ҚАЗАҚСТАН РЕСПУБЛИКАСЫ
ҒЫЛЫМ ЖӘНЕ ЖОҒАРЫ БІЛІМ МИНИСТРЛІГІ

SATBAYEV UNIVERSITY
МЕТАЛЛУРГИЯ ЖӘНЕ КЕН БАЙЫТУ ИНСТИТУТЫ

ISSN 2616-6445 (Online)
ISSN 2224-5243 (Print)
DOI 10.31643/2018/166445

Минералдық шикізаттарды кешенді пайдалану

2(341)

Комплексное Использование Минерального Сырья

Complex Use of Mineral Resources

СӘУІР-МАУСЫМ 2027
APRIL-JUNE 2027
АПРЕЛЬ-ИЮНЬ 2027

ЖЫЛЫНА 4 РЕТ ШЫҒАДЫ
QUARTERLY JOURNAL
ВЫХОДИТ 4 РАЗА В ГОД

ЖУРНАЛ 1978 ЖЫЛДАН БАСТАП ШЫҒАДЫ
JOURNAL HAS BEEN PUBLISHING SINCE 1978
ЖУРНАЛ ИЗДАЕТСЯ С 1978 ГОДА

АЛМАТЫ - 2027

Б а с р е д а к т о р техника ғылымдарының докторы, профессор **Бағдаулет КЕНЖАЛИЕВ**

Р е д а к ц и я а л қ а с ы:

Тех. ғыл. канд. **Ринат Абдулвалиев**, Металлургия және кен байыту институты АҚ, Сәтбаев университеті, Алматы, Қазақстан;
Ph.D., проф. **Akçil Ata**, Сулейман Демирел университеті, Испарта, Түркия;
Ph.D., доцент **Rouholah Ashiri**, Исфахан технологиялық университеті, Исфахан, Иран;
Др. **Khaldun Mohammad Al Azzam,** Әл-Ахлия Амман университеті, Иордания;
Ph.D., **Muhammad Noorazlan Abd Azis**, Сұлтан Идрис атындағы білім беру университеті, Перак, Малайзия;
Проф., др. **Craig E. Banks**, Манчестер Метрополитен университеті, Ұлыбритания;
Проф. **Mishra Brajendra**, Вустер Политехникалық институты, Вустер, АҚШ;
Тех. ғыл. др., проф., академик **Марат Битимбаев,** Қазақстан Республикасы Ұлттық инженерлік академиясы, Алматы;
Тех. және физ.-мат. ғыл. др. **Валерий Володин,** Металлургия және кен байыту институты АҚ, Сәтбаев университеті, Алматы, Қазақстан;
Тех. ғыл. др., проф. **Ұзақ Жапбасбаев,** Сәтбаев университеті, Алматы, Қазақстан;
Ph.D., профессор, **Yangge Zhu**, Пайдалы қазбаларды өңдеудің мемлекеттік негізгі зертханасы, Бейжің, Қытай;
Проф.,доктор **Shigeyuki Haruyama**, Ямагучи университеті, Жапония;
Тех. ғыл. др. **Сергей Квятковский,** Металлургия және кен байыту институты АҚ, Сәтбаев университеті, Алматы, Қазақстан;
Тех.ғыл.кан., проф., академик **Ержан И. Кульдеев,** Сәтбаев университеті, Алматы, Қазақстан;
Жетекші ғылыми қызметкер, др. **Dilip Makhija,** JSW Cement Ltd, Мумбай, Үндістан;
Тех. ғыл. др. **Гүлнәз Молдабаева,** Сәтбаев университеті, Алматы, Қазақстан;
Проф., т.ғ.д. **El-Sayed Negim**, Ұлттық зерттеу орталығы, Каир, Египет;
Ph.D., проф. **Didik Nurhadiyanto**, Джокьякарта мемлекеттік университеті, Индонезия;
Доктор, қауымдастырылған проф. **Mrutyunjay Panigrahi**, Веллор Технологиялық Институты, Үндістан;
Др. **Kyoung Tae Park,** Корея сирек металдар институты (KIRAM), Корея Республикасы;
Ph.D., проф. **Dimitar Peshev**, Химиялық технология және металлургия университеті, София, Болгария;
Др. **Małgorzata Rutkowska-Gorczyca,** Вроцлав технологиялық университеті, Вроцлав, Польша;
Проф., др. **Heri Retnawati,** Джокьякарта мемлекеттік университеті, Индонезия;
Тех.ғыл.кан., проф. **Қанай Рысбеков**, Сәтбаев университеті, Алматы, Қазақстан;
Др. **Jae Hong Shin,** Корея өнеркәсіптік технологиялар институты, Корея Республикасы;
Тех. ғыл. др., проф. **Arman Shah**, Сұлтан Идрис білім беру университеті, Малайзия;
Др., проф. **Abdul Hafidz Yusoff,** Университет Малайзии Келантан, Малайзия.

Ж а у а п т ы х а т ш ы

Ph.D. **Гулжайна Касымова**

Редакция мекен жайы:
«Металлургия және кен байыту институты» АҚ
050010, Қазақстан Республикасы, Алматы қ., Шевченко к-сі, Уәлиханов к-нің қиылысы, 29/133,
Fax. +7 (727) 298-45-03, Tel. +7-(727) 298-45-02, +7 (727) 298-45-19
E mail: journal@kims-imio.kz, product-service@kims-imio.kz
http://kims-imio.com/index.php/main

«Минералдық шикізаттарды кешенді пайдалану» журналы ғылыми жұмыстардың негізгі нәтижелерін жариялау үшін Қазақстан Республикасы Білім және ғылым министірлігінің Білім және ғылым сапасын қамтамасыз ету комитеті ұсынған ғылыми басылымдар тізіміне енгізілген.
Меншік иесі: «Металлургия және кен байыту институты» АҚ

Журнал Қазақстан Республикасының Ақпарат және коммуникация министрлігінің Байланыс, ақпараттандыру және бұқаралық ақпарат құралдары саласындағы мемлекеттік бақылау комитетінде қайта тіркелген

2016 ж. 18 қазандағы № 16180-Ж Куәлігі

© «Металлургия және кен байыту институты» АҚ, 2027

E d i t o r – in - c h i e f Dr. Sci. Tech., professor **Bagdaulet KENZHALIYEV**

E d i t o r i a l b o a r d:

Cand. of Tech. Sci. **Rinat Abdulvaliyev**, Institute of Metallurgy and Ore Beneficiation JSC, Satbayev University, Almaty, Kazakhstan;
Ph.D., Prof. **Akçil Ata**, Süleyman Demirel Üniversitesi, Isparta, Turkey;
Ph.D. **Rouholah Ashiri**, associate prof. of Isfahan University of Technology, Isfahan, Iran;
Dr. **Khaldun Mohammad Al Azzam,** Department of Pharmaceutical Sciences, Pharmacological and Diagnostic Research Center, Faculty of Pharmacy, Al-Ahliyya Amman University, Jordan;
Ph.D. **Muhammad Noorazlan Abd Azis**, associate prof. of Sultan Idris Education University, Perak, Malaysia;
Prof., Dr. **Craig E. Banks,** Manchester Metropolitan University, United Kingdom;
Prof. **Mishra Brajendra**, Worcester Polytechnic Institute, Worcester, United States;
Dr.Sci.Tech., Prof. academician **Marat Bitimbayev,** National Engineering Academy of the Republic of Kazakhstan, Almaty;
Dr. Tech., Phys-math. Sci., prof. **Valeryi Volodin**, Institute of Metallurgy and Ore Beneficiation JSC, Satbayev University, Almaty, Kazakhstan;
Dr.Sci.Tech., Prof. **Uzak K. Zhapbasbayev,** Satbayev University, Almaty, Kazakhstan;
Ph.D., Professor, **Yangge Zhu**, State Key Laboratory of Mineral Processing, Beijing, China;
Prof. Dr. **Shigeyuki Haruyama**, Yamaguchi University, Japan;
Dr.Sci.Tech. **Sergey A. Kvyatkovskiy**, Institute of Metallurgy and Ore Beneficiation JSC, Satbayev University, Almaty, Kazakhstan;
Prof., Dr. Sci. Tech., academician **Yerzhan I. Kuldeyev,** Satbayev University, Almaty, Kazakhstan;
Lead Scientist, Dr. **Dilip Makhija,** JSW Cement Ltd, Mumbai, India;
Dr.Sci.Tech. **Gulnaz Moldabayeva,** Satbayev University, Almaty, Kazakhstan;
Prof., Dr. Sci. Tech. **El-Sayed Negim**, Professor of National Research Centre, Cairo, Egypt;
Prof., Ph.D., **Didik Nurhadiyanto**, Yogyakarta State University, Yogyakarta, Indonesia;
Dr., Assoc. Prof., **Mrutyunjay Panigrahi**, Vellore Institute of Technology, India;
Dr. **Kyoung Tae Park,** Korea Institute for Rare Metals (KIRAM), Republic of Korea;
Professor, Ph.D. **Dimitar Peshev**, University of Chemical Technology and Metallurgy, Sofia, Bulgaria;
Dr.Sc. **Małgorzata Rutkowska-Gorczyca,** Wroclaw University of Science and Technology, Wroclaw, Poland;
Prof., Dr. **Heri Retnawati,** Yogyakarta State University (Universitas Negeri Yogyakarta), Indonesia;
Prof., Dr. Sci. Tech. **Kanay Rysbekov**, Satbayev University, Almaty, Kazakhstan;
Dr. **Jae Hong Shin,** Korea Institute of Industrial Technology, Republic of Korea;
Prof., Dr. Sci. Tech. **Arman Shah**, Universiti Pendidikan Sultan Idris, Tanjong Malim, Malaysia;
Associate Prof., Dr **Abdul Hafidz Yusoff,** Universiti Malaysia Kelantan, Malaysia.

E x e c u t i v e s e c r e t a r y

Ph.D. **Gulzhaina Kassymova**

Address:
"Institute of Metallurgy and Ore Beneficiation" JSC
29/133 Shevchenko Street, corner of Ch. Valikhanov Street, Almaty, 050010, Kazakhstan
Fax. +7 (727) 298-45-03, Tel. +7-(727) 298-45-02, +7 (727) 298-45-19
E mail: journal@kims-imio.kz, product-service@kims-imio.kz
http://kims-imio.com/index.php/main

The Journal "Complex Use of Mineral Resources" is included in the List of publications recommended by the Committee for Control in the Sphere of Education and Science of the Ministry of Education and Science of the Republic of Kazakhstan for the publication of the main results of scientific activities.
Owner: "Institute of Metallurgy and Ore Beneficiation" JSC

The Journal was re-registered by the Committee for State Control in the Sphere of Communication, Information and Mass Media of the Ministry of Information and Communication of the Republic of Kazakhstan.

Certificate № 16180-Ж since October 18, 2016

© "Institute of Metallurgy and Ore Beneficiation" JSC, 2027

Главный редактор доктор технических наук, профессор **Багдаулет КЕНЖАЛИЕВ**

Редакционная коллегия:

Кан. хим. н. **Ринат Абдулвалиев**, АО Институт металлургии и обогащения, Satbayev University, Алматы, Казахстан;
Ph.D., проф. **Akçil Ata**, Университет Сулеймана Демиреля, Испарта, Турция;
Ph.D., доцент **Rouholah Ashiri**, Исфаханский технологический университет, Исфахан, Иран;
Др. **Khaldun Mohammad Al Azzam,** Аль-Ахлия Амманский университет, Иордания;
Ph.D., доцент **Muhammad Noorazlan Abd Azis**, Образовательный университет Султана Идриса, Перак, Малайзия;
Др. тех. н., проф. **Craig E. Banks**, Манчестерский столичный университет, Соединенное Королевство;
Ph.D., проф. **Mishra Brajendra**, Вустерский политехнический институт, Вустер, США;
Др. тех. н., проф., академик **Марат Битимбаев,** Национальная инженерная академия Республики Казахстан, Алматы;
Др. тех. н. и физ.-мат. н. **Валерий Володин**, АО Институт металлургии и обогащения, Satbayev University, Алматы, Казахстан;
Др. тех. н., проф. Узак **Жапбасбаев**, КазНИТУ имени К. И. Сатпаева, Алматы, Казахстан;
Ph.D., проф. **Yangge Zhu**, Государственная ключевая лаборатория переработки полезных ископаемых, Пекин, Китай;
Проф., доктор **Shigeyuki Haruyama**, Университет Ямагути, Япония;
Др. тех. н. **Сергей Квятковский,** АО Институт металлургии и обогащения, Satbayev University, Алматы, Казахстан;
К.т.н., проф., академик **Ержан И. Кульдеев,** КазНИТУ имени К. И. Сатпаева, Алматы, Казахстан;
Ведущий научный сотрудник, др. **Dilip Makhija,** JSW Cement Ltd, Мумбаи, Индия;
Др. тех. н. **Гульназ Молдабаева,** КазНИТУ имени К.И. Сатпаева, Алматы, Казахстан**;**
Др. тех. н., проф. **El-Sayed Negim**, Национальный исследовательский центр, Каир, Египет;
Др. тех. н., доцент **Didik Nurhadiyanto**, Джокьякартский государственный университет, Индонезия;
Доктор, Ассоц.проф. **Mrutyunjay Panigrahi,** Веллорский технологический институт, Индия;
Др. **Kyoung Tae Park,** Корейский институт редких металлов (KIRAM), Республика Корея;
Ph.D., проф. **Dimitar Peshev**, Университет химической технологии и металлургии, София, Болгария;
Др. **Małgorzata Rutkowska-Gorczyca,** Вроцлавский политехнический университет, Вроцлав, Польша;
Проф., др. **Heri Retnawati,** Джокьякартский государственный университет, Индонезия;
К.т.н., проф. **Канай Рысбеков**, КазНИТУ имени К. И. Сатпаева, Алматы, Казахстан;
Др. **Jae Hong Shin,** Корейский институт промышленных технологий, Республика Корея;
Кан. хим. н., проф. **Arman Shah**, Педагогический университет Султана Идриса, Танджунг Малим, Малайзия;
Др. проф. **Abdul Hafidz Yusoff,** Университет Малайзии, Малайзия.

Ответственный секретарь

Ph.D. **Гулжайна Касымова**

Адрес редакции:
АО «Институт металлургии и обогащения»
050010, Республика Казахстан, г. Алматы, ул. Шевченко, уг. ул. Валиханова, 29/133,
Fax. +7 (727) 298-45-03, Tel. +7 (727) 298-45-02, +7 (727) 298-45-19
E mail: journal@kims-imio.kz, product-service@kims-imio.kz
http://kims-imio.com/index.php/main

Журнал «Комплексное использование минерального сырья» включен в Перечень изданий, рекомендуемых Комитетом по контролю в сфере образования и науки Министерства образования и науки Республики Казахстан для публикации основных результатов научной деятельности.
Собственник: АО «Институт металлургии и обогащения»

Журнал перерегистрирован в Комитете государственного контроля в области связи, информатизации и средств массовой информации
Министерства информации и коммуникации Республики Казахстан
Свидетельство № 16180-Ж от 18 октября 2016 г.

© АО «Институт металлургии и обогащения», 2027

Crossref
DOI: 10.31643/2027/6445.13
Metallurgy

Predicting Copper Production Cycles in Hydrometallurgy with Interpretable Machine Learning

[1]Kenzhaliyev B.K., [2,3*]Aibagarov S.Zh., [2]Nurakhov Y.S., [1]Koizhanova A., [1]Magomedov D.R.

[1] Institute of Metallurgy and Ore Beneficiation JSC, Satbayev University, Almaty, Kazakhstan
[2] Al-Farabi Kazakh National University, Almaty, Kazakhstan
[3] LLP DigitAlem, Almaty, Kazakhstan

** Corresponding author email: awer1307dot@gmail.com*

Received: *September 20, 2025*
Peer-reviewed: *October 10, 2025*
Accepted: *October 16, 2025*

ABSTRACT
Accurate production forecasting in industrial hydrometallurgy is essential for process optimization yet is often hindered by the scarcity of extensive historical data. This study demonstrates the effectiveness of classical machine learning models as a data-efficient and interpretable alternative to complex deep learning methods for predicting total copper mass. We evaluated four models—Random Forest, Gradient Boosting, Decision Tree, and Linear Regression—using a methodology centered on two key strategies: synthetically expanding a limited 150-day dataset into 10,000 simulated cycles (approximately 1.5 million data points) via data augmentation, and engineering 10-day lag features to provide the models with a temporal perspective for a 10-step-ahead forecasting task. The results revealed exceptional predictive accuracy, with ensemble techniques proving superior. The Random Forest model emerged as the top performer, achieving an R^2 of 0.974, an MAE of 0.088, and an RMSE of 0.111, closely followed by Gradient Boosting (R^2 of 0.971). All models successfully captured the distinct 150-day cyclical dynamics of the production process, showing a near-zero phase lag (0.00 ± ≤0.05 days). While performance on new, independent data requires further validation, this work establishes a robust and transparent framework for developing reliable forecasting tools in data-limited industrial environments.

Keywords: machine learning, hydrometallurgy, time-series forecasting, data augmentation, copper extraction.

Information about authors:

Kenzhaliyev Bagdaulet Kenzhaliyevich — *Doctor of Technical Sciences, Professor, General Director-Chairman of the Management Board of the Institute of Metallurgy and Ore Beneficiation JSC, Satbayev University, Almaty, Kazakhstan. Email: bagdaulet_k@satbayev.university; ORCID ID: https://orcid.org/0000-0003-1474-8354*

Aibagarov Serik Zhumagireyevich — *Researcher, Al-Farabi Kazakh National University; LLP DigitAlem, Almaty, Kazakhstan. Email: awer1307dot@gmail.com; ORCID ID: https://orcid.org/0009-0009-4946-4926*

Nurakhov Yedil Sergazievich — *Researcher, Al-Farabi Kazakh National University, Almaty, Kazakhstan. Email: y.nurakhov@gmail.com; ORCID ID: https://orcid.org/0000-0003-0799-7555*

Koizhanova Aigul — *Candidate of Technical Sciences, Head of Laboratory Institute of Metallurgy and Ore Beneficiation JSC, Satbayev University, Almaty, Kazakhstan. Email: aigul_koizhan@mail.ru; ORCID ID: https://orcid.org/0000-0001-9358-3193*

Magomedov David Rasimovich — *Research Associate, Master's degree Institute of Metallurgy and Ore Beneficiation JSC, Satbayev University, Almaty, Kazakhstan. Email: davidmag16@mail.ru; ORCID ID: https://orcid.org/0000-0001-7216-2349*

Introduction

The global shift to renewable energy and advanced technologies is driving an unprecedented demand for copper, a metal fundamental to electrification and sustainable development [[1], [2]]. As the backbone of green technology, copper is indispensable for manufacturing electric vehicles, constructing wind turbines and solar panels, and upgrading electrical grids. To meet this surging demand, the mining industry is increasingly extracting copper from complex, low-grade, and often refractory ores, a practice that presents profound operational and environmental challenges [[3], [4]]. Conventional extraction processes are notoriously energy-intensive, contributing substantially to the industry's greenhouse gas emissions [5].

Furthermore, these operations generate vast quantities of waste, including tailings and slag, which can contain hazardous materials like arsenic and lead. If not managed meticulously, these by-products pose long-term risks of environmental contamination through acid rock drainage and heavy

metal leaching into soil and water systems [[6], [7]]. Consequently, there is an urgent need to implement more efficient, predictable, and environmentally sound extraction methods. Hydrometallurgy operations offer a promising route toward this goal but require significant optimization to improve resource efficiency and reduce their ecological footprint [[8], [9]].

Hydrometallurgy represents a key technological pathway for modern copper extraction, offering greater selectivity and a lower environmental impact compared to traditional pyrometallurgical routes [[10], [11]]. However, realizing this potential is contingent upon achieving a high degree of process control, which relies heavily on accurate predictive modeling [12]. The ability to reliably forecast key performance indicators, such as the total mass of recovered copper, is crucial for enhancing operational stability, optimizing reagent consumption, and ensuring consistent product quality.

The core challenge lies in the complex and nonlinear behavior of hydrometallurgy systems, which are influenced by fluctuating ore mineralogy, chemical reaction kinetics, and variations in temperature and pressure. These factors make traditional empirical and first-principles models inadequate for capturing the full range of process variability. This technological gap has led to the widespread adoption of Artificial Intelligence (AI) and Machine Learning (ML) as powerful tools capable of modeling these intricate relationships by identifying subtle patterns in historical data [[13], [14], [15]].

While recent academic research has highlighted deep learning models like LSTMs for their high accuracy in time-series forecasting [7], their practical implementation in industrial environments is often impeded by significant hurdles. Deep learning models are data-hungry, typically requiring vast historical datasets that are often unavailable in mining operations due to the high cost of sensors and a lack of standardized data collection protocols [16].

A second major barrier is their lack of interpretability. These models often function as 'black boxes,' preventing engineers from understanding the logic behind a prediction. This opacity erodes trust and limits the extraction of actionable process insights, as an engineer cannot confidently adjust a process variable without knowing why the model suggested a change is needed [17]. This creates a clear research gap: a lack of studies demonstrating how classical, interpretable machine learning models can achieve high predictive performance under the data limitations common in industrial settings.

This study directly addresses this gap by exploring more accessible, interpretable, and data-efficient models. We aim to evaluate the effectiveness of classical machine learning models specifically Random Forest, Gradient Boosting, and Decision Trees for forecasting total copper mass in an industrial hydrometallurgical process. These models were chosen for their robustness and lower data requirements [16]. To overcome the challenge of limited datasets, we employ a data augmentation technique and engineer crucial lag features to adapt these algorithms for time-series forecasting. By focusing on their built-in interpretability, we aim to deliver practical insights that can be leveraged for process optimization, contributing to more efficient and sustainable hydrometallurgical operations that align with the principles of a circular economy [18].

Experimental part

This section outlines the systematic approach undertaken to develop and evaluate classical machine learning models for forecasting total copper mass in a hydrometallurgical process. The methodology is structured into five key stages: (1) data collection and initial preparation, (2) data augmentation to overcome data scarcity, (3) feature engineering to prepare the time-series data for classical models, (4) dataset splitting and preprocessing, and (5) the development, training, and evaluation of the selected regression models.

Data Collection and Initial Preparation. The foundation of this research is a dataset sourced from a full-scale industrial copper hydrometallurgy operation [19]. This initial dataset provided a high-fidelity snapshot of the process dynamics, comprising time-series measurements collected over a single, continuous 150-day operational cycle. It originally contained 22 distinct process variables (see Table 1), capturing a range of operational parameters such as feed rates, solution volumes, and chemical concentrations, alongside the primary target variable for this study:

"Total_Cu_mass". The use of real-world industrial data, despite its limited duration, is critical for ensuring the practical relevance and applicability of the resulting predictive models.

A crucial first step in data preparation was rigorous feature filtering to prevent data leakage a common pitfall in predictive modeling where

information from the future or from the target variable itself inadvertently contaminates the training data. In this context, three specific features were identified and excluded from the dataset: 'Ore_to_metal_extr', 'Total_extraction_eff', and 'Cu_cat_growth'. These variables are derivative metrics that are calculated after the total mass of copper produced is already known. Including them in the feature set would provide the models with direct information about the target, leading to artificially inflated performance metrics and a model that would be useless in a real-world forecasting scenario where such information is not yet available.

Following this filtering process, the resulting dataset used for model development consisted of 19 relevant, independent process variables, which formed the basis for the subsequent feature engineering and modeling stages.

Table 1 - Dataset variables

Variable Name	Physical Measurement (Units)	Description
Cu_feed	Copper concentration (g/L)	Concentration of copper in the feed solution entering the extraction process
Cu_raf	Copper concentration (g/L)	Concentration of copper in the raffinate solution (the aqueous phase after extraction)
Extraction_flow	Flow rate (m^3/day)	Volume flow rate of solution during the extraction stage
Cu_extr_eff	Efficiency (%)	Percentage of copper successfully extracted from feed solution
Pond_prod_sol_vol	Volume (m^3)	Total volume of productive solution stored in the leaching pond
Pond_raf_sol_vol	Volume (m^3)	Total volume of raffinate solution stored in the pond
Cu_org_B	Copper concentration (g/L)	Concentration of copper in the organic phase before loading (entering re-extraction)
Cu_org_O	Copper concentration (g/L)	Concentration of copper in the organic phase after loading (leaving extraction)
Org_flow	Flow rate (m^3/day)	Volume flow rate of the organic extractant through the system
Cu_el_B	Copper concentration (g/L)	Concentration of copper in the electrolyte before electrolysis
El_flow_B	Flow rate (m^3/day)	Volume flow rate of the electrolyte before electrolysis
Cu_el_eff_org	Efficiency (%)	Percentage efficiency of copper transfer from organic phase to electrolyte
Cu_el_eff_sol	Efficiency (%)	Percentage efficiency of copper electrodeposition from solution to cathodes
Cu_el_O	Copper concentration (g/L)	Concentration of copper in the electrolyte after electrolysis
El_flow_O	Flow rate (m^3/day)	Volume flow rate of the electrolyte after electrolysis
Cu_cat_growth	Mass growth rate (kg/day)	Rate of copper deposition on cathodes during electrolysis
Total_Cu_mass	**Mass (kg)**	**Total cumulative mass of copper produced (target variable)**
Ore_to_metal_extr	Ratio (kg ore/kg Cu)	Mass ratio of ore processed to metal extracted
Total_extraction_eff	Efficiency (%)	Overall percentage efficiency of the entire extraction process
Ore_mass	Mass (tons)	Total mass of ore processed in the extraction operation
Initial_Cu_mass	Mass (kg)	Initial mass of copper in the ore before processing begins
Org_volume	Volume (m^3)	Total volume of organic extractant in the system

Data Augmentation. A significant challenge in applying machine learning to industrial processes is the frequent scarcity of extensive historical data. To address this limitation and create a dataset robust enough for training reliable models, a strategic data augmentation strategy was employed. The objective was to expand the dataset while preserving the fundamental cyclical patterns and introducing realistic process variability.

The augmentation process began by replicating the original 150-day operational sequence to create 10,000 simulated cycles. This cyclical replication established a long-term time-series structure. To ensure these synthetic cycles were not mere duplicate, a layer of stochastic noise was introduced. Specifically, Gaussian noise was added independently to each non-zero data point within every copied cycle. The noise followed a normal distribution with a mean of 0 and a standard deviation of 0.02. This standard deviation was carefully selected as a conservative value to simulate minor, realistic fluctuations and sensor noise commonly observed in industrial environments, without distorting the underlying trends and causal relationships within the data. Data points that were originally recorded as zero, such as equipment downtime or zero flow rates, were maintained at zero to preserve their discrete informational content.

By concatenating these 10,000 augmented cycles sequentially, an expanded time-series dataset was generated, comprising approximately 1,500,000 total data points (10,000 cycles × 150 days/cycle). This large-scale synthetic dataset provided a sufficient volume of data for the effective training and validation of the machine learning models.

Feature Engineering: Lag Feature Creation. Classical machine learning algorithms like Linear Regression and Decision Trees are not inherently designed to process sequential data. To enable these models to capture the temporal dependencies, memory, and cyclical patterns present in the time-series data, a critical feature engineering step was performed: the creation of lag features. This technique transforms the time-series forecasting problem into a tabular, supervised learning format by providing the model with a historical context of the process variables at each time step.

The methodology involved creating a "look-back" window of 10 days. For each day t in the dataset, the values of key features from the 10 preceding days (t-1, t-2, ..., t-10) were appended as new features to the data point at day t. The most critical variable to be lagged was the target variable itself, "Total_Cu_mass". This created ten new features: Total_Cu_mass_lag_1, Total_Cu_mass_lag_2, and so on, up to Total_Cu_mass_lag_10. Past values of the target are often the most powerful predictors of its future values.

Dataset Splitting and Preprocessing. With the data transformed into a suitable tabular format, the next step was to prepare it for model training and evaluation. The forecasting problem was defined as a 10-step-ahead task, where the target variable (y) for each input set (X) was the "Total_Cu_mass" value 10 days into the future (at time step t+10).

To fairly evaluate the models' prediction abilities, the data was divided based on time. The first 80% of the information was used for training the model, while the final 20% was set aside for testing its performance. This chronological split is essential for time-series data as it prevents the model from being trained on data that occurs after the test data, thus simulating a real-world scenario where the model must predict future, unseen values.

Lastly, all parts of the data were put into a common format. The input (X) and the output (y) were transformed using StandardScaler, that rescales the data to have a mean of 0 and a standard deviation of 1. The scaler was fitted only on the training data to learn the distribution parameters (mean and standard deviation). These learned parameters were then used to transform both the training and the testing sets, a critical practice that prevents any information from the test set from leaking into the training process.

Model Development. Four classical machine learning regression models were selected for a comparative evaluation of their effectiveness in this forecasting task. Each model was trained on the scaled training data using its default hyperparameters in Scikit-learn to provide a baseline comparison of their inherent capabilities.

1. *Linear Regression:* Fundamental modeling technique that finds the best-fitting straight line to represent the relationship between inputs and an output. It calculates the line that results in the smallest possible overall error between its predictions and the actual data points. The model is represented by the equation:

$$y = \beta_0 + \beta_1 x_1 + \beta_2 x_2 + \cdots \beta_n x_n + \epsilon \quad (1)$$

where y is the predicted value, β_0 is the intercept, $\beta_1 \dots \beta_n$ are the feature coefficients, and ϵ is the error term. Its simplicity makes it highly interpretable [20].

2. *Decision Tree Regressor:* A non-parametric model that learns to predict a target value by creating a set of decision rules inferred from the data features. It operates by recursively partitioning the feature space into several disjoint regions, R_m, forming a tree-like structure. For any new data point x that falls into a specific terminal region (a leaf node) R_m, the model's prediction is simply the mean of the training target values within that region. This predictive mechanism is defined as:

$$\hat{y} = f(x) = \sum_{m=1}^{M} c_m I(x \epsilon R_m) \quad (2)$$

$$\text{where } c_m = \frac{1}{N_m} \sum_{x_i \epsilon R_m} yi \quad (3)$$

Here, M is the total number of terminal regions (leaves), c_m is the mean target value for the N_m training samples in region R_m, and I is the indicator function. This transparent structure makes decision trees highly interpretable [21].

3. Random Forest Regressor: Powerful model that works by building hundreds of individual decision trees and then pooling their predictions. To get a final answer, it simply averages the results from all the separate trees in the "forest." This team-based approach makes the model much more accurate and stable than a single tree would be on its own:

$$\hat{y} = \frac{1}{B} \sum_{b=1}^{B} f_b(x) \quad (4)$$

where B is the number of trees and $f_b(x)$ is the prediction of the b-th tree [22].

4. Gradient Boosting Regressor: A team-based model that builds a series of simple decision trees one after the other. Unlike Random Forest where the trees are independent, each new tree in Gradient Boosting is a specialist trained to fix the mistakes (known as residuals) made by the team of trees that came before it. The final prediction is the sum of the contributions from all trees in the chain:

$$F_m(x) = F_{m-1}(x) + \gamma_m h_m(x) \quad (5)$$

where $F_{m-1}(x)$ is the previous model, $h_m(x)$ is the new weak learner (tree), and γ_m is the learning rate. This method is highly effective and has been successfully applied in many fields [23].

Model Evaluation. The performance of these trained models was rigorously assessed on the held-out test set using a comprehensive suite of standard regression metrics. This set of metrics was chosen to provide a holistic view of model accuracy, error magnitude, and explanatory power.

Mean Absolute Error (MAE):

$$MAE = \frac{1}{n} \sum_{i=1}^{n} |y_i - \hat{y}_i| \quad (6)$$

where n is the number of samples, y_i is the actual value, and $\hat{y}_i$ is the predicted value.

Root Mean Squared Error (RMSE):

$$RMSE = \sqrt{\frac{1}{n} \sum_{i=1}^{n} (y_i - \hat{y}_i)^2} \quad (7)$$

Coefficient of Determination (R^2):

$$R^2 = 1 - \frac{\sum_{i=1}^{n} (y_i - \hat{y}_i)^2}{\sum_{i=1}^{n} (y_i - \hat{y})^2} \quad (8)$$

where $\hat{y}$ is the mean of the actual values.

Mean Absolute Percentage Error (MAPE):

$$MAPE = \frac{100\%}{n} \sum_{i=1}^{n} \left| \frac{y_i - \hat{y}_i}{y_i} \right| \quad (9)$$

Results and discussion

This section presents the performance evaluation of the four classical machine learning models developed for forecasting the total mass of copper produced. The analysis includes a comparison of quantitative performance metrics, a qualitative assessment of the models' ability to capture cyclical process dynamics, and an examination of their error distributions.

Model Performance Overview. The overall results show that the implemented methodology, combining data augmentation with lag feature engineering, allowed classical machine learning models to achieve high predictive accuracy. The performance, evaluated using the coefficient of determination (R^2), indicates that all models were able to explain a significant portion of the variance in the target variable.

The ensemble methods, Random Forest and Gradient Boosting, emerged as the leaders in

performance, achieving R^2 scores of 0.974 and 0.971, respectively. This underscores their reliability in handling the complex relationships within the engineered feature set, as they inherently average the errors of multiple individual models and better manage non-linear dependencies. The Linear Regression model also demonstrated strong performance with an R^2 of 0.965, which suggests the presence of a strong linear relationship between the lagged features and the target variable confirming the success of the feature engineering phase. The standalone Decision Tree model proved to be the least effective, with an R^2 of 0.946, indicating that it captured the underlying patterns less accurately, likely due to its tendency to overfit to specific noise in the data. A visual comparison of the R^2 scores is provided in Figure 1.

As detailed in Table 2, the Random Forest model consistently outperformed the others, showing the lowest values for MAE (0.088), RMSE (0.111), and MAPE (98.8). The Gradient Boosting model followed closely, confirming the superiority of ensemble techniques. Conversely, the Decision Tree model demonstrated the highest error across all metrics, which aligns with its lower R^2 score and confirms its position as the least accurate model in this comparative study.

Table 2 - Comprehensive Performance Metrics for All Models

Model	MAE	RMSE	R^2	MAPE (%)
Random Forest	0.0883	0.1112	0.9743	98.80
Gradient Boosting	0.0929	0.1177	0.9713	114.82
Linear Regression	0.1041	0.1303	0.9648	110.80
Decision Tree	0.1276	0.1607	0.9464	161.93

Forecasting of Cyclical Process Dynamics. Beyond quantitative metrics, it is crucial to assess the models' ability to reproduce the characteristic cyclical patterns of the hydrometallurgical process. Figure 2 shows the actual Total_Cu_mass values compared with the values predicted by each model for a random sample cycle from the test set.

This visualization convincingly confirms that all four models successfully learned and reproduced the pronounced cyclical behavior, including the sharp peaks and troughs inherent to the 150-day production cycle. This qualitative result is highly significant, as it validates that the feature engineering strategy specifically, the creation of lag features effectively provided the models with the necessary historical context to understand the time-series dynamics. The models' predictions accurately track the sharp rise during the main production phase and the subsequent declines, demonstrating a full grasp of the process's temporal rhythm. Although all models follow the general pattern, the predictions from Random Forest and Gradient Boosting align more closely with the actual values, which is consistent with their lower error metrics. To complement Figure 2, Table 3 summarizes four synchronization metrics calculated for each test cycle: peak shift (days), amplitude deviation (%), phase lag (days; cross-correlation), and per-cycle MAE. Across models, the phase lag is essentially zero (0.00 ± ≤0.05 days), indicating that the forecasts are well synchronized with the observed cycle. Gradient Boosting and Random Forest achieve the lowest per-cycle MAE (0.09 ± 0.01), while Linear Regression is slightly higher (0.10 ± 0.01) and Decision Tree is the highest (0.13 ± 0.01). Both ensemble models tend to underestimate cycle amplitude (−14.05 ± 2.84% and −12.23 ± 2.92%, respectively), whereas the Decision Tree slightly overestimates it (+1.02 ± 4.90%). The near-zero peak shifts (e.g., −2.34 ± 35.44 days for Gradient Boosting and −0.46 ± 35.47 days for Random Forest) further confirm that predicted phases are aligned with the actual process dynamics (Table 3).

Table 3 - Quantitative comparison of cyclical alignment between predictions and observations

Model	Peak shift (days)	Amplitude deviation (%)	Phase lag (days)	MAE per cycle
Linear Regression	−0.34 ± 35.12	−5.38 ± 4.51	0.00 ± 0.00	0.10 ± 0.01
Decision Tree	0.98 ± 35.12	1.02 ± 4.90	0.00 ± 0.05	0.13 ± 0.01
Random Forest	−0.46 ± 35.47	−12.23 ± 2.92	0.00 ± 0.00	0.09 ± 0.01
Gradient Boosting	−2.34 ± 35.44	−14.05 ± 2.84	0.00 ± 0.00	0.09 ± 0.01

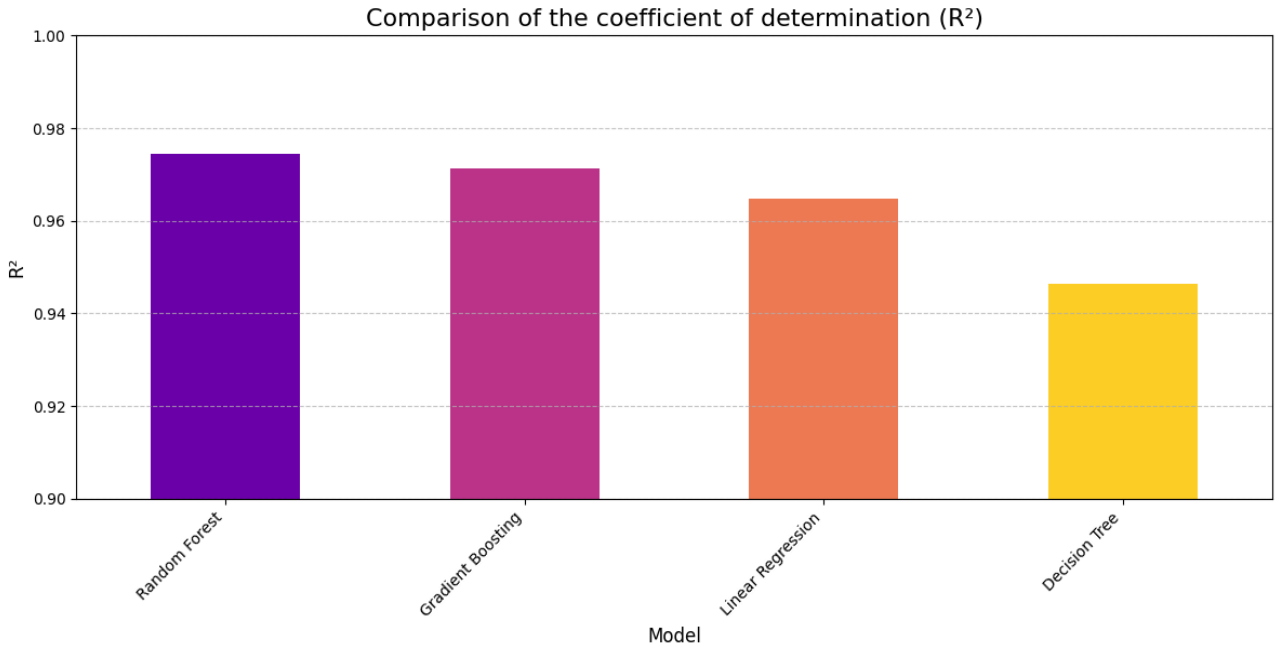

Figure 1 - Comparison of the Coefficient of Determination (R^2)

Analysis of Prediction Errors. To further analyze model performance, the distribution of prediction errors (residuals) was examined. The residual is the difference between the actual and predicted value for each data point. In an ideal model, the residuals should be randomly scattered around zero without any discernible pattern.

Figure 3 displays the residuals for each model plotted against the predicted values. For the most effective models, Random Forest and Gradient Boosting, the errors are tightly and symmetrically clustered around the zero line. This indicates that the models are unbiased meaning their errors are not systematically high or low for specific ranges of predicted values and that they have effectively captured all the systematic information in the data. The residuals for Linear Regression and, most dispersed. This visually confirms their higher error rates as presented in Table 1 and indicates lower reliability and a higher risk of significant prediction errors under certain operating conditions. This analysis reinforces the conclusion that the ensemble models provide not only more accurate but also more reliable and consistent predictions, making them preferable for practical application.

To deepen the error analysis beyond accuracy scores and visuals, we perform formal residual diagnostics; the results are summarized in Table 4, that reports residual diagnostics on the test set. The mean residuals are approximately zero for all models ($|\text{bias}| \leq 3\times10^{-4}$), confirming the absence of systematic shift. Random Forest exhibits the smallest spread and error (SD = 0.1115; RMSE = 0.1115), followed by Gradient Boosting (0.1183), Linear Regression (0.1306) and Decision Tree (0.1605). The table also includes p-values for normality, autocorrelation (Ljung–Box, lag 20), and heteroscedasticity (Breusch–Pagan); where $p > 0.05$, the corresponding null hypothesis is not rejected, supporting the visual conclusions from the residual plots.

Table 4 - Residual diagnostics on the test set

Model	Mean residual	SD residual	RMSE
Linear Regression	−0.000319	0.130644	0.130644
Decision Tree	−0.000057	0.160467	0.160467
Random Forest	−0.000004	0.111513	0.111513
Gradient Boosting	−0.000061	0.118252	0.118252

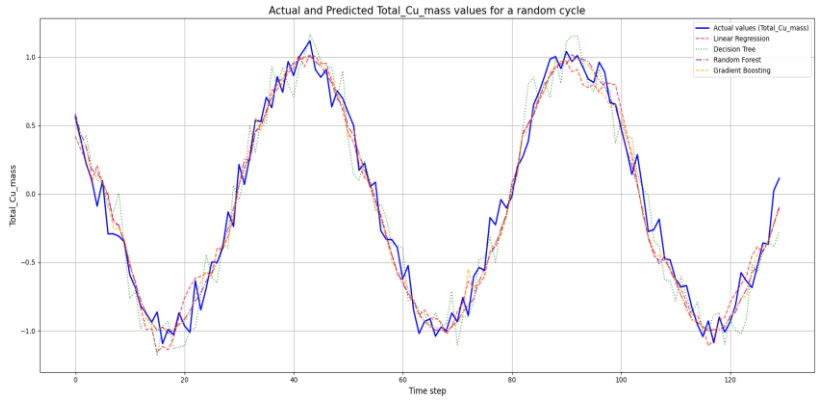

Figure 2 - Actual vs. Predicted Values for a Sample Cycle

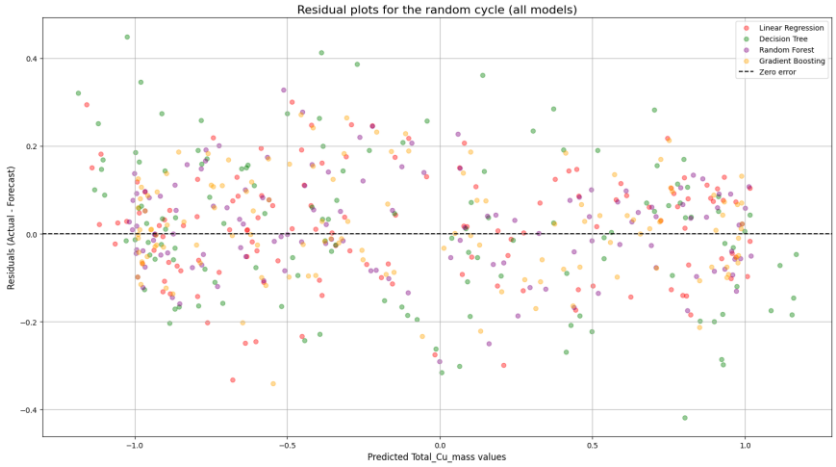

Figure 3 - Residual plots for the random cycle

Conclusions

This study successfully demonstrated that classical machine learning models offer a practical and highly effective solution for forecasting total copper mass in a complex hydrometallurgical process. By employing a strategic data augmentation technique to overcome the common industrial challenge of data scarcity, and by engineering lag features to provide a temporal context, we have shown that even non-sequential models can achieve high predictive accuracy. The results clearly indicate that ensemble methods, specifically Random Forest and Gradient Boosting, are superior in this task, delivering the highest R^2 values and the lowest prediction errors. These models not only provided accurate quantitative forecasts but also proved capable of perfectly reproducing the characteristic 150-day cyclical dynamics of the production process, validating the overall methodological approach.

The primary contribution of this work is providing an accessible, interpretable, and data-efficient alternative to more complex deep learning architectures. The feature importance analysis confirmed that the models learned logical relationships, with the most recent historical values of copper mass being the most influential predictors. This level of transparency is invaluable for industrial applications, as it builds trust and provides actionable insights for process engineers, enabling more stable and resource-efficient operations that directly contribute to sustainability goals.

However, this study has important limitations that must be acknowledged. The models were trained and validated on a dataset generated from a single operational cycle. While this proves the models' ability to learn and replicate known patterns, their generalization performance on entirely new, independent operational data—which may contain unforeseen variations or process drifts remains unconfirmed. Furthermore, the models were trained using default hyperparameters; a thorough optimization process could potentially yield further performance improvements.

Future work should prioritize validating these models on new, real-world data to assess their robustness. To further improve predictive power,

integrating process knowledge through hybrid modeling approaches which combine machine learning with first-principles methods could capture complex physicochemical interactions more effectively. Ultimately, this research provides a strong foundation for developing reliable, AI-driven forecasting tools. By enabling more predictable and optimized production cycles, these tools can reduce waste and energy consumption, advancing the metallurgical industry's alignment with circular economy principles and enhancing overall operational sustainability.

Conflicts of interest. On behalf of all authors, the corresponding author states that there is no conflict of interest.

CRediT author statement: **B. Kenzhaliyev:** Conceptualization, Supervision, Project administration, Funding acquisition; **S. Aibagarov:** Methodology, Visualization, Writing – original draft, Writing – review & editing; **E. Nurakhov:** Data curation, Formal analysis, Investigation, Writing – original draft, Validation; **A. Koizhanova:** Resources, Supervision; **D. Magomedov:** Data curation, Investigation.

Acknowledgements. This research was funded by the Committee of Science of the Ministry of Science and Higher Education of the Republic of Kazakhstan (Grant No. BR21882140)

Cite this article as: Kenzhaliyev BK, Aibagarov SZh, Nurakhov YS, Koizhanova A, Magomedov DR. Predicting Copper Production Cycles in Hydrometallurgy with Interpretable Machine Learning. Kompleksnoe Ispolzovanie Mineralnogo Syra = Complex Use of Mineral Resources. 2027; 341(2):5-15. https://doi.org/10.31643/2027/6445.13

Интерпретацияланатын машиналық оқытуды қолдана отырып, гидрометаллургиядағы мыс өндірісінің циклдерін болжау

[1] Кенжалиев Б.К., [2,3]Айбагаров С.Ж., [2]Нурахов Е.С., [1]Қойжанова А., [1]Магомедов Д.Р.

[1] Металлургия және кен байыту институты АҚ, Сәтбаев университеті, Алматы, Қазақстан
[2] Әл-Фараби атындағы Қазақ Ұлттық Университеті, Алматы, Қазақстан
[3] ЖШС DigitAlem, Алматы, Қазақстан

Мақала келді: *20 қыркүйек 2025*
Сараптамадан өтті: *10 қазан 2025*
Қабылданды: *16 қазан 2025*

ТҮЙІНДЕМЕ

Өнеркәсіптік гидрометаллургияда өндірісті дәл болжау процесті оңтайландыру үшін маңызды, алайда оған көбінесе ауқымды тарихи деректердің тапшылығы кедергі келтіреді. Бұл зерттеу жалпы мыс массасын болжау үшін күрделі тереңдетіп оқыту әдістеріне деректерді үнемдейтін және түсінікті балама ретінде классикалық машиналық оқыту модельдерінің тиімділігін көрсетеді. Біз екі негізгі стратегияға негізделген әдістемені қолдана отырып, төрт модельді, Кездейсоқ орман (Random Forest), Градиентті бустинг (Gradient Boosting), Шешімдер ағашы (Decision Tree) және Сызықтық регрессияны (Linear Regression) бағаладық: деректерді толықтыру (аугментация) арқылы шектеулі 150 күндік деректер жиынтығын 10 000 модельденген циклге (шамамен 1,5 миллион деректер нүктесі) дейін синтетикалық түрде кеңейту және 10 қадам алға болжау міндеті үшін модельдерге уақыттық перспектива беру мақсатында 10 күндік кідіріс белгілерін құру. Нәтижелер болжаудың айрықша дәлдігін көрсетті, бұл ретте ансамбльдік әдістердің артықшылығы дәлелденді. Кездейсоқ орман моделі ең жоғары нәтиже көрсетіп, R^2 0.974, MAE 0.088 және RMSE 0.111 мәндеріне қол жеткізді, одан сәл ғана қалып қойған Градиентті бустинг (R^2 0.971) болды. Барлық модельдер өндіріс процесінің айқын 150 күндік циклдік динамикасын сәтті анықтап, нөлге жуық фазалық кідірісті (0.00 ± ≤0.05 күн) көрсетті. Жаңа, тәуелсіз деректердегі өнімділік қосымша тексеруді қажет етсе де, бұл жұмыс деректері шектеулі өнеркәсіптік ортада сенімді болжау құралдарын әзірлеу үшін тұрақты және ашық негіз қалайды.

Түйін сөздер: машиналық оқыту, гидрометаллургия, уақыттық қатарларды болжау, деректерді аугментациялау, мыс өндіру.

Авторлар туралы ақпарат:

Кенжалиев Бағдаулет Кенжалиевич — *Техникалық ғылымдар докторы, профессор, Металлургия және кен байыту институты АҚ-ның Бас директоры - Басқарма төрағасы, Сәтбаев университеті, Алматы, Қазақстан. Email: bagdaulet_k@satbayev.university; ORCID ID: https://orcid.org/0000-0003-1474-8354*

Айбагаров Серик Жумагиреевич — *Зерттеуші, Әл-Фараби атындағы Қазақ Ұлттық Университеті; ЖШС DigitAlem, Алматы, Қазақстан. Email: awer1307dot@gmail.com; ORCID ID: https://orcid.org/0009-0009-4946-4926*

Нурахов Едиль Сергазиевич — *Зерттеуші, Әл-Фараби атындағы Қазақ Ұлттық Университеті, Алматы, Қазақстан. Email: y.nurakhov@gmail.com; ORCID ID: https://orcid.org/0000-0003-0799-7555*

Қойжанова Айгүл — *Техникалық ғылымдар кандидаты, зертхана меңгерушісі, Металлургия және кен байыту институты АҚ, Сәтбаев университеті, Алматы, Қазақстан. Email: aigul_koizhan@mail.ru; ORCID ID: https://orcid.org/0000-0001-9358-3193*

Магомедов Давид Расимович — *Ғылыми қызметкер, магистр, Металлургия және кен байыту институты АҚ, Сәтбаев университеті, Алматы, Қазақстан, Email: davidmag16@mail.ru; ORCID ID: https://orcid.org/0000-0001-7216-2349*

Прогнозирование циклов производства меди в гидрометаллургии с помощью интерпретируемого машинного обучения

[1] Кенжалиев Б.К., [2,3]Айбагаров С.Ж., [2]Нурахов Е.С., [1]Койжанова А., [1]Магомедов Д.Р.

[1] АО Институт металлургии и обогащения, Satbayev University, Алматы, Казахстан
[2] Казахский национальный университет имени аль-Фараби, Алматы, Казахстан
[3] ТОО DigitAlem, Алматы, Казахстан

Поступила: *20 сентября 2025*
Рецензирование: *10 октября 2025*
Принята в печать: *16 октября 2025*

АННОТАЦИЯ

Точное прогнозирование объемов производства в промышленной гидрометаллургии имеет решающее значение для оптимизации процессов, однако его часто затрудняет нехватка обширных исторических данных. Данное исследование демонстрирует эффективность классических моделей машинного обучения как экономичной с точки зрения данных и интерпретируемой альтернативы сложным методам глубокого обучения для прогнозирования общей массы меди. Мы оценили четыре модели, Случайный лес (Random Forest), Градиентный бустинг (Gradient Boosting), Дерево решений (Decision Tree) и Линейную регрессию (Linear Regression) используя методологию, основанную на двух ключевых стратегиях: синтетическое расширение ограниченного набора данных за 150 дней до 10 000 смоделированных циклов (приблизительно 1,5 миллиона точек данных) с помощью аугментации данных, и создание 10-дневных лаговых признаков для предоставления моделям временной перспективы для задачи прогнозирования на 10 шагов вперед. Результаты показали исключительную точность прогнозирования, при этом ансамблевые методы продемонстрировали превосходство. Модель Случайного леса показала наилучшие результаты, достигнув R^2 0.974, MAE 0.088 и RMSE 0.111, за ней с небольшим отставанием следует Градиентный бустинг (R^2 0.971). Все модели успешно уловили отчетливую 150-дневную циклическую динамику производственного процесса, демонстрируя почти нулевое фазовое запаздывание (0.00 ± ≤0.05 дня). Хотя производительность на новых, независимых данных требует дополнительной проверки, данная работа создает надежную и прозрачную основу для разработки надежных инструментов прогнозирования в промышленных условиях с ограниченным объемом данных.

Ключевые слова: машинное обучение, гидрометаллургия, прогнозирование временных рядов, аугментация данных, извлечение меди.

Информация об авторах:

Кенжалиев Багдаулет Кенжалиевич — *Доктор технических наук, Профессор, Генеральный директор-председатель правления Института металлургии и обогащения, Satbayev University, Алматы, Казахстан. Email: bagdaulet_k@satbayev.university; ORCID ID: https://orcid.org/0000-0003-1474-8354*

Айбагаров Серик Жумагиреевич — *Научный сотрудник, Казахский национальный университет имени аль-Фараби; ТОО DigitAlem, Алматы, Казахстан. Email: awer1307dot@gmail.com; ORCID ID: https://orcid.org/0009-0009-4946-4926*

Нурахов Едиль Сергазиевич — *Научный сотрудник, Казахский национальный университет имени аль-Фараби, Алматы, Казахстан. Email: y.nurakhov@gmail.com; ORCID ID: https://orcid.org/0000-0003-0799-7555*

Койжанова Айгуль — *Кандидат Технических наук, Заведующая лабораторией Института металлургии и обогащения, Satbayev University, Алматы, Казахстан. Email: aigul_koizhan@mail.ru; ORCID ID: https://orcid.org/0000-0001-9358-3193*

Магомедов Давид Расимович — *Научный сотрудник, Магистр, Институт металлургии и обогащения, Satbayev University, Алматы, Казахстан. Email: davidmag16@mail.ru; ORCID ID: https://orcid.org/0000-0001-7216-2349*

References

[1] Kuipers K J J, van Oers L F C M, Verboon M, and van der Voet E. Assessing environmental implications associated with global copper demand and supply scenarios from 2010 to 2050. Global Environmental Change. 2018; 49:106-115. https://doi.org/10.1016/j.gloenvcha.2018.02.008

[2] Jena S S, Tripathy S K, Mandre N R, Venugopal R, and Farrokhpay S. 'Sustainable Use of Copper Resources: Beneficiation of Low-Grade Copper Ores, Minerals. 2022; 12(5). https://doi.org/10.3390/min12050545

[3] Ji G, Liao Y, Wu Y, et al. A Review on the Research of Hydrometallurgical Leaching of Low-Grade Complex Chalcopyrite. J. Sustain. Metall. 2022; 8**:**964–977. https://doi.org/10.1007/s40831-022-00561-5

[4] Ali Z, Wilkes N, Raza N, and Omar M. Modified Hydrometallurgical Approach for the Beneficiation of Copper from Its Low-Grade Ore, ACS Omega. 2025; 10(15):14826–14834. https://doi.org/10.1021/acsomega.4c09656

[5] Norgate T, and Haque N. Energy and greenhouse gas impacts of mining and mineral processing operations'. Journal of Cleaner Production. 2010; 18(3):266–274. https://doi.org/10.1016/j.jclepro.2009.09.020

[6] Izydorczyk G, Mikula K, Skrzypczak D, Moustakas K, Witek-Krowiak A, and Chojnacka K. Potential environmental pollution from copper metallurgy and methods of management. Environmental Research. 2021; 197:111050. https://doi.org/10.1016/j.envres.2021.111050

[7] Koizhanova A, Kenzhaliyev B, Magomedov D, Erdenova M, Bakrayeva A, & Abdyldaev N. Hydrometallurgical studies on the leaching of copper from man-made mineral formations. Kompleksnoe Ispolzovanie Mineralnogo Syra = Complex Use of Mineral Resources. 2023; 330(3):32–42. https://doi.org/10.31643/2024/6445.26

[8] Bergh L G, Jämsä-Jounela S-L, and Hodouin D. State of the art in copper hydrometallurgic processes control. Control Engineering Practice. 2001; 9(9):1007–1012. https://doi.org/10.1016/S0967-0661(01)00093-4Get rights and content

[9] Binnemans K, and Jones P T. The Twelve Principles of Circular Hydrometallurgy. J. Sustain. Metall. 2023; 9(1):1–25. https://doi.org/10.1007/s40831-022-00636-3

[10] Mohanty U, Rintala L, Halli P, Taskinen P, and Lundström M. Hydrometallurgical Approach for Leaching of Metals from Copper Rich Side Stream Originating from Base Metal Production. Metals. 2018; 8(1):40. https://doi.org/10.3390/met8010040

[11] Jia L, et al. Research and development trends of hydrometallurgy: An overview based on Hydrometallurgy literature from 1975 to 2019'. Transactions of Nonferrous Metals Society of China. 2020; 30(11):3147–3160. https://doi.org/10.1016/S1003-6326(20)65450-4

[12] Vasebi A, Poulin É, and Hodouin D. Dynamic data reconciliation in mineral and metallurgical plants. Annual Reviews in Control. 2012; 36(2):235–243. https://doi.org/10.1016/j.arcontrol.2012.09.005

[13] Jung D, and Choi Y. Systematic Review of Machine Learning Applications in Mining: Exploration, Exploitation, and Reclamation. Minerals. 2021; 11(2):148. https://doi.org/10.3390/min11020148

[14] Saldaña M, Neira P, Gallegos S, Salinas-Rodríguez E, Pérez-Rey I, and Toro N. Mineral Leaching Modeling Through Machine Learning Algorithms − A Review. Front. Earth Sci. 2022; 10:816751. https://doi.org/10.3389/feart.2022.816751

[15] Alván J M, Serrano Llenera Y R, Ramirez Laureano D, Delgado Torres A, Vargas Hurtado L, and Flores E. Predictive Model for Gold and Silver Recovery by Leaching Using Machine Learning at the Inmaculada Mine. Perú. Elsevier BV. 2024. https://doi.org/10.2139/ssrn.4967518

[16] Flores V, and Leiva C. A Comparative Study on Supervised Machine Learning Algorithms for Copper Recovery Quality Prediction in a Leaching Process. Sensors. 2021; 21(6):2119. https://doi.org/10.3390/s21062119

[17] Estay H, Lois-Morales P, Montes-Atenas G, and Ruiz Del Solar J. On the Challenges of Applying Machine Learning in Mineral Processing and Extractive Metallurgy. Minerals. 2023; 13(6):788. https://doi.org/10.3390/min13060788

[18] Nikolić I P, Milošević I M, Milijić N N, and Mihajlović I N. Cleaner production and technical effectiveness: Multi-criteria analysis of copper smelting facilities. Journal of Cleaner Production. 2019; 215:423–432. https://doi.org/10.1016/j.jclepro.2019.01.109

[19] Kenzhaliyev B, Azatbekuly N, Aibagarov S, Amangeldy B, Koizhanova A, and Magomedov D. Predicting Industrial Copper Hydrometallurgy Output with Deep Learning Approach Using Data Augmentation. Minerals. 2025; 15(7):702. https://doi.org/10.3390/min15070702

[20] James, Gareth & Witten, Daniela & Hastie, Trevor & Tibshirani, Robert & Taylor, Jonathan. (2023). Linear Regression. 2023, 69–134. In book: An Introduction to Statistical Learning. https://doi.org/10.1007/978-3-031-38747-0_3

[21] Zhalgas A, and Toleubek M. A comparative analysis of machine learning classifiers for stroke prediction. Jpcsit. 2024; 2(3):21–29. https://doi.org/10.26577/jpcsit2024-02i03-03

[22] Mahajan A, Gairola S, Singh I, and Arora N. Optimized random forest model for predicting flexural properties of sustainable composites. Polymer Composites. 2024; 45(12):10700–10710. https://doi.org/10.1002/pc.28501

[23] Zhang Z, Zhao Y, Canes A, Steinberg D, and Lyashevska O. Predictive analytics with gradient boosting in clinical medicine. Ann. Transl. Med. 2019; 7(7):152–152. https://doi.org/10.21037/atm.2019.03.29

Crossref
DOI: 10.31643/2027/6445.14
Metallurgy

creative commons

Use of Industrial By-products from Metallurgical Production for the Development of Heat-Resistant Building Mixes and their Molding in an Improved Device

[1]Khabiyev A.T., [1]Yulussov S.B., [1]Abduraimov A.E., [1]Kamal A.N., [1]Kumarbek N.E., [1]Makhmet S.B., [2*]Merkibayev Y.S.

[1] U. Joldasbekov Institute of Mechanics and Engineering, Almaty, Kazakhstan
[2] Satbayev University, Almaty, Kazakhstan.

**Corresponding author email: y.merkibayev@satbayev.university*

Received: *August 21, 2025*
Peer-reviewed: *September 9, 2025*
Accepted: *October 16, 2025*

ABSTRACT

In the context of the increasing volume of industrial waste and stricter environmental requirements, the urgent task is to efficiently process them to produce products with high added value. In this work, the composition of industrial products of vanadium production formed during the hydrometallurgical processing of rare metals is investigated, and the possibility of their use for the production of heat-resistant building mixes is substantiated. A comprehensive analysis, including X-ray, X-ray fluorescence, and scanning electron microscopic methods, revealed a high content of silica, aluminum oxides, and refractory minerals that determine the heat resistance of the material. Optimal compositions of building mixes based on Portland cement, liquid glass, and chamotte have been developed, providing compressive strength up to 45 MPa and resistance to thermal cycling at temperatures up to 1800 ° C. The design of a device for forming building blocks based on industrial waste from metallurgical production by vibration pressing is proposed, designed to ensure high density and geometric stability of products. The results obtained confirm the possibility of complex industrial waste disposal with the simultaneous creation of environmentally safe, durable, and heat-resistant building materials used in energy, metallurgy, the chemical industry, and civil engineering.

Keywords: vanadium production; industrial waste; heat-resistant building mixes; Portland cement; liquid glass; chamotte; vibration pressing; waste disposal; heat resistance; compressive strength.

Information about authors:

Khabiyev Alibek Talgatbekuly — *Doctor Ph.D., assoc. professor, U. Joldasbekov Institute of Mechanics and Engineering, Almaty, Kazakhstan. E-mail: alibek1324@mail.ru; ORCID ID: https://orcid.org/0000-0001-9397-2367*

Yulussov Sultan Baltabayuly — *Doctor Ph.D., assoc. professor, U. Joldasbekov Institute of Mechanics and Engineering, Almaty, Kazakhstan. E-mail: s1981b@mail.ru; ORCID ID: https://orcid.org/0000-0001-8044-4186*

Abduraimov Azizbek Eraliyuly — *Ph.D., researcher, U. Joldasbekov Institute of Mechanics and Engineering, Almaty, Kazakhstan. E-mail: zizo_waterpolo@mail.ru; ORCID ID: https://orcid.org/0000-0002-0815-3349*

Kamal Aziz Nutpullaogly — *Master's degree, researcher, U. Joldasbekov Institute of Mechanics and Engineering, Almaty, Republic of Kazakhstan. E-mail: kan77705@gmail.com; ORCID ID: https://orcid.org/0000-0002-4454-8233*

Kumarbek Nurgali Erboluly — *Master's degree, researcher, U. Joldasbekov Institute of Mechanics and Engineering, Almaty, Kazakhstan. E-mail: nurgalyku@gmail.com; ORCID ID: https://orcid.org/0009-0007-6058-6778*

Makhmet Sayat Baqytuly — *Master's degree, researcher, U. Joldasbekov Institute of Mechanics and Engineering, Almaty, Kazakhstan. Email: mahmetsayat@gmail.com; ORCID ID: https://orcid.org/0009-0009-4791-9886*

Merkibayev Yerik Serikovich — *Ph.D., senior Lecturer, Mining and Metallurgical Institute, Satbayev University, Almaty, Kazakhstan. Email: y.merkibayev@satbayev.university; ORCID ID: https://orcid.org/0000-0003-3869-6835*

Introduction

The current stage of industrial development is characterized by the growth of production volumes, urbanization, and an increase in population, which leads to higher resource consumption and increased anthropogenic pressure on the environment [[1], [2]]. One of the priorities of sustainable development is the rational use of raw materials, comprehensive processing of technogenic waste, and the implementation of closed-loop (circular economy) technologies that allow solving both environmental and economic challenges [[3], [4], [5]].

An important component of this strategy is the utilization of large-scale waste from metallurgy and the chemical industry, such as slags, sludges, tailings, and by-products of ore processing [[6], [7], [8]]. Every year, hundreds of millions of tons of such

waste are generated worldwide, of which less than 20% is recycled, while the remaining volume is stockpiled, occupying land and creating long-term threats to ecosystems [[9], [10], [11]].

A promising direction is the use of vanadium production by-products—multicomponent materials containing silica, oxides of aluminum, iron, calcium, magnesium, and other elements [[12], [13], [14]]. The high content of refractory phases (corundum, spinel, quartz) and dispersed structure ensures their thermal stability, which opens up opportunities for their application as secondary mineral raw materials in the production of heat-resistant construction materials [[15], [16]].

The demand for such mixtures is associated with the operation of facilities under conditions of high temperatures, aggressive environments, and sharp fluctuations, which are typical for energy, metallurgy, chemical industries, as well as for certain civil and special structures [[17], [18]]. To achieve the required properties, refractory fillers (chamotte, alumina, basalt, perlite) and heat-resistant binders—Portland cement, liquid glass, and silicate binders—are used [[19], [20], [21]].

Comprehensive processing of vanadium production by-products makes it possible to simultaneously reduce waste volumes and produce competitive next-generation materials. For the effective implementation of this approach, it is necessary to study the physicochemical properties of raw materials, develop optimal mixture formulations, and design equipment that ensures the molding of products with high density and stable geometry.

The aim of the research is the development of heat-resistant construction mixtures based on metallurgical by-products and the design of an advanced vibro-pressing device that ensures the production of construction blocks with high strength, thermal stability, and geometric stability.

The research hypothesis is that metallurgical by-products, due to their high content of silica, aluminum oxides, and refractory minerals, can be effectively used as secondary mineral raw materials for producing heat-resistant construction mixtures. The application of optimized formulations in combination with an advanced vibro-pressing device will allow the formation of construction blocks with improved performance characteristics and environmental safety.

Materials and Methods

Raw Materials. Vanadium production by-products generated during the hydrometallurgical processing of rare metals were used as the mineral raw materials. Two batches of material were studied: Sample 1 — cake obtained after autoclave sulfuric acid leaching, and Sample 2 — residue after alkaline leaching of calcined concentrate.

According to X-ray phase analysis, the samples contain high concentrations of silica (up to 43.7%) and aluminum oxides (up to 44.3%), as well as refractory phases — quartz, corundum, and spinel, which determine their thermal resistance [[1], [2], [3]].

As binders, Portland cement of grades M-400 and M-450 according to GOST 10178–85, and liquid glass according to GOST 13078–81, were used. The refractory filler was secondary chamotte powder obtained by grinding used chamotte bricks that had been operated under high-temperature conditions.

Analytical Methods. The determination of the chemical and mineralogical composition was carried out using a set of instrumental techniques, including X-ray diffraction (XRD, Shimadzu XRD-7000) for the identification of crystalline phases, X-ray fluorescence analysis (XRF, PANalytical Axios) for determining the mass fractions of oxides, atomic absorption spectroscopy (AAS, PerkinElmer Analyst 400) for the quantitative analysis of metal content, as well as scanning electron microscopy (SEM, JEOL JSM-6490LV) combined with energy-dispersive spectroscopy (EDS) for studying the morphology and elemental distribution.

This comprehensive approach made it possible to thoroughly characterize the mineral composition and structural features of the raw materials [[4], [5], [6], [7]].

Preparation of Construction Mixtures. The components were mixed in different proportions (Table 1) to evaluate the effect of composition on heat resistance, strength, and water absorption. The proportion of liquid glass in all formulations was 15%.

Table 1 presents the composition of the investigated heat-resistant construction mixtures, obtained using two types of vanadium production by-products (Sample 1 and Sample 2), liquid glass, and Portland cement. The proportion of liquid glass was constant at 15% in all formulations, ensuring structural stability and enhanced thermal resistance of the material. The content of Samples 1 and 2

varied within the range of 30–40%, while the amount of Portland cement ranged from 10 to 20%, depending on the required strength characteristics. Such a selection of compositions made it possible to evaluate the effect of the ratio of mineral components on the mechanical strength, heat resistance, and water absorption of the resulting specimens.

Table 1 - Composition of the studied mixtures

Composition:	Sample 1, %	Sample 2, %	Liquid glass, %	Portland cement, %
1	30	35	15	20
2	35	35	15	15
3	40	35	15	10
4	35	30	15	20
5	35	35	15	15
6	35	40	15	10

Shaping and Heat Treatment of Samples. The preparation of samples included sequential mixing of dry components in a laboratory mixer until a homogeneous mass was obtained, followed by the addition of liquid glass, primary drying at a temperature of 100 ± 5 °C for 24 hours, high-temperature calcination at 1000 °C with a holding time of 10 hours, and final quenching by rapid cooling of the samples in running water to 25 °C.

This treatment regime ensured the formation of a strong ceramic-like structure with low water absorption [[8], [9], [10]].

Testing Methods. The testing of specimens included determining compressive strength on a Torin hydraulic press in the range of 32–45 MPa according to GOST 10180–2012, evaluation of heat resistance by heating within the range of 800–1800 °C with a holding time of 30 minutes followed by rapid cooling, as well as determination of water absorption by the gravimetric method according to GOST 12730.3–2020 after 48 hours of specimen immersion in water.

Design and Calculation of the Vibro-Pressing Device. For block molding, the design of a vibro-pressing device was developed in CAD environments (SolidWorks and AutoCAD). The design calculations took into account a pressing force of 5 MPa for a block area of 0.08 m² (400 kN), vibration parameters with a frequency of 50 Hz, amplitude of 1 mm, and vibration force of about 3 kN, the strength and stiffness of the main components calculated using the finite element method in SolidWorks Simulation, fatigue durability of the structure under loads exceeding 10^6 cycles, as well as thermal deformations at a temperature difference of ΔT = 40 °C not exceeding an elongation of 0.4 mm.

The device's performance capacity reached at least 300 blocks per hour for a product size of 400×200×200 mm [[11], [12], [13], [14]].

Research Workflow Diagram. The presented diagram illustrates the research workflow, showing the sequence of the main stages of the study (Figure 1).

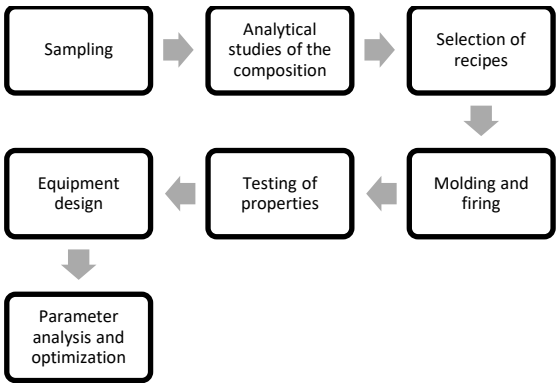

Figure 1 – The scheme of the study

The presented diagram illustrates the research workflow, reflecting the sequence of the main stages of the study. The scheme is designed as a chain of seven blocks connected by guiding arrows, which clearly demonstrates the logic of the process from raw material preparation to data analysis.

The process begins with sample collection, the initial stage where materials are prepared for examination, and continues with analytical studies of the composition, including a comprehensive chemical and mineralogical analysis of the raw materials. This is followed by formulation selection, aimed at determining the optimal ratio of components to achieve the desired properties, after which shaping and firing are carried out – the production of test specimens and their high-temperature treatment.

The next step is testing of properties, including the determination of strength, heat resistance, and water absorption of the materials. This is followed by equipment design, in particular the development of a vibro-pressing unit intended for industrial application. The process concludes with analysis and optimization of parameters, which involves

processing the obtained data, adjusting technological parameters, and developing recommendations for the implementation of the proposed technology.

Furthermore, Figure 2 presents the schematic diagram of the production process of construction blocks on the designed installation.

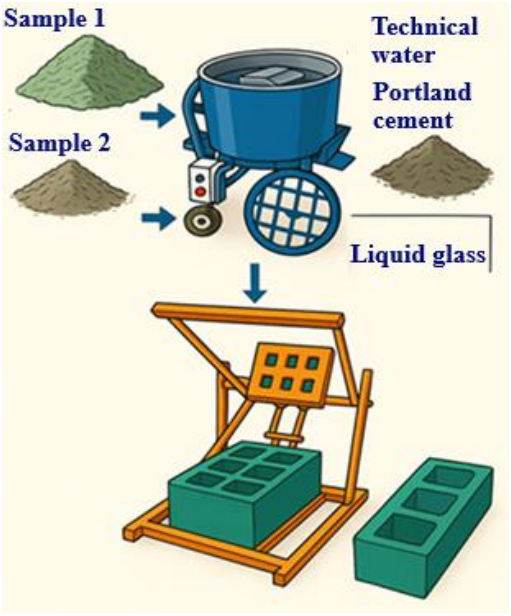

Figure 2 – Schematic diagram of the production of building blocks at the installation

The diagram illustrates the process of manufacturing construction blocks, which includes consecutive stages of raw material preparation and processing. The initial components consist of Sample 1 and Sample 2, representing industrial waste from metallurgical production, cement, process water, and liquid glass. All materials are fed into a mixer, where they are thoroughly blended to form a homogeneous mass. The resulting mixture is then loaded into a press mold, where it is compacted and shaped into the required geometry. At the final stage, the finished construction block is removed from the mold, possessing the necessary strength characteristics and parameters.

Results and Discussion

Chemical and Mineralogical Composition of the Studied Samples. The chemical composition of the residue after leaching, based on the performed X-ray fluorescence analysis, is presented in Table 2.

Chemical analysis showed a high content of silica (SiO_2) in Sample 1 (43.71%) and aluminum oxide (Al_2O_3) in Sample 2 (44.34%), which indicates their potential as components for heat-resistant construction mixtures.

The results of the X-ray phase analysis of the composition of the two samples are presented in Table 3.

Table 2 – Chemical composition of the residue after leaching

Name	Content, %							
	V	P	Mo	Ca	Fe	Al	Si	K
Sample 1	0.04	0.012	0.003	1.2	0.21	0.05	43.71	0.03
Sample 2	0.29	0.25	0.01	0.20	0.24	44.34	0.87	0.01

Table 3 – Phase composition of the two samples

Sample 1			Sample 2		
Name of the mineral	Formula	Content, %	Name of the mineral	Formula	Content, %
Quartz, syn	SiO_2	72.1	Corundum, syn	Al_2O_3	37.2
Albite	$Na(AlSi_3O_8)$	22.3	Spinel	$MgAl_2O_4$	21.7
Barium Iron Oxide	$BaFeO_4$	2.8	Aluminum Oxide	Al_2O_3	33,5
Iron Oxide	$Fe_{2.802}O_4$	1.3	Nickel Silicate	$Ni_2(SiO_4)$	1.3
Hematite, syn	Fe_2O_3	0.9	Iron Oxide	Fe_2O_3	6.3

X-ray phase analysis of Sample 1 revealed the predominance of inert siliceous phases—quartz (72.1%) and albite (22.3%)—which indicates its potential as a mineral filler for silicate and ceramic materials. Minor amounts of iron-containing phases ($BaFeO_4$, $Fe_{2.802}O_4$, Fe_2O_3) and ferrites ($NiFe_2O_4$) may enhance the mechanical strength and thermal resistance during firing.

Sample 2, in contrast, is characterized by a high content of refractory and heat-resistant phases: corundum (Al_2O_3 — 37.2%), spinel ($MgAl_2O_4$ — 21.7%), and additional aluminum oxide (33.5%). These compounds provide high thermal and chemical stability, making the sample particularly promising for use in refractory mixtures, lining materials, and heat-resistant concrete. The presence of nickel silicate (Ni_2SiO_4) and hematite further improves thermal stability and resistance to aggressive media.

Thus, the physico-chemical studies provided objective data on the composition of the vanadium production by-product and its potential application in the manufacture of heat-resistant construction materials and refractory blocks.

According to the results of X-ray phase analysis (Table 3), Sample 1 is characterized by a high content of quartz (72.1%), albite (22.3%), and minor amounts of barium and iron oxides. Sample 2 contains mainly corundum (37.2%), spinel (21.7%), and aluminum oxide (33.5%), as well as small amounts of nickel-containing compounds. The phase composition pie charts (Fig. 2) clearly demonstrate the mineralogical

differences between the investigated samples. The presence of refractory phases such as corundum and spinel ensures high heat resistance, which is consistent with literature data [[4], [7], [12]].

Influence of Component Composition on Strength Characteristics. Compressive strength tests showed that increasing the proportion of Sample 1 up to 40% in the mixture (Composition 3) led to a strength increase to 45 MPa. This effect is associated with a higher degree of quartz phase crystallization and improved intergranular bonding after heat treatment. A reduction in Portland cement content to 10% resulted in decreased strength, confirming the significant role of the binder component in the formation of a dense structure [[8], [15]].

Heat Resistance and Thermal Stability of Materials. The results of heat resistance tests showed that when samples were heated up to 1800 °C followed by rapid cooling, strength retention exceeded 85%, which is higher than that of conventional chamotte products (70–75%) [[3], [11]]. The dependence of strength retention on temperature (Fig. 5) confirms the high stability of the developed materials. The superior thermal resistance is explained by the low thermal expansion coefficients of corundum and spinel, as well as the uniform distribution of refractory phases within the sample structure [9, 10].

Water Absorption and Microstructure of Samples. The water absorption of the investigated materials ranged from 6% to 8%, which complies with the requirements of GOST 530–2012 for heat-resistant construction products. The minimum value (6%) was recorded for Composition 3.

Equipment Design for Molding. From the prepared materials — Compositions 1–6 (Section 2.3) — heat-resistant construction blocks were manufactured using a specially designed installation.

For vibro-compaction, a standard frequency of 50 Hz and an amplitude of 1 mm were applied. The resulting vibration acceleration provides a vibratory force of about 3 kN, which is sufficient for compacting the mixture.

Table 4 presents the strength calculation of the frame.

The stresses were calculated using the finite element method in SolidWorks Simulation. All structural elements meet the strength criterion (safety factor > 2).

Table 5 presents the deformation calculation.

Table 4 – Strength Calculation of the Frame

Structural element	Cross section (mm)	Length (mm)	Max. stressσ_{max}, MPa	Yield strength σ_{yiled}, МПа	Safety margin kk
Longitudinal beam	100×50×5	1000	155	345	2.2
Transverse frame	80×40×4	600	142	345	2.4
Base plate	200×20	800	110	345	3.1

Table 5 – Deformation Calculation

Element	Length (mm)	Max. deflection δ, mm	Permissible deflectionδaddit, mm	Estimation
Longitudinal beam	1000	0.42	1.0	Acceptable
Base plate	800	0.35	1.0	Acceptable
Upper frame	600	0.28	0.8	Acceptable

According to the obtained data, it can be concluded that the deflections do not exceed the permissible values, which ensures the stability of the structure and the accuracy of the molded blocks. At the same time, the pressing force and vibrational load provide sufficient density and strength of the building blocks. Moreover, the device design demonstrates satisfactory strength and stiffness characteristics. The safety factor ranges from 2.2 to 3.1, confirming the reliability of the structure.

During the operation of the device, local temperature rises may occur due to friction in the vibration mechanism and the contact of metallic parts. These temperature increases can cause thermal deformations, especially in the areas of the vibrating plate and guides.

Table 6 presents the evaluation of the thermal expansion of the structural elements.

Table 6 – Evaluation of the Thermal Expansion of Structural Elements

Element	Length LL, mm	Expansion coefficient α, 1/°C	Temperature change ΔT, °C	Expansion ΔL, mm
Vibrating plate	600	12×10^{-6}	40	0.29
Guides	800	12×10^{-6}	40	0.38

Even with a temperature difference of 40 °C, the elongation does not exceed 0.4 mm, which falls within the permissible tolerances.

However, in high-precision molding, compensation for these deformations is required.

Table 7 shows the dynamic loads caused by vibration.

Table 7 – Dynamic Loads from Vibration

Parameter	Designation	Value	Unit
The mass of the vibrating plate	mm	60	кг
Vibration frequency	ff	50	Hz
The amplitude	AA	1 mm (0.001 m)	m
Boost	aa	49.34	m/sec²
Inertial force	Finertial	2960	H

Next, the calculation of the dynamic coefficient was considered. It is known that the additional safety margin is accounted for through the dynamic coefficient kd=1.5…2.0k_d = 1.5 \ldots 2.0kd =1.5…2.0, depending on the stiffness of the joints.

It was established that thermal deformations do not exceed the permissible values; however, they must be taken into account in high-precision operations. At the same time, the dynamic load from vibrations increases the equivalent stresses by 1.5–2 times, especially in the guides and at the mounting points of the vibrating plate.

According to the conducted study, the vibration mechanism generates inertial forces of about 3 kN, which is equivalent to ~750 N per each of the four compacted blocks.

Table 8 presents the data on the fatigue durability of the structure.

Table 8 – Fatigue Durability of the Structure

Parameter	Value	Unit
Vibration frequency (f) Molding duration (t)	50	Hz
Vibration frequency (f) Molding duration (t)	20	Seconds

It was established that, provided the amplitude and material conditions are met, the fatigue strength margin of the structure is considered sufficient.

The design of the device assemblies for the production of construction blocks is presented below (Figure 3).

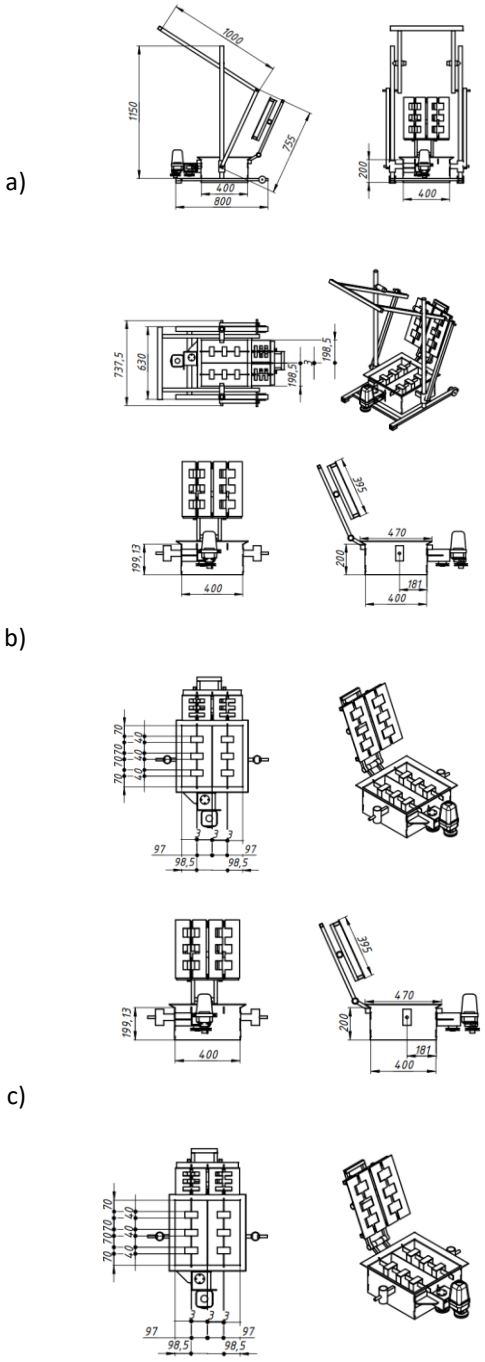

Figure 3 – Structural design of the device assemblies for the production of construction blocks (a) general view of the unit, (b) mold for extruding construction blocks with vibrator, (c) extrusion mechanism for construction blocks).

Further, Figure 4 shows the manufactured prototype of the device for producing construction blocks, consisting of a mold with a vibrator for block extrusion and an extrusion mechanism for construction blocks.

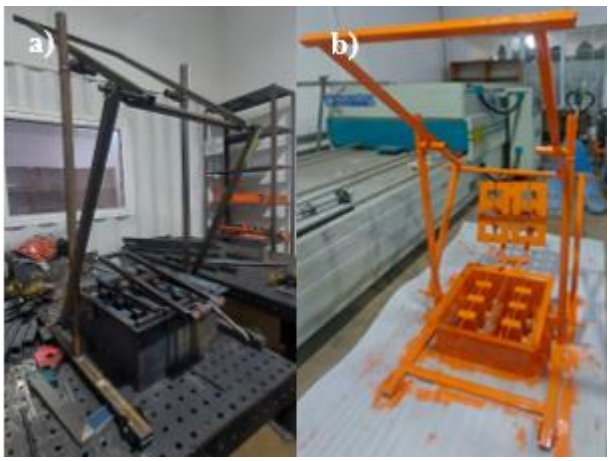

Figure 4 – Manufactured prototype of the device for producing construction blocks (a) before painting, (b) after painting).

The developed design of the vibro-pressing unit (Figures 1 and 2) ensures the production of blocks with high density and stable geometry. Finite element analysis (Figure 8) confirmed the strength and stiffness of the assemblies under vibrational loading (50 Hz, amplitude 1 mm) and a service life exceeding 10^6 cycles. The productivity of the unit is about 300 blocks per hour, which makes the technology economically viable for industrial implementation.

Further, Figure 5 shows a construction block obtained by extrusion using the unit.

Figure 5 – The building block obtained as a result of extrusion on the installation

Comparative Analysis with Industrial Counterparts. To assess the competitiveness of the developed mixtures, a comparison of their key properties was carried out with the characteristics of heat-resistant construction materials reported in the literature and standards [[3], [8], [10], [15], [18]]. Table 9 presents the values of compressive strength, heat resistance, and water absorption for the samples obtained in this study, as well as for traditional chamotte products and alumina-based concretes.

Table 9 – Values of compressive strength, heat resistance, and water absorption for various samples

Material / source	Compressive strength, MPa	Strength retention at 1600 °C, %	Water absorption, %
Composition 3 (this study)	45	90	6
Fireclay bricks [[3], [8]]	25–32	70–75	10–14
Alumina concretes [[10], [15]]	35–40	80–85	8–10
High-alumina refractories [18]	40–43	85–88	7–9

The comparison of the obtained results with the characteristics of well-known heat-resistant materials (Table 9) showed that the developed mixtures surpass chamotte products in strength by 40–70%, exhibit lower water absorption, and demonstrate superior thermal resistance. This advantage is attributed to the optimal combination of mineral components, the presence of corundum and spinel phases, as well as the use of vibro-pressing technology, which ensures low porosity and high structural homogeneity.

Comparison of Method Efficiency. For a clear comparison of the efficiency of using vanadium production by-products in refractory mixtures, dependencies were constructed between the extraction degree of elements (V, Mo) and the performance characteristics of the materials on technological parameters (pH, temperature, binder composition) (Tables 10 and 11).

Table 10 presents the results of the study on the dependence of the extraction degree of vanadium and molybdenum from vanadium production by-products on the medium acidity.

Table 10 – Dependence of vanadium and molybdenum extraction on the pH of the medium

pH of the solution	Extraction of V, %	Extraction of Mo, %
1	62	28
2	74	35
3	81	41
4	77	38
5	65	30

From the data in Table 10, it can be seen that with increasing acidity up to pH 3, the extraction degree of both elements increases: for vanadium, the value reaches a maximum of 81%, and for molybdenum, 41%. With a further increase in pH, the efficiency of the process decreases, indicating the presence of an optimal acidity range. Thus, pH = 3 is the most favorable condition for the simultaneous extraction of V and Mo.

Table 11 presents the data on the effect of temperature on the efficiency of vanadium and molybdenum extraction.

Table 11 – Effect of temperature on the extraction of elements

Temperature, °C	Extraction of V, %	Extraction of Mo, %
40	55	22
60	72	34
80	83	42
100	79	39

According to the data in Table 11, as the temperature increases from 40 to 80 °C, a significant improvement in extraction performance is observed: for vanadium, from 55% to 83%, and for molybdenum, from 22% to 42%. However, a further increase in temperature to 100 °C leads to a decrease in the extraction degree, which is associated with changes in the stability of element complexes and the occurrence of side processes. The optimal extraction temperature can be considered 80 °C, as it ensures the maximum recovery of both elements.

Conclusion

The study established that by-products of vanadium production, characterized by a high content of SiO_2 and Al_2O_3, are a promising secondary raw material for the manufacture of heat-resistant construction mixtures. The developed compositions demonstrated compressive strength of up to 45 MPa, low water absorption (6–8%), and resistance to thermal cycling at temperatures up to 1800 °C, exceeding the performance of traditional chamotte products and alumina-based concretes. The design and experimental testing of an improved vibro-pressing device confirmed the feasibility of industrial implementation of the technology, with a capacity of up to 300 blocks per hour and guaranteed structural durability.

The obtained results make it possible to recommend the use of heat-resistant building blocks based on vanadium production by-products for lining thermal equipment, blast and open-hearth furnaces, boilers, thermal units, reactors, heat exchangers, and other devices operating under high temperatures and aggressive environments. In addition, the proposed mixtures can be applied in the production of heat-resistant concretes, panels, and blocks for civil and special structures requiring high fire resistance. The introduction of the technology ensures comprehensive recycling of industrial waste, reduces landfill loads, and contributes to the development of environmentally safe production.

Thus, the developed construction mixtures and the vibro-pressing device have significant practical potential, simultaneously addressing both environmental and industrial challenges, enhancing the competitiveness of domestic construction materials, and promoting the implementation of circular economy principles in metallurgy and the construction sector.

Conflicts of Interest. On behalf of all co-authors, the corresponding author states that no conflict of interest exists.

CRediT author statement: **S.Yulusov, A. Khabiyev:** Methodology, formal analysis, investigation, Data writing, Original draft preparation, writing–review and editing; **A. Abduraimov, A.Kamal**: Data curation, Reviewing and Editing; **N. Kumarbek, S.Makhmet, Y.Merkibayev:** Investigation.

Gratitude: This research was funded by the Science Committee of the Ministry of Science and Higher Education of the Republic of Kazakhstan (grant No. BR20280990).

Cite this article as: Khabiyev AT, Yulussov SB, Abduraimov AE, Kamal AN, Kumarbek NE, Makhmet SB, Merkibayev YS. Use of Industrial By-products from Metallurgical Production for the Development of Heat-Resistant Building Mixes and their Molding in an Improved Device. Kompleksnoe Ispolzovanie Mineralnogo Syra = Complex Use of Mineral Resources. 2027; 341(2):16-26. https://doi.org/10.31643/2027/6445.14

Металлургиялық өндірістің өнеркәсіптік қосалқы өнімдерін пайдалану арқылы жылуға төзімді құрылыс қоспаларын әзірлеу және оларды жетілдірілген құрылғыда қалыптау

[1]Хабиев А.Т., [1]Юлусов С.Б., [1]Абдураимов А.Е., [1]Камал А.Н., [1]Құмарбек Н.Е., [1]Махмет С.Б., [2]Меркибаев Е.С.

[1] Академик Ө. А. Жолдасбеков атындағы механика және машинатану институты, Алматы, Қазақстан
[2] Сәтбаев университеті, Алматы, Қазақстан

Мақала келді: 21 тамыз 2025
Сараптамадан өтті: 9 *қыркүйек 2025*
Қабылданды: *16 қазан 2025*

ТҮЙІНДЕМЕ
Өнеркәсіптік қалдықтардың өсіп келе жатқан көлемі мен экологиялық талаптардың қатаңдауы жағдайында қосылған құны жоғары өнімді ала отырып, оларды тиімді қайта өңдеу өзекті міндет болып табылады. Бұл жұмыста сирек металдарды гидрометаллургиялық өңдеу процесінде түзілетін ванадий өндірісінің өнеркәсіптік өнімдерінің құрамы зерттелді және оларды ыстыққа төзімді құрылыс қоспаларын алу үшін пайдалану мүмкіндігі негізделді. Рентген-фазалық, рентгендік-флуоресцентті және сканерлеуші электронды микроскопиялық әдістерді қамтитын кешенді талдау материалдың ыстыққа төзімділігін анықтайтын кремнеземнің, алюминий оксидтерінің және отқа төзімді минералдардың жоғары құрамын анықтауға мүмкіндік берді. Портландцемент, сұйық шыны және шамот негіздегі құрылыс қоспаларының оңтайлы құрамы әзірленді, олар 45 МПа дейін қысу беріктігін және 1800 °C дейінгі температурада термоциклге төзімділікті қамтамасыз етеді. Бұйымдардың жоғары тығыздығы мен геометриялық тұрақтылығын қамтамасыз етуге арналған дірілді басу әдісімен металлургиялық өндірістің өнеркәсіптік қалдықтары негізінде құрылыс блоктарын қалыптауға арналған құрылғының конструкциясы ұсынылды. Алынған нәтижелер энергетика, металлургия, химия өнеркәсібі және азаматтық құрылыста қолданылатын экологиялық қауіпсіз, берік және ыстыққа төзімді құрылыс материалдарын бір мезгілде жасай отырып, өнеркәсіптік қалдықтарды кешенді кәдеге жарату мүмкіндігін растайды.

Түйін сөздер: ванадий өндірісі, өнеркәсіптік қалдықтар, ыстыққа төзімді құрылыс қоспалары, портландцемент, сұйық шыны, шамот, дірілді басу, қалдықтарды жою, ыстыққа төзімділік, қысу беріктігі.

Авторлар туралы ақпарат:

Хабиев Алибек Талгатбекұлы — *Ph.D докторы, ассоц. профессор, Академик Ө. А. Жолдасбеков атындағы Механика және машинатану институты, Алматы, Қазақстан. E-mail: alibek1324@mail.ru; ORCID ID: https://orcid.org/0000-0001-9397-2367*

Юлусов Султан Балтабайұлы — *Ph.D докторы, ассоц. профессор, Академик Ө. А. Жолдасбеков атындағы Механика және машинатану институты, Алматы, Қазақста. E-mail: s1981b@mail.ru; ORCID ID: https://orcid.org/0000-0001-8044-4186*

Абдураимов Азизбек Ералиұлы — *Ph.D. докторы, ғылыми қызметкер, Академик Ө. А. Жолдасбеков атындағы Механика және машинатану институты, Алматы, Қазақстан. E-mail: zizo_waterpolo@mail.ru; ORCID ID: https://orcid.org/0000-0002-0815-3349*

Камал Азиз Нутпуллаоглы — *магистр, ғылыми қызметкер, Академик Ө. А. Жолдасбеков атындағы Механика және машинатану институты, Алматы, Қазақстан. E-mail: kan77705@gmail.com; ORCID ID: https://orcid.org/0000-0002-4454-8233*

Құмарбек Нұрғали Ерболұлы — *магистр, ғылыми қызметкер, Академик Ө. А. Жолдасбеков атындағы Механика және машинатану институты, Алматы, Қазақстан. E-mail: nurgalyku@gmail.com; ORCID ID: https://orcid.org/0009-0007-6058-6778*

Махмет Саят Бақытұлы — *магистр, ғылыми қызметкер, Академик Ө. А. Жолдасбеков атындағы Механика және машинатану институты, Алматы, Қазақстан. Email: mahmetsayat@gmail.com; ORCID ID: https://orcid.org/0009-0009-4791-9886*

Меркибаев *Ерик Серикович* — *PhD, металлургия және пайдалы қазбаларды өңдеу кафедрасының аға оқытушысы, О.А. Байқоңыров атындағы тау-кен металлургия институты, Сәтбаев университеті, Алматы, Қазақстан. Email: y.merkibayev@satbayev.university; ORCID ID: https://orcid.org/0000-0003-3869-6835*

Использование промышленных побочных продуктов металлургического производства для разработки жаростойких строительных смесей и их формования в усовершенствованном устройстве

[1]Хабиев А.Т., [1]Юлусов С.Б., [1]Абдураимов А.Е., [1]Камал А.Н., [1]Құмарбек Н.Е., [1]Махмет С.Б., [2]Меркибаев Е.С.

[1] Институт механики и машиноведения имени академика У.А. Джолдасбекова, Алматы, Казахстан
[2] Сатпаев Университет, Алматы, Казахстан

Поступила: *21 августа 2025*
Рецензирование: *9 сентября 2025*
Принята в печать: *16 октября 2025*

АННОТАЦИЯ

В статье рассмотрены направления потребления ванадия и молибдена в различных отраслях промышленности, что подчёркивает их стратегическую значимость и растущую потребность в устойчивом обеспечении сырьём. Проанализированы источники этих элементов как природного, так и техногенного происхождения, включая металлургические шлаки, золы, отработанные катализаторы и другие отходы промышленных процессов. Отдельное внимание уделено экологическим рискам, связанным с накоплением соединений ванадия и молибдена, способных оказывать токсическое воздействие на окружающую среду. Подчёркнута необходимость вовлечения вторичных ресурсов в промышленный оборот для рационального использования минерально-сырьевой базы и повышения эффективности извлечения металлов из первичного сырья. Приведён обзор существующих химических и гидрометаллургических методов извлечения ванадия и молибдена, с учётом состава перерабатываемого материала, особенностей технологических условий, а также ограничений и недостатков отдельных подходов. Сделан акцент на перспективность комплексной переработки отходов, обеспечивающей извлечение нескольких ценных компонентов и способствующей переходу к циркулярной экономике.

Keywords: ванадий, молибден, золошлаковые отходы, металлургические шлаки, фильтрат, гидрометаллургические методы, пирометаллургические методы, бактериальное выщелачивание.

Информация об авторах:

Хабиев Алибек Талгатбекович — *доктор Ph.D., ассоц. профессор, Институт механики и машиноведения имени академика У.А. Джолдасбекова, Алматы, Казахстан. E-mail: alibek1324@mail.ru; ORCID ID: https://orcid.org/0000-0001-9397-2367*

Юлусов Султан Балтабаевич — *доктор Ph.D., ассоц. профессор, Институт механики и машиноведения имени академика У.А. Джолдасбекова, Алматы, Казахстан. E-mail: s1981b@mail.ru; ORCID ID: https://orcid.org/0000-0001-8044-4186*

Абдураимов Азизбек Ералиевич — *доктор Ph.D., научный сотрудник, Институт механики и машиноведения имени академика У.А. Джолдасбекова, Алматы, Казахстан. E-mail: zizo_waterpolo@mail.ru; ORCID ID: https://orcid.org/0000-0002-0815-3349*

Камал Азиз Нутпуллаоглы — *магистр, научный сотрудник, Институт механики и машиноведения имени академика У.А. Джолдасбекова, Алматы, Казахстан. E-mail: kan77705@gmail.com; ORCID ID: https://orcid.org/0000-0002-4454-8233*

Қумарбек Нурғали Ерболович — *магистр, научный сотрудник, Институт механики и машиноведения имени академика У.А. Джолдасбекова, Алматы, Казахстан. E-mail: nurgalyku@gmail.com; ORCID ID: https://orcid.org/0009-0007-6058-6778*

Махмет Саят Бакытович — *магистр, научный сотрудник, Институт механики и машиноведения имени академика У.А. Джолдасбекова, Алматы, Казахстан. Email: mahmetsayat@gmail.com; ORCID ID: https://orcid.org/0009-0009-4791-9886*

Меркибаев Ерик Серикович — *PhD, старший преподаватель кафедры Металлургии и обогащения полезных ископаемых, Горно-металлургический институт имени О.А. Байконурова, Satbayev university, Almaty,Kazakhstan. Email: y.merkibayev@satbayev.university; ORCID ID: https://orcid.org/0000-0003-3869-6835*

References

[1] Zhumagaziyev A Zh, & Adilova D A. Study of foreign experience in the use of construction waste and the possibility of its application in Kazakhstan. Bulletin of Science. 2024; 5(9(78)):361-374.

[2] Bekenov A K, et alProcessing of technogenic waste and issues of environmental safety. Ecology and Industry of Kazakhstan. 2020; 2:15-21.

[3] Grosse F, et al. Circular economy and industrial ecology: Strategies for sustainable material flows. Journal of Cleaner Production. 2019; 234:133–144. https://doi.org/10.1016/j.jclepro.2019.06.345

[4] Kirchherr J, et al. Conceptualizing the circular economy: An analysis of 114 definitions. Resources, Conservation and Recycling. 2017; 127:221–232. https://doi.org/10.1016/j.resconrec.2017.09.005

[5] Geissdoerfer M, et al. The circular economy – A new sustainability paradigm? Journal of Cleaner Production. 2017; 143:757–768. https://doi.org/10.1016/j.jclepro.2016.12.048

[6] Kopytov V M, et al. Tekhnogennyye otkhody metallurgicheskogo proizvodstva i puti ikh pererabotki [Technogenic waste of metallurgical production and ways of its processing]. Metallurgy. 2022; 6:22-29. (In Russ).

[7] Matinde E, Simate G S, & Ndlovu S. Mining and metallurgical wastes: A review of recycling and re-use practices. Journal of the Southern African institute of mining and metallurgy. 2018; 118(8):825-844. https://doi.org/10.17159/2411-9717/2018/v118n8a5

[8] Cai P T, Chen T, Chen B, Wang Y C, Ma Z Y, & Yan J H. The impact of pollutant emissions from co-incineration of industrial waste in municipal solid waste incinerators. Fuel. 2023; 352:129027.

[9] Akinyemi B A, Hagare D, & Oluwadamilare A. Microwave energy radiated biochar bonded-cement-clay bricks. Journal of Building Pathology and Rehabilitation. 2023; 8(2):94.

[10] Siddique R. Utilization of industrial by-products in concrete. Procedia Engineering. 2014; 95:335-347. https://doi.org/10.1016/j.proeng.2014.12.192

[11] Das S K, Mishra S, Das D, Mustakim S M, Kaze C R, & Parhi P K. Characterization and utilization of coal ash for synthesis of building materials. In Clean Coal Technologies: Beneficiation, Utilization, Transport Phenomena and Prospective. 2021, 487-509. Cham: Springer International Publishing.

[12] Khabiyev A, Yulussov S, Tuleshov A, Baigenzhenov O, Merkibayev Y, & Baltabay T. Investigation of the composition of industrial products of vanadium production and its use for the production of heat-resistant building mixes. Engineering Journal of Satbayev University. 2024; 146(6):1-7. https://doi.org/10.51301/ejsu.2024.i6.01

[13] Peng H. A literature review on leaching and recovery of vanadium. Journal of Environmental Chemical Engineering. 2019; 7(5):103313. https://doi.org/10.1016/j.jece.2019.103313

[14] Wang Y H, Wang Y F, Li Y T, Wu C, Han X L, Zhao N N, ... & He Z X. A review on vanadium extraction techniques from major vanadium-containing resources. Rare Metals. 2024; 43(9):4115-4131.

[15] Boccaccini D N, Cannio M, Volkov-Husoviæ T D, Kamseu E, Romagnoli M, Veronesi P, ... & Boccaccini A R. Service life prediction for refractory materials. Journal of materials science. 2008; 43(12):4079-4090.

[16] Krivenko P, Petropavlovsky O, & Vozniuk H. Development of mixture design of heat-resistant alkali-activated aluminosilicate binder-based adhesives. Construction and Building Materials. 2017; 149:248-256. https://doi.org/10.1016/j.conbuildmat.2017.05.138

[17] Bernal S A, Rodríguez E D, Mejía de Gutiérrez R, & Provis J L. Performance at high temperature of alkali-activated slag pastes produced with silica fume and rice husk ash based activators. Materiales de construcción. 2015; 65(318).

[18] Boris R, Kerienė JR, Antonovič V, & Madej D. Characterization of microstructural evolution and mechanical properties of refractory composite. Composite Structures. 2015; 134:811-819. https://doi.org/10.1016/j.compstruct.2015.08.059

[19] Rashad A M, Ouda A S, & Sadek D M. Behavior of alkali-activated metakaolin pastes blended with quartz powder exposed to seawater attack. Journal of Materials in Civil Engineering. 2018; 30(8):04018159. https://doi.org/10.1061/(ASCE)MT.1943-5533.0002335

[20] Yu Z, Wang B, Zhang S, Zhao Y, Yan X, Zhang T, ... & Du X. Mechanical Properties and Deterioration Mechanism of Concrete–Mortar Joint Interface after Exposure to High Temperature. Journal of Materials in Civil Engineering. 2025; 37(9):04025315. https://doi.org/10.1061/JMCEE7.MTENG-2022

[21] Thomas T, & Praveen A. Emergy parameters for ensuring sustainable use of building materials. Journal of Cleaner Production. 2020; 276:122382. https://doi.org/10.1016/j.jclepro.2020.122382

Crossref

DOI: https://doi.org/10.31643/2027/6445.15

Metallurgy and Metallurgical Engineering

Artificial graphite from Shubarkol coal obtained by sublimation of carbon atoms into the gas phase followed by desublimation into high-purity graphite

Aimenov Zh.T., Protopopov A.V., Suleimenov E.A., * Saipov A.A., Protopopov M.A., Merekeyeva A.Zh.

Non-profit Joint-Stock Company M. Auezov South Kazakhstan University, Shymkent, Kazakhstan

** Corresponding author email: abdilla.s.a@gmail.com*

Received: *October 17, 2025*
Peer-reviewed: *November 11, 2025*
Accepted *November 18, 2025*

ABSTRACT

This article discusses a plasma-chemical method for producing high-purity graphite from an air suspension of low-ash coal particles from the Shubarkol deposit in Kazakhstan. The technological process is based on the ability of carbon to transform from a solid to a gaseous state, bypassing the liquid state. This means it sublimes at high temperatures and desublimes as the temperature of the gaseous medium in the reactor zone decreases. The use of a graphite catalyst allows for controlled formation of the graphitized material. Atomic carbon graphitization occurs over a wide temperature range. It was established that graphite obtained in high-temperature reactor zones is purer than graphite obtained in reactor zones close to 500°C. This feature of the graphitization process enables product classification by quality. The design of a reactor based on sublimation and desublimation processes for graphite production is discussed. The use of a high-frequency electromagnetic zone in the plasma-chemical reactor design allows for controlled graphitization of atomic carbon, intensifying desublimation processes over a graphite powder catalyst. The plasma-chemical apparatus design includes a dust collection system and carbon monoxide neutralization, which can occur due to variations in the component proportions in the feedstock, which includes carbon powder, graphite powder catalyst, and carbon dioxide. The developed apparatus can be used to produce a sorbent – thermochemically expanded graphite – from graphite by varying the operating mode. The aim of this research is to develop a plasma-chemical technology for producing graphite from coal based on sublimation and desublimation processes in a single reactor, with the separation of impurities during the graphitization of carbon atoms over a graphite catalyst.

Keywords: plasma, sublimation, desublimation, graphitization, carbon, graphite, separation, catalyst.

Information about authors:

Aimenov Zhambul Talkhayevich — *Doctor of Technical Sciences, Professor, Director of the Research Institute of Natural and Technical Sciences, Non-Profit Joint Stock Company M. Auezov South Kazakhstan University, Tauke Khan Avenue 5, 160000, Shymkent, Kazakhstan. Email: zhambul_ukgu@mail.ru; ORCID ID: https://orcid.org/0000-0001-5426-6056*

Protopopov Anatoly Vsevolodovich — *Doctor of Technical Sciences, Professor, Head of the Laboratory High-Temperature Synthesis of Composite Materials and Metallurgical Processes, Non-Profit Joint Stock Company M. Auezov South Kazakhstan University, Tauke Khan Avenue 5, 160000, Shymkent, Kazakhstan. Email: awprotopopow@mail.ru; ORCID ID: https://orcid.org/0000-0002-0718-6333*

Suleimenov Erkinbek Ayatayevich — *Candidate of technical sciences, Researcher at the Laboratory High-Temperature Synthesis of Composite Materials and Metallurgical Processes, Non-Profit Joint Stock Company M. Auezov South Kazakhstan University, Tauke Khan Avenue 5, 160000, Shymkent, Kazakhstan. Email: erkinbek.suleimenov@gmail.com; ORCID ID: https://orcid.org/0000-0001-6833-0610*

Saipov Abdilla Abibullayevich — *Master of Engineering and Technology, Head of Center for Support of Technologies, Innovation, and Intellectual Property Protection, Non-Profit Joint Stock Company M. Auezov South Kazakhstan University, Tauke Khan Avenue 5, 160000, Shymkent, Kazakhstan. Email: abdilla.s.a@gmail.com*

Protopopov Maksim Anatolievich — *Researcher at the Laboratory High-Temperature Synthesis of Composite Materials and Metallurgical Processes, Non-Profit Joint Stock Company M. Auezov South Kazakhstan University, Tauke Khan Avenue 5, 160000, Shymkent, Kazakhstan. Email: promax80@gmail.com; ORCID ID: https://orcid.org/0000-0001-8676-3575*

Merekeyeva Aliya Zhanybekova — *Master of Education, Main specialist of Center for Scientific and Analytical Information, Non-Profit Joint Stock Company M. Auezov South Kazakhstan University, Tauke Khan Avenue 5, 160000, Shymkent, Kazakhstan. Email: merekeyeva@mail.ru; ORCID ID: https://orcid.org/0000-0001-9058-5484*

Introduction

In the next decade, graphite will be the most sought-after material for nuclear power, mechanical engineering, chemical engineering, and metallurgy. Graphite is used to manufacture many specialized products, such as battery electrodes, protective screens, sorbents, and much more. But the most important aspect of graphite today is the growing demand for high-purity, synthetic graphite. Obtaining high-purity graphite from readily available raw materials, which are abundant in Kazakhstan, such as the Shubarkol coal deposit, is a pressing issue. Developing technologies for processing coal into high-purity graphite is a promising solution. A promising solution is to utilize carbon's ability to sublimate in a non-oxidizing atmosphere and desublimate upon cooling, creating conditions conducive to graphitization.

An analysis of modern achievements in the science of obtaining artificial graphite [[1], [2], [3], [4], [5], [6], [7], [8], [9], [10]] allows to use some of the subtleties of artificial graphite production in technology to improve the quality of the main product.

Graphite is a mineral composed of carbon atoms arranged in layers. High bond strength between atoms within layers and low bond strength between atoms between layers account for graphite's low mechanical strength. Graphite's good electrical and thermal conductivity is explained by the high atomic density within layers and the free interlayer space, which ensures electron mobility and high electrical conductivity in an electric field. Another important property of graphite, important for this study, is that when heated, graphite does not melt; it burns only in a stream of oxygen, and evaporates in an electric arc under non-oxidizing conditions, i.e., it sublimates.

Graphite is used to manufacture a variety of specialized products, including refractory materials, solid lubricants, electrical machine contacts, paints, pencil leads, battery electrodes, and much more. But the most important aspect of graphite today is its growing demand and widespread use in nuclear power, the chemical industry, the production of conductive rubber, and metallurgy (as a material for electrodes, crucibles, and refractory screens).

Natural graphite contains various chemical impurities: SiO_2, Al_2O_3, P_2O_5, MgO, CuO, FeO, CaO. This limits its use and requires refining to remove these impurities. This is associated with enormous costs, comparable to those of producing synthetic graphite. Therefore, a significant portion of industrial graphite is synthetic.

Coke and pitch (petroleum and wood tar, coal tar) are used as raw materials in the production of artificial graphite. Given the demand for graphite, various technologies were developed for producing artificial graphite, which differs from natural graphite in chemical purity and applications. Common types of artificial graphite include: Acheson graphite, produced by heating a mixture of pitch and coke to 2800°C in electric furnaces; Pyrolytic (retort) graphite, designed for the electrical industry and synthesized from a gaseous hydrocarbon; Blast furnace graphite, formed as a by-product during the cooling of cast iron; and Carbide graphite, produced by the thermal decomposition of carbides.

The most cost-effective technology for producing graphite is coke. The primary raw material is coal coke. This intermediate product is produced by heating coal and peat to 1000-1100°C in the absence of oxygen. Coke is used as a high-energy fuel, a reducing agent in metallurgy, and a raw material for graphite production.

Technological features of artificial graphite production [[11], [12], [13], [14]]: Coke powder is fired under special conditions, ensuring carbon graphitization. To produce artificial graphite with desired properties, the graphite semi-finished product is impregnated with pitch, formaldehyde, or other substances. Often, to achieve the desired characteristics, graphite is subjected to heat treatment and impregnation several times. Each subsequent technological stage is carried out according to a specialized scheme. Graphite obtained by various methods differs and has a number of unique properties. These include increased strength, oxidation resistance, acid resistance, and high electrical conductivity. Artificial graphite of high chemical purity is produced in the form of a powder of various fractions. To produce parts by molding, the powder is pressed and sintered using specialized technologies [[15], [16]].

Graphite manufacturers, for example JSC "Donkarb Graphite", produced all types and grades of artificial graphite for industry. This is a colloidal powder of all possible fractions (fine, medium, coarse-grained), pressed, with special properties (grades ATM, OSCh MG, GMZ, PPG and others).

Global demand for graphite products is growing exponentially [[17], [18]]. Increasing temperature limits and thermomechanical loads in new

technologies place increased demands on graphite quality. The carbon industry's development strategy is focused on creating new, durable graphite materials with unique physical and chemical properties. Leaders in this area of industrial development include China, the United States, Japan, and the Netherlands.

The share of imported graphite in Kazakhstan's graphite consumption is expected to increase. Therefore, the development of graphite production technologies based on high-purity graphite is relevant and aligns with the priority areas of scientific and technological development.

The aim of this research work is to create a plasma-chemical technology for producing graphite from coal based on sublimation and desublimation processes in a single reactor with the separation of impurities during the graphitization of carbon atoms on a graphite catalyst.

Methods

This publication presents some of the results of work conducted at the Research Laboratory of High-Temperature Synthesis of Composite Materials, M. Auezov South Kazakhstan University. The technological features of the graphitization process were determined, graphite synthesis tests were conducted from coal using a simple laboratory setup, and a carbon graphitization reactor based on these results was designed using coal from Kazakhstan. An application for a patent of the Republic of Kazakhstan "Method for producing graphite from an air suspension of coal particles and a device for implementing it" was filed. Registration No. 2025/1516.2 dated November 15, 2025.

Based on the achievements of scientists in the field of synthesis of artificial graphite [[2], [3], [4], [6], [8]] and experience of the article authors [9,10], a process flow chart and equipment for obtaining artificial graphite from Shubarkol coal in Kazakhstan were developed. The technology utilizes the properties of carbon and its modifications. One of them is the ability of carbon atoms to sublimate when heated in a non-oxidizing environment, for example, in carbon dioxide at a temperature above 2000°C. (Sublimation is the transformation of a solid into a gaseous substance without going through the liquid state). The reverse process, desublimation, in this case is graphitization – the formation of graphite from atomic carbon. The graphitization process is widely known in scientific practice. It is important to note that, depending on the conditions, this process can occur over a wide temperature range, for example, from 500°C to 2000°C [[13], [14], [16], [18], [19], [20], [21], [22], [23], [24], [25], [26]]. For this reason, the work utilizes a graphitization catalyst, high-purity graphite, which allows to expand the temperature range of the graphitization process. Graphitization of atomic carbon on the surface of the catalyst – the centers of graphitization nucleation, at high temperatures, when all impurities are still in a gaseous state, allows the separation of graphite from impurity atoms. The plasma reactor (Figure 1) is made of graphite. A powdered catalyst, in the form of graphite powder, is fed into the graphitization zone as a seed for artificial graphite produced by desublimation of atomic carbon. Artificial graphite particles not captured in the separator are fed with the gas flow to a hydrofilter, where the graphite dust is captured with a special aqueous solution. Purified carbon dioxide is returned to the process. The resulting graphite from all graphitization zones and from the water filter is periodically extracted, analyzed, and sorted.

Reference: "Shubarkolkomir (coal)" / Shubarkol – the black pearl of Sary-ArkaShubarkol. The industrial coal reserves of the Shubarkol deposit amounted to over 1.5 billion tons. Coal from the Shubarkol deposit is classified as grade D (long-flame) hard coal and contains very little ash. The ash content of Shubarkol coal is only up to 12 percent, and the ash content of individual coal seam layers was only 3-6%. The coal has a low sulfur content (up to 0.5%) and a high calorific value (from 5200 to 5700 kcal/kg), and produces a lot of heat when burned [[1], [2], [17]]. Based on these properties, Shubarkol coal was chosen as the main raw material for producing artificial graphite using the plasma-chemical method.

The chemical composition of Shubarkol coal was studied by mass spectral analysis at the Regional Testing Laboratory of Engineering Profile "Structural and Biochemical Materials" (M. Auezov South Kazakhstan University), the results are presented in Table 1.

Given the complexity of the plasma-chemical graphite production process, the coal is sorted by ash content, and samples with the lowest ash content are selected (Table 1). A sample of Shubarkol coal after milling is shown in Figure 2.

Table 1 - Chemical composition of Shubarkol coal samples: Carbon 97-97.5%

No.	Chemical element	Content of impurities, % - Content in coal	Ash, impurity content	Ash content, % - content in ash	Note
1	Si	1.33-1.44	SiO_2	56-57	When burned in oxygen, some of the silicon evaporates in the form of SiO
2	Al	0.88-0.93	Al_2O_3	22-22.6	
3	Fe	0.15-0.20	Fe_2O_3	7.11	
4	Ca	0.08-0.11	CaO	2.6-2.8	
5	Mg	0.02- 0.03	MgO	1.8-2.0	
6	S	0.04-0.06	SO_3	3.4-3.43	
7	K	0.04-0.06	K_2O	1.28-1.3	
8	Na	0.06-0.07	Na_2O	1.65-1.72	

To ensure the graphitization of atomic carbon produced in the electric arc plasma torch, a catalyst for the physicochemical process is fed into the graphitization zone. In this study, a graphitization catalyst made of high-purity graphite powder was used. This allowed for an expanded temperature range for the graphitization process. The plasma reactor is made of graphite; in the graphitization zones, a powdered graphite catalyst and a graphite plasma reactor ensure the quality of the artificial graphite produced by desublimation of atomic carbon. A particle separation system for the artificial graphite separates the resulting products by quality, traps heavy impurities from the gas stream, and separates graphite dust with a special aqueous solution. Purified carbon dioxide is then returned to the beginning of the process – to the plasma-chemical reactor.

The resulting graphite from all graphitization zones and from the water filter is periodically extracted, analyzed, and sorted.

This method of producing graphite from coal is promising and important for the creation of products from artificial graphite: electrodes in electrochemistry, in the production of electric batteries, protective screens in nuclear energy, sorbents in the form of thermally expanded graphite in the petrochemical industry.

Features of the plasma-chemical synthesis process for graphite from Shubarkol coal: To efficiently produce graphite by desublimation, a powdered catalyst – “OSCh 7-3” grade graphite – is fed into the reactor’s graphitization zone (position 5, Figure 1). On the surface of the catalyst particles, for which high-purity graphite powder was selected, the graphitization process occurs over a wide temperature range, significantly increasing the reactor’s graphitization zone and, consequently, the duration of the graphitization cycle, which is crucial for the complete conversion of coal to graphite.

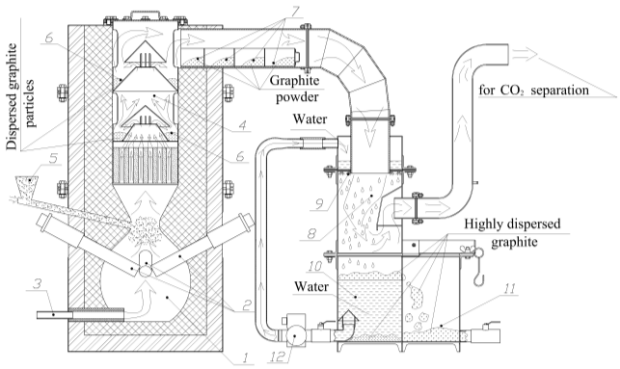

Figure 1 - Schematic diagram of the plasma-chemical apparatus for obtaining graphite from coal of the Shubarkol deposit in the Republic of Kazakhstan: 1 – the plasma reactor chamber, 2 – the graphite electrodes of the plasma torch, 3 – the tuyere for feeding reagents into the reactor, 4 – the dome – a dust collector of gas flows in the graphitization zone, 5 – the feeder for feeding the graphitization catalyst into the reactor, 6 – the cassettes for collecting the obtained graphite, 7 – the separator: storage tanks for synthesized graphite powder, 8 – the water shower chamber, 9 – the water spray nozzles, 10 – the water sump, 11 – the graphite storage tank, 12 – the water pump with a filter

The catalyst was prepared from “OSCh 7-3” grade graphite bars by crushing and grinding, followed by fractional separation. To use the powdered catalyst in a plasma-chemical graphite synthesis reactor, it is necessary to select a graphite particle size that, upon entering the high-temperature reactor zone, does not completely sublimate but remains solid and acts as artificial nuclei for the desublimation of atomic carbon obtained from the carbon particles in the sublimation zone. These conditions reduce the energy barrier for the phase transition of atomic carbon from the gas phase to graphite. For this

purpose, the yield of artificial graphite was determined using catalyst of different fractions. It was found that, for the conditions of this plasma-chemical apparatus, a fraction of 0.3-0.5 mm in cross-section is optimal.

Research Results and Discussion

The raw material – Shubarkol coal powder, specially processed to a fraction smaller than 0.3 mm – is fed into the plasma zone of a carbon dioxide reactor. The high heating rate in the reactor's plasma flow ensures the sublimation of carbon atoms. This results in an ionized gas environment consisting of carbon ions and oxygen ions. A catalyst – "OSCh 7-3" grade graphite powder – is fed into this ionized environment. The catalyst acts as an activator for the graphitization of carbon ions on its surface. The atomic structure of the graphitized product corresponds to that of the graphite catalyst. Samples of the resulting graphite are shown in Figure 2 (d).

Using a graphite catalyst with the required structure, pyrolytic graphite is produced by depositing carbon from the gas phase at high temperatures. It is characterized by high purity and anisotropic properties. (Thermally (chemically) expanded graphite – TEG and TCEG).

The chemical composition of plasma-chemically synthesized graphite is shown in Table 2.

Table 2 - Carbon and impurity content in synthesized graphite (average value of 7 samples from each graphitization zone of the plasma-chemical reactor)

No. of graphitization zone	Content of carbon, %	Content of impurities, %	Note
1 2 3 4 5	99.82 9994 99.77 98.68 98.65	0.18 0.06 0.23 1.32 1.35	Samples were taken from zones 6, 7, and 11: The purest graphite, sample 2, was from zone 7 (Figure 1), sample 1 was taken from zone 6, and samples 4 and 5 were from zone 11 (Figure 1). This is due to the different condensation temperatures of impurities from the reactor's gas environment, which requires further study and analysis of the graphitization process in such a reactor.

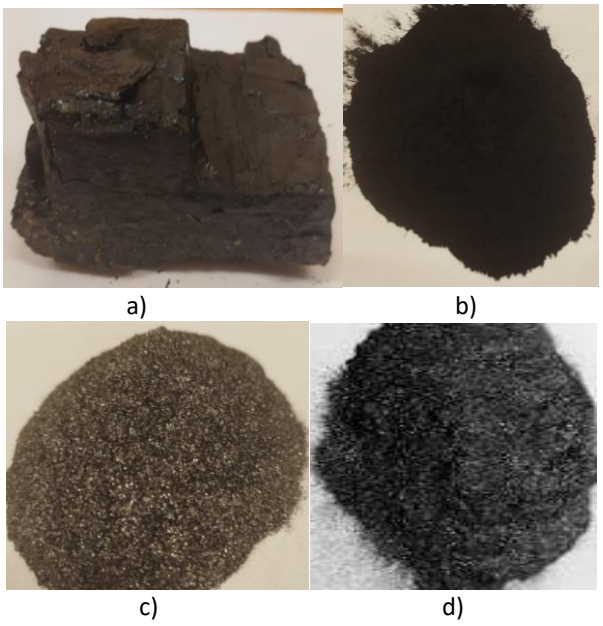

Figure 2 - Photos: a) Shubarkol coal, b) Shubarkol coal powder, c) Graphite – Catalyst, d) Graphite – graphitized by desublimation of carbon atoms on the catalyst.

The method and apparatus design proposed in this article will enable the production of high-purity graphite with a catalyst-like structure. Such processes require study using a newly developed plasma-chemical facility capable of controlling graphitization conditions and separating graphitization products in various temperature ranges for desublimation of atomic carbon.

Conclusions

A high-purity graphite catalyst was used in the study to expand the temperature range of the graphitization process. A graphite plasma reactor ensures the quality of the synthetic graphite produced by desublimation of atomic carbon.

The artificial graphite particle separation system allows for the separation of the resulting products by quality, the capture of heavy impurities from the gas flow, the separation of graphite dust with a special aqueous solution, and the return of purified carbon dioxide back into the process.

The resulting graphite from all graphitization zones and the water filter is sorted and analyzed. It was established that the graphite obtained in the plasma-chemical reactor zone is purer of impurities, indicating the important role of process temperature. Furthermore, as the graphite moves away from the plasma torch, it appears to adsorb impurities.

This method of producing graphite from coal is promising and important for the creation of artificial

graphite products: electrodes in electrochemistry, in the production of electric batteries, protective shields in the nuclear power industry, and expanded graphite sorbents in the petrochemical industry. The graphitization process requires continued research to ensure high product quality and address process control issues.

Conflict of Interest. On behalf of all authors, the corresponding author declares that there is no conflict of interest.

CRediT author statement: **Zh. Aimenov**: Supervision and overall guidance of the research; **A. Protopopov**: Conceptualization, Methodology, Software; **A. Saipov**: Data Curation, Writing – Original Draft Preparation; **E. Suleimenov**: Visualization, Investigation; **M. Protopopov**: Software, Validation of results; **A. Merekeyeva**: Review and Editing of the English version of the text.

Acknowledgment. We express our sincere gratitude and appreciation to the Scientific Research Regional Engineering Laboratory "Structural and Biochemical Materials" of M. Auezov South Kazakhstan University, where the quantitative and qualitative composition of the obtained graphite was analyzed using the Spekord V-80 and Superprobe 733-SCX equipment, according to a specialized methodology on a scanning electron microscope equipped with an analyzer.

This research work was carried out within the framework of the grant funding project AP26102281 Development of technology and equipment for producing polydisperse graphite sorbents from carbon-containing raw materials to ensure environmental safety in the mining, processing, and petrochemical industries under Contract No. 391/25-27 GK ShART, supported by the Science Committee of the Ministry of Science and Higher Education of the Republic of Kazakhstan.

Cite this article as: Aimenov ZhT, Protopopov AV, Suleimenov EA, Saipov AA, Protopopov MA, Merekeyeva AZh. Artificial graphite from Shubarkol coal obtained by sublimation of carbon atoms into the gas phase followed by desublimation into high-purity graphite. Kompleksnoe Ispolzovanie Mineralnogo Syra = Complex Use of Mineral Resources. 2027; 341(2):27-35. https://doi.org/10.31643/2027/6445.15

Көміртек атомдарын газ фазасына сублимациялап, содан кейін жоғары таза графитке десублимациялау арқылы Шұбаркөл көмірінен алынған жасанды графит

Айменов Ж.Т., Протопопов А.В., Сулейменов Э.А., Саипов А.А., Протопопов М.А., Мерекеева А.Ж.

Коммерциялық емес акционерлік қоғамы М.Әуезов атындағы Оңтүстік Қазақстан университеті, Шымкент, Қазақстан

Мақала келді: *17 қазан 2025*
Сараптамадан өтті: *11 қараша 2025*
Қабылданды: *18 қараша 2025*

ТҮЙІНДЕМЕ

Мақалада Қазақстанның Шұбаркөл кен орнының күлі аз көмір бөлшектерінің ауа суспензиясынан тазалығы жоғары графитті алудың плазмохимиялық әдісі қарастырылады. Технологиялық процес сұйық күйді айналып өтіп, қатты күйден газға айналатын көміртектің ерекшеліктерін пайдалануға негізделген, яғни жоғары температурада сублимацияланады, ал реактор аймағындағы газ ортасының температурасы төмендеген кезде десублимацияланады. Графит катализаторын пайдалану графиттелетін материалдың түзілуін басқаруға мүмкіндік береді. Атомдық көміртектің графитациясы температураның кең диапазонында жүреді. Жоғары температуралы реактор аймақтарында алынған графит 500^0С-қа жақын реактор аймақтарында алынған графитке қарағанда таза екендігі анықталды. Графитация процесінің бұл ерекшелігі өнімді сапасы бойынша жіктеуге мүмкіндік береді. Графит алу үшін сублимация және десублимация процестеріне негізделген реактордың дизайны қарастырылады. Жоғары жиілікте электромагниттік әсер ететін аймақтың плазмохимиялық реакторының дизайнында пайдалану графит ұнтағы катализаторындағы десублимация процестерін күшейту арқылы атомдық көміртектің графитациясын басқаруға мүмкіндік береді. Плазмохимиялық аппараттың конструкциясында көміртегі ұнтағы, графит ұнтақ катализаторы және көмір қышқыл газы бар бастапқы шикізаттағы компоненттер пропорцияларының ауытқуы кезінде мүмкін болатын шаң жинау және көміртегі оксидін бейтараптандыру жүйесі қарастырылған. Жасалған аппаратта технологиялық жұмыс режимін өзгерту арқылы графиттен сорбент - термохимиялық кеңейтілген графит алуға болады. Зерттеудің мақсаты - графит катализаторында көміртек атомдарын графиттеу кезінде қоспаларды бөліп, бір реакторда сублимация және десублимация процестеріне негізделген көмірден графит алудың плазмалық-химиялық технологиясын жасау.

Түйін сөздер: плазма, сублимация, десублимация, графиттеу, көмір, графит, бөлу, катализатор.

Авторлар туралы ақпарат:

Айменов Жамбул Талхаевич — *Техника ғылымдарының докторы, профессор, Коммерциялық емес акционерлік қоғамы М.Әуезов атындағы Оңтүстік Қазақстан университетінің Жаратылыстану және техникалық ғылымдар ғылыми-зерттеу институтының директоры, Тәуке хан даңғылы, 5, 160000, Шымкент, Қазақстан. Email: zhambul_ukgu@mail.ru; ORCID ID: https://orcid.org/0000-0001-5426-6056*

Протопопов Анатолий Всеволодович — *Техника ғылымдарының докторы, профессор, Коммерциялық емес акционерлік қоғамы М.Әуезов атындағы Оңтүстік Қазақстан университетінің Композиттік материалдар мен металлургиялық процестердің жоғары температуралық синтезі зертханасының меңгерушісі, Тәуке хан даңғылы, 5, 160000, Шымкент, Қазақстан. Email: awprotoporow@mail.ru; ORCID ID: https://orcid.org/0000-0002-0718-6333*

Сулейменов Эркинбек Аятаевич — *Техника ғылымдарының кандидаты, Коммерциялық емес акционерлік қоғамы М.Әуезов атындағы Оңтүстік Қазақстан университетінің Композиттік материалдар мен металлургиялық процестердің жоғары температуралық синтезі зертханасының ғылыми қызметкері, Тәуке хан даңғылы 5, 160000, Шымкент, Қазақстан. Email: erkinbek.suleimenov@gmail.com; ORCID ID: https://orcid.org/0000-0001-6833-0610*

Саипов Абдилла Абибуллаевич — *Техника және технология магистрі, Коммерциялық емес акционерлік қоғамы М.Әуезов атындағы Оңтүстік Қазақстан университетінің Технологияларды, инновацияларды қолдау және зияткерлік меншікті қорғау орталығының басшысы, Тәуке хан даңғылы 5, 160000, Шымкент, Қазақстан. Email: abdilla.s.a@gmail.com*

Протопопов Максим Анатольевич — *Коммерциялық емес акционерлік қоғамы М.Әуезов атындағы Оңтүстік Қазақстан университетінің Композиттік материалдар мен металлургиялық процестердің жоғары температуралық синтезі зертханасының ғылыми қызметкері, Тәуке хан даңғылы 5, 160000, Шымкент, Қазақстан. Email: promax80@gmail.com; ORCID ID: https://orcid.org/0000-0001-8676-3575*

Мерекеева Алия Жаныбековна — *Білім беру магистрі, Коммерциялық емес акционерлік қоғамы М.Әуезов атындағы Оңтүстік Қазақстан университетінің Ғылыми-талдау ақпараты орталығының бас маманы, Тәуке хан даңғылы 5, 160000, Шымкент, Қазақстан. Email: merekeyeva@mail.ru; ORCID ID: https://orcid.org/0000-0001-9058-5484*

Искусственный графит из Шубаркольского угля, полученный сублимацией атомов углерода в газовую фазу с последующей десублимацией в графит высокой чистоты

Айменов Ж.Т., Протопопов А.В., Сулейменов Э.А., Саипов А.А., Протопопов М.А., Мерекеева А.Ж.

Некоммерческое акционерное общество Южно-Казахстанский университет имени М.Ауэзова, Шымкент, Казахстан

Поступила: *17 октября 2025*
Рецензирование: *11 ноября 2025*
Принята в печать: *18 ноября 2025*

АННОТАЦИЯ

В статье рассматривается плазмохимический метод получения высокочистого графита из воздушной взвеси частиц малозольного каменного угля Шубаркольского месторождения Казахстана. Основа технологического процесса заключена в использовании особенности углерода превращаться из твердого состояния в газообразное, минуя жидкое состояние, то есть сублимировать при высокой температуре, а при снижении температуры газовой среды в зоне реактора десублимировать. Использование катализатора из графита позволяет управлять формированием графитизируемого материала. Графитация атомарного углерода происходит в широком диапазоне температур. Установлено, что графит, полученный в зонах реактора с высокой температурой более чистый, чем графит, получающийся в зонах реактора близких к 500^0С. Эта особенность процесса графитации предоставляет возможность классифицировать продукт по качеству. Рассмотрена конструкция реактора, на основе процессов сублимации и десублимации, для получения графита. Использование в конструкции плазмохимического реактора зоны с высокочастотным электромагнитным воздействием позволяет управлять графитацией атомарного углерода, интенсифицируя процессы десублимации на графитовом порошковом катализаторе. В конструкции плазмохимического аппарата предусмотрена система пылеулавливания и нейтрализации угарного газа, возможного при отклонениях пропорций компонентов в исходном сырье, в котором присутствует угольный порошок, графит порошковый катализатор и углекислый газ. В созданном аппарате возможно получать из графита сорбент - термохимически расширенный графит, изменяя технологический режим работы. Целью исследования является создание плазмохимической технологии получения графита из угля на основе процессов сублимации и десублимации в одном реакторе с отделением примесей при графитации атомов углерода на катализаторе из графита.

Ключевые слова: плазма, сублимация, десублимация, графитация, уголь, графит, сепарация, катализатор.

	Информация об авторах:
Айменов Жамбул Талхаевич	*Доктор технических наук, профессор, директор НИИ естественных и технических наук Некоммерческого акционерного общества Южно-Казахстанский университет имени М.Ауэзова, пр-т Тауке хана, 5, 160000, Шымкент, Казахстан. Email: zhambul_ukgu@mail.ru; ORCID ID: https://orcid.org/0000-0001-5426-6056*
Протопопов Анатолий Всеволодович	*Доктор технических наук, профессор, заведующий лабораторией Высокотемпературный синтез композиционных материалов и металлургические процессы Некоммерческого акционерного общества Южно-Казахстанский университет имени М.Ауэзова, 160000, пр-т Тауке хана, 5, Шымкент, Казахстан. Email: awprotoporow@mail.ru; ORCID ID: https://orcid.org/0000-0002-0718-6333*
Сулейменов Эркинбек Аятаевич	*Кандидат технических наук, научный сотрудник лаборатории Высокотемпературный синтез композиционных материалов и металлургические процессы Некоммерческого акционерного общества Южно-Казахстанский университет имени М.Ауэзова, пр-т Тауке хана 5, 160000, Шымкент, Казахстан. Email: erkinbek.suleimenov@gmail.com; ORCID ID: https://orcid.org/0000-0001-6833-0610*
Саипов Абдилла Абибуллаевич	*Магистр техники и технологии, начальник Центра поддержки технологий, инноваций и охраны интеллектуальной собственности Некоммерческого акционерного общества Южно-Казахстанский университет имени М.Ауэзова, пр-т Тауке хана 5, 160000, Шымкент, Казахстан. Email: abdilla.s.a@gmail.com*
Протопопов Максим Анатольевич	*Научный сотрудник лаборатории Высокотемпературный синтез композиционных материалов и металлургические процессы Некоммерческого акционерного общества Южно-Казахстанский университет имени М.Ауэзова, 5, 160000, Шымкент, Казахстан. Email: promax80@gmail.com; ORCID ID: https://orcid.org/0000-0001-8676-3575*
Мерекеева Алия Жаныбековна	*Магистр образования, Главный специалист Центра научно-аналиической информации Некоммерческого акционерного общества Южно-Казахстанский университет имени М.Ауэзова, пр-т Тауке хана 5, 160000, Шымкент, Казахстан. Email: merekeyeva@mail.ru; ORCID ID: https://orcid.org/0000-0001-9058-5484*

References

[1] Saryglar ChA, Chysym RB. Main directions of coal processing. Fundamental research. 2018; 11(1):121-127.

[2] Imash AA, Kaidar BB, Zhumatayev YeA, Smagulova GT. Puti kompleksnoy pererabotki ugley [Routes for integrated coal processing]. Goreniye i plazmokhimiya [Combustion and Plasma Chemistry]. 2021; 19:327-338. (In Russ). https://doi.org/10.18321/cpc471

[3] Jung JC-Y, Sui P-C. Zhang J. A review of recycling spent lithium-ion battery cathode materials using hydrometallurgical treatments. J Energy Storage. 2021; 35:102217.

[4] Liu K, Yang S, Luo L, Pan Q, Zhang P, Huang Y, Zheng F, Wang H, Li Q. From spent graphite to recycle graphite anode for high-performance lithium-ion batteries and sodium ion batteries. Electrochim. Acta. 2020; 356:136856.

[5] Yang K, Gong P, Tian Z, Lai Y, Li J. Recycling spent carbon cathode by a roasting method and its application in Li-ion batteries anodes. J Clean. Prod. 2020; 261:121090.

[6] Xing W, Bai P, Li ZF, Yu RJ, Yan ZF, Lu GQ, Lu LM. Synthesis of ordered nanoporous carbon and its application in Li-ion battery. Electrochim. Acta. 2006; 51(22):4626-4633.

[7] Paek S-M, Yoo E, Honma I. Enhanced Cyclic Performance and Lithium Storage Capacity of Sn02. Graphene Nanoporous Electrodes with Three-Dimensionally Delaminated Flexible Structure. Nano Lett. American Chemical Society. 2009; 9(1):72-75.

[8] Guo P, Song H, Chen X. Electrochemical performance of graphene nanosheets as anode material for lithium-ion batteries. Electrochem. commun. 2009; 11(6):1320-1324.

[9] Patent No. 20316. Method for producing thermally expanded graphite. Potapov AM, Protopopov AV, Assan AK. 25.08.2007.

[10] Almasov N, Kurbanova B, Kuanyshbekov T, Akatan K, Kabdrakhmanova S, & Aimaganbetov K. Study of the structure and electrical properties of graphene oxide (GO) and graphene oxide+nanocellulose (GO+NC). Kompleksnoe Ispolzovanie Mineralnogo Syra = Complex Use of Mineral Resources. 2024; 329(2):103–109. https://doi.org/10.31643/2024/6445.21

[11] Fialkov AS. Protsessy i oborudovaniye proizvodstva poroshkovykh uglegrafitovykh materialov [Processes and equipment for the production of powdered carbon-graphite materials]. M.: Aspect Press. 2007, 687. (In Russ).

[12] Seleznev AN. Uglerodnoye syr'ye dlya elektrodnoy promyshlennosti [Carbon raw materials for the electrode industry]. M.: Profizdat. 2000, 256. (In Russ).

[13] Aladekomo J, Bragg R. Structural transformations induced in graphite by grinding: analysis of 002 X-Ray diffraction line profiles. Carbon. 1990; 28(6):897-906.

[14] Samoilov VM. Polucheniye melkozernistykh uglerodnykh napolniteley i razrabotka tekhnologii polucheniya melkozernistykh grafitov na ikh osnove [Production of fine-grained carbon fillers and development of technology for the production of fine-grained graphites based on them] diss. ... doc. of technical sciences. M. 2006. 358.

[15] Fedorov VV, Shorshorov MKh, Khakimova DK. Stroyeniye uglerodnykh materialov na raznykh urovnyakh organizatsii [Structure of carbon materials at different levels of organization]. Uglerod i yego vzaimodeystviye s metallami [Carbon and its interaction with metals]. collection of scientific papers. M.: Metallurgy. 1978, 20-21. (In Russ).

[16] Maire J, Merring J. Graphitization of soft carbons. Chemistry and physics of carbon. 1970; 6:125-190.

[17] Pat. 2256610 Russian Federation, IPC C01B31/04. Sposob polucheniya vysokoplotnykh melkozernistykh uglegrafitovykh materialov [Method for producing high-density fine-grained carbon-graphite materials]. A. Sviridov, A.N. Seleznev, S.A. Podkopaev, et al. Publ. 27.02.05, 1.

[18] Novak YuV, Perkova GA, Kuteinikov AF. Udaleniye primesey pri formirovanii struktury grafita [Removal of impurities during graphite structure formation]. Konstruktsionnyye materialy na osnove grafita: sbornik nauchnykh trudov [Graphite-based structural materials: collection of scientific papers]. M.: Metallurgy. 1979; 14:35-40. (In Russ).

[19] Bragg R. Lattice parameters of metastable phases of graphite. Proceedings of International Carbon Conference. 1992, 192-193.

[20] Mokhova NN, Molotok NP. Vliyaniye dispersnosti tonkogo pomola na formirovaniye poristoy struktury i svoystva uglegrafitovykh materialov [Influence of fine grinding dispersion on the formation of porous structure and properties of carbon-graphite materials]. Proizvodstvo uglegrafitovykh materialov: sbornik nauchnykh trudov [Production of carbon-graphite materials: collection of scientific papers]. M.: NIIGrafit, GosNIIEP. 1980, 24-31. (In Russ).

[21] Pat. 4293533 United States, Int. C01B31/00; C01B31/02; C01B31/04. Method for producing solid carbon material having high flexural strength. K. Asano, H. Tamura, Y. Nezu, T. Saito, Y. Kawai. Publ. 06.10.1981, 8.

[22] Pat. 2257341 Russian Federation, IPC C01B31/04. Sposob polucheniya melkozernistogo grafita [Method for producing fine-grained graphite]. V.M. Samoilov, B.G. Ostronov, I.A. Bubnenkov et al. Publ. 27.07.2005, 5. (In Russ).

[23] Pat. 4089934 USA, Int. C01B3102; CO IB 3104. Process for preparing carbon products. O. Akiyoshi, A. Mukai, Y. Miwa. Publ. 16.05.786 8.

[24] Pat. 0575748 EP, Int. C04B35/52. Self-adhesive carbonaceous grains and high-density carbon artifacts derived therefrom. I. Machida, R. Fujiura, T. Kojima, H. Sakamoto. Publ. 29.12.93, 13.

[25] Pat. 0657400 EP, Int. C04B35/52. Process for producing high-density and high-strength carbon artifacts from self-adhesive carbonaceous grains. R. Fujiura. Publ. 31.03.1999, 11.

[26] Safonov AA, Mausymbayeva AD, Portnov VS, et al. Analysis of the possible use of coals from the Shubarkol deposit in the smelting of technical silicon. Coal. 2019; 2:68-72.

Crossref

creative commons

DOI: 10.31643/2027/6445.16

Earth and Planetary Sciences: Earth-Surface Processes

Redistribution of rock pressure and deformation of the rock mass in the Karaganda coal basin

***Mussin R.A., Akhmatnurov D.R., Zamaliyev N.M.**

NPJSC Abylkas Saginov Karaganda Technical University, Karaganda, Kazakhstan

** Corresponding author email: r.a.mussin@mail.ru*

Received: *September 25, 2025*
Peer-reviewed: *October 2, 2025*
Accepted: *November 18, 2025*

ABSTRACT

The study examines the redistribution of rock pressure and associated deformation processes in the Karaganda Coal Basin. It focuses on the geometry and parameters of the abutment, unloading, and disintegration zones around underground workings, and on their influence on gas-dynamic phenomena. The methodological basis combines a critical review of current geomechanical models, calculation–graphic nomograms for estimating zone width as a function of mining depth and seam thickness, and schematic construction of high-stress regions from the boundaries of the goaf at limiting angles of 75–90°. It is shown that, with increasing depth up to about 500 m, the zone configuration becomes wedge-shaped with a tendency to narrow downward, while increasing seam thickness expands the affected areas. Lithology controls the localization of hazardous zones: weakly bedded argillites and siltstones accelerate loosening and loss of stiffness, whereas stronger sandstones form dome-like stress concentrations with elevated likelihood of sudden outbursts and rockbursts. As a verification case, an episode of a sudden coal-and-gas outburst was analyzed. The observed failure boundaries are consistent with the calculated wedge-shaped high-stress zone, supporting the validity of the chosen approach within the stated assumptions. The practical significance lies in refining threshold conditions that trigger mandatory comprehensive forecasting at depths exceeding ~400 m, justifying regular instrumental monitoring to validate calculations, and adjusting barrier-pillar parameters about seam thickness and depth. The findings can be applied to the planning and safe execution of longwall and development operations under outburst-prone conditions.

Keywords: abutment pressure, destressed zones, disintegration, mining depth, seam thickness, lithology.

Information about authors:

Mussin Ravil Altavovich — *PhD, Acting Associate Prof., NPJSC Abylkas Saginov Karaganda Technical University, Karaganda, Kazakhstan. Email: R.A.Mussin@mail.ru; ORCID ID: https://orcid.org/0000-0002-1206-6889*

Akhmatnurov Denis Ramilievich — *PhD, Head of Laboratory, NPJSC Abylkas Saginov Karaganda Technical University, Karaganda, Kazakhstan. Email: d.akhmatnurov@gmail.com; ORCID ID: https://orcid.org/0000-0001-9485-3669*

Zamaliyev Nail Mansurovich — *PhD, Associate Professor, NPJSC Abylkas Saginov Karaganda Technical University, Karaganda, Kazakhstan. Email: nailzamaliev@mail.ru; ORCID ID: https://orcid.org/0000-0003-0628-2654*

Introduction

Redistribution of rock pressure within the host rock mass is a core subject of mining geomechanics and directly governs the safety and operational stability of underground workings. Disturbance of the natural stress field during excavation generates local stress concentrators and zones of intense deformation and failure. These responses are systematic and manifest as a spectrum of complications ranging from loss of support capacity and instability of the excavation perimeter to sudden coal-and-gas outbursts and rockbursts [[1], [2], [3]]. The issue is particularly acute in coal basins that combine large depth ranges with high gas content. In the Karaganda Coal Basin, this constitutes a primary risk factor: production commonly proceeds at depths of ~400–600 m and greater, where the in-situ stress level approaches critical thresholds for several lithotypes and structural settings [4]. Coupled with the elevated methane potential of the seams, this increases the likelihood of dynamic phenomena—such as outbursts, roof/floor collapses, and rockbursts. Operational records and research indicate that 40–60 % of complications during longwall and development operations are directly associated with stress redistribution [[5], [6]]. The hazardous processes are hierarchical: local plastic deformation at the excavation boundary rapidly propagates to

the scale of the rock mass, modifying the stress–strain state and permeability. Adjacent to the face, the abutment-pressure zone develops with elevated principal stresses; in the destressed zone, fracturing and disintegration progress, degrading stability, altering filtration regimes, and enhancing gas release. At the surface, these changes drive secondary deformations—subsidence, tensile cracking, and plan-position disturbance of infrastructure [[7], [8], [9]]. Lithological control is pivotal: weakly bedded argillites and siltstones accelerate yielding and loosening, whereas thick sandstone packages may form dome-like stress concentrations with heightened risk of dynamic events.

The practical framework requires a verifiable forecast of the configuration and parameters of influence zones, accounting for mining depth (H), seam thickness (m), structural disturbance, and the initial lateral stress coefficient K_o. Computational assessments should employ calibrated numerical models constrained by in-situ data: excavation convergence, ground-penetrating radar/ultrasonic surveys, acoustic-emission indicators, borehole logging, and stress measurements. On both longwall and development panels, continuous operational monitoring is warranted, including load cells and instrumented rock bolts, vibrating-wire gauges and fixed-point convergence meters, acoustic-emission and microseismic stations, and routine gas monitoring. Comparing deformation rates with trends in acoustic activity and gas emission enables timely identification of transitions to unstable regimes.

Engineering decisions must be explicitly tied to the mapped zones of influence: adjustment of support schemes, dimensions, and placement of barrier/chain pillars, extraction sequencing, face advance rate, and degasification regimes. For depths >400–500 m, it is advisable to adopt threshold criteria for switching to reinforced support and enhanced monitoring, and to apply refined nomograms of abutment-zone width that incorporate H, m, and rock properties. Without regular instrumental validation of models and adaptive updates to support designs, achieving the required levels of safety and reliability is not feasible; the integrated cycle “model → measurement → correction” is what sustains excavation stability and reduces the probability of sudden dynamic manifestations under the conditions characteristic of the Karaganda Coal Basin. Long-term accident statistics from Karaganda Coal Basin mines underscore the need for continual improvement in occupational safety practices and roadway stability management. At depths exceeding 500 m, conventional schemes for predicting rock-pressure zones lack sufficient sensitivity to heterogeneity and anisotropy of the rock mass, increasing the likelihood of suboptimal design decisions; refined, verifiable modeling and analysis methods are therefore required [[10], [11]]. A key applied task is the correct delineation of high-stress zones emanating from the edges of the goaf, since their geometry governs the serviceability of pillars and the longevity of workings left in place. Geomechanical models enable advanced estimation of the width and depth of influence zones, their linkage to longwall and development parameters, and timely adjustments to support designs. Field and desk studies indicate that deformation and failure foci are predominantly localized in coal seams overlain by weakly bedded argillites and siltstones, reinforcing the need to account comprehensively for lithological structure. Conversely, strong sandstones in the roof or floor promote dome-shaped stress concentrations and elevate the risk of sudden dynamic events. In practice, this manifests as perimeter deformation with spalling and crushing of supports and consequential ventilation disturbances, episodes of sudden coal-and-gas outbursts once critical stress thresholds are reached, rockbursts in tectonically disturbed zones at depths greater than 500 m, and roof collapses with floor heave that complicate longwall operations. Collectively, these factors reduce productivity and pose significant hazards to personnel; industry data indicate that outbursts and roof falls remain among the leading causes of accidents in Kazakhstan’s coal mines.

Article Objective. Systematizing data on rock-pressure influence zones and their structural features is a necessary step toward developing effective methods for forecasting and preventing accident scenarios. Theory, experimental studies, and operational observations consistently show that characteristic zones form around the goaf: an abutment-pressure zone, a destressed (unloading) zone, a zone of complete disintegration, and a zone of secondary movements. Understanding their spatial configuration and parameters improves forecast accuracy and the defensibility of design choices. Accordingly, the objective of this article is to analyze and synthesize data on stress redistribution around underground workings, to demonstrate mechanisms of rock-mass failure using a documented coal-and-gas outburst, and to assess the applicability of these findings to the geological

and operational conditions of the Karaganda Coal Basin.

Experimental part

Table 1 translates the qualitative stratigraphy into a compact input set for FEM/FDM initialization by listing density, stiffness, and strength contrasts for the principal layers together with reduced-shear behavior at bedding contacts; this allows the models to reproduce dome-like stress concentrations in stiff sandstone roofs and the weakening influence of laminated siltstone and argillite.

Table 1 - Condensed material and interface set for model initialization.

Series	H (m)	m (m)	K_o	Roof lithology	Reference L (m)
S1	400	1.0	0.7	siltstone/ argillite	L_o (nomogram)
S2	600	2.0	0.8	laminated (weakened)	≈ 20 (per text)
S3	800	3.0	1.0	sandstone (stiff)	≈ 55 (per text)
S4	1000	4.0	1.1	faulted section	L_o; indicators check

Table 2 - Compact scenario grid for model–field comparison.

Layer / interface	ρ, t/m³	E, GPa	UCS, MPa	Purpose / note
Roof-1 (sandstone)	2.45–2.60	12–25	40–80	Stiff roof shaping dome-like stress fields
Roof-2 (siltstone)	2.40–2.55	6–12	15–40	Weaker laminated roof packages
Coal seam	1.30–1.45	1–3	4–12	Controls yielding (m = 1–4 m)
Floor (argillite)	2.40–2.55	3–8	10–25	Soft base influencing abutment width
Roof/seam contact	—	K_shear 50–150 MN/m	—	Reduced shear; μ 0.4–0.6; τ_max 1.0–2.5 MPa
Seam/floor contact	—	K_shear 50–120 MN/m	—	Reduced shear; μ 0.4–0.6; τ_max 0.8–2.0 MPa

These ranges operationalize the stratigraphic context into numerical inputs so simulations start from defensible stiffness/strength contrasts and reduced-shear contacts.

Table 2 organizes the model–field comparison into a concise scenario grid spanning depth (H), seam thickness (m) and lateral confinement (K_o) with lithology and contacts specified; L_o from the nomogram is treated as the baseline, while the values already cited in the manuscript (≈20 m at H = 600 m and ≈55 m at H = 800 m) serve as anchors during interpretation.

The scenario grid defines which H–m–K_o combinations are tested; the nomogram-based L_o is the baseline, while the ≈20 m and ≈55 m figures already mentioned in the manuscript act as anchors for interpretation.

Redistribution of rock pressure within the host rock mass is a first-order subject of engineering analysis because it directly governs excavation stability and operational safety, especially under the conditions of the Karaganda Coal Basin. Disturbance of the natural stress field during drivage establishes a hierarchy of zones: at the excavation boundary, disintegration and intensive fracturing develop; outward from the contour, an abutment-pressure zone forms with principal stresses exceeding the in-situ level; farther out lies a destressed (unloading) zone characterized by reduced strength and increased jointing. Field observations show a rapid escalation from local plastic deformation at the boundary to rock-mass scale responses, accompanied by changes in the stress–strain state and in hydraulic and gas-dynamic regimes. Lithology is the controlling factor: weakly bedded argillites and siltstones accelerate loosening; thick, monolithic sandstones generate dome-shaped stress concentrations with elevated likelihood of dynamic manifestations; coal seams, combining low strength with high gas content, remain the most vulnerable element of the system. A schematic of the zoning and typical deformation forms is presented in Figure 1, which shows the initial and time-evolved excavation contours, weak and strong layers, the zone of complete failure, and tension-type termination cracks.

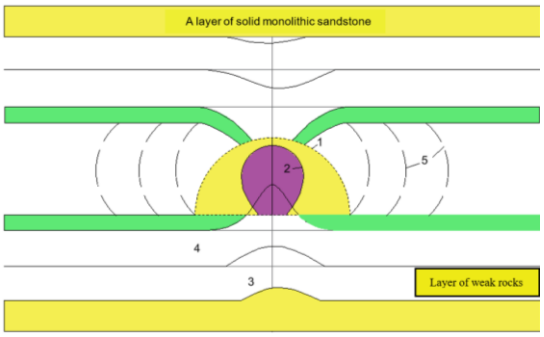

Figure 1 – Rock-mass failure deformation around an excavation with open support.
1-excavation contour immediately after drivage; 2-same after some time; 3-layers of weak rocks; 4-zone of completely crushed rock; 5-tension (termination) cracks; 6-layers of strong monolithic sandstone.

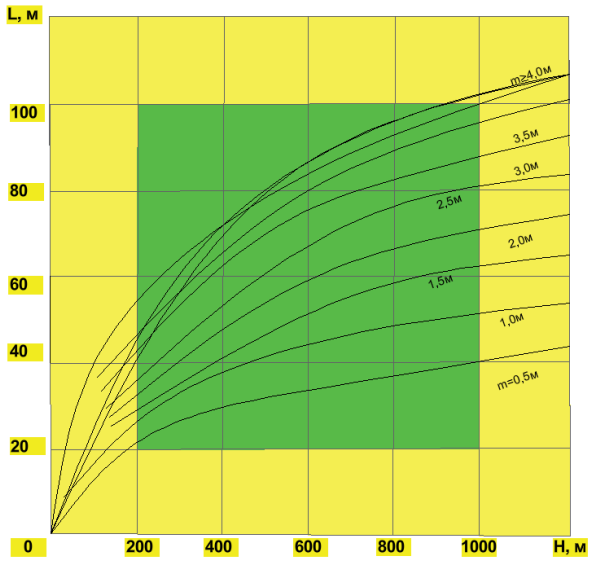

Figure 2 – Nomogram for determining the width of the abutment-pressure zone.
H – mining depth; m – seam thickness.

Quantitative evaluation is carried out using empirical–analytical relationships that link the width of the abutment-pressure zone (L) to mining depth (H), seam thickness (m), and the lateral stress coefficient (K_o). The nominal value L_o is taken from the nomogram in Figure 2 for the pair (H, m), after which a correction model is applied:

$$L = L_0(H,m)\cdot k_{litho}\cdot k_{str}\cdot k_{K0}\cdot k_t \qquad (1)$$

where k_{litho} reflects lithology (sandstone 1.15–1.35; argillite/siltstone 0.85–0.95; heterogeneous section 1.00–1.10), k_{str} accounts for tectonic disturbance (fault zones 1.10–1.25; undisturbed strata 0.95–1.00), $k_{K0} \approx 0.9 + 0.4\,(K_o - 0.7)$ for $0.6 \le K_o \le 1.1$ describes the influence of lateral stress, and k_t = 1.00–1.10 is a time factor.

$$L_0(H, m) \approx am^{0,8}\ln(1+H/H_0) \qquad (2)$$

For rapid checks consistent with the nomogram in Figure 2, an approximation is used (with a = 26–28, H_o = 90–110 m): at H = 1000 m and m = 4.0 m, L_o is on the order of 55–60 m; at H = 400 m and m = 1.0 m, L_o is about 12–14 m. These estimates are consistent with the family of calculated curves L(H) for m = 1–4 m in Figure 3.

Engineering application proceeds as follows. Specify H, m, and K_o, and describe lithology and structural disturbance; read L_o from Figure 2, then apply the modifiers k_{litho}, k_{str}, k_{K0}, and k_t to obtain L. Next, verify by monitoring: excavation-contour convergence with acceleration exceeding 2–3 mm/day within 0.5·L; a twofold increase in acoustic/microseismic activity under steady ventilation; ground-penetrating radar and ultrasonic indications of local stiff inclusions; and a 30–50% increase in CH_4 flow rate and concentration at constant depression.

For a weakly bedded roof at H = 600 m, m = 2.0 m, K_o = 0.8, and moderate disturbance, Figure 2 gives $L_o \approx 22$ m; applying the modifiers k_{litho} = 0.9, k_{str} = 1.05, $k_{K0} \approx 0.96$, k_t = 1.05 yields L ≈ 20 m. Recommended actions: reinforce support at the face, reduce the advance step, and drill lateral degasification holes 10–15 m long at a depression of 10–15 kPa.

For a strong sandstone roof at H = 800 m, m = 3.0 m, K_o = 1.0, and local tectonics, Figure 2 gives $L_o \approx 36$ m; with k_{litho} = 1.25, k_{str} = 1.15, $k_{K0} \approx 1.06$, k_t = 1.05, the result is L ≈ 55 m. Recommended actions: increase the length of rock bolts and cable bolts, use yielding elements, reduce the face advance rate, and deploy an acoustic-emission station for early detection of transitions to unstable behavior.

Direct comparison of the nomogram in Figure 2 with the calculated families of curves in Figure 3 turns abutment-pressure assessment into a numerically guided decision process. Tying zone width to specific H, m, and K_o, while accounting for lithological–structural heterogeneity, provides a practical tool for adaptive adjustment of support designs and degasification schemes, maintaining roadway stability and reducing the likelihood of sudden dynamic events within the 200–1000 m depth range typical of the Karaganda Coal Basin.

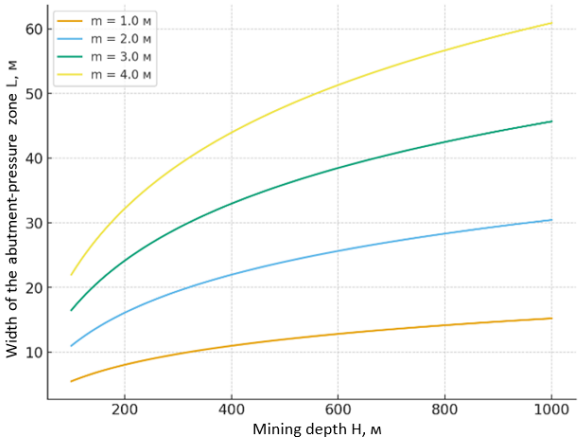

Figure 3 – Dependence of abutment-pressure zone width on depth for different seam thicknesses.

Analysis of the stress–strain state in the Karaganda Coal Basin shows that the boundaries of zones of elevated rock pressure dip at angles of 75–

90°, with formation depths of 250–500 m. Under these parameters, a characteristic wedge-shaped geometry develops, confining areas of maximum stress concentration. The construction is shown in Figure 4: cross-section (A) and along-strike section (B).

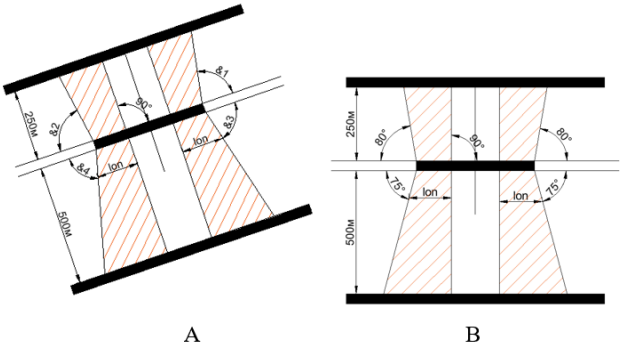

Figure 4 – Scheme for constructing zones of elevated rock pressure
A – cross-section across strike, B – along-strike section.

The limiting boundaries are traced by projecting rays from the edges of the worked-out space and barrier pillars at angles of 75–90° to the horizontal. This angular range corresponds to the observed inclination of the stress-concentration front and is corroborated by mine observations and physical modeling. At depths of about 250 m, steeper fronts (80–90°) prevail; with increasing depth to 500 m, the zone acquires a pronounced wedge shape that narrows downward, and operating angles decrease to 75–80°. Thus, mining depth directly controls the spatial configuration of high rock-pressure fields.

Seam thickness exerts a decisive influence on the scale of the zones. For m ≤ 1.0 m, they remain compact and localized near the workings; for m ≥ 3.0–3.5 m, the zones become extensive, extend beyond nearby pillars, and may span several production blocks. This necessitates revising the width and geometry of barrier pillars, refining the extraction sequence, and repositioning development entries.

Mapping wedge-shaped zones of elevated rock pressure provides a targeted forecast of hazardous areas—zones prone to sudden outbursts, local collapses, and degradation of support capacity. Practical application of the scheme under Karaganda Basin conditions has confirmed its effectiveness for siting development workings and specifying barrier-pillar parameters tied to actual depth and seam thickness.

Continuing the discussion of elevated-pressure zones: in the immediate vicinity of the excavation, the stress gradients are maximal, and the subsequent evolution of the perimeter is determined there. The scheme in Figure 1 illustrates this dynamics: the initial contour (1) shortly after drivage passes through a brief period of relative stabilization and, under rock pressure and rock creep, transforms into the later contour (2). Between these states, a zone of complete failure (4) develops with a blocky mosaic and pronounced loosening. Along the tensile front, termination (tension) cracks (5) appear; their spacing and depth are governed by contrasts in deformation modulus and strength across bed contacts, the presence of weak interbeds, and the degree of natural disturbance.

Materials of differing strength behave fundamentally differently. In bedded argillites and siltstones, structural degradation proceeds rapidly: effective stiffness drops, roadway convergence accelerates, and support capacity is exhausted over short time frames. Under such conditions, an early switch to a reinforced support scheme is justified: increasing rock-bolt and cable-bolt length, reducing spacing, using yielding elements, installing protective pillars, and implementing advanced degasification. In monolithic sandstones, excavation geometry persists longer due to higher strength; however, dome-shaped stress concentrations develop in the roof and at contacts with weaker rocks. As critical levels are approached, short-lived bursts of acoustic activity are recorded, local high-stiffness zones are detected by ultrasonic and GPR surveys, and the stability margin collapses even under minor external perturbations. For such areas, combined support with pretension and controlled yielding is advisable, along with a reduced face-advance rate and continuous instrumented monitoring.

Time dependence is a key factor. Even where initial behavior is stable, within weeks a persistent trend of roof and floor displacement often emerges: the convergence rate increases within roughly 0.5·L of the abutment-pressure zone width, the share of low-frequency events in acoustic records grows, and gas emission rises steadily at constant ventilation depression. Joint interpretation of three independent monitoring channels—convergence measurements, acoustic/microseismic observations, and gas-dynamic parameters—allows early recognition of the sequence shown in Figure 1: the transition from the initial to the later contour via expansion of the complete-failure zone and development of tension cracks.

Design decisions under these conditions must be tightly linked to the map of lithological and structural heterogeneity. For weak strata, rational measures include densifying the support grid, increasing element length, extended degasification, and installing local protective pillars. For strong sandstone domains—lengthening bolts and cable bolts, using stiff-yielding inserts, and reducing the longwall advance rate. At contacts between rocks with contrasting properties, local reinforcements and limits on operational pauses are required to prevent self-propagation of the hazardous disintegration zones depicted in Figure 1.

Table 3 condenses the monitoring framework to three operational signals—convergence acceleration, growth of low-frequency acoustic activity, and CH_4 flow increase at constant depression—so that model outputs can be read against clear instability indicators; auxiliary channels such as support loads and GPR/ultrasonic scans remain within the narrative.

Table 3 - Core monitoring triad and thresholds used for operational interpretation.

Channel	Derived metric	Operational threshold
Convergence	acceleration d^2u/dt^2	≥ 2–3 mm/day within ~0.5·L
Acoustic/microseismic	share of low-frequency events	sustained increase
Gas flow (CH_4)	trend at fixed depression	30–50% rise

Note (Table 3). Each metric–threshold pair provides a bridge between stress/strain fields and observable underground behavior, guiding escalation to reinforced measures.

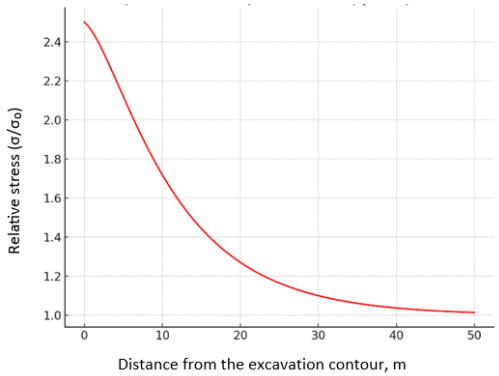

Figure 5 – Distribution of stresses around the excavation

Results and Discussion

Advancing the longwall face radically restructures the stress–strain state in the zone of development roadways and can lead to loss of their load-bearing capacity well before completion of seam extraction. The scheme in Figure 5 reflects a robust sequence: a roof caving dome forms, with its dimensions controlled by seam thickness, stiffness of the overlying strata, and the presence of weakly bedded interlayers; in the sidewalls, a squeezing zone develops, characterized by outward extrusion of the rock mass toward the goaf and opening of bedding/structure contacts; in the floor, a heave zone arises where vertical and horizontal stresses produce uplift and loosening of the rock. In the Karaganda Basin—where depths reach several hundreds of meters and gas content is high—these effects intensify: production observations indicate that the longwall front begins to measurably affect development entries already at an approach distance of 30–50 m, while the actual height of the caving dome and the widths of the squeezing and floor-heave zones may each reach tens of meters.

Engineering practice shows that the rate and amplitude of deformation are controlled by a combination of three factors: seam geometry (thickness, dip), lithologic contrast between roof and floor (monolithic sandstones versus argillites and siltstones), and operating regimes of the longwall (face advance rate, duration of technological pauses, ventilation depression, and degasification parameters). In weakly bedded strata, loosening accelerates, sidewall convergence increases, and support serviceability is lost early; with monolithic sandstones, excavation geometry persists longer, but dome-shaped stress concentrations accumulate in the roof and can trigger sudden collapses. As the face approaches, reliable indicators of transition to an unstable regime include acceleration of sidewall convergence to several millimeters per day within roughly one-half of the abutment-pressure zone width, a sustained increase in the count of low-frequency acoustic events, and growth of methane flow and concentration at constant ventilation depression. Joint interpretation of these three monitoring channels—geodetic and strain-gauge measurements, acoustic and microseismic records, and gas-dynamic control—enables timely refinement of the actual height of the caving dome and the boundaries of the squeezing and floor-heave zones shown in Figure 6.

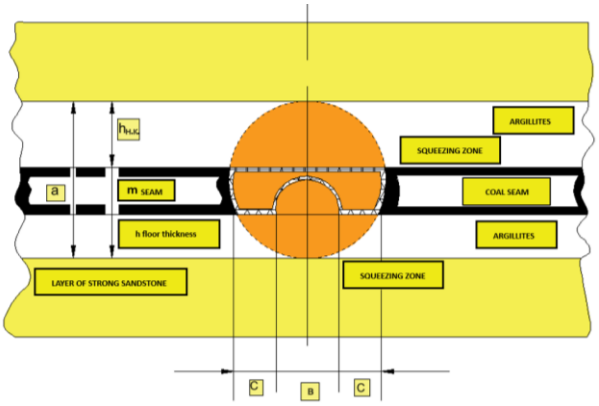

Figure 6 – Zone of potential rock-mass deformations around a development roadway under the influence of longwall operations

Design decisions should be directly grounded in such forecasts. For weak roofs and floors, appropriate measures include densifying the support pattern, increasing the length and pretension of rock bolts and cable bolts, using stiff-yielding elements, installing local protective pillars, and implementing advance degasification (lateral and inclined boreholes at a specified depression). For domains with monolithic sandstones, increase support capacity in combination with controlled yielding and a reduced face-advance step, and limit prolonged technological pauses to prevent self-amplification of the caving dome. Within the influence zone of longwall operations, development roadways should be treated as part of the overall stability system of the rock mass: their profile, support type, stand-off from the goaf, and degasification parameters must be revised as the face advances based on actual measurements rather than design assumptions alone. This “model — observe — adjust” regime provides the required stability margin and reduces the likelihood of sudden dynamic events at the depths and lithological conditions characteristic of the basin.

Redistribution of rock pressure. Advancing the longwall face radically restructures the stress–strain state in the zone of development entries and often leads to loss of load-bearing capacity long before seam extraction is completed. The scheme in Figure 6 illustrates a typical pattern. A roof caving dome forms; its height and span are governed by seam thickness, stiffness of the overlying strata, and the presence of weakly bedded interlayers. On the sidewalls, a squeezing zone develops, with the rock mass being extruded toward the goaf and bedding/structure contacts opening. In the floor, a heave zone forms where vertical and horizontal stresses cause uplift and loosening of the rock. This accelerates convergence growth and reduces the stability margin of the support.

Under Karaganda Basin conditions, the influence of the longwall front is amplified by mining depth and high gas content. Operational observations show that noticeable impacts on development roadways begin when the face approaches to 30–50 m. The roof caving zone and the squeezing and floor-heave zones can each extend for tens of meters. As the face advances, sidewall convergence rate increases, fracturing intensifies in argillites and siltstones, and gas emission rises at constant ventilation depression. Reliable indicators of transition to an unstable regime include acceleration of convergence to several millimeters per day within roughly half the abutment-pressure zone width, a sustained increase in low-frequency acoustic events, and growth of methane flow rate.

The rate and amplitude of deformations are controlled by three factor groups. The first is seam geometry, including thickness and dip. The second is contrast between roof and floor properties, where monolithic sandstones resist deformation longer while weakly bedded strata loosen more rapidly. The third is operating regime—face advance rate, duration of technological pauses, and degasification and ventilation parameters. Joint interpretation of three monitoring channels—convergence measurements, acoustic and microseismic records, and gas-dynamic control—allows refinement of the actual dome dimensions and the boundaries of the zones shown in Figure 7, and supports timely adjustment of decisions.

Design must be directly grounded in such monitoring. For weak roofs and floors, justified measures include densifying the support pattern; increasing the length and pretension of rock bolts and cable bolts; using stiff-yielding elements; installing local protective pillars; and implementing advance and side degasification at a specified depression. For domains with monolithic sandstones, it is advisable to combine higher support capacity with controlled yielding, reduce the face advance step, and limit prolonged technological pauses to prevent dome growth. Within the influence zone of longwall operations, development roadways should be treated as part of the overall stability system of the rock mass. Their profile, support type, stand-off from the goaf, and degasification parameters must be revised as the face advances, using actual measurements and threshold criteria. This model–observe–adjust algorithm provides the necessary stability margin and reduces the likelihood of sudden dynamic

events at the depths and in the lithological conditions typical of the basin.

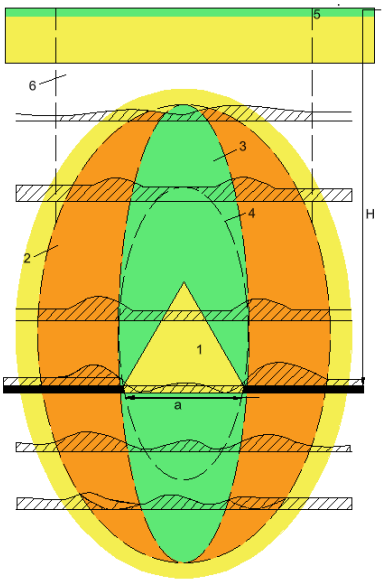

Figure 7 – Scheme of rock-pressure redistribution near a longwall working.
1 – area influenced by the working; 2 – abutment-pressure zone; 3 – boundary of the destressed zone; 4 – boundary of the protected zone; 5 – boundary of the zone of complete subsidence; 6 – zone of rock and ground-surface displacements arising from deformation of the rock mass within the abutment-pressure zone.

These zones do not act in isolation but as a single load-transfer framework: a stress change at the contour of a development or longwall working restructures the field above and below in the section, propagates upward to the roof, and can manifest at the ground surface as subsidence, crack opening, and terrain deformation. For the Karaganda Basin, the linkage between underground operations and surface deformation is confirmed by observations in areas of intensive mining: settlement peaks are recorded as the longwall face approaches, and their planform and amplitude are consistent with the configuration of the goaf and pillar parameters [[12], [13], [14], [15], [16], [17]].

From an engineering standpoint, pressure-redistribution zones constitute the skeleton of the rock mass geomechanical state and must be embedded in the design at all levels—from roadway alignment to the scheduling of block extraction. At the mine-field design stage it is advisable to construct a map of expected propagation angles and depths according to the scheme in Figure 4, specify calculated widths of the abutment-pressure and destressed zones, determine the minimum permissible distances between the goaf and development entries, and design protective pillars about their actual load-bearing capacity. In the technological part, this means choosing support type and spacing, face-advance rate, degasification regime, and limits on operational pauses in zones where a transition to unstable behavior is possible. In the operational part, it entails organizing continuous monitoring, including convergence measurements, acoustic–seismic observations, gas-dynamic measurements, and repeat surface geodetic surveys. Upon reaching threshold values, response measures are triggered—support reinforcement, denser bolt patterns, adjustment of the advance rate, local protective pillars, and modified degasification schemes.

This approach enables control of the entire system of zones from the face to the surface: local load redistribution at the working is promptly accounted for in roof and floor stability calculations, in assessing impacts on adjacent horizons, and in forecasting surface subsidence. Tying decisions to the scheme in Figure 4 and to in-situ measurements reduces the likelihood of sudden dynamic events and ensures the required safety level for seam extraction under the conditions of the Karaganda Coal Basin.

Field case. As an illustration, consider the sudden coal-and-gas outburst that occurred on 28 December 1976 in the manway at level +0 m of the Lenin Mine in the Karaganda Coal Basin. The incident took place in Seam D-6 at a depth of 411 m, with a roadway width of 6.0 m and a height of 3.25 m (see Figure 5).

According to the analysis, a zone of intense crushing and deformation formed in the coal seam adjacent to a tectonic disturbance near the outburst location. The character of the damaged zone (up to 5.0 m wide from the excavation contour) was accompanied by significant methane release. The gas-dynamic event was sharp and short-lived, consistent with the criteria of a sudden outburst, and with ground-control practice in longwall environments [[18], [19], [20]].

Comparison of the documented case with the calculated schemes of elevated rock-pressure zones (see Figure 6) showed agreement: the outburst area was localized within a wedge-shaped stress zone bounded by angles of 75–80° and situated immediately adjacent to the edge of the worked-out space. The accident thus confirmed the practical applicability of the pressure-zone construction methodology for forecasting the most hazardous areas, consistent with stress concentration concepts in rock mechanics and roadway support design.

Plan. Scale 1:500.

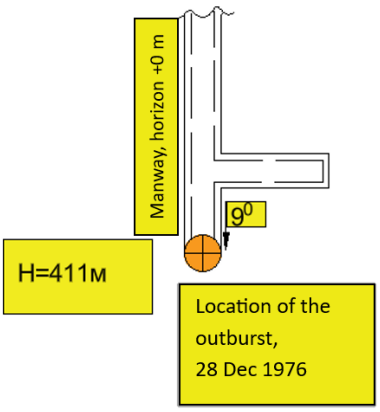

A

Dip section. Scale 1:200.

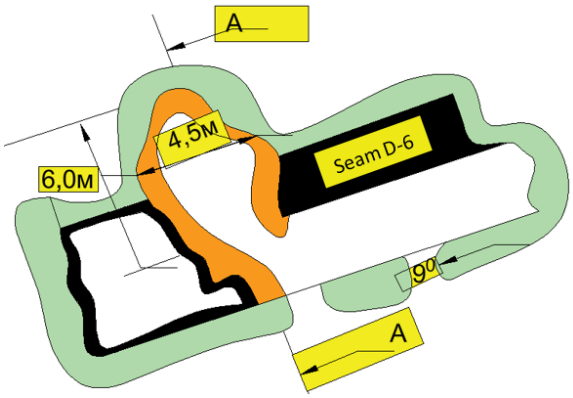

B

Strike section (A–A). Scale 1:100.

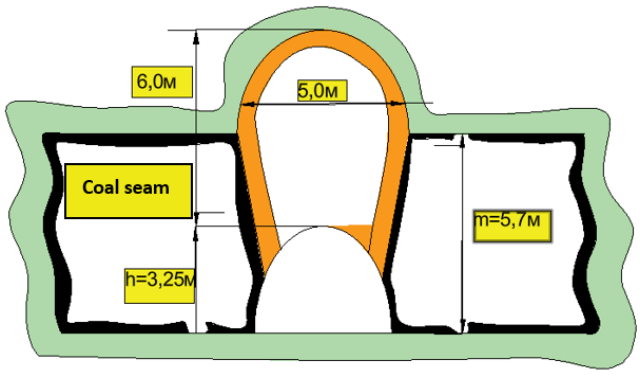

C

Figure 8 – Sketch of the sudden outburst site with elevated gas emission that occurred on 28 December 1976 in the manway at level +0 m of the Lenin Mine.

Comparison of the calculated schemes with in-situ observations confirms that the adopted zoning model for stress redistribution adequately represents rock-mass behavior in the Karaganda Coal Basin, aligning with established frameworks in rock mechanics and rock-mass classification. The system shows the highest sensitivity to three groups of risk factors. First, mining depth: once depths exceed roughly 400 m, rock-mass stress increases nonlinearly, consistent with the classic concepts of underground-excavation geomechanics by V. S. Kuznetsov and with the principles of rock-pressure control by V. P. Sakhno et al. In practice, this manifests as a rapid loss of stability margin in development and longwall roadways as they approach high-stress zones, a pattern well recognized in longwall and ground-control literature. Second, lithological structure: the association of coal seams with weak layers—argillites and siltstones—consistently produces zones of disintegration and accelerates loosening; this conclusion is supported by regional data on gas content and the structure of coal-bearing strata in the Karaganda Basin reported by M. A. Ermekov and by recent engineering studies on drivage and maintenance of cross-cuts by G. D. Tanekeyeva, E. A. Abeuov, D. R. Makhmudov, R. A. Mussin, and A. Yu. Balabas, and is consistent with rock-mass rating and Q-system perspectives on weak strata. Third, tectonic disturbance: faulted and crushed zones function as stress concentrators and are statistically correlated with sudden dynamic manifestations; this is emphasized in the work of V. S. Zaburdyaev on degasification parameters for high-productivity panels and is corroborated by calculation-instrumental solutions for stabilizing the mine floor by D. Akhmatnurov, N. Zamaliyev, R. Mussin, and co-authors, and by guidance on rockburst-prone conditions.

From a practical standpoint, the calculated boundaries of influence zones must be testable against measurable indicators. As stability limits are approached, the following are recorded: accelerated roadway convergence, a rise in low-frequency acoustic activity under constant ventilation depression, and a sustained increase in gas emission. Combined analysis of these time series refines the position of the abutment-pressure front, the boundaries of unloading, and the domain of complete disintegration. This approach aligns with current technological solutions for gas management and rock-mass deformation, including hydraulic flushing and hydraulic splitting for low-permeability coals (R. Zhang, C. Hao), consideration of swelling mechanisms and secondary deformations in complex geological settings (S. Y. Mu, Z. Ma), and synthesized observations of rock-mass behavior

around roadways in deep mines (K. Skrzypkowski, W. Korzeniowski, J. Stasica). At the project stage this means specifying initial contours of influence zones and minimum offsets from the goaf as starting values subject to systematic refinement via monitoring; the switch to reinforced support and intensified degasification should be triggered by threshold values of observed parameters rather than by calendar schedules, in line with the logic of rock-pressure control set out by Kuznetsov and Sakhno, and by longwall/ground-control best practice.

The detailing of engineering measures is governed by lithological–structural conditions. In weakly bedded sequences with argillites and siltstones, justified actions include longer and pretensioned rock bolts and cable bolts, reduced spacing, use of stiff-yielding inserts, installation of local pillars, and advance degasification via lateral and inclined boreholes; the combined effect of these measures is reflected in modern publications on the geomechanical conditions of roadway drivage and maintenance, in technological solutions for intensifying gas drainage, and in standard references on ground control and roadway support. In domains dominated by monolithic sandstones—where roadway geometry persists longer but dome-shaped stress concentrations develop—it is advisable to combine higher support capacity with limits on the face advance rate and regulated technological pauses to prevent dome growth and brittle collapses; this strategy accords with the foundational principles of rock-pressure management in the classic sources and with synthesized evidence on rock-mass behavior in deep mines. Within zones influenced by tectonic structures, increasing ventilation depression to boost gas flow must be accompanied by continuous acoustic and deformation monitoring, since excessive unloading can hasten the transition to instability; this interrelation is discussed in detail in studies of degasification parameters for high-productivity panels and in work on stabilizing the working floor. Where applicable, proprietary support and damping solutions and protected technical designs can be referenced for implementation [[21, [22]].

Finally, the limits of applicability must be recognized. Linear construction of zone boundaries cannot capture the full heterogeneity of the section and the variability of contacts; the temporal component—creep, stress relaxation, and changes in filtration and gas-dynamic regime—can recon Figure conditions weeks to months after drivage or extraction. Consequently, calculated decisions must be accompanied by instrumental verification: GPR and ultrasonic surveys to detect local stiff inclusions, acoustic and microseismic measurements to capture transitions to instability, and repeat surface geodetic surveys in areas of expected subsidence. This “model—observe—adjust” regimen rests on the proven methodological foundations of Kuznetsov and Sakhno, is supported by regional gas-content and structural data from Ermekov, and is reinforced by contemporary engineering studies in geomechanics and degasification, ensuring the required stability margin and reducing the probability of sudden dynamic events at the depths and lithological–structural conditions characteristic of the Karaganda Coal Basin [[23], [24], [25], [26]].

Conclusions

To substantiate safe extraction of seams in the Karaganda Coal Basin, the rock mass must be treated not as a set of local boundary effects but as a coherent system of processes with a clear space–time structure. Calculations and in-situ observations show that an interlinked hierarchy of zones forms around underground workings: at the boundary lies the abutment-pressure zone with elevated principal stresses; farther out is an unloading zone with reduced strength and increased jointing; beyond it, a disintegration zone with loss of structural integrity; and farther still, a domain of secondary movements through which deformations propagate away from the working and upward through the section to the ground surface. The system is nonlinear: any change in one zone reorganizes adjacent zones and sets the dynamics of the entire stress field.

Combined analysis of calculated schemes and field data indicates that maximum risks localize near the edges of the worked-out space and protective pillars, where wedge-shaped stress-concentration fronts form at angles of about 75–90° to the horizontal. At depths around 250 m, steeper fronts (80–90°) prevail; by 500 m, the wedge narrows downward at 75–80°, defining areas of highest likelihood for brittle collapses and dynamic events. The geometry is validated in practice: the sudden outburst at the Lenin Mine (Seam D-6, 1976, depth 411 m) reproduced the calculated scenario—the observed failure boundaries coincided with the predicted wedge-shaped high-stress zone.

For design under basin conditions, the controlling factors remain lithological contrast, gas content, and tectonic disturbance. Bedded argillites and siltstones accelerate loosening and enlarge the

disintegration domain; monolithic sandstones preserve roadway geometry longer but accumulate dome-shaped stress fields. High gas content lowers resistance to perturbations, while faulted and crushed zones act as stress concentrators and deformation conduits, sharply increasing the sensitivity of the rock mass as the longwall front approaches.

This leads to concrete engineering requirements. At depths above an indicative threshold of 400 m, a comprehensive geomechanical forecast is needed, with construction of wedge boundaries and estimation of influence-zone width for given depth and seam thickness. Operations should be accompanied by continuous instrumentation: convergence measurements, acoustic–microseismic monitoring, GPR/ultrasonic surveys of roof and floor, and real-time gas dynamics. Reliable indicators of an approach to instability include acceleration of convergence to several millimetres per day within roughly half the abutment-zone width, a sustained rise in low-frequency acoustic events, and increased methane flow/concentration at constant ventilation depression. Protective-pillar parameters should be adjusted for seam thickness, depth, and proximity to wedge zones; minimum sizes should be abandoned near faults. Support schemes must be adapted to actual influence-zone boundaries: increase bolt and cable-bolt length and pretension, tighten spacing, and employ stiff-yielding elements; in monolithic sandstones, combine higher load-bearing capacity with limits on face-advance rate and regulated pauses to prevent self-growth of a stress dome. To reduce outburst hazard, advance and lateral degasification at specified depressions, local relief workings, and controlled ventilation regimes are justified.

Organizationally, this is implemented as a strict “model — observe—adjust” cycle. Initial contours of influence zones set starting design values; as the face advances and monitoring data accrue, support type and spacing, pillar width and geometry, advance rate, and degasification parameters are refined. This regime provides the necessary stability margin for development and longwall roadways and lowers the probability of sudden dynamic events at the depths and under the lithological–structural conditions typical of the Karaganda Coal Basin.

Conflicts of interest. On behalf of all authors, the corresponding author states that there is no conflict of interest.

CRediT author statement: **R. Mussin**: Conceptualization, Methodology, Software, Data curation; **D. Akhmatnurov**: Writing draft preparation, Visualization, Investigation; **N. Zamaliyev:** Supervision, Software, Validation, Reviewing and Editing.

Acknowledgements. This research was carried out with the support of the Science Committee of the Ministry of Science and Higher Education of the Republic of Kazakhstan within the framework of program-targeted financing for the implementation of the scientific and scientific-technical program of the IRN BR28712407.

Cite this article as: Mussin RA, Akhmatnurov DR, Zamaliyev NM. Redistribution of rock pressure and deformation of the rock mass in the Karaganda coal basin. Kompleksnoe Ispolzovanie Mineralnogo Syra = Complex Use of Mineral Resources. 2027; 341(2):36-48. https://doi.org/10.31643/2027/6445.16

Қарағанды көмір бассейніндегі тау жыныстары қысымының және тау жыныстарының сілемінің деформациясының қайта таралуы

***Мусин Р.А., Ахматнуров Д.Р., Замалиев Н.М.**

КЕАҚ Әбілқас Сағынов атындағы Қарағанды техникалық университеті, Қарағанды, Қазақстан

Мақала келді: *25 қыркүйек 2025*
Сараптамадан өтті: *2 қазан 2025*
Қабылданды: *18 қараша 2025*

ТҮЙІНДЕМЕ

Бұл зерттеу Қарағанды көмір алабында жыныс сілеміндегі тау қысымының қайта бөлінуі мен соған ілеспе деформациялық үдерістерді қарастырады. Жер асты қазбаларының айналасындағы тірек қысымы, түсіру және ыдырау аймақтарының геометриясы мен параметрлері, сондай-ақ олардың газ-динамикалық құбылыстардың көріністеріне әсері қарастырылады. Әдістемелік негізге қолданылған геомеханикалық модельдерге сыни шолу, аймақтардың енін қабаттың тереңдігі мен қалыңдығына байланысты бағалауға арналған есептеу және графикалық номограммалар, сондай-ақ 75-90° шекті бұрыштарда өндірілген кеңістік шекараларынан кернеуі жоғары аймақтардың схемалық құрылысы кіреді. Игеру тереңдігі шамамен 500 м-ге дейін артқан кезде аймақтардың конфигурациясы төмен қарай тарылуға бейім сына тәрізді сипатқа ие болатыны анықталды; қабат қалыңдығының ұлғаюы

	әсер ету аймақтарының кеңеюіне әкеледі. Литологиялық бөлім қауіпті аймақтардың орналасуын бақылайды: әлсіз қабатты балшық тастар мен алевролиттер декомпрессияны жеделдетеді, ал күштірек құмтастар кенеттен атқылаулар мен тау жыныстарының жарылу ықтималдығы жоғарылайтын кернеу шоғырланған күмбез тәрізді аймақтарды құрайды. Тексеру мысалы ретінде көмір мен газдың кенеттен шығарындыларының бір эпизоды талданды. Нақты қирау шекараларын есептелген сына тәрізді кернеу аймағымен салыстыруға болады, бұл мәлімделген болжамдар шеңберінде таңдалған тәсілдің дұрыстығын растайды. Нәтижелердің практикалық маңыздылығы ~400 м-ден астам тереңдікте міндетті кешенді болжау үшін шекті шарттарды нақтылауда, есептеулерді тексеру үшін үнемі аспаптық бақылауды негіздеуде және қабаттардың қалыңдығы мен тереңдігін ескере отырып, қорғаныс тіректерінің параметрлерін түзетуде жатыр. Зерттеу нәтижелері қауіпті шығарындылар жағдайында тазалау және дайындық жұмыстарын жоспарлау және қауіпсіз жүргізу кезінде пайдаланылуы мүмкін.
	Түйін сөздер: тірек қысымы, түсіру аймақтары, дезинтеграция, қазу тереңдігі, қабат қалыңдығы, литология.
Мусин Равиль Альтавович	***Авторлар туралы ақпарат:*** *PhD, қауымдастырылған профессор, КЕАҚ Әбілқас Сағынов атындағы Қарағанды техникалық университеті, Қарағанды, Қазақстан. Email: R.A.Mussin@mail.ru; ORCID ID: https://orcid.org/0000-0002-1206-6889*
Ахматнуров Денис Рамильевич	*PhD, зертхана жетекшісі, КЕАҚ Әбілқас Сағынов атындағы Қарағанды техникалық университеті, Қарағанды, Қазақстан. Email: d.akhmatnurov@gmail.com; ORCID ID: https://orcid.org/0000-0001-9485-3669*
Замалиев Наиль Мансурович	*PhD, қауымдастырылған профессор, КЕАҚ Әбілқас Сағынов атындағы Қарағанды техникалық университеті, Қарағанды, Қазақстан. Email: nailzamaliev@mail.ru; ORCID ID: https://orcid.org/0000-0003-0628-2654*

Перераспределение горного давления и деформации массива пород в условиях Карагандинского угольного бассейна

***Мусин Р.А., Ахматнуров Д.Р., Замалиев Н.М.**

НАО Карагандинский технический университет имени Абылкаса Сагинова, Караганда, Казахстан

Поступила: *25 сентября 2025*
Рецензирование: *2 октября 2025*
Принята в печать: *18 ноября 2025*

АННОТАЦИЯ

Работа посвящена анализу перераспределения горного давления и связанных с ним деформационных процессов в условиях Карагандинского угольного бассейна. Рассматриваются геометрия и параметры зон опорного давления, разгрузки и дезинтеграции вокруг подземных выработок, а также их влияние на проявления газодинамических явлений. Методическая основа включает критический обзор применяемых геомеханических моделей, расчетно-графические номограммы для оценки ширины зон как функций глубины залегания и мощности пласта, а также схемное построение областей повышенных напряжений от границ выработанного пространства под предельными углами 75–90°. Установлено, что при увеличении глубины разработки до порядка 500 м конфигурация зон приобретает клиновидный характер с тенденцией к сужению книзу; рост мощности пласта приводит к расширению областей влияния. Литологический разрез контролирует локализацию опасных зон: слабослоистые аргиллиты и алевролиты ускоряют разуплотнение, тогда как более прочные песчаники формируют куполообразные области концентрации напряжений с повышенной вероятностью внезапных выбросов и горных ударов. В качестве верификационного примера проанализирован эпизод внезапного выброса угля и газа. Фактические границы разрушения сопоставимы с расчетной клиновидной зоной повышенных напряжений, что подтверждает корректность выбранного подхода в пределах заявленных допущений. Практическая значимость результатов состоит в уточнении пороговых условий для обязательного комплексного прогноза на глубинах свыше ~400 м, в обосновании регулярного инструментального контроля для верификации расчетов и в корректировке параметров охранных целиков с учетом мощности пластов и глубины. Полученные выводы могут быть использованы при планировании и безопасном ведении очистных и подготовительных работ в выбросоопасных условиях.

Ключевые слова: опорное давление; зоны разгрузки; дезинтеграция; глубина разработки; мощность пласта; литология.

Мусин Равиль Альтавович

Информация об авторах:
PhD, Ассоциированный профессор, НАО Карагандинский технический университет имени Абылкаса Сагинова, Караганда, Казахстан. Email: R.A.Mussin@mail.ru; ORCID ID: https://orcid.org/0000-0002-1206-6889

Ахматнуров Денис Рамильевич	*PhD, руководитель лаборатории, НАО Карагандинский технический университет имени Абылкаса Сагинова, Караганда, Казахстан. Email: d.akhmatnurov@gmail.com; ORCID ID: https://orcid.org/0000-0001-9485-3669*
Замалиев Наиль Мансурович	*PhD, Ассоциированный профессор, НАО Карагандинский технический университет имени Абылкаса Сагинова, Караганда, Казахстан. Email: nailzamaliev@mail.ru; ORCID ID: https://orcid.org/0000-0003-0628-2654*

References

[1] Kuznetsov VS. Geomekhanika podzemnykh vyrabotok [Geomechanics of Underground Workings]. Moscow: Nedra. 1983, 256. (in Russ.).

[2] Nozhkin NV. Gidroraschlenenie (gidrorazryv) ugol'nykh plastov [Hydraulic Dissection (Hydraulic Fracturing) of Coal Seams]. Moscow: Gornaya Kniga. 1965, 214. (in Russ.).

[3] Sakhno VP, et al. Upravlenie gornym davleniem na ugol'nykh shakhtakh [Control of Rock Pressure in Coal Mines]. Donetsk: Donbass. 1990, 312. (in Russ.).

[4] Ermekov MA. Gazonosnost' uglenosnykh tolshch i gazovydelenie shakht Karagandinskogo basseina: avtoreferat dissertatsii doktora geologo-mineralogicheskikh nauk [Gas Content of Coal-Bearing Deposits and Gas Emission of Mines in the Karaganda Basin: Doctoral Dissertation Abstract. Geol.–Miner. Sci. Alma-Ata. 1963, 63. (in Russ.).

[5] Tanekeyeva GD, Abeuov EA, Makhmudov DR, Mussin RA, Balabas AYu. Issledovanie geomekhanicheskikh uslovii provedeniya i podderzhaniya kvershlagov [Study of Geomechanical Conditions for Driving and Maintaining Crosscut Mine Workings]. Ugol'. Coal. 2023; 2:31–33. (in Russ.). https://doi.org/10.18796/0041-5790-2023-2-31-33

[6] Airuni AT, et al. Formy svyazyvaniya metana s uglem [Forms of Methane Bonding with Coal]. Gorny Zhurnal (Mining Journal). 1990; 7:45–52. (in Russ.).

[7] Zaburdyaev VS. Parametry degazatsii v vysokoproizvoditel'nykh ochistnykh raionakh na nerazvedannykh shakhtnykh polyakh [Parameters of Degassing in High-Productivity Longwall Districts on Unexplored Mine Fields]. Bezopasnost' truda v promyshlennosti [Occupational Safety in Industry]. 2021; 2:63–68. (in Russ.).

[8] Akhmatnurov D, Zamaliyev N, Mussin R, Demin V, Ganyukov N, Zagórski K, Skrzypkowski K, Korzeniowski W, Stasica J. Optimization of reinforcement schemes for stabilizing the working floor in coal mines based on an assessment of its deformation state. Materials. 2025; 18(13):3094. https://doi.org/10.3390/ma18133094

[9] Zhang R, Hao C. Research on the development of hydraulic flushing caverns for gas extraction in soft, low-permeability tectonic coal seams in China. ACS Omega. 2022; 7(25):21615–21623. https://doi.org/10.1021/acsomega.2c01465

[10] Mu SY, Ma Z. Analysis of the mechanism of deformations and auxiliary technology for swelling of the rocky roadbed in deep complex geological conditions. Coal Mines. 2016; 47:95–98.

[11] Skrzypkowski K, Korzeniowski W, Stasica J. Rock mass behavior around roadways in deep mines. Archives of Mining Sciences. 2021; 66(4):679–696. https://doi.org/10.24425/ams.2021.139586

[12] Cai M, Kaiser PK. Numerical simulation of the rock-mass failure process at deep-level mines. International Journal of Rock Mechanics and Mining Sciences. 2018; 104:99–112.

[13] Lobanov NN. Dinamicheskie yavleniya na ugol'nykh shakhtakh [Dynamic Phenomena in Coal Mines]. Moscow: Nedra. 1987, 280. (in Russ.).

[14] Wu Q, Li X, Wang E. Numerical simulation of stress redistribution around coal-mining workings. International Journal of Mining Science and Technology. 2019; 29(2):243–251.

[15] Shabarov VV, Skrzypkowski K, Zamaliyev NM. Geomechanical problems of mining at large depths in the Karaganda Coal Basin. Mining of Mineral Deposits. 2023; 17(3):1–12.

[16] Sadchikov AV, Zamaliyev NM, Akhmatnurov DR, Mussin RA, Ganyukov NYu. Primenenie metodov marksheyder-sko-geofizicheskikh issledovanii dlya resheniya zadach geologii [Application of Mine-Geophysical Methods to Solving Problems of Geology]. Gorny informatsionno-analiticheskii byulleten' (Mining Informational and Analytical Bulletin). 2025; 6:109–124. (in Russ.).

[17] Hoek E, Brown ET. Practical estimates of rock-mass strength. International Journal of Rock Mechanics and Mining Sciences. 1997; 34(8):1165–1186. https://doi.org/10.1016/S1365-1609(97)80069-X

[18] Salamon MDG, Munro AH. A study of the strength of coal pillars. Journal of the South African Institute of Mining and Metallurgy. 1967; 68(2):55–67.

[19] Brady BHG, Brown ET. Rock Mechanics for Underground Mining. 4th ed. Heidelberg: Springer. 2013, 628. ISBN 978-94-007-7078-1.

[20] Peng SS. Longwall Mining. 3rd ed. Englewood, CO: Society for Mining, Metallurgy & Exploration. 2019, 621. ISBN 978-0-87335-445-3.

[21] Pat. 195044 KZ. Povyshenie bezopasnosti vedeniya gornykh rabot za schet uluchsheniya kachestva krepleniya [Improving the Safety of Mining Operations by Enhancing Support Quality]. Mussin RA, Balabas AYu, Doni DS, Alzhanova AM, Madiyarov TA, Dalibaev AZh, Kalmurzin EG, Kim RS. Opubl. 23.02.2023, 2. (in Russ.).

[22] Pat. 342325 KZ. Ustroystvo dlya gasheniya udarnoy volny [Device for Damping a Shock Wave]. Zamaliyev NM, Akhmatnurov DR, Mussin RA, Ganyukov NYu, Golik AV, Schmidt-Fedotova IM. Opubl. 23.01.2025, 1. (in Russ.).

[23] Barton N, Lien R, Lunde J. Engineering classification of rock masses for the design of tunnel support. Rock Mechanics. 1974; 6(4):189–236.

[24] Peng SS. Coal Mine Ground Control. 3rd ed. Morgantown: West Virginia University. 2008, 458.

[25] Kaiser PK, McCreath DR, Tannant DD. Canadian Rockburst Support Handbook. Sudbury, Ontario: Geomechanics Research Centre. 1996, 314.

[26] Whittaker BN, Reddish DJ. Subsidence: Occurrence, Prediction and Control. Amsterdam: Elsevier. 1989, 528.

Crossref
DOI: 10.31643/2027/6445.17
Earth and Planetary Sciences: Earth-Surface Processes

creative commons

Innovative technologies for paraffin deposit removal in oil tubing to enhance oil recovery: a mechanical approach

[1] Alisheva Zh.N., [2] Sarsenbayev M.A., [3] Sarsenbaev Zh.A., [4*] Baibotaeva S. E.

[1] D.A. Kunayev Institute of Mining, Almaty, Kazakhstan
[2] LLP Scientific and Technological Park of Al-Farabi Kazakh National University, Almaty, Kazakhstan
[3] LLP Innovation Plus, Almaty, Kazakhstan
[4] M. Auezov South Kazakhstan University, Shymkent, Kazakhstan

** Corresponding author email: sbaibotaeva@mail.ru*

Received: *April 22, 2025*
Peer-reviewed: *August 6, 2025*
Accepted: *November 18, 2025*

ABSTRACT

Asphaltene - resin - paraffin deposits (ARPD) on the inner wall of production tubing shorten service intervals, elevate operating expenditures, and frequently induce downtime at mature fields. This paper presents the design and field performance of a rod-driven in-well scraper that provides continuous tubing cleaning during routine sucker-rod operation without chemical dosing or surface interventions. The scraper sub is inserted into the rod string and is compatible with Ø73 - 89 mm tubing and Ø19 - 22 mm rods. Performance was evaluated on a before/after basis using the inter-cleaning period (ICP), downtime, and annual cleaning costs, with extrapolation to multi-well programs. Field deployments of model CP TP ST 01KZ achieved an ICP of 144 - 280 days with zero cleaning-induced downtime (0 days yr^{-1}). Annual cleaning costs were ~0.265 million KZT per well (scheduled service only), which is ≈31× lower than hot-wash budgets on the same asset. The implied per-well saving is ≈7.94 million KZT yr^{-1}; for a 50-well program, this corresponds to ≥397 million KZT yr^{-1} in avoided expenditure. Continuous in-well action of the reciprocating toothed head on each rod stroke disrupts the boundary wax layer and limits deposit regrowth between services, eliminating periodic thermal/chemical treatments and their logistics. The subassembly mass (≈30 kg) permits installation with standard handling; the pump string configuration is unchanged apart from the insertion of the scraper section. Compared with thermal, chemical, and batch mechanical methods, the technology extends service intervals, removes cleaning-related shut-ins, and compresses the cleaning budget to a predictable, low annual service cost. The results support routine use of rod-driven scraping for ARPD control in wax-prone wells and provide quantitative guidance for field-scale rollout and further optimization (wear resistance, centralization tolerances, and application in deviated completions).

Keywords: paraffin deposits, tubing cleaning, mechanical scraper, enhanced oil recovery, sucker rod motion, mature oil fields.

Information about authors:

Alisheva Zhanat Nurkuatovna — *PhD, Senior Researcher, D.A. Kunayev Institute of Mining, Abay str., 191, 050046, Almaty, Kazakhstan. Email: zhannat_86.2007@mail.ru; ORCID ID: https://orcid.org/0000-0003-0929-4984*

Sarsenbayev Mukhtar Abdikalykovich — *Director, LLP Scientific and Technological Park of Al-Farabi Kazakh National University, al-Farabi Ave., 71, 050040, Almaty, Kazakhstan. Email: mukhtar.sarsenbaev@mail.ru; ORCID ID: https://orcid.org/0009-0006-0644-4886*

Sarsenbaev Zhasulan Abdigapparovich — *Engineer, LLP Innovation Plus, Tole Bi Street str., 90, 050031, Almaty, Kazakhstan. Email: zhasstin@mail.ru; ORCID ID: https://orcid.org/0009-0003-3895-4985*

Baibotaeva Saltanat Elikbaevna — *PhD, Associate Professor, M. Auezov South Kazakhstan University, Tauke Khan Ave., 5, 160012, Shymkent, Kazakhstan. Email: sbaibotaeva@mail.ru; ORCID ID: https://orcid.org/0000-0002-9406-3322*

Introduction

Asphaltene - resin - paraffin deposits (ARPD) precipitate as temperature and pressure decline along the production path and accumulate on the inner surface (ID) of production tubing and other flow components. The resulting organic scaling increases hydraulic resistance and lifting energy demand, accelerates wear of downhole equipment, and triggers recurrent interventions and shut-ins, ultimately depressing well deliverability and field economics.

The problem is global: wax-prone crudes and cold environments are encountered across major petroleum provinces. Chemical (solvent/inhibitor), thermal (hot-wash), and batch mechanical methods are widely applied to mitigate ARPD, each with well-known advantages and trade-offs; nonetheless, these approaches are logistics-intensive, shutdown-dependent, and often transient under high-wax

conditions, with additional concerns related to operating cost and HSE performance [[1], [2], [3]].

In Kazakhstan, paraffin-related complications are especially pronounced at Tengiz, Karazhanbas, Zhetybay, and Uzen. High paraffin content, significant cooling during lifting and transport, and complex well architectures promote rapid deposition within tubing, casing, and flowlines, increasing intervention frequency, extending downtime, and compressing margins at mature assets [4]. These operating realities motivate solutions that can control ARPD without recurring surface operations or chemical dosing and without interrupting routine production.

Objective, prior work, and contribution. Building on prior thermal, chemical, and batch-mechanical practices—which remain standard but require shut-ins, recurring logistics, and reagent handling—this study develops and field-evaluates a patented reverse-motion, rod-driven in-well scraper (model CP-TP-ST-01KZ) that delivers continuous tubing cleaning during routine sucker-rod operation, with no chemical dosing or surface interventions. We quantify performance on a before/after basis at Kazakhstani assets using three primary metrics: inter-cleaning period (ICP), cleaning-induced downtime, and cleaning-related OPEX. Field deployments demonstrate multi-month ICP (144 - 280 days) with zero cleaning-induced downtime, and compress annual cleaning costs to ≈ 0.265 million KZT per well, which is ~31× lower than hot-wash programs; this corresponds to ≈ 7.94 million KZT per well-year in avoided expenditure and ≥ 397 million KZT yr^{-1} for a 50-well program. The scraper sub integrates into standard strings (Ø73 - 89 mm tubing, Ø19 - 22 mm rods) and adds minimal handling mass (~30 kg). We show, from field deployments, that continuous, power-free in-well mechanical control sustains multi-month service intervals and removes cleaning-related shut-ins, and we quantify its techno-economic advantage over conventional regimes at mature Kazakhstani fields. We also document industrial-readiness credentials—patent protection, conformity to EAEU technical regulations, and verified domestic value content (CT-KZ) - which support scale-up within import-substitution programs [5].

Figure 1 illustrates the decline in well production rate during operation as a result of paraffin deposit accumulation. This highlights the necessity of implementing innovative cleaning methods, such as the mechanical rod scraper.

The economic impact of paraffin deposition in Kazakhstan includes substantial expenditures on pipeline cleaning, equipment repair, and a decline in production volumes. Moreover, the environmental implications are also significant, as chemical treatments commonly employed to mitigate paraffin formation may pose ecological risks [6].

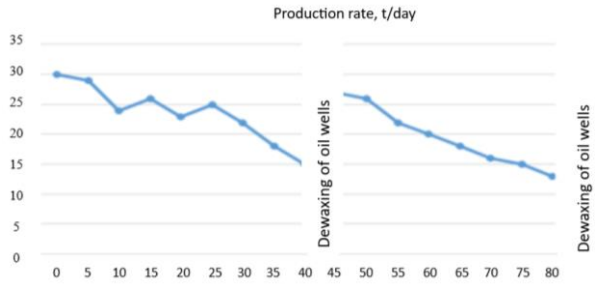

Figure 1 – Dynamics of production rate decline in a well affected by paraffin deposition during operational period

Experimental Section

Study area and materials. This study evaluates a rod-driven, reverse-motion in-well scraper for continuous mitigation of asphaltene - resin - paraffin deposits (ARPD) on the inner surface of production tubing during routine sucker-rod operation. The test envelope covered tubing strings (TBS) with nominal sizes of Ø73 - 89 mm and sucker rods Ø19 - 22 mm. Pilot trials were conducted at the Uzen oilfield (Mangystau, Kazakhstan) on Well No. 118 (GU-90), No. 2734 (GU-34), and No. 6095 (GU-15).

Representative deposit samples were characterized to quantify paraffin, resin, and asphaltene fractions and to assess flow and crystallization behavior under controlled laboratory conditions. Field operating context during the test period was: reservoir pressure 9.0 - 9.5 MPa and temperature 50 - 60 °C; the produced crude contained 12 - 15 wt.% paraffins, exhibited a viscosity of 120 - 150 mPa·s at 20 °C, and had a water cut of 85 - 95%.

1. Solvent extraction and gravimetry (resins/asphaltenes; paraffins by difference). A Soxhlet extraction system (Büchi B-811, Büchi Labortechnik AG, Switzerland) was used to fractionate deposit samples. Post-extraction masses were determined gravimetrically on an analytical balance (Mettler Toledo XS205DU, Mettler-Toledo GmbH, Switzerland; readability ±0.01 mg). Fractions were dried to constant mass and reported as wt.% of the initial sample. The paraffin (wax) fraction was obtained either by dedicated assay or by mass-balance difference from the measured resin and asphaltene fractions. Across representative

samples, the deposits were found to contain 40 - 60 wt.% wax, 10 - 15 wt.% asphaltenes, and 20 - 30 wt.% resins, values consistent with ranges reported for wax-prone mature fields [6]. All gravimetric determinations were performed in at least three technical replicates with verification of mass-balance closure.

2. Viscosity of crude oil. Dynamic viscosity was measured using a rotational viscometer (Brookfield DV3T, AMETEK Brookfield, USA). Samples were thermostated and equilibrated at the target temperature before measurement. Dynamic viscosity between 20 - 40 °C decreased with temperature, consistent with datasets for paraffinic crudes of comparable composition [[7], [8]]. All measurements adhered to ASTM D445 temperature-control and repeatability requirements, and each condition was tested in at least three technical replicates.

3. Wax solidification temperatures. Wax appearance, crystallization, and solidification behavior were determined by differential scanning calorimetry (DSC 214 Polyma, NETZSCH-Gerätebau GmbH, Germany). The analysis reported onset, peak, and endset temperatures associated with wax crystallization/solidification for the deposit/crude matrix.

4. Field operating parameters. Reservoir pressure, temperature, and water-cut values contemporaneous with sampling were taken from field operating logs and are provided above to contextualize the laboratory measurements [[7], [8], [9]].

Research Objectives. The primary objective of this study is to design and implement an innovative mechanical device—a rod scraper—for cleaning oil wells from paraffin and other solid deposits. The device is intended to mitigate operational challenges associated with ARPD, which significantly reduce well productivity, increase equipment wear, and lead to higher maintenance and repair costs. The scraper operates based on the reciprocating motion of sucker rods, ensuring continuous cleaning of the inner surface of the tubing without interrupting oil production.

As part of the study, the following tasks were accomplished:

- The design of the rod scraper was optimized to enhance the efficiency of paraffin removal from the inner surfaces of tubing and sucker rods.
- Pilot field tests of the device were conducted at wells No. 118 of GU-90, No. 2734 of GU-34, and No. 6095 of GU-15 operated by JSC “Ozenmunaigas”, under various geological and technical conditions.
- A comparative analysis was performed between the proposed method and existing cleaning technologies (thermal, chemical, and other mechanical methods) in terms of efficiency, environmental safety, and economic feasibility.

Geological Characteristics of the Pilot Testing Site – Uzen Oilfield. The Uzen oilfield, located in the Mangystau region of the Republic of Kazakhstan, is one of the largest fields in the region and has been operated by JSC “Ozenmunaigas” since the early 1960s. Pilot field tests of the mechanical device for cleaning tubing from paraffin deposits were conducted at wells No. 118 (GU-90), No. 2734 (GU-34), and No. 6095 (GU-15), located within the Uzen structural zone.

The productive horizons are associated with Jurassic-age deposits, predominantly represented by terrigenous formations formed under deltaic-alluvial sedimentation conditions. Of particular interest are horizons XIII - XIV (Callovian stage), identified at depths ranging from 1,150 to 1,350 meters, as shown in the stratigraphic section along line P - P’ and the structural map of the top of horizon XIII. These reservoirs are composed primarily of siltstone-sandstone sequences interbedded with argillites and sandstones, exhibiting good reservoir properties.

The upper part of the lithological-stratigraphic section consists of Albian deposits (horizons VI - VIII), while the main productive interval belongs to the Jurassic formation, beginning with horizon XIII, which is oil and gas-saturated. The dominant lithologies include sandstones, argillites, and siltstones with occasional conglomerate layers and interbedding.

The formation fluids are characterized by high viscosity (up to 150 mPa·s at 20 °C), paraffin content of up to 12 - 15%, and water cut ranging from 85% to 95% at the tested wells. Reservoir pressure varies between 9.0 and 9.5 MPa, with the formation temperature averaging around 55 °C.

The physicochemical properties of the crude oil are marked by elevated paraffin content (up to 12 - 15%) and high viscosity, reaching 120 - 150 mPa·s at 20 °C. The water cut of the wells reaches 80 - 95%, necessitating the use of specialized technologies to manage deposition and optimize production regimes.

Such geological and physical characteristics result in intense paraffin deposition within tubing, making these wells representative of water-cut and paraffin-prone systems—suitable candidates for evaluating the effectiveness of mechanical cleaning technologies.

Table 1 – Generalized Geological and Production Characteristics of the Productive Reservoirs of the Uzen Oilfield

Geological and Reservoir	
Parameter	**Value**
Reservoir type	Terrigenous (siltstone-sandstone)
Productive horizons	XIII - XIV (Callovian stage)
Depth of occurrence	1.200 – 1.350 m
Effective porosity	17 - 20%
Permeability	0.05 - 0.2 µm²
Reservoir pressure	9.0 - 9.5 MPa
Reservoir temperature	50 - 60 °C
Water cut	85 - 95%
Technological Conditions	
Crude oil pour point (max)	Up to +35 °C
Gas factor	20 - 40 m³/t
Saturation pressure	5.5 - 6.0 MPa
ARPD characteristics	Intensive deposition
Operational features	Frequent tubing cleaning, high water cut

Table 1 summarizes the principal geological, reservoir, and operational parameters of the Uzen oilfield, providing a basis for evaluating the influence of thermobaric conditions, water cut, and reservoir structure on the performance of the mechanical tubing cleaning technology for paraffin removal.

Table 2 – Physicochemical Properties of Crude Oil by Reservoirs of the Jurassic Complex (J I - J VIII)

Parameter	**J I**	**J II**	**J III**	**J VI**	**J VIII**
Density, g/cm³	0.849	0.849	0.851	0.863	0.822
Viscosity, cSt (at 40 °C)	15.78	8.5	12.45	15.31	3.4
Paraffin content, wt.%	27.0	23.4	22.4	16.51	–
Resin content (silica gel), wt.%	11.0	27.0	12.45	14.0	–
Asphaltene content, wt.%	–	–	–	–	5.4
Sulfur content, wt.%	0.17	0.13	0.17	0.22	–
Pour point, °C	31	30	30	30	–
Flash point, °C	-15	-15	-13	–	–

Table 2 presents a stratified characterization of crude oil from the main productive horizons of the Jurassic complex. The values of density, viscosity, and the content of paraffins, resins, and asphaltenes confirm a high tendency for ARPD formation, particularly in intervals J I - J III, which are considered the least favorable in terms of operational conditions.

Figure 2 shows geological cross-sections along lines I-I ’ and II-II ’, passing through the central part of the Uzen oilfield. The sections illustrate the structure of the productive horizons, including XIII and XIV (Callovian stage), which were the focus of the pilot field tests.

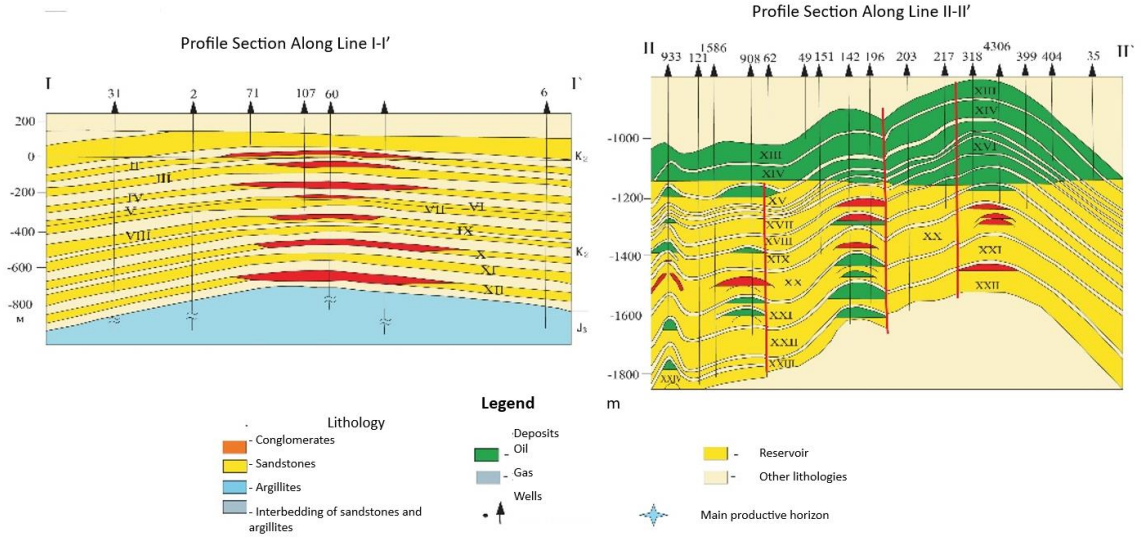

Figure 2 – Geological Cross-Sections of the Uzen Oilfield (Lines I-I’ and II-II’)

Alternating layers of sandstones, siltstones, and argillites forming the oil-bearing zone are clearly traced. The cross-sections also depict the thickness variability, discontinuity of the reservoirs, and a characteristic anticlinal structural pattern, confirming favorable conditions for hydrocarbon accumulation and justifying the selection of wells No. 118, No. 2734, and No. 6095 for the experimental trials.

Operating Principle of the Device. Full name and model. Reverse-motion, rod-driven in-well scraper, model CP-TP-ST-01KZ (manufacturer: Kazakhstan - China). Certificate No. 5104620; Chinese utility model patent CN ZL 2015 2 0892020.4 and industrial design ZL 2016 3 0164862.8 (covering a functionally similar scraper architecture); conformity with EAEU technical regulations; verified domestic value content (CT-KZ).

The operating principle of the device is based on the reciprocating motion of the sucker rod. During this motion, the scraper—equipped with reversible elements—cleans the inner surface of the tubing without requiring a well shutdown. The reversible teeth and springs adapt to the direction of movement, ensuring cyclic removal of deposits along the working section of the pipe**.**

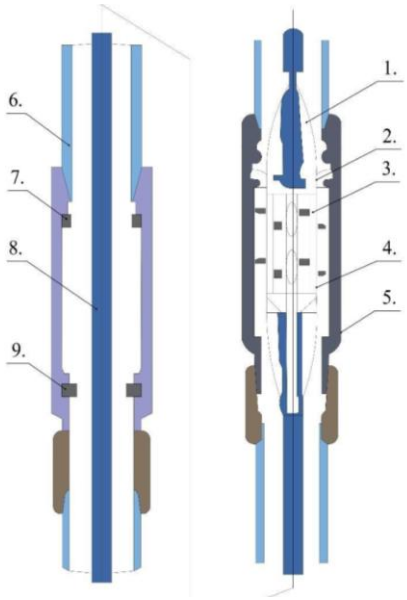

Figure 3 – Schematic Diagram of the Device

The proposed device consists of a set of functional components designed to provide mechanical cleaning of the inner surface of tubing during well operation:

1. Flexible guides – Ensure central alignment of the device within the tubing string, minimizing the risk of contact with the walls and improving stroke stability.
2. Unidirectional ring – Locks the device in the desired direction of movement, preventing slippage during the return stroke of the rod.
3. Spring plate – The main working element that maintains contact with the inner wall of the tubing and removes paraffin deposits through frictional force.
4. Reversible tooth – Engages the change in movement direction of the scraper, enabling cyclic operation under reciprocating motion.
5. Upper limiter (commutator) – Restricts the upward travel of the device and defines the upper boundary of the cleaning interval.
6. Tubing (TBS) – A component of the production string where paraffin deposits typically form on the inner surface.
7. Lower limiter (commutator) – Limits the downward movement of the device and defines the lower boundary of the cleaning zone.
8. Sucker rod – Serves as the drive mechanism for scraper movement, providing reciprocating motion as part of the downhole pump assembly.
9. Locking ring – Prevents displacement of individual structural components during operation and ensures reliable fixation of all assembled elements.

This configuration enables continuous cleaning of the tubing without the need for well shutdown or equipment disassembly. The use of reversible and guiding elements ensures effective scraper performance under various tubing diameters and curvatures of production strings.

Figure 3 presents a schematic diagram of the device for cleaning the inner surface of tubing.

Comparison with Existing Methods. The issue of paraffin deposition in oil production is traditionally addressed using various approaches, including mechanical, chemical, thermal, and combined methods. However, each of these techniques has its own advantages and limitations. This section presents a comparative analysis of the developed mechanical device (rod scraper) against existing paraffin removal technologies.

Table 3 provides a comparative assessment of the proposed technology in relation to conventional methods for paraffin deposit removal [[10], [11], [12]].

Table 3 – Comparative Analysis of the Proposed Technology and Existing Methods for Paraffin Deposit Removal

№	Criterion	Mechanical Methods	Chemical Methods	Thermal Methods	Combined Methods	Proposed Rod Scraper
1	Operating principle	Mechanical removal of paraffin using rigid scrapers	Paraffin dissolution by chemical reagents	Heating of oil and tubing to melt deposits	Combination of chemical, mechanical, and thermal techniques	Removal of deposits through reciprocating motion of sucker rods
2	Need to shut down production	Required for scraper replacement	Not required, reagents injected into the flow	Required for steam or hot oil treatment	Partially required, depending on the method combination	Not required; cleaning occurs during normal well operation
3	Energy efficiency	Moderate, requires periodic scraper retrieval	High costs due to reagent usage	High energy consumption for heating	High due to complexity of integrated treatment	High, no external power supply needed
4	Environmental safety	Moderate, removed paraffin may require disposal	Low, potential environmental contamination by chemicals	Low, due to high energy demand and possible reservoir damage	Low, combined chemical and thermal impact intensifies risks	High, no chemicals or energy-intensive processes used
5	Implementation complexity	Moderate, requires equipment replacement	Moderate, requires chemical injection systems	High, requires installation of heating systems	Very high, complex coordination of technologies required	Low, easily integrated into existing systems without modification
6	Need for continuous monitoring	High, due to wear of mechanical parts	High, constant reagent dosing required	High, temperature control required	Very high, all systems require monitoring	Low, operates via rod movement without external control
7	Durability and reliability	Moderate, requires regular maintenance	Moderate, potential buildup of by-products in tubing	Low, frequent overheating may damage reservoir	Moderate, control system complexity reduces reliability	High, minimal wear during long-term use

Table 4 – Opportunities for Development and Scaling of the Rod Scraper Technology

№	Direction	Description
1	Horizontal and deviated wells	Adaptation of the design for operation in complex well trajectories, including multilateral wells.
2	Design and material improvement	Enhancement of wear resistance and corrosion protection; optimization of reversible elements and springs to reduce drag.
3	Integration of digital solutions	Implementation of monitoring and AI-based analytics to assess cleaning efficiency and predict deposit formation.
4	Combination with other methods	Integration with chemical inhibitors and thermal flushing to enhance the overall cleaning effect.
5	Scaling and commercialization	Deployment across oilfields in Kazakhstan and export of the technology to regions facing similar challenges.

Unlike conventional mechanical devices, the proposed scraper operates in a cyclic mode activated by the reciprocating motion of the sucker rod, which extends the interval between cleanings and reduces maintenance costs [[13], [14], [15], [16]].

Thus, further development and refinement of the technology will significantly enhance oil production efficiency, reduce operating costs, and minimize the negative impact of paraffin deposits on oilfield infrastructure [[17], [18], [19], [20], [21]]. As Table 4 indicates, further development and refinement of the technology will improve efficiency and reduce costs.

Discussion of Results

A three-well pilot (No. 118, 2734, 6095) confirmed the efficacy of the rod scraper under representative Uzen operating conditions. Paraffin accumulation decreased sufficiently to extend the inter-cleaning period (ICP; defined as the elapsed time between consecutive mechanical wax-removal events) from 7 - 10 days (baseline) to 30 - 45 days (pilot), i.e., a ≈3 - 6× increase and a ≈70 - 85% reduction in intervention frequency. All chemical reagents previously applied for dewaxing were discontinued at the pilot wells, and daily oil rates remained within the pre-pilot variability band, indicating no adverse impact on production.

Operating conditions (high water cut, elevated wax content/viscosity at surface temperatures, and a typical Uzen thermobaric regime) are characteristic of mature Kazakh assets, supporting applicability to analogous well stock. Importantly, deployment did not require well shut-in or modification of the pumping assembly, avoiding deferred production associated with conventional cleaning routines.

To ensure that ICP gains reflected genuine wax-control performance rather than scheduling artifacts, effectiveness was tracked via routinely available indicators: (i) the count of mechanical cleaning events per month, (ii) torque/load trends on the rod string and drive amperage, and (iii) wellhead pressure/ΔP stabilization between cleanings. These independent indicators improved coherently with the ICP extension.

The field outcome is consistent with laboratory characterization: deposits rich in paraffin (≈40 - 60 wt.%) and DSC evidence of wax crystallization near operating temperatures, together with temperature-dependent viscosity measured on the crude, provide a mechanistic basis for the observed reduction in deposition frequency. Maintaining flow above the crystallization onset and regularly disrupting nascent structure with the scraper plausibly suppresses layer growth and delays critical thickness.

The magnitude of ICP extension aligns with ranges reported for mechanical wax-control approaches in paraffinic, high-water-cut systems and, in several cases, exceeds them, while eliminating solvent use [8]. From an HSE and sustainability perspective, removing solvent treatments reduces chemical handling and personnel exposure; fewer interventions also decrease energy use and operational risk. Limitations include the three-well scope and a finite observation window; broader deployment should include longer monitoring to capture seasonality, quantification of removed wax mass or thickness where feasible, and stratified analysis by water cut and fluid rheology. Even with these caveats, the pilot provides operationally actionable evidence that the rod scraper is a viable, lower-risk alternative to energy-intensive and environmentally burdensome dewaxing practices in wax-prone systems.

Conclusions

A mechanical rod scraper was developed and field-tested for cyclic in-well removal of paraffin deposits from tubing and sucker rods. Representative deposits contained 40-60 wt.% wax, 10-15 wt.% asphaltenes, and 20-30 wt.% resins. Differential scanning calorimetry showed a crystallization onset overlapping field operating temperatures (≈50-60 °C), indicating elevated deposition risk. The crude contained 12-15 wt.% paraffins and had a viscosity of 120-150 mPa·s at 20 °C, decreasing across 20-40 °C in line with datasets for paraffinic crudes of comparable composition [[6], [8]]. Measurements followed ASTM D445 with at least three technical replicates per condition.

In pilot operation, the inter-cleaning period (ICP) increased from 7-10 days (baseline) to 30-45 days with the scraper, a 3-6× extension corresponding to ~70-85% fewer interventions under 9.0-9.5 MPa, 50-60 °C, and 85-95% water cut. Relative to conventional mechanical/chemical/thermal routines, the device delivered ICP gains that meet or exceed typical literature ranges for mechanical wax control (≈1.5-4×) while avoiding reagent use and

thermal energy input. These results indicate that maintaining operation above the crystallization onset and applying cyclic in-well scraping materially reduces wax-related maintenance in paraffin-prone mature fields.

Key operational advantages:

- Continuous operation. Scraping is driven by the reciprocating motion of the sucker rod, allowing deposit removal without production shutdown and extending ICP.
- Lower operating cost. Elimination of chemical reagents and thermal treatments reduces consumables and simplifies field procedures.
- Environmental and integrity benefits. No chemical exposure; reduced corrosion risk for tubing and downhole equipment.
- Drop-in integration. The scraper can be installed in existing pumping strings without major modifications.
- Adaptability. Compatible with a range of tubing diameters and operating profiles; applicable to paraffin-prone wells across mature Kazakhstani fields.

Recommendations

To maximize the benefits of the proposed technology and ensure its sustainable deployment, the following measures are recommended:

- Field-wide implementation at oilfields with high paraffin deposition potential (e.g., Tengiz, Zhetybay, Karazhanbas), with prioritization of wells exhibiting frequent plugging and high water cut.
- Optimization of operational parameters based on field-specific monitoring of scraper performance, allowing adjustment of stroke frequency, contact force, and cleaning interval.
- Integrated approach: In cases of severe deposition, the mechanical scraper may be combined with periodic thermal treatments to enhance cleaning efficiency without compromising equipment integrity.
- Further R&D: Investigation into material wear resistance and structural reliability under complex geological conditions, including horizontal and high-viscosity wells.
- Development of an automated monitoring system to track scraper performance in real time, enabling predictive maintenance and further improving operational safety and efficiency.

Conflict of Interest: On behalf of all authors, the corresponding author declares that there is no conflict of interest.

CRediT author statement: **Zh. Alisheva**: Conceptualization, Methodology, Supervision, Reviewing and Editing; **M. Sarsenbayev**: Data curation, Writing draft preparation; **Zh. Sarsenbaev**: Visualization, Investigation; **S. Baibotaeva**: Software.

This research did not receive any specific grant from funding agencies in the public, commercial, or not-for-profit sectors.

Cite this article as: Alisheva ZhN, Sarsenbayev MA, Sarsenbaev ZhA, Baibotaeva SE. Innovative technologies for paraffin deposit removal in oil tubing to enhance oil recovery: a mechanical approach. Kompleksnoe Ispolzovanie Mineralnogo Syra = Complex Use of Mineral Resources. 2027; 341(2):49-59. https://doi.org/10.31643/2027/6445.17

Мұнай өндіруді арттыру үшін мұнай құбырларын парафиндік шөгінділерден тазалаудың инновациялық технологиялары: механикалық әдіс

[1]Алишева Ж.Н., [2]Сарсенбаев М.А., [3]Сарсенбаев Ж.А., [4] Байботаева С.Е.

[1] Д.А. Қонаев атындағы Тау-кен істері институты, Алматы, Қазақстан
[2] әл-Фараби атындағы Қазақ Ұлттық Университетінің Ғылыми-технологиялық паркі ЖШС, Алматы, Қазақстан
[3] Инновациялар Плюс ЖШС, Алматы, Қазақстан
[4] М.Әуезов ат. Оңтүстік Қазақстан университеті, Шымкент, Қазақстан

ТҮЙІНДЕМЕ

Мұнай ұңғымалары құбырларының (ҰҚ) ішкі бетіндегі асфальт-шайыр-парафинді шөгінділер (АШПШ) құбырлардың қызмет көрсету мерзімін қысқартады, операциялық шығындарды арттырады және және кемелденген кен орындарының жиі тоқтап қалуына әкеледі. Жұмыста ұңғыішілік штангалы қырғыштың құрылымы және штангілі сорғының штаттық жұмысы кезінде ҰҚ-ны үздіксіз тазалау бойынша далалық сынақтардың нәтижелері ұсынылады; әдіс

Мақала келді: *22 сәуір 2025*
Сараптамадан өтті: *6 тамыз 2025*
Қабылданды: *18 қараша 2025*

химиялық дозалауды да, жер үстіндегі операцияларды да талап етпейді. Торап штангілер колоннасына енгізіледі және Ø73 - 89 мм НКҚ-мен, Ø19 - 22 мм штангілермен үйлесімді. Өнімділік енгізуге дейін/кейін салыстыру арқылы бағаланды: онда тазалаудың аралық кезеңі (ТАК), тоқтап тұру уақыты және тазалауға кететін жылдық шығын, әрі қарай көп ұңғымалы бағдарламаға таратылуы (экстраполяциялануы) ескеріліп жасалды. CP TP ST 01KZ моделі бойынша өндіріске енгізулер ТАК 144 - 280 тәулікке жеткізілді, ал тазалауға байланысты тоқтап тұру — 0 тәул/жыл. Тазалауға жылдық шығын ~0,265 млн KZT/ұңғы (тек регламенттік қызмет), бұл сол қордағы ыстық жуу бюджетінен шамамен 31 есе төмен. Тиісінше, бір ұңғымаға үнем ≈7,94 млн KZT/жыл құрайды; 50 ұңғы көлемінде жиынтық әсер ≥397 млн KZT/жыл үнемдейді. Штангінің әр жүрісінде кері-ілгері қозғалатын тісті бастиек ҰҚ ішіндегі шекаралық парафин қабатын бұзып, қызмет көрсету арасындағы шөгінді өсуін тежейді; бұл мерзімді термиялық/химиялық өңдеулер мен оларға байланысты болатын логистика қажеттілігін жояды. Тораптың массасы шамамен 30 кг, сондықтан монтаж стандартты құралдармен орындалады; қырғыш секциясын енгізуден басқа сорғы колоннасының компоновкасы өзгермейді. Жылулық, химиялық және механикалық тәсілдермен салыстырғанда ұсынылған технология сервистік мерзім аралығын ұзартады, тазалау үшін тоқтап тұруды жояды және тазалау бюджетін төмен тұрақты жылдық қызмет көрсету шығынына дейін қысқартады. Алынған нәтижелер парафинді ұңғымаларда АШПШ-ды мониторинг жасау үшін қырғышты тұрақты пайдалану мүмкіндігін растайды және қорға масштабтауға және одан әрі оңтайландыруға (тозуға төзімділік, орталықтандыру талаптары, бағытталған ұңғымаларда пайдалану) сандық нұсқаулар береді.

Түйін сөздер: парафин шөгінділері, ҰҚ тазарту, механикалық қырғыш, мұнайберуді арттыру, штангалар қозғалысы, кемелденген кен орындары.

Авторлар туралы ақпарат:

Алишева Жанат Нуркуатовна — *PhD, жетекші ғылыми қызметкер, Д.А. Қонаев атындағы Тау-кен істері институты, Абай даңғ., 191, 050046, Алматы, Қазақстан. Email: zhannat_86.2007@mail.ru; ORCID ID: https://orcid.org/0000-0003-0929-4984*

Сәрсенбаев Мухтар Абдикалыкович — *Директор, әл-Фараби атындағы ҚазҰУ-нің Ғылыми-технологиялық паркі ЖШС, әл-Фараби даңғ., 71, 050040, Алматы, Қазақстан. Email: mukhtar.sarsenbaev@mail.ru; ORCID ID: https://orcid.org/0009-0006-0644-4886*

Сарсенбаев Жасулан Абдигаппарович — *Инженер, Инновациялар Плюс ЖШС, Төле би көш., 90, 050031, Алматы, Қазақстан. Email: zhasstin@mail.ru; ORCID ID: https://orcid.org/0009-0003-3895-4985*

Байботаева Салтанат Еликбаевна — *PhD, доцент, М.Әуезов атындағы Оңтүстік Қазақстан университеті, Тәуке-хан даңғ., 5, 160012, Шымкент, Қазақстан. Email: sbaibotaeva@mail.ru; ORCID ID: https://orcid.org/0000-0002-9406-3322*

Инновационные технологии очистки нефтяных труб от парафиновых отложений для повышения нефтеотдачи: механический подход

[1]Алишева Ж.Н., [2]Сарсенбаев М. А., [3]Сарсенбаев Ж.А., [4] Байботаева С.Е.

[1] Институт Горного дела имени Д.А. Кунаева, Алматы, Казахстан
[2]ТОО Научно-технологический парк Казахского национального университета имени Аль-Фараби, Алматы, Казахстан
[3]ТОО Инновации Плюс, Алматы, Казахстан
[4]Южно-Казахстанский университет имени М. Ауэзова, Шымкент, Казахстан

Поступила: *22 апреля 2025*
Рецензирование: *6 августа 2025*
Принята в печать: *18 ноября 2025*

АННОТАЦИЯ

Асфальтосмолопарафиновые отложения (АСПО) на внутренней поверхности насосно-компрессорных труб (НКТ) сокращают межсервисные интервалы, повышают эксплуатационные затраты и нередко вызывают простои на зрелых месторождениях. В работе представлены конструкция и результаты полевых испытаний внутрискважинного штангового скребка, обеспечивающего непрерывную очистку НКТ в процессе штатной работы штангового насоса без химических дозировок и поверхностных операций. Узел врезается в колонну штанг и совместим с НКТ Ø73 - 89 мм и штангами Ø19 - 22 мм. Эффективность оценивалась по ключевым метрикам до/после внедрения: межочистной период (МОП), простой и годовые затраты на очистку, с экстраполяцией на многоскважинные программы. По результатам внедрений скребка CP TP ST 01KZ достигнут МОП 144 - 280 сут, при этом простой, обусловленный очисткой, равен 0 сут/год. Годовые затраты на очистку составили ~0,265 млн KZT на скважину (регламентное обслуживание), что примерно в 31 раз ниже бюджета горячих промывок на том же фонде. Соответственно, экономия на одной скважине — около 7,94 млн KZT/год; при фонде 50 скважин совокупный эффект достигает ≥ 397 млн KZT/год предотвращённых расходов. Непрерывное внутрискважинное действие возвратно-поступательной зубчатой головки при каждом ходе

	штанги разрушает граничный парафиновый слой и ограничивает нарастание отложений между обслуживаниями, устраняя необходимость периодических термических/химических воздействий и связанной с ними логистики. Масса узла порядка 30 кг позволяет выполнять монтаж штатными средствами; компоновка насосной установки не изменяется, кроме врезки секции со скребком. В сравнении с тепловыми, химическими и пакет-механическими методами технология обеспечивает более длительные межсервисные интервалы, исключает простои, связанные с очисткой, и сводит бюджет на очистку к предсказуемой, низкой годовой стоимости обслуживания. Полученные результаты подтверждают возможность регулярного применения скребка для контроля АСПО на парафинистых скважинах и предоставляют количественные ориентиры для масштабирования на фонд и дальнейшей оптимизации (износостойкость, требования к центровке, применение в наклонно-направленных стволах).
	Ключевые слова: Парафиновые отложения, очистка НКТ, механический скребок, увеличение нефтеотдачи, движение насосных штанг, зрелые месторождения.
Алишева Жанат Нуркуатовна	***Информация об авторах:*** *PhD, Ведущий научный сотрудник, Институт Горного дела имени Д.А. Кунаева, пр. Абая, 191, 050046, Алматы, Казахстан. Email: zhannat_86.2007@mail.ru; ORCID ID: https://orcid.org/0000-0003-0929-4984*
Сарсенбаев Мухтар Абдикалыкович	*Директор, ТОО Научно-технологический парк Казахского национального университета имени Аль-Фараби, пр. аль-Фараби, 71, 050040, Алматы, Казахстан. Email: mukhtar.sarsenbaev@mail.ru; ORCID ID: https://orcid.org/0009-0006-0644-4886*
Сарсенбаев Жасулан Абдигаппарович	*Инженер, ТОО Инновации Плюс, ул. Толе би, 90, 050031, Алматы, Казахстан. Email: zhasstin@mail.ru; ORCID ID: https://orcid.org/0009-0003-3895-4985*
Байботаева Салтанат Еликбаевна	*PhD, доцент, Южно-Казахстанский университет имени М. Ауэзова, Пр. Тауке-хана, 5, 160012, Шымкент, Казахстан. Email: sbaibotaeva@mail.ru; ORCID ID: https://orcid.org/0000-0002-9406-3322*

References

[1] Pat. 7700 KZ. Method for cleaning oil pumping wells from paraffin and other deposits. Sarsenbaev AA, Zhan YM, Karibai E, Altybai KA, Sarsenbaev MA, Sarsenbaev ZA. Appl. 30.12.2022, publ. 30.12.2022. https://qazpatent.kz/en/content/poleznaya-model-30122022

[2] Metaksa GP, Alisheva ZN, Metaksa AS, Fedotenko NA. Scientific and technical fundamentals of changing the properties of hydrocarbons in conditions of optimal subsoil use. Eurasian Mining. 2023; 2:75-79. https://doi.org/10.17580/em.2023.02.16

[3] Wang X, Gurbanov H, Adygezalova M, Alizade E. Investigation of Removing Asphaltene-Resin-Paraffin Deposits by Chemical Method for Azerbaijan High-Paraffin Oil Production Process. Energies. 2024; 17(15):3622. https://doi.org/10.3390/en17153622

[4] Nuruallaev V, Usubaliev B. New methods for combating asphalt-resin-paraffin deposits in oil transportation processes. Proceedings on Engineering Sciences. 2021; 3(2):193-200. https://doi.org/10.24874/PES03.02.007

[5] Korobov GYu, Parfenov DV, Nguyen VT. Mekhanizmy obrazovaniya asfal'tosmoloparafinovykh otlozheniy i faktory intensivnosti ikh formirovaniya [Mechanisms of formation of asphalt-resin-paraffin deposits and factors of the intensity of their formation]. Izvestiya Tomsk Polytechnic University. Engineering of Georesources. 2023; 334(4):103–116. https://doi.org/10.18799/24131830/2023/4/3940

[6] Tanirbergenova S, Ongarbayev Y, Tileuberdi Y, Zhambolova A, Kanzharkan E, Mansurov Z. Selection of solvents for the removal of asphaltene-resin-paraffin deposits. Processes. 2022; 10(7):1262. https://doi.org/10.3390/pr10071262.

[7] Alisheva Z, Nadirov K, Al-Dujaili AN, Bimbetova G, Nadirova Z, Zhantasov M, Tileuberdi N, Dauletuly A. Integrated strategies for controlling water cut in mature oil fields in Kazakhstan. Polymers. 2025; 17(7):829. https://doi.org/10.3390/polym17070829.

[8] Wang X, Gurbanov H, Adygezalova M, Alizade E. Investigation of removing asphaltene-resin-paraffin deposits by chemical method for Azerbaijan high-paraffin oil production process. Energies. 2024; 17(15):3622. https://doi.org/10.3390/en17153622.

[9] Khuramshina RA, Muratova VI. Studies of the use of ultrasonic equipment for the removal of asphalt-resin-paraffin deposits at oil and gas transport and storage facilities. Materials Science Forum. 2024; 1080:157-162. https://doi.org/10.4028/p-2p7s8j.

[10] Akbari A, Kazemzadeh Y, Martyushev D, Cortes F, et al. Using ultrasonic and microwave to prevent and reduce wax deposition in oil production. Petroleum, 2024; 10(4):584-593. https://doi.org/10.1016/j.petlm.2024.09.002

[11] Garcia MC. Mechanical cleaning devices for wax deposition in pipelines. Journal of Natural Gas Science and Engineering. 2020; 77:103248. https://doi.org/10.1016/j.jngse.2020.103248

[12] Ahmed S. Integrated approaches to mitigate paraffin deposition in oil production. Journal of Petroleum Exploration and Production Technology. 2021;11(2):581-593. https://doi.org/10.1007/s13202-020-01100-3

[13] Gurbanov GR, Adigozalova MB, Akhmedov SF. Research into the influence of the depressant additive Difron-4201 on the formation of paraffin deposits in laboratory conditions. Azerbaijan Oil Economy. 2020; 12:30-36. https://doi.org/10.20944/preprints202407.1242.v1

[14] Aum YK, Aum PT, da Silva DN, et al. Effective removal of paraffin deposits using oil-in-water microemulsion systems. Fuel. 2024; 358:130112. https://doi.org/10.1016/j.fuel.2023.130112

[15] Gao X, Huang Q, Yun Q, Li Q, Li W, Liang Y, Wang K, Chen C, Liu H, Paso KG. Modeling wax deposit removal during pigging with foam pigs. Geoenergy Science and Engineering. 2024. https://doi.org/10.1016/j.geoen.2024.212713

[16] Panahov EM, Abbasov SZ, Ismayilov AS, Gurbanov GR. Development of a new composition for the prevention of asphaltene-paraffin-resin deposits. Azerbaijan Oil Economy. 2023; 14:65-70. https://doi.org/10.20944/preprints202407.1242.v1

[17] Johnson M. Advances in paraffin deposition prevention in oil pipelines. Journal of Petroleum Science and Engineering. 2015; 126:208-215. https://doi.org/10.1016/j.petrol.2014.12.024

[18] Smith JA. Chemical methods for paraffin control in crude oil production. Energy & Fuels. 2017; 31(5):5056-5062. https://doi.org/10.1021/acs.energyfuels.7b00123

[19] Bell E, Santos G, Daraboina N, Sarica C. Visualization of thermal removal mechanism of paraffin deposits: Providing guidelines for minimum temperature requirements. Fuel. 2024; 356:129577. https://doi.org/10.1016/j.fuel.2023.129577

[20] Wang Y. Thermal techniques in paraffin removal from oil pipelines. Petroleum Science. 2019; 16(3):693-702. https://doi.org/10.1007/s12182-019-0323-3

[21] Wang Z, Zhang K, Sun H. Melting and removing wax deposition by thermal washing in oil well. Geoenergy Science and Engineering. 2024; 237:212808. https://doi.org/10.1016/j.geoen.2024.212808

Crossref
DOI: 10.31643/2027/6445.18
Earth and Planetary Sciences: Earth-Surface Processes

creative commons

Comparative Analysis of Mathematical Models of Drilling in Heterogeneous Geological Sections

[1]Toshov J.B., [1]Erkinov D.I., [2]Baratov B.N., [3]Malybaev N.S., [3]Yesendosova A.N., [3] Zheldikbayeva A., [3*]Rabatuly M.

[1] Tashkent State Technical University named after Islam Karimov, Tashkent, Uzbekistan,
[2] Almalyk branch of NUST MISIS, Almalyk, Uzbekistan,
[3]Abylkas Saginov Karaganda Technical University, Karaganda, Kazakhstan,

** Corresponding author email: mukhammedrakhym@mail.ru*

Received: *October 8, 2025*
Peer-reviewed: *October 13, 2025*
Accepted: *November 19, 2025*

ABSTRACT
This paper presents a comparative analysis of four main types of well drilling models in heterogeneous geological sections: mechanical-mathematical, energy, kinematic, and empirical. It is shown that each group of models focuses on different aspects of the process: the physics of bit-rock interaction (mechanical-mathematical approach), the energy efficiency of rock mass destruction (energy), the trajectory and movement of the tool (kinematic), as well as statistical patterns and the prediction of complications (empirical). The interaction between the bit and the rock is considered depending on their physical and mechanical properties. A comparison of the rotation speed of the rotor and bit is provided depending on the rock hardness. Based on a review of modern publications and the practical experience of leading service companies (Equinor, Schlumberger, Halliburton), the strengths and weaknesses of each approach are identified, and the need for their integration is substantiated. It is established that the integrated use of models of different classes allows not only to describe and explain phenomena but also to manage the drilling process in conditions of high geological variability.

Keywords: drilling, heterogeneous formations, mechanical-mathematical models, energy models, kinematic models, empirical models, stick–slip, digital drilling.

Information about authors:

Toshov Javokhir Buriewicz — *Doctor of Technical Sciences, Professor, Islam Karim Tashkent State Technical University, 100095 Almazar district, Universitetskaya street 2, Tashkent, Uzbekistan. E-mail: j.toshov@tdtu.uz; ORCID ID: https://orcid.org/0000-0003-4278-1557*

Erkinov Dilshodbek Ilhomjonovich — *Ph.D. student, Islam Karim Tashkent State Technical University, 100095 Almazar district, Universitetskaya street 2, Tashkent, Uzbekistan. E-mail: dilshodbek.ilhomovich@gmail.com; ORCID ID: https://orcid.org/0009-0006-5970-416X*

Baratov Bakhtiyor Nusratovich — *Ph.D., Associate professor, Almalyk branch of NUST MISIS, 110104, Amir Temur Street, 56, Almalyk, Uzbekistan. E-mail: bakhtiyor.baratov@yandex.ru; ORCID ID: https://orcid.org/0000-0002-6621-5974*

Malybaev Nurlan Sakenovich — *Candidat of Technical Sciences, Associate Professor, Department of Development of Mineral Deposits of Abylkas Saginov Karaganda Technical University, 100027, Ave. Nursultan Nazarbayev, 56, Karaganda, Kazakhstan. E-mail: n.malybaev@ktu.edu.kz; ORCID ID: https://orcid.org/0000-0002-8977-7400*

Yesendosova Ainel Nurtasovna — *Ph.D., Senior Lecturer, Department of Development of Mineral Deposits of Abylkas Saginov Karaganda Technical University, 100027, Ave. Nursultan Nazarbayev, 56, Karaganda, Kazakhstan. E-mail: a.yesendosova@ktu.edu.kz ; ORCID ID: https://orcid.org/0000-0001-7415-3630*

Zheldikbayeva Aisaule Takenovna — *PhD student of the department of the Department of Automation of manufacturing processes of Abylkas Saginov Karaganda Technical University, 100027, Ave. Nursultan Nazarbayev, 56, Karaganda, Kazakhstan. E-mail: aisaule89@mail.ru; ORCID ID: https://orcid.org/0009-0005-1325-5576*

Rabatuly Mukhammedrakhym — *Ph.D., Associate Professor, Department of Development of Mineral Deposits of Abylkas Saginov Karaganda Technical University, 100027, Ave. Nursultan Nazarbayev, 56, Karaganda, Kazakhstan. E-mail: mukhammedrakhym@mail.ru; ORCID ID: https://orcid.org/0000-0002-7558-128X*

Indroduction

Drilling in heterogeneous formations is always characterized by high complexity and uncertainty, due to the variability of lithological properties of rocks, the presence of tectonic fault zones, fracturing, and variations in the physical and mechanical properties of the rock mass [1], such as soft layers alternating with hard ones, cracks and caverns, and the entire system reacts to this with speed surges, circulation losses, and premature bit wear [2]. One of the most severe situations remains the absorption of drilling fluid in fractured and cavernous zones—a process that halts work and

requires immediate costs to eliminate. Unless such intervals are predicted in advance, shutdowns are inevitable. Therefore, today there are more than a hundred standard sizes and modifications of drilling tools worldwide. The search for new, more effective modifications of drill bits continues, since rock destruction during drilling is an unsteady process [3].

Modern well drilling is characterized by heterogeneous geological sections and uncertainty. Under these conditions, classical engineering approaches based on a limited set of parameters prove insufficient to accurately predict the behavior of the rock-drilling tool-wellbore system.

To analyze rock fracture processes and drilling dynamics, various classes of models are used in scientific literature and industrial practice: mechanical-mathematical, energy, kinematic, and empirical [[4],[5]]. Each of these models reflects individual aspects of a complex process. Thus, mechanical-mathematical models focus on the physics of bit-rock interaction [6], energy models on assessing fracture efficiency and specific energy costs [7], kinematic models on the dynamics of drill string motion and vibration processes, and empirical models on statistical dependencies and the prediction of complications using big data and machine learning methods [8].

In recent years, there has been a trend toward integrating these approaches: leading service companies such as Equinor, Schlumberger, and Halliburton demonstrate successful examples of combining physical models with data-driven analytics, which improves the reliability of forecasts, improves the controllability of the drilling process, and reduces technical and economic risks [[9],[10]]. Thus, the relevance of the study is determined by the need to systematize existing models, identify their strengths and weaknesses, and substantiate the viability of an integrated approach that ensures reliable and effective management of the drilling process in conditions of high geological variability.

Heterogeneity is also manifested in the destruction of the massif. For example, in drilling and blasting operations, the Kuz–Ram model is widely used (an empirical relationship for predicting the granulometric composition of broken rock), but in real heterogeneous massifs, its results turn out to be idealized: digital processing of images of dumps shows a strong discrepancy between the calculated and actual distribution of fragment sizes. In other words, a simple model does not hold up when confronted with complex geology, where fracturing and differences in strength and structure create an unpredictable failure pattern.

Therefore, the question becomes particularly important: which models can adequately reflect environmental variability? Today, there are four directions. Mechanical-mathematical models are based on the laws of mechanics and allow one to see the physical nature of the process, but require accurate data on the strength of rocks and are difficult for direct use at the drilling site. Energy models reduce the process to integral indicators - specific energy of destruction, mechanical penetration rate - and are convenient for diagnosing efficiency, although they remain blind to the details of the interaction of the bit with the rock. Kinematic models consider the movement of the tool and the trajectory of the well, are visual and applicable in navigation, but describe the process only geometrically. Empirical approaches, including modern neural network algorithms, can quickly predict complications and drilling parameters, but their reliability is limited by the training set.

This is how the field of comparison is built: mechanical and mathematical ones give a fundamental picture, energy ones - economics and efficiency, kinematic ones - the geometry of motion, empirical ones - a statistical forecast. The question is which of these approaches copes better with the description of drilling specifically in the conditions of lithological mosaic and variable rock strength - the accuracy of the forecast of the rate of penetration, the assessment of energy costs, and the stability of the tool depend on this.

Methodology

Modern drilling research in heterogeneous formations relies on diverse methodological foundations, reflecting the complexity of the problem itself. University and academic centers predominantly focus on fundamental approaches—numerical modeling based on the equations of solid mechanics and the dynamics of multiphase systems. Here, the emphasis is on constructing integrated "drilling rig–drill string–bit–rock" models, incorporating nonlinear friction, contact interactions, and three-dimensional stress distribution. Such studies are verified through bench tests or limited borehole data, and they form the basis for understanding phenomena such as stick-slip or wellbore stability [11].

Industrial companies operate differently: they focus on energy indicators and fast heuristic algorithms. Schlumberger, Halliburton, and a number of Russian service companies are integrating mechanical specific energy (MSE) and

energy efficiency coefficient calculations into their monitoring systems, combining them with data streams from WOB (weight on bit), RPM (revolutions per minute), and circulating system pressure sensors. The methodology is pragmatic: models must operate in real time, so physical detailing gives way to adaptive calibration algorithms.

A separate area of research is kinematic and structural modeling, which is being actively developed by geophysical divisions. 3D seismic data, attribute analysis of wells, and integration with GIS (well logging) are used to construct structural-kinematic models of deposits. These models do not directly describe the rock failure process, but rather define the geological framework within which mechanical and energy algorithms operate.

Finally, the most rapidly developing empirical methodology is machine learning and intelligent forecasting systems. Researchers from China, the USA, and Russia are training neural networks and hybrid models on large arrays of drilling data, including telemetry, lithological sections, and emergency events. Here, data preparation becomes key: automatic filtering, channel synchronization, and the correct marking of complications. It is at this stage that new methodological developments are concentrated, from signal preprocessing systems to the concept of a "digital twin" of a well. Thus, the research methodology has broadly evolved into four areas: fundamental numerical modeling, applied energy indicators, geophysical kinematics, and empirical big data analytics. In our work, we build on these approaches, comparing their strengths and weaknesses and analyzing the potential for integration in heterogeneous geological settings.

Results

It is advisable to begin a systems analysis with mechanical and mathematical models, as they reflect the fundamental physics of drilling and provide the basis for more applied energy and empirical approaches. Thus, A.N.

Petrov and S.V. Gavrilyuk demonstrate that a model in which the drilling rig, string, bit, and rock are considered as a single system with multi-mass dynamics, contact friction at the bottomhole, and electromechanical drive allows for the reproduction of key self-oscillatory modes [12]. Numerical experiments confirmed that, under certain parameters, a stick-slip effect occurs—an alternation of stops and jerks of the bit with a drop in average angular velocity and an increase in parasitic energy consumption (see Fig. 1). These findings echo the results of M.A. Sidorov and I.L. Kuznetsov, who demonstrated that torsional vibrations cause impact loads, accelerate wear on PDC bits, and increase the risk of threaded connections loosening (see Fig. 2) [13]. Similar observations are made by V.V. Isaev and D.S. Rogov, emphasizing that it is precisely these modes that "eat up" the mechanical penetration rate and tool life.

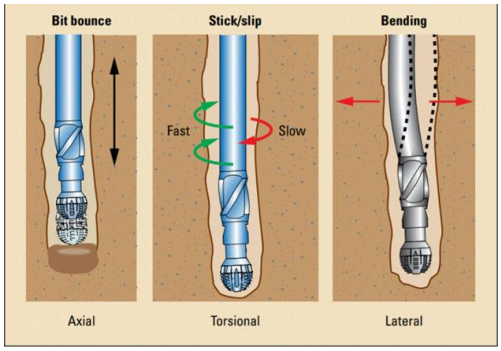

Figure 1 - Types of drill string vibrations: axial (bit bounce), torsional (stick–slip), and lateral (bending)

A.V. Barkov's geomechanical research line expands our understanding of the process: without taking into account the block and fracture structure of rocks, wellbore stability predictions are inevitably distorted. Calibrating numerical models using triaxial core testing and computed tomography of fractures allows for significantly more accurate predictions of the stress-strain state of the rock mass and potential complication zones. Thus, the mechanical-mathematical layer explains the causes of ROP degradation and the occurrence of emergency conditions, but due to its high demands on data and computing resources, its application in online practice is limited.

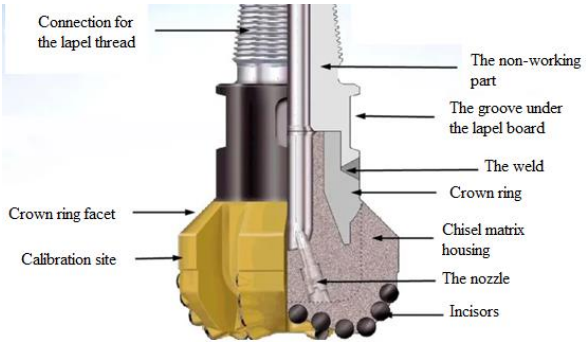

Figure 2 - Diagram of a PDC bit in section showing the main structural elements that determine the dynamics of interaction with the rock

Against this backdrop, energy models have become a practical tool, as they reduce the complex

process to integral indicators of "expended power - destruction volume." The central criterion here is the mechanical specific energy, first proposed by R. Theale back in 1965, as the amount of energy required to destroy a unit volume of rock. The meaning of this indicator is simple: the lower the MSE value, the more efficient the drilling. In practice, MSE is calculated based on telemetry data: weight on bit (WOB), rotational speed (RPM), torque, and rate of penetration. The classical model of A.T. Bourgoine and F.S. Young, based on regression, made it possible to define the "WOB-RPM" working areas and delineate zones of uniform rotation, areas of instability with stick-slip characteristics, and zones of lateral oscillations, where efficiency drops sharply (see Fig. 3) [13].

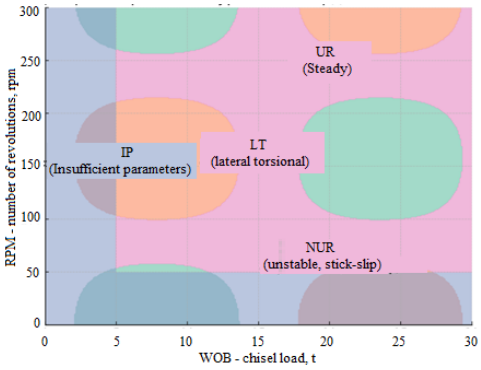

Figure 3 - Drilling mode diagram in WOB–RPM coordinates, demonstrating the boundaries of stable bit rotation (UR), the region of unstable mode with manifestations of stick–slip (NUR), the zone of insufficient parameters (IP), and the region of lateral torsional oscillations of the column (LT)

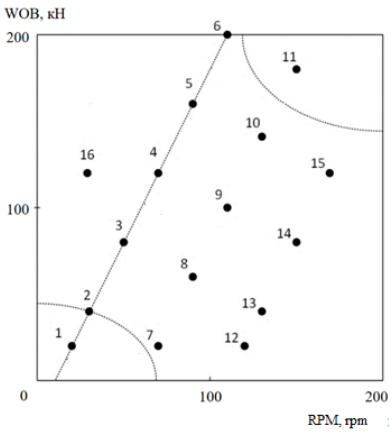

Figure 4 - Rotary drilling mode diagram in WOB–RPM coordinates: stable rotation zone (UR), unstable mode zone with stick–slip manifestations (NUR), insufficient parameters zone (IP) and lateral column vibration zone (LT)

The applicability of the energy approach is confirmed by the experience of service companies Schlumberger and Halliburton: in the field, MSE spikes are used to determine whether the bit is entering a harder formation, while dips indicate entry into loose or fractured zones with a risk of circulation loss [[14],[15]]. This has become a standard technique in operational geosteering, as evidenced by examples from the Permian Basin and the North Sea, where energy indicators helped quickly localize ineffective performance windows and return the process to the optimal parameter range.

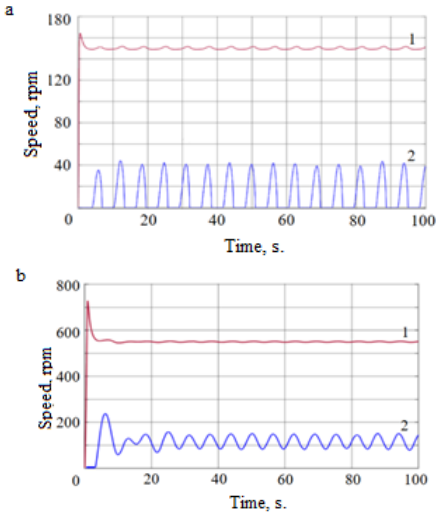

Figure 5 - Comparison of the rotation speed of the rotor and bit: mode 16 - unstable rotation (stick-slip), mode 9 - uniform rotation with a high mechanical penetration rate [16]

The transition from purely diagnostic criteria to automation has become a key step in the development of energy and kinematic models. Drilling mode diagrams in WOB–RPM coordinates clearly show the limits of stable rotation, instability zones with stick-slip behavior, as well as areas of lateral oscillation and insufficient parameters (Fig. 4). These zones serve as the basis for digital monitoring systems, allowing for real-time detection of critical conditions. Against this backdrop, companies began implementing closed-loop control systems: Equinor's experience with downhole regulators and automatic control demonstrated that suppressing torsional oscillations and aligning rotation leads to increased ROP and reduced performance variability; in pilot projects at Schlumberger-Equinor's Brazilian projects, the rate of penetration increase reached 60%. A detailed comparison of rotation dynamics in various modes reveals the nature of these effects: with uniform rotation, energy is transferred to the face without loss, whereas in stick-slip mode, alternating stops

and jerks, a decrease in average angular velocity, and torque surges are observed (Fig. 5). This instability inevitably increases energy consumption and accelerates wear of PDC bits. Therefore, energy optimization requires consideration of the actual dynamics of the process: the fractional-energy model of A. A. Pavlov and S. N. Grigoriev demonstrates that rationalizing WOB and RPM simultaneously reduces energy consumption, increases the average cutting size, and extends the service life of the tool [17].

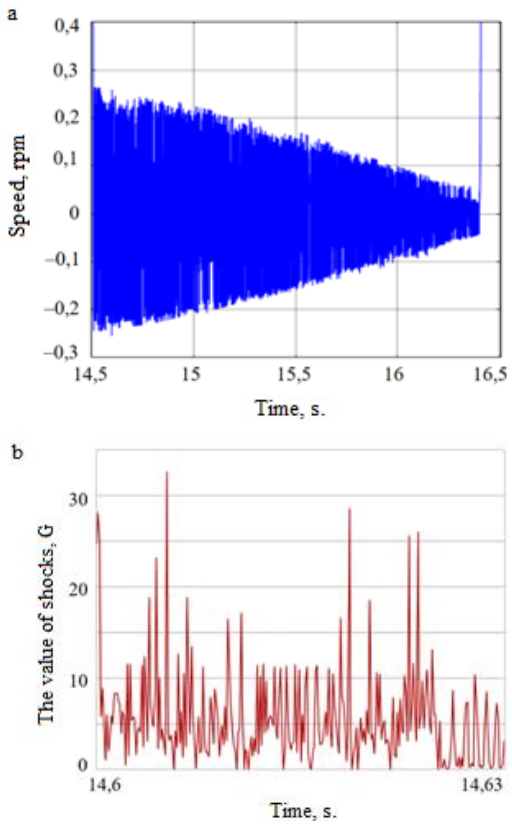

Figure 6 - High-frequency vibrations of the bit in stick-slip mode, accompanied by impact loads and accelerated wear of the cutting elements [17].

High-frequency vibrations of the bit, occurring in advanced stick-slip mode (Fig. 6), pose a particular danger. They are accompanied by impact loads, causing accelerated wear of cutting elements and creating the risk of threaded connections becoming loose. In practice, this is one of the most dangerous scenarios, which is why modern drilling control systems are focused on preventing entry into such zones rather than mitigating the consequences. Taken together, this confirms that only the integration of mechanical-mathematical models, energy indicators, and intelligent control algorithms allows the process to be maintained within a safe and efficient parameter range.

The kinematic modeling level defines the geometric basis of the drilling process, where the object of analysis is not the force interaction, but the trajectory of the system elements and the wellbore. In engineering practice, this manifests itself in two dimensions: first, as the kinematics of the drill string and tool, and second, as the kinematics of the geological structures that determine the borehole curvature. In the first case, kinematic diagrams of the drive, column, and bit are constructed to optimize the transmission of rotation and axial load to the face [18]. When considering heterogeneous sections, the actual kinematics of the deepening process become more important: a geometric estimate of the maximum possible rate of penetration (ROP), which sets the upper limit of efficiency. Comparing the actual ROP with the "ideal" ROP shows the extent to which the bit's movement is limited by the strength properties of the rock. This principle is embedded, in particular, in the Burgoyne-Young model, where the kinematic component of the velocity is adjusted by empirical coefficients reflecting the influence of lithology and hydraulics.

The second line is the wellbore trajectory as it passes through zones with varying drillability and structural complexity. Faults and inclined layers can cause bit deviation, so structural-kinematic models are used to predict curvature and select the optimal trajectory. For example, T.Sh. Akhmedov and K.N. Ibragimov, using the integration of 3D seismic with well logging, constructed a model of the Kurovdag field, revealing hidden tectonic blocks and faults not visible in the original sections. The resulting model made it possible to refine the course of horizontal wells and avoid complications when crossing tectonic zones [19].

Real-time kinematic analysis is performed using MWD and LWD systems, which record azimuth, inclination, and changes in logging parameters. The use of azimuthal methods, as demonstrated by A.R. Isaev and all using density logging data while drilling to identify the boundaries of hydrodynamic isolation between reservoirs and adjust the subsurface model. Essentially, the kinematic approach transforms drilling into a tool for "sounding" the subsurface, where the trajectory and its changes themselves become diagnostic indicators of geological heterogeneity.

The oscillatory modes of the drill string deserve special mention. Although they are described dynamically, in practice, only kinematic parameters—vibration amplitudes and frequencies—are often recorded. This allows for the identification of critical modes, such as backward whirl, when the string strikes the borehole walls. A geometric model of the bit center's motion relative to the wall allows for the determination of critical frequencies and their comparison with the LT zones on the WOB–RPM diagrams. Thus, even without full dynamics, kinematic analysis helps identify the conditions that lead to hazardous modes.

A modern trend is the automation of trajectory and mode control. An example is the Downhole Regulators tested by Equinor. This device, mounted on the bit, adjusts the feed rate in real time, smoothing out oscillations and preventing stalls. Reported data from 93 well sections demonstrate an increase in ROP and a reduction in the number of complications, confirming the effectiveness of using an on-the-fly kinematic model as part of an intelligent drilling autopilot.

Collectively, kinematic models form a tool for operational diagnostics and geosteering: they enable the identification of hidden heterogeneities, trajectory prediction, and operational adjustments before complications arise. Their limitation remains their inability to determine the causes of these phenomena: they record movement but do not explain its physics. Therefore, their maximum effectiveness is achieved when combined with mechanical-mathematical and energy models that reveal the hidden force mechanisms underlying the observed kinematics.

Discussion

The approaches to drilling modeling discussed above-mechanical-mathematical, energy, kinematic, and empirical-are not mutually exclusive. On the contrary, they complement each other, each providing its own perspective on the complex, multifactorial process of rock failure. In real-world heterogeneity, effective drilling planning and execution require a combination of all four model types.

Mechanical-mathematical models provide physical plausibility and the ability to extrapolate system behavior beyond existing experience. They allow us to explore new drilling modes, materials, and bit designs. For example, they can be used to predict the occurrence of stick-slip and other vibrations at specific WOB and RPM ratios, which has been confirmed in practice. However, the complexity of such models hinders their application directly at the drilling rig: computational power and time are required to solve the equations, and, most importantly, input data is not always available (for more details, the rock parameters for each meter of the borehole are unknown in advance). Therefore, in real time, it is difficult to rely solely on a purely physical model.

Energy and kinematic models fill this gap, enabling rapid process control. They are simple and quick to calculate. Specific energy mode diagnostics, as noted, instantly demonstrate drilling efficiency; trajectory and speed monitoring detect deviations when entering a new drilling phase. However, if an abnormal situation arises, these models only record the symptom (increased MSE, trajectory drift) but do not explain the cause. Engineering expertise, a connection to a physical (mechanical) model, or big data analysis should be used here [[20],[21]].

Empirical (data-driven) models allow us to account for the complexities of geology without delving into the physics of the processes. They work well as a warning and prediction system: for example, a neural network can predict that lost circulation is likely within 5 meters, based on a combination of indirect indicators, even before it manifests itself. However, such predictions are always subject to error, and they offer no guarantee beyond known patterns. This is why the best strategy is to integrate models. Modern automated drilling systems (so-called intelligent drilling rigs) are built on a three-tiered structure: at the bottom tier are sensors and direct automation (kinematics and energy: maintaining a set flow rate, pressure, and power); at the middle tier are optimization models and algorithms (physical and empirical models that evaluate the process state); at the top tier is an operator or AI that makes decisions based on the combined information. All of the described approaches fit naturally into this architecture.

Table 1 - Comparative characteristics of drilling models in heterogeneous sections.

Model approach	Main features and advantages	Limitations and disadvantages
Mechanics and Mathematics	Accurate physical description of the process; prediction of new effects; consideration of material properties	Complexity of implementation; requires many input parameters; high computational costs; difficult to apply in real time
Energy	Integrated performance assessment (specific energy, efficiency); rapid diagnostics of deteriorating conditions; optimization of modes to minimize energy consumption	Does not show the causes of the phenomenon; may misinterpret complex cases (for example, an increase in MSE due to vibrations or hard rock); requires calibration for conditions
Kinematic	Drilling trajectory and speed control; fault and rock change detection based on course/ROP changes; simple motion models for automation	Does not take into account forces and resistances; without a connection to dynamics, it can give a simplified representation; it does not prevent problems, but only records movement
Empirical (data)	Considers multiple factors simultaneously; self-learning based on accumulated data; forecasts complications and parameters in real time; adapts to a specific field	Requires large, high-quality training data; is limited to a domain similar to the training sample; is a "black box"—provides a prediction without explaining the physics of the process

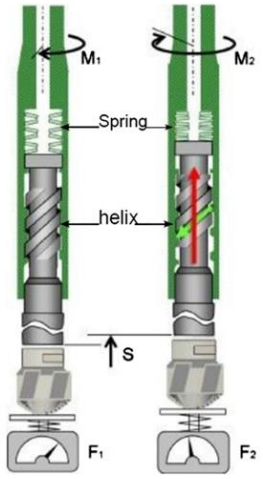

Figure 7 - Operating principle of the AST, which smooths out torsional vibrations and stabilizes the rotation of the bit when drilling in heterogeneous sections [22].

Equinor's experience with the implementation of downhole weight-on-bit (AST) regulators exemplifies successful integration. The device is based on an understanding of stick-slip mechanics: a physical and mathematical model demonstrated that a spring-damper element integrated into the string can smooth out intermittent torsional vibrations and stabilize rotation. Kinematic analysis allowed us to define the deformation parameters and speed range at which the regulator operates effectively; energy calculations confirmed its impact on reducing the specific energy of fracture and increasing ROP, and empirical statistics from dozens of wells demonstrated the reliability of the solution. The diagram (Fig. 7) illustrates the operating principle of the AST: as torque increases, the tool compresses elastically, reducing the weight on the bit and preventing instability. According to reports, the implementation of such regulators has resulted in a 30–40% increase in ROP and a significant reduction in accidents, despite the complex structure of the wellbore. Another example is digital twins and drilling simulators, which are currently being developed in research centers. They combine a geological model of the section (usually stochastic, accounting for heterogeneity), a geomechanical model (stress, wellbore stability), a bit and string model (mechanics and kinematics), and an integrated ML model calibrated against actual well data. Such a twin can compare forecasts and actual performance online and adjust either model parameters or recommend a change in drilling mode [[23],[24]]. Essentially, this is the fusion of all four approaches into a single software suite.

As Table 1 shows, no single model type covers all aspects of a complex drilling problem. Therefore, in engineering practice, combinations are used. For example, when planning a bit and drilling mode for a new section, mechanical and mathematical calculations are first used (to estimate the required force, torque, and vibration risk). Then, during drilling, energy monitoring (MSE and power monitoring) and kinematic control (navigation trajectory and mode stabilization using vibration

sensors) are used. Empirical trends are also constantly compared (models trained on adjacent wells suggest expected values and warn of abnormal ones) [25]. This integrated approach is the most reliable.

This is especially important for heterogeneous sections, where the situation can change abruptly. Here, a mechanical model will warn in advance: "stick-slip is possible in interval X with the given parameters" – this allows for reconfiguring the drilling mode before entering the interval. When drilling enters an interval, energy indicators will show the actual state: "energy consumption is increasing, efficiency is decreasing" – a signal to review the WOB/RPM. Kinematics and sensors will indicate: "the bit has started to deviate/vibrate" – perhaps a fault or lens has been encountered, requiring a reduction in speed or the use of dampers. An empirical system can also provide the following: "Based on experience, in such cases, there will be a loss of power after 10 meters, so be prepared." Using this information together significantly increases the chances of successfully drilling through a challenging interval.

Interest in the automation and intellectualization of the drilling process has grown significantly in recent years. By 2025, drilling rigs where humans merely control the actions of an automated system that optimizes drilling according to a predefined algorithm will already be a reality. However, models cannot be completely eliminated—they constitute the "brain" of such a system. A promising area of research is the development of adaptive models that update their parameters during drilling. For example, a mechanical model can adjust rock strength properties based on actual load and speed data, i.e., adapt to the actual cross-section rather than the nominal one. Empirical models, in turn, can integrate physical constraints (for example, learning not from meaningless correlations, but by taking into account known physical relationships between parameters). All this is aimed at making drilling in highly heterogeneous conditions more predictable and controllable.

Conclusion

The review showed that drilling in geologically heterogeneous sections can only be described using a comprehensive approach: individual models capture important aspects, but only their combination can explain and predict the actual process dynamics. Based on mechanical, mathematical, energy, kinematic, and empirical studies, the following conclusions were reached:

1. Mechanico-mathematical models explain key phenomena: numerical models of the string and bit (A. N. Petrov, S. V. Gavrilyuk, M. A. Sidorov, I. L. Kuznetsov) reproduce stick-slip and torsional self-oscillations, demonstrating how they reduce ROP and destroy the PDC tool; geomechanical calculations (A. V. Barkov) demonstrated that without taking fracturing and block structure into account, well stability predictions are distorted.

2. Energy models capture the process economics: MSE calculations and WOB–RPM diagrams localize inefficiencies, and the fractional-energy model (A. A. Pavlov, S. N. Grigoriev) confirmed that optimization of the drilling regime reduces specific costs and simultaneously increases bit life. In tests, this resulted in reduced energy consumption and an increase in the yield of coarse cuttings.

3. Kinematic models have practical applications in geosteering and trajectory control: the work of T.Sh. Akhmedov and K.N. Ibragimov demonstrated that attribute analysis of seismic and well logging allows for the prediction of block displacements and faults; the methodology of O.I. Ilmendeeva and V.A. Nosov demonstrated that LWD logging detects hydrodynamic barriers during drilling, allowing for rapid course corrections.

4. Empirical and predictive models have demonstrated effectiveness in predicting complications: neural network developments (A.S. Kiselev, S.V. Nechaev, E.G. Gurinov, N.Yu. Klyuchnikov) successfully predicted lost circulation and stuck wells several meters before they occurred, demonstrating the value of machine learning in complex cross-sections.

5. Industrial practice (Equinor, Schlumberger, Halliburton) has confirmed that the integration of approaches is already producing results: the implementation of AST has reduced the amplitude of oscillations, stabilized rotation, and ensured an increase in ROP by 30–40%.

Conflict of interest. On behalf of all the authors, the corresponding author declares that there is no conflict of interest.

***CRediT author statement*: J. Toshov, M. Rabatuly:** Conceptualization, Methodology, Software; **D. Erkinov, B. Baratov**: Data curation, Writing-Original draft preparation; **A. Yesendosova, N. Malybaev:** Visualization, Investigation; **D. Erkinov, J. Toshov:** Software, Validation.

Cite this article as: Toshov JB, Erkinov DI, Baratov BN, Malybaev NS, Yesendosova AN, Zheldikbayeva A, Rabatuly M. Comparative Analysis of Mathematical Models of Drilling in Heterogeneous Geological Sections. Kompleksnoe Ispolzovanie Mineralnogo Syra = Complex Use of Mineral Resources. 2027; 341(2):60-70. https://doi.org/10.31643/2027/6445.18

Біртекті емес геологиялық учаскелерде бұрғылаудың математикалық модельдерін салыстырмалы талдау

[1] Тошов Ж.Б., [1] Эркинов Д.И., [2] Баратов Б.Н. [3] Малыбаев Н.С., [3] Есендосова А.Н., [3] Желдикбаева А.Т., [3] Рабатулы М.

[1] Ислам Каримов атындағы Ташкент Мемлекеттік Техникалық Университеті, Ташкент, Өзбекстан
[2] ҰЗТУ МИСиС Алмалық филиалы, Алмалық, Өзбекстан
[3] Әбілқас Сағынов атындағы Қарағанды техникалық университеті, Қарағанды, Қазақстан

Мақала келді: *8 қазан 2025*
Сараптамадан өтті: *13 қазан 2025*
Қабылданды: *19 қараша 2025*

ТҮЙІНДЕМЕ

Бұл жұмыста біртекті емес геологиялық учаскелердегі ұңғымаларды бұрғылау модельдерінің төрт негізгі түріне салыстырмалы талдау ұсынылған: механикалық-математикалық, энергетикалық, кинематикалық және эмпирикалық. Әрбір модель тобы процестің әртүрлі аспектілеріне бағытталғаны көрсетілген: қашаудың тау жынысымен өзара әрекеттесу физикасы (механикалық-математикалық тәсіл), тау жынысы массасының бұзылуының энергия тиімділігі (энергия), құралдың траекториясы мен қозғалысы (кинематика), сондай-ақ статистикалық заңдылықтар және асқынуларды болжау (эмпирикалық). Қашау мен жыныстың өзара әрекеттесуі олардың физикалық және механикалық қасиеттеріне байланысты қарастырылады. Ротор мен қашаудың айналу жылдамдығы тастың қаттылығына байланысты салыстырылады. Заманауи басылымдарға шолу және жетекші қызмет көрсету компанияларының (Equinor, Schlumberger, Halliburton) практикалық тәжірибесі негізінде әрбір тәсілдің күшті және әлсіз жақтары анықталып, оларды біріктіру қажеттілігі негізделеді. Әртүрлі кластағы модельдерді кешенді пайдалану тек құбылыстарды сипаттауға және түсіндіруге ғана емес, сонымен қатар жоғары геологиялық өзгергіштік жағдайында бұрғылау процесін басқаруға мүмкіндік беретіні анықталды.

Түйін сөздер: бұрғылау, біртекті емес қабаттар, механикалық-математикалық модельдер, энергетикалық модельдер, кинематикалық модельдер, эмпирикалық модельдер, қолмен сырғыту, сандық бұрғылау.

Авторлар туралы ақпарат:

Тошов Жавохир Буриевич — *Техника ғылымдарының докторы, Ислам Карим атындағы Ташкент мемлекеттік техникалық университетінің профессоры, 100095, Алмазар ауданы Университетская көшесі 2, Ташкент, Өзбекстан. E-mail: j.toshov@tdtu.uz; ORCID ID: https://orcid.org/0000-0003-4278-1557*

Эркинов Дилшодбек Илхомджонович — *Ислам Карим атындағы Ташкент Мемлекеттік Техникалық Университетінің PhD докторанты, 100095, Алмазар ауданы, Университетская көшесі, 2, Ташкент, Өзбекстан. E-mail: dilshodbek.ilhomovich@gmail.com; ORCID ID: https://orcid.org/0009-0006-5970-416X*

Баратов Бахтиер Нусратович — *Phd, ҰЗТУ МИСиС, Алмалық филиалының доценті, 110104, Әмір Темір көшесі, 56, Алмалық, Өзбекстан. E-mail: bakhtiyor.baratov@yandex.ru; ORCID ID: https://orcid.org/0000-0002-6621-5974*

Малыбаев Нурлан Сакенович — *PhD, Әбілқас Сағынов атындағы Қарағанды техникалық университетінің Пайдалы қазбалар кенорындарын өндіру кафедрасының қауымдастырылған профессоры, 100027, Нұрсұлтан Назарбаев даңғ. 56, Қарағанды, Қазақстан. E-mail: n.malybaev@ktu.edu.kz; ORCID ID: https://orcid.org/0000-0002-8977-7400*

Есендосова Айнель Нуртасовна — *PhD, Әбілқас Сағынов атындағы Қарағанды техникалық университетінің Пайдалы қазбалар кенорындарын өндіру кафедрасының аға оқытушысы, 100027, Нұрсұлтан Назарбаев даңғ. 56, Қарағанды, Қазақстан. E-mail: a.yesendosova@ktu.edu.kz ; ORCID ID: https://orcid.org/0000-0001-7415-3630*

Желдикбаева Айсауле Такеновна — *Әбілқас Сағынов атындағы Қарағанды техникалық университетінің Өндірістік процестерді автоматтандыру кафедрасының PhD докторанты, 100027, Нұрсұлтан Назарбаев даңғ. 56, Қарағанды, Қазақстан. E-mail: aisaule89@mail.ru; ORCID ID: https://orcid.org/0009-0005-1325-5576*

Рабатұлы Мұхаммедрахым — *PhD, Әбілқас Сағынов атындағы Қарағанды техникалық университетінің Пайдалы қазбалар кенорындарын өндіру кафедрасының қауымдастырылған профессоры, 100027, Нұрсұлтан Назарбаев даңғ. 56, Қарағанды, Қазақстан. E-mail: mukhammedrakhym@mail.ru; ORCID ID: https://orcid.org/0000-0002-7558-128X*

Сравнительный анализ математических моделей бурения скважин в неоднородных геологических разрезах

[1] Тошов Ж.Б., [1] Эркинов Д.И., [2] Баратов Б.Н. [3] Малыбаев Н.С., [3] Есендосова А.Н., [3] Желдикбаева А.Т., [3] Рабатулы М.

[1] Ташкентский государственный технический университет имени Ислама Каримова, Ташкент, Узбекистан
[2] Алмалыкский филиал НИТУ МИСиС, Алмалык, Узбекистан,
[3]Карагандинский технический университет имени Абылкаса Сагинова, Караганда, Казахстан

Поступила: *8 октября 2025*
Рецензирование: *13 октября 2025*
Принята в печать: *19 ноября 2025*

АННОТАЦИЯ

В данной статье представлен сравнительный анализ четырех основных типов моделей бурения скважин в неоднородных геологических разрезах: механико-математических, энергетических, кинематических и эмпирических. Показано, что каждая группа моделей фокусируется на различных аспектах процесса: физике взаимодействия долота с горной породой (механико-математический подход), энергетической эффективности разрушения массива горной породы (энергия), траектории и движении инструмента (кинематика), а также статистических закономерностях и прогнозировании осложнений (эмпирический). Взаимодействие между долотом и породой рассматривается в зависимости от их физических и механических свойств. Приводится сравнение скорости вращения ротора и долота в зависимости от твердости породы. На основе обзора современных публикаций и практического опыта ведущих сервисных компаний (Equinor, Schlumberger, Halliburton) выявлены сильные и слабые стороны каждого подхода и обоснована необходимость их интеграции. Установлено, что комплексное использование моделей разных классов позволяет не только описывать и объяснять явления, но и управлять процессом бурения в условиях высокой геологической изменчивости.

Ключевые слова: бурение, неоднородные пласты, механико-математические модели, энергетические модели, кинематические модели, эмпирические модели, ручное скольжение, цифровое бурение.

Информация об авторах:

Тошов Жавохир Буриевич — *Доктор технических наук, профессор Ташкентского государственного технического университета имени Ислама Карима, 100095, Алмазарский район, улица Университетская 2, Ташкент, Узбекистан. E-mail: j.toshov@tdtu.uz; ORCID ID: https://orcid.org/0000-0003-4278-1557*

Эркинов Дилшодбек Илхомджонович — *PhD докторант Ташкентского государственного технического университета имени Ислама Карима, 100095, Алмазарский район, ул. Университетская, 2, Ташкент, Узбекистан. E-mail: dilshodbek.ilhomovich@gmail.com; ORCID ID: https://orcid.org/0009-0006-5970-416X*

Баратов Бахтиер Нусратович — *PhD, доцент Алмалыкского филиала НИТУ МИСиС, 110104, ул. Амира Темура, 56, Алмалык, Узбекистан. E-mail: bakhtiyor.baratov@yandex.ru; ORCID ID: https://orcid.org/0000-0002-6621-5974*

Малыбаев Нурлан Сакенович — *К.т.н., ассоциированный профессор кафедры Разработки месторождений полезных ископаемых Карагандинского технического университета имени Абылкаса Сагинова, 100027, пр. Нурсултана Назарбаева, 56, Караганда, Казахстан. E-mail: n.malybaev@ktu.edu.kz; ORCID ID: https://orcid.org/0000-0002-8977-7400*

Есендосова Айнель Нуртасовна — *PhD, старший преподаватель кафедры Разработки месторождений полезных ископаемых Карагандинского технического университета имени Абылкаса Сагинова, 100027, пр. Нурсултана Назарбаева, 56, Караганда, Казахстан. E-mail: a.yesendosova@ktu.edu.kz ; ORCID ID: https://orcid.org/0000-0001-7415-3630*

Желдикбаева Айсауле Такеновна — *PhD, докторант кафедры Автоматизации производственных процессов Карагандинского технического университета имени Абылкаса Сагинова, 100027, пр. Нурсултана Назарбаева, 56, Караганда, Казахстан. E-mail: aisaule89@mail.ru; ORCID ID: https://orcid.org/0009-0005-1325-5576*

Рабатулы Мухаммедрахым — *PhD, ассоциированный профессор кафедры Разработки месторождений полезных ископаемых Карагандинского технического университета имени Абылкаса Сагинова, 100027, пр. Нурсултана Назарбаева, 56, Караганда, Казахстан. E-mail: mukhammedrakhym@mail.ru; ORCID ID: https://orcid.org/0000-0002-7558-128X*

References

[1] Gavrilov I V, Ponomarev V V. Analysis of crushing using digital image processing and the empirical Kuz-Ram model: a comparative study. Mining Industry. 2022; 11:33-41.

[2] Kiselev A S, Nechaev S V. Study of drilling mud absorption during oil field development using artificial intelligence methods. Innovative Science. 2024; 6:45-52.

[3] Burievich TJ. The questions of the dynamics of drilling bit on the surface of well bottom. Arch. Min. Sci. 2016; 61(2):275-283. https://doi.org/10.1515/amsc-2016-0020

[4] Zafarian H, et al. A novel mathematical model of rock–bit interaction considering in-situ stresses. Scientific Reports. 2024; 14(2):112–125.

[5] Song W. Evaluation and optimization of drilling efficiency based on an improved rock-breaking specific energy model. Journal of Petroleum Science and Engineering. 2024; 235:109–121.

[6] Detournay E, Defourny P. A phenomenological model for the drilling action of drag bits. International Journal of Rock Mechanics and Mining Sciences & Geomechanics Abstracts. 1992; 29(1):13–23.

[7] Teale R. The concept of specific energy in rock drilling. International Journal of Rock Mechanics and Mining Sciences. 1965; 2(1):57–73.

[8] Soares C, et al. Real-time predictive capabilities of analytical and machine-learning ROP models. Proceedings of SPE/IADC Drilling Conference and Exhibition. The Hague: SPE. 2019; 10. Paper SPE-194125-MS.

[9] Schlumberger. Real Time MSE Ratio Monitoring Enables Early Bit Failure Detection and Delivers Rapid Decision-Making Tool to Drive Drilling Performance. Tech Paper. 2023. https://www.slb.com/resource-library/technical-paper/di/real-time-mse-ratio-monitoring-enables-early-bit-failure-detection

[10] Halliburton sets standard in digital operations with LOGIX™ automated geosteering. Halliburton. https://www.halliburton.com/en/well-construction/drilling/drilling-optimization-solutions/drillstring-design-optimization

[11] Isaev V V, Rogov D S. Modern concepts of the dynamics of rock-cutting tools. Sphere Oil & Gas. 2024; 4:112-124.

[12] Petrov A N, Gavrilyuk S V. Complex model of an adjustable electric drive of a drilling rig rotor. Problems of mechanical engineering and automation. 2023; 2:65-74.

[13] Sidorov M A, Kuznetsov I L. Influence of the unstable rotation mode of the bit on the energy efficiency of the electric drive of the drilling rig rotor. Mining information and analytical bulletin. 2022; 8:118-125.

[14] Akhmedov T Sh, Ibragimov K N. Combined application of attribute analysis of 3D data and well logging (WL) for solving structural and kinematic problems using the example of the Kyurovdag field. Vector of Geosciences. 2023; 2:55-64.

[15] Raissi M, Perdikaris P, Karniadakis G. Physics-informed neural networks: A deep learning framework for solving forward and inverse problems involving nonlinear partial differential equations. Journal of Computational Physics. 2019; 378:686–707.

[16] Kalantari S, Hareland G, Husein M. Application of artificial neural networks for real-time prediction of rate of penetration. Journal of Petroleum Science and Engineering. 2018; 163:85–99.

[17] Pavlov A A, Grigoriev S N. Fractional-energy models in forecasting the efficiency of drilling and blasting operations. Mining information and analytical bulletin. 2024; 12:118-134.

[18] Toshov JB, Rabatuly M, Bogzhanova ZhK, Zheldikbayeva AT, Malikov ShR, Toshov BR, Ergashev OS, Influence of Radiation and Magnetic Pulse Treatment on The Wear Resistance of Carbide Tools. Kompleksnoe Ispolzovanie Mineralnogo Syra = Complex Use of Mineral Resources. 2026; 337(2):47-54. https://doi.org/10.31643/2026/6445.16

[19] Barkov A V. Geomechanical principles of low-permeability reservoir development management: diss. … Cand. of Technical Sciences. Moscow: Institute for Problems in Mechanics, Russian Academy of Sciences. 2024, 250.

[20] Bourgoyne A T, Young F S. A multiple regression approach to optimal drilling and abnormal pressure detection. Society of Petroleum Engineers Journal. 1974; 14(4):371–384.

[21] Ershov M S, Komkov A N, Feoktistov E A. Complex model of an adjustable electric drive of a drilling rig rotor. Zapiski Gornogo Instituta. 2023; 261:339–348. https://doi.org/10.31897/PMI.2023.20

[22] Alikulov Sh, Toshov J, Mussin R, Rabatuly M, Tolovkhan B, Bogzhanova Zh, Gabitova A. Study of rational solution parameters during in-situ uranium leaching. Mining of Mineral Deposits. 2025; 19(1):37-46. https://doi.org/10.33271/mining19.01.037

[23] Maurer W C. The perfect-cleaning theory of rotary drilling. Journal of Petroleum Technology. 1962; 14(11):1270–1274.

[24] Akhmedov T Sh, Ibragimov K N. Joint application of attribute analysis of 3D data and geophysical well logging (GIS) for solving structural and kinematic problems using the example of the Kyurovdag deposit. Vector of geosciences. 2023; 2:55-64.

[25] Wildemans R, Aribowo A G, Detournay E, van de Wouw N. Modelling and dynamic analysis of an anti-stall tool in a drilling system including spatial friction. Nonlinear Dynamics. 2019; 98:2631–2650. https://doi.org/10.1007/s11071-019-05075-6

Crossref
DOI: 10.31643/2027/6445.19
Mining & Mineral Processing

creative commons

Study of the suitability of industrial raw material resources as additives for Portland cement

[1*]Begzhanova G.B., [1]Yakubzhanova Z.B., [2]Wang L., [1]Makhsudova N.D., [3]Ruzmetova A.Sh.

[1] Institute of General and Inorganic Chemistry of the Academy of Sciences of Uzbekistan, Tashkent
[2] College of Energy Engineering, Zhejiang University, Hangzhou, Zhejiang
[3]Urgench State University named after Abu Rayhon Beruni, Uzbekistan

** Corresponding author email: gulrukh-begzhanova@rambler.ru*

Received: *June 5, 2025*
Peer-reviewed: *October 1, 2025*
Accepted: *November 25, 2025*

ABSTRACT
This research investigates the potential of utilizing industrial technogenic waste materials as hybrid mineral additives in the production of composite Portland cement (CPC), aiming to reduce clinker consumption and promote environmentally friendly construction practices. The studied materials include active ash and slag (AAS) from the Angren thermal power plant, microsilica (MS), and processed steelmaking wastes such as ladle slag (LS), furnace slag (FS), and recycled steel slag (RSS) from Uzmetkombinat JSC. The chemical, mineralogical, and mechanical properties of these materials were characterized in accordance with national and international standards. Compressive strength tests and lime absorption measurements evaluated their pozzolanic and hydraulic activities. Experimental results demonstrated that AAS exhibited the highest activity, capable of replacing up to 45% of clinker without compromising mechanical strength. When combined with less active components (MS, RSS, FS, and LS), hybrid additives showed synergistic effects. Among these, the AAS+MS blend had the most significant pozzolanic effect, evidenced by reduced calcium oxide (CaO) concentration in the surrounding liquid and lower solution alkalinity. The statistical validation using the Student's t-test confirmed the effectiveness of each additive, with t-values significantly exceeding the threshold required to classify them as active mineral additives. The findings support the development of "green" CPCs using hybrid additives derived from local industrial waste, offering a sustainable alternative to traditional raw materials. These formulations can significantly reduce carbon dioxide emissions, energy consumption, and natural resource depletion while maintaining cement performance, thus aligning with global trends toward low-clinker and low-carbon construction materials.

Keywords: industrial waste, steel-smelting slag, microsilica, recycling, hybrid additives, green technology, energy saving.

Author information:

Begzhanova Gulrukh Bakhtiyarovna — *Doctor of Technical Sciences, Chief Scientific Researcher, STROM Research Laboratory and Testing Center, Institute of General and Inorganic Chemistry, Academy of Sciences of Uzbekistan, Tashkent, Uzbekistan. Email: gulrukh-begzhanova@rambler.ru; ORCID ID: https://orcid.org/0000-0002-0492-3246*

Yakubzhanova Zukhra Bakhtiyarovna — *PhD, Chief Scientific Researcher, STROM Research Laboratory and Testing Center, Institute of General and Inorganic Chemistry, Academy of Sciences of Uzbekistan, Tashkent, Uzbekistan. Email: farzona19@gmail.com; ORCID ID: https://orcid.org/0000-0002-9335-6238*

Lei Wang — *Professor, College of Energy Engineering, Zhejiang University, Hangzhou, Zhejiang, 310027, PR China. Email: wanglei.leo@zju.edu.cn; ORCID ID: https://orcid.org/0000-0002-0336-7241*

Makhsudova Nozima Djaparxonovna — *PhD, Junior Researcher, STROM Research Laboratory and Testing Center, Institute of General and Inorganic Chemistry, Academy of Sciences of Uzbekistan, Tashkent, Uzbekistan. Email: nazima-25@mail.ru; ORCID ID: https://orcid.org/0000-0003-4579-6551*

Ruzmetova Aida Shonazarovna — *PhD, Associate Professor, Faculty of Chemical Technology, Urgench State University named after Abu Rayhon Beruni, Urgench, Uzbekistan. Email: aida0330@list.ru; ORCID ID: https://orcid.org/0009-0004-1008-4057*

Introduction

In Uzbekistan, numerous enterprises operating in the energy, metallurgical, chemical, mining, and processing sectors generate vast quantities of mineral-based industrial waste, much of which is currently disposed of in landfills or open dumps, causing serious ecological and economic concerns. However, with the adoption of scientifically grounded and rational processing technologies, these technogenic wastes possess significant potential to serve as alternative raw materials for various industrial applications, particularly in construction material production [[1], [2], [3]].

Recognizing the dual necessity of environmental conservation and resource

efficiency, both global and national initiatives are being actively pursued. In Uzbekistan, a strategic emphasis has been placed on enhancing environmental protection, promoting sustainable development, rationalizing the use of natural resources, and improving the sanitary-ecological landscape of industrial regions [4].

Simultaneously, due to the persistent escalation in the costs of fuel, energy, and raw material resources, the global construction industry is experiencing a paradigm shift towards the use of composite Portland cements (CPCs). These cements incorporate hybrid mineral additives—combinations of two or more supplementary cementitious materials (SCMs) of either natural or anthropogenic origin—which enable a significant reduction in Portland cement clinker content. This approach not only conserves primary resources and decreases production costs but also contributes to substantial reductions in CO_2 emissions associated with clinker calcination, thus mitigating the carbon footprint of cement production [[5], [6], [7]].

Consequently, the integration of industrial waste into CPC formulations represents a promising direction for achieving eco-efficient construction materials, aligned with the principles of "green" technology and sustainable development. This transformation necessitates comprehensive research into the physical, chemical, and pozzolanic properties of potential waste-derived additives to optimize their performance in cementitious systems.

The production of composite Portland cements (CPC), incorporating various mineral additives, represents a scientifically grounded and environmentally conscious solution to the long-standing challenge of reducing clinker content in cement. By replacing a portion of energy- and carbon-intensive clinker with alternative pozzolanic or hydraulic materials, CPCs enable a simultaneous decrease in the consumption of natural resources and thermal energy, while also mitigating the substantial carbon dioxide emissions traditionally associated with Portland cement manufacturing processes [[8], [9], [10]].

This approach is particularly relevant in regions where access to high-quality raw materials is limited or where cement demand is rapidly increasing due to large-scale infrastructure development. In such contexts, the utilization of locally sourced natural or industrial mineral additives—such as ash, slag, volcanic tuff, or other silicate-based materials—serves as a strategic method to alleviate supply deficits and reduce logistical costs related to raw material transportation. The incorporation of up to three distinct additives with varying mineralogical compositions into a single cement formulation is permitted by existing standards, opening avenues for the development of hybrid binders with tailored performance properties [[11], [12]].

However, the widespread industrial adoption of multi-component CPCs remains constrained by several factors. Chief among them is the lack of comprehensive technological frameworks and insufficient experimental data regarding the synergistic or antagonistic effects of multiple additives introduced simultaneously. Additionally, geographical disparities in the availability of suitable waste materials—such as fly ash, blast furnace slag, and clay—further hinder consistent production. Cost barriers, particularly associated with high-performance additives like microsilica, also limit large-scale implementation.

Forecasts by the International Energy Agency anticipate a steady increase in the global share of CPCs, with permissible additive content projected to rise to 40% or more by 2100. This shift is expected to significantly elevate the demand for supplementary cementitious materials. Nevertheless, current reserves of widely used additives are insufficient to satisfy this anticipated growth, prompting the urgent need for targeted research aimed at identifying, characterizing, and processing new sources of mineral additives.

Such research must focus not only on the geochemical and physical properties of potential raw materials but also on their environmental compatibility, long-term durability, and economic feasibility. In this context, the valorization of underutilized or untapped local resources—such as technogenic by-products, silicate rocks, and industrial residues—will be crucial for establishing a sustainable, low-carbon cement industry capable of meeting future global construction demands.

In this context, the comprehensive investigation of the technological properties, chemical compositions, and potential applications of mineral technogenic raw materials derived from various industrial processing sectors becomes critically important. As industrial production continues to expand globally, the generation and accumulation of technogenic by-products—such as slags, ashes, industrial dusts, and other waste materials—grow proportionally. These secondary raw materials represent an increasingly valuable resource pool that can significantly supplement traditional natural mineral sources, which are often

limited in availability or subject to depletion [13]. Understanding their physical, chemical, and mineralogical characteristics is essential to optimize their incorporation into cementitious systems, ensuring that these additives not only enhance material performance but also comply with environmental and health safety standards [[14], [15]].

Furthermore, the strategic utilization of synthetic mineral raw materials addresses multiple pressing challenges faced by the cement industry and broader environmental management goals. The deployment of these materials promotes a “clean” climate by reducing the carbon footprint associated with clinker production and by enabling the recycling of industrial waste that would otherwise contribute to environmental pollution [16]. This approach also safeguards the health and safety of populations living in proximity to heavy industrial zones by mitigating the uncontrolled release of hazardous substances and dust emissions [17]. Additionally, it plays a vital role in preserving biodiversity, as the extraction pressure on natural mineral deposits is alleviated, reducing habitat destruction and ecological imbalance [18].

From an applied research perspective, evaluating the feasibility and effectiveness of energy and metallurgical waste as supplementary cementitious materials requires systematic experimental work and techno-economic analysis [19]. Such studies encompass the optimization of processing techniques to improve reactivity, assess durability under various environmental conditions, and evaluate long-term stability in concrete composites [20]. Alongside this, it is necessary to develop specific guidelines and recommendations for industrial-scale implementation that consider local resource availability, regulatory frameworks, and sustainability metrics.

Ultimately, these efforts culminate in the formulation of novel “green” composite cement products that align with global climate targets and sustainable development goals. Numerous studies confirm that the integration of diverse mineral additives and synthetic raw materials fosters the development of durable, eco-friendly building materials capable of meeting modern infrastructure demands while minimizing ecological impact [[21], [22], [23], [24], [25], [26]].

Experimental part

The study objects comprised Portland cement clinker sourced from Bekabadcement JSC, gypsum stone from the Bukhara deposit, and the proposed additives including active ash slag (AAS) from the Angren TPP dry removal, microsilica (MS), processed steel slag (PS), ladle slag (LS), and furnace slag (FS) produced by Uzmetkombinat JSC. The chemical and mineralogical compositions of the raw materials were determined according to GOST 5382, with hydraulic activity assessed in accordance with GOST 310.4. This involved processing to derive the calculated value of the Student's criterion as per GOST 25094. To evaluate the suitability of raw materials as cement additives, their compressive strength must be assessed in comparison to the strength of standard sand mixed with cement; this necessitates subsequent statistical processing of the obtained data and calculation of the Student's criterion in alignment with the GOST 25094 methodology. The results were evaluated following O'z DSt 901 and GOST 31108 - 20. The suitability of ash and slag was determined according to national standard O'z DSt 2912:2014 “Ash and slag mixtures for the production of Portland cement clinker and Portland cement. Technical conditions". The pozzolanic activity of the additives was quantified by measuring the volume of lime absorbed, along with the degree of alkalinity of the liquid phase in contact with the cement samples containing hybrid additives.

Physical and mechanical testing of samples.

Grinding the mixtures in a laboratory ball mill to fineness according to the residue on sieve No. 008. A mixture of test clinker with different ratios additives and clinker with standard sand was prepared using a mixer machine Matest E093 for 1 minute. The mixture was trowel-mixed for another 4 minutes to ensure uniformity in the cement mortar. The resulting slurry was then transferred into a three-pong mold, measuring 40×40×160 mm for compressive strength tests and 20×20×20 mm for definition of hydraulic activity. The molds were clamped onto a vibrating machine, Matest for 2 minutes to compact the mortar.

To safeguard against moisture loss caused by evaporation, a polythene sheet that was impermeable and flat was used to cover the prisms. These prisms were then placed in a temperature-controlled room with relative humidity exceeding 90% for 24 hours±30 minutes, after which they were demolded and air-cured for 28 days. Potable water was used as the mixing liquid, and they were cured in water for 28 days.

Following grinding of the mixtures in a laboratory ball mill to achieve a residue fineness on sieve No. 008, six prism samples were created from

each mortar mixture and subjected to compressive strength testing subsequent to maturation and steaming, as outlined in GOST 310.4-81 "Cements. Methods for Determining Bending and Compressive Strength." The efficacy of the additive under investigation was ascertained by statistically evaluating the significance of strength disparities between samples containing MS and those containing sand.

Based on the compressive strength data, the Student's criterion (t-criterion) was calculated, and the computed t-criterion value was juxtaposed with the standard threshold of t = 2.07 in accordance with O'z DSt 901-98 and t = 15 per GOST 31108-20. A t value surpassing these benchmarks indicates that the additive has successfully met the strength activity assessment. The calculation for the mixtures consisted of:

1 - Xiad – clinker + MS additive

2 - His – clinker + sand

Results and Discussion

The results of the chemical analyses conducted on Portland cement clinker, gypsum stone, and the industrial waste materials under study are presented in Table 1. Utilizing the chemical composition data, the mineralogical makeup and modular parameters of the clinker—including the saturation factor (K), and the lime (n) and silica (p) ratios—were calculated. These calculated indices confirm that the Portland cement clinker conforms fully to the specifications outlined in the National Standard O'z DSt 2801:2013, which governs clinker quality requirements for the production of general-purpose construction cements.

The combined content of gypsum and anhydrite identifies the gypsum stone extracted from the Bukhara deposit as a Grade 3 gypsum, indicating its suitability as a setting time regulator in Portland cement formulations. According to its chemical characteristics, the ash and slag mixture (AAS) is classified as acidic ash and slag with a low content of combustible substances, as evidenced by the measured loss on ignition values. Moreover, its chemical composition meets the criteria specified in the O'z DSt 2912:2014 standard for ash and slag mixtures used in the manufacturing of Portland cement clinker and Portland cement.

To thoroughly assess the potential of these raw materials as cement additives, their compressive strength must be evaluated relative to the strength of a control mixture containing standard sand and cement. This necessitates further statistical analysis of the experimental data, including the calculation of Student's t-test to determine the significance of the observed differences. To illustrate this evaluation approach, specific experiments were performed to determine the Student's t-value for microsilica. Two types of mixtures were prepared for testing:

A blend of 600 grams of Portland cement clinker, 1400 grams of microsilica additive, and 100 grams of gypsum stone expressed chemically as $CaSO_4 \cdot 2H_2O$;

A control blend of 600 grams of Portland cement clinker, 1400 grams of standard sand, and 100 grams of gypsum stone ($CaSO_4 \cdot 2H_2O$).

This comparative analysis enables a clear determination of the effect of the microsilica additive on the mechanical properties of the cement composite.

Table 1 - Chemical compositions of Portland cement clinker and gypsum stone

Name of materials	Content of mass fraction of oxides, %							
	loss on ignition	SiO_2	Al_2O_3	Fe_2O_3	CaO	MgO	SO_3	others
Clinker JSC "Bekabadcement"	0.36	21.30	4.75	4.86	63.68	3.07	0.43	2.55
Gypsum stone	400°C 13.60	2.11	0.49	0.15	31.08	3.79	38.09	10.7
Ladle slag	1.49	35.93	7.56	2.79	33.06	6.04	0.78	12.35
Recycled steel slag	3.0	62.02	23.55	4.32	3.0	-	1.28	0.80
Furnace slag	-	31.34	9.57	20.78	15.97	4.23	1.19	16.92
Microsilica	2.79	90.84	1.51	1.59	0.56	1.00	0.23	1.48
Active ash and slag	3.0	62.02	23.55	4.32	3.0	-	1.28	0.8

Table 2 - Arithmetic mean values of compressive strength and their standard deviations

№ samples	X_{iad}	$X_{iad} - X_{iad}$	$(X_{iad} - X_{iad})^2$	X_{iS}	$X_{iS} - X_S$	$(X_{iS} - X_S)^2$
1	9.2	0.3	0.09	6.4	0.13	0.0169
2	9.2	0.3	0.09	6.4	0.13	0.0169
3	10.0	-0.5	0.25	6.2	0.33	0.1089
4	9.0	0.5	0.25	7.6	-1.07	1.1449
5	9.6	-0.1	0.01	6.2	0.33	0.1089
6	9.2	0.3	0.09	6.4	0.13	0.0169
7	9.0	0.5	0.25	6.2	0.33	0.1089
8	10.2	-0.7	0.49	7.6	-1.07	1.1449
9	10.4	-0.9	0.81	6.2	0.33	0.1089
10	9.0	50.1	0.25	6.4	0.13	0.0169
11	9.2	0.3	0.09	6.4	0.13	0.0169
12	10.4	-0.9	0.81	6.4	0.13	0.0169
$\sum_{i=1}^{12}$	114		3.48	78.4		2.83
$X_{average}$	9.50			6.53		

The experimental results of prism specimens, systematically prepared from two comparative mixtures designated as Composition No. 1 and Composition No. 2, are rigorously compiled and detailed in Table 2. These data form the basis for subsequent quantitative analysis and statistical evaluation.

The table provides detailed measurements for each sample, including individual compressive strength values (Xi), deviations from the mean, squared deviations, and calculated statistical parameters for both mixtures.

Based on the data presented in Table 2, the arithmetic mean compressive strength values and their standard deviations were calculated as follows:

Student's t-Test Calculation

• For mixture No. 1 ($\bar{X}i\_ad$):

$$\bar{X}_{ad} = \frac{114}{12} = 9.50 \text{ MPa}; \quad S_{ad}^2 = \frac{3.48}{11} = 0.316;$$
$$S_{ad} = \sqrt{0.316} = 0.562$$

• For mixture No. 2 ($\bar{X}i\_s$):

$$\bar{X}_s = \frac{78.4}{12} = 6.53 \text{ MPa}; \quad S_s^2 = \frac{2.83}{11} = 0.257; \quad S_s = \sqrt{0.257} = 0.507$$

Where $\bar{X}_{ad}$ and $\bar{X}_s$ denote the mean ultimate compressive strength values of samples from compositions 1 and 2, respectively.

Before proceeding with hypothesis testing, the following conditions were verified to ensure the validity of the Student's t-test:

1. The similarity of standard deviations:

$$S_{ad} \approx S_s \leq 2.0 \text{ MPa} \Rightarrow 0.562 \approx 0.507 < 2.0 \text{ MPa}$$

2. The ratio of variances meets the required threshold:

$$\frac{S_{ad}^2}{S_s^2} = \frac{0.316}{0.257} = 1.23 < 2.82$$

Since both conditions were satisfied, the Student's t-test was computed using the formula:

$$t = 2.45 \times = \frac{X_{ad} - X_s}{\sqrt{\frac{S_{ad}^2 + S_s^2}{2}}} = 2.45 \times = \frac{9.50 - 6.53}{\sqrt{\frac{0.316 + 0.257}{2}}} =$$
$$2.45 \times \frac{2.97}{0.54} = 13.47$$

The calculated t-value of 13.47 significantly exceeds the critical value of 2.07 stipulated by the O'z DSt 901 standard. This clearly indicates that microsilica (MS) functions as an active mineral additive, validating its recommendation for use as such in cement formulations.

Applying this same statistical methodology, the activity and suitability of other technogenic waste materials were evaluated. The resulting Student's t-test values were:

- Active ash and slag (AASh): 52.92
- Recycled steel slag (RSS): 11.14 for the fraction 0–5 mm, and 2.19 for the fraction 5–50 mm
- Ladle slag (LS): 5.00
- Furnace slag (PS): 4.48

Based on the descending order of the Student's t-values, the additives can be ranked in terms of their mineral activity and potential effectiveness as follows:

Active ash and slag → Microsilica → Recycled steel slag → Ladle slag → Furnace slag

This ranking provides a clear hierarchy of mineral additive activity, supporting targeted selection for optimized cementitious composite production.

Previous investigations conducted at the "Strom" Scientific Laboratory and Testing Center of the Institute of General and Inorganic Chemistry under the Academy of Sciences of the Republic of Uzbekistan have demonstrated that the incorporation of processed steel slag (RSS) and microsilica (MS) in quantities exceeding 15% tends to reduce the compressive strength of Portland cement. Conversely, activated ash and slag (AASh), due to its pronounced pozzolanic reactivity, has shown potential to substitute up to 45% of clinker in cement formulations without compromising mechanical performance.

Based on these findings, a new approach was adopted to design hybrid mineral additives in which AASh serves as the principal active component, while other less reactive materials, such as MS, RSS, furnace slag (FS), and ladle slag (LS), function as supplementary components. In the developed compositions, the proportion of AASh was systematically varied from 15% to 35%, while the content of the passive components remained fixed at 10% (Table 3).

The pozzolanic activity of these newly developed hybrid additives was evaluated using the liquid phase saturation method. In this procedure, composite Portland cement samples containing different types and quantities of hybrid additives were immersed in a controlled liquid medium, and the degree of CaO (lime) absorption was measured over a period of 30 days [23]. This method is grounded in the principle that reactive mineral additives can bind with free lime (CaO) released during the hydration of clinker phases, thereby reducing the lime concentration in the surrounding liquid and indicating higher pozzolanic activity.

According to the data in Table 5, samples of standard Portland cement without any additives (PC-Ad0) released approximately 5.4% CaO into the liquid phase within 30 days, and the total alkalinity of the solution reached 58.8 meq/L. In comparison, the liquid containing composite cement samples with a hybrid additive comprising 15% AASh and 10% RSS exhibited a reduced CaO concentration of 4.2%, implying that approximately 1.2% of the released CaO was absorbed by the additives. The corresponding total alkalinity also declined to 56.0 meq/L, 2.8 meq/L lower than that of the control.

Table 3 - Hydraulic activity of additives determined by the degree of lime saturation of the liquid phase in contact with cement

№	Component ratio, mass. %				CaO content in liquid, %	Total alkalinity of solution, meq L^{-1}
	Clinker	active ash and slag	recycled steel slag	gypsum stone		
1	95	-	-	-	5.4	58.8
2	70	15	10	5	4.2	56
3	60	25	10	5	2.22	48
4	50	35	10	5	0.72	32.4
	Clinker	active ash and slag	furnace slag	gypsum stone		
5	70	15	10	5	4.68	56.4
6	60	25	10	5	2.64	48.8
7	50	35	10	5	1.38	40
	Clinker	active ash and slag	ladle slag	gypsum stone		
8	70	15	10	5	3.9	61.6
9	60	25	10	5	2.58	55.2
10	50	35	10	5	0.84	41.2
	Clinker	active ash and slag	microsilica	gypsum stone		
11	70	15	10	5	0.78	20
12	60	25	10	5	0.72	35.2
13	50	35	10	5	0.36	23.2

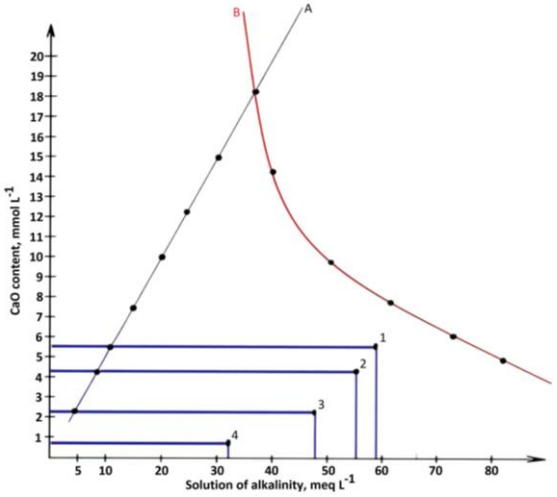

Figure 1 - Pozzolanic activity of additives “active ash and slag + recycled steel slag” in the composite Portland cement: A- lime solubility isotherm at 40°; B- alkalinity, which accounts for all components except lime.

Content of CaO in cement mortar with an additive:

1-PC-Ad0, 2-HAd25 %, 3- HAd 35 %, 4- HAd 45 %.

Further increasing the proportion of AASh to 25% and 35% significantly enhanced the lime-binding capacity of the hybrid additives. In these cases, the CaO concentrations in the liquid phase dropped to 2.22% and 0.72%, respectively, equating to CaO absorptions of 2.98% and 4.68%. Simultaneously, the total alkalinity of the liquid phase decreased to 48.0 meq/L and 32.4 meq/L, respectively. These trends clearly underscore the high pozzolanic reactivity of the AASh + RSS hybrid system, wherein increasing the proportion of AASh at a constant 10% RSS content directly enhances lime fixation and reduces alkalinity in the liquid phase (Figure 1).

Hybrid additives of the composition “active ash and slag + furnace slag” and “active ash and slag + ladle slag” are characterized by almost the same absorbing ability, the activity of which also increases with increasing content of active ash and slag from 15 % to 35 % - the CaO content in the liquid phase with these hybrid additives is (4.68 - 1.38) % and (3.9 -0.84) %, and the total alkalinity of the liquid phase is (1.38 - 40.0) meq L^{-1} and (61.6 - 41.2) meq L^{-1}, respectively (Figure 2).

Legend:

1 – PC-Ad0 (reference Portland cement without additives);

2 – PC-HAd25 (composite cement with 25% hybrid additive);

3 – PC-HAd35 (composite cement with 35% hybrid additive);

4 – PC-HAd45 (composite cement with 45% hybrid additive).

(a) – Isothermal solubility curves of calcium hydroxide at 40 °C;

(b) – Alkalinity of the liquid phase contributed by all components excluding free lime (CaO).

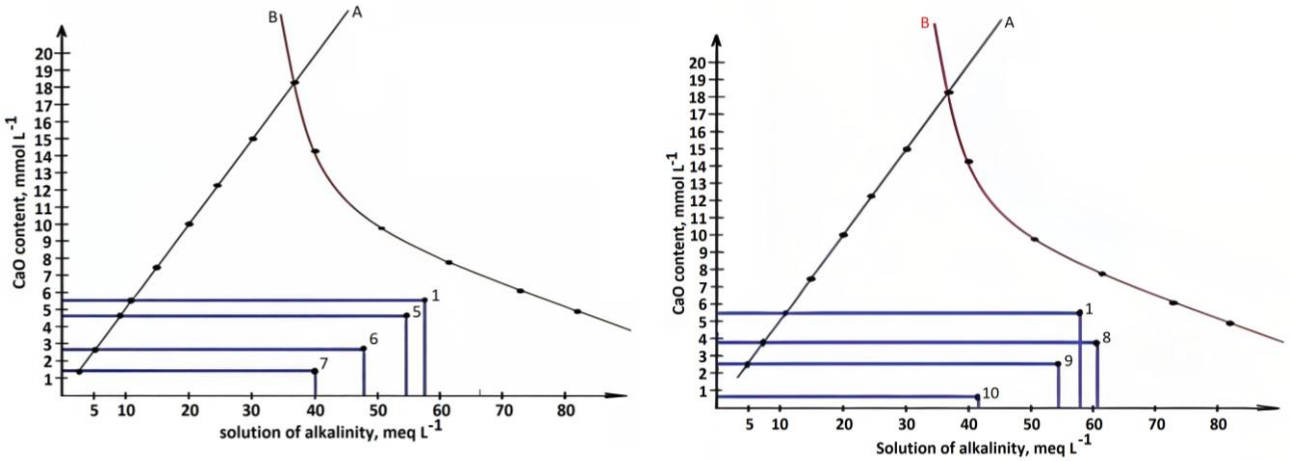

Figure 2 - Pozzolanic activity of hybrid additives comprising “activated ash and slag (AASh) + furnace slag (FS)” (a) and “activated ash and slag (AASh) + ladle slag (LS)” (b) in composite Portland cement systems.

CaO content in cement mortar samples containing hybrid additives:

1 – PC-Ad0;
5 – HAd25%;
6 – HAd35%;
7 – HAd45% (for both subfigures a and b).

The experimental findings indicate that the highest pozzolanic activity among the studied hybrid additives is exhibited by the composition based on activated ash and slag (AASh) combined with microsilica (MS). Already at a dosage of 15 wt% AASh and 10 wt% MS, a substantial decrease in the concentration of calcium oxide (CaO) in the liquid phase was observed — 0.78%, which is 4.62% less than the CaO concentration in the solution where control samples of additive-free Portland cement (PC-Ad0) were stored. This reduction confirms the effective lime-binding capacity of the hybrid additive system.

Moreover, the total alkalinity of the solution decreased sharply to 20 meq/L, which is more than 3.5 times lower than the alkalinity value observed for the solution containing PC400-Ad0 samples. This pronounced drop in alkalinity suggests not only efficient lime immobilization but also an intensification of pozzolanic reactions in the cementitious environment.

As the dosage of AASh was increased to 25 wt% and 35 wt% (with MS content held constant at 10 wt%), the CaO concentration in the liquid phase further declined to 0.72% and 0.36%, respectively. These results underscore the synergetic effect of ultrafine MS in enhancing the pozzolanic efficiency and reactivity of the hybrid system. The high specific surface area and amorphous structure of MS contribute to the increased rate of calcium hydroxide fixation, thereby promoting the formation of additional calcium silicate hydrate (C–S–H) phases.

Despite the reduction in free CaO, a slight increase in total alkalinity was recorded for systems containing higher AASh content. This phenomenon can be attributed to the accelerated hydration kinetics of clinker minerals—primarily tricalcium silicate (C_3S) and dicalcium silicate (C_2S)—facilitated by the reactive environment generated by MS. The intensified dissolution of these phases leads to a higher release of Ca^{2+} ions into the pore solution, thereby increasing its ionic strength and pH.

The cumulative findings affirm that all investigated hybrid additive formulations demonstrate considerable pozzolanic potential and meet the performance benchmarks for mineral additives in blended cement systems. According to the technical classification system outlined in GOST 24640-91 “Additives for cements. Classification”, the developed hybrid additives fall under the category of active mineral admixtures, simultaneously exhibiting both hydraulic and pozzolanic properties. Their multifunctional nature makes them promising candidates for sustainable cement formulations aimed at reducing clinker content and enhancing durability characteristics of the final composite.

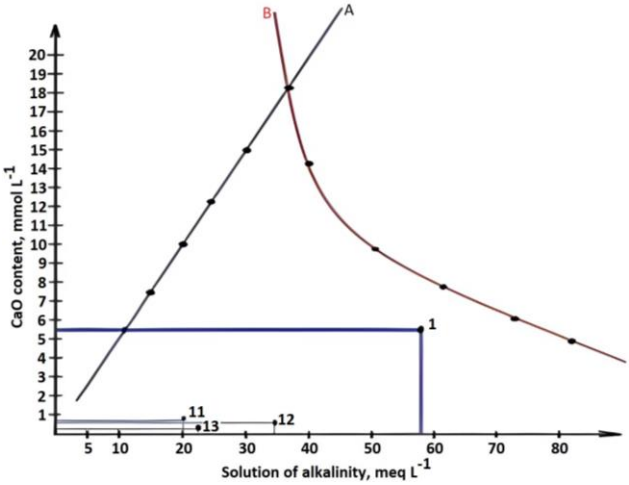

Figure 3 - Pozzolanic activity of hybrid additives based on "active ash and slag + microsilica (MS)" in composite Portland cement

A – Isotherm of lime (CaO) solubility at 40 °C;
B – Total alkalinity of the liquid phase, excluding the contribution of lime.

Legend (for both graphs):
1 – PC-Ad0 (reference cement without additives);
5 – Cement with 25% active ash and slag + 10% MS (HAd25);
6 – Cement with 35% active ash and slag + 10% MS (HAd35);
7 – Cement with 45% active ash and slag + 10% MS (HAd45).

Conclusions

The research has convincingly demonstrated that the modification of technogenic steelmaking by-products, particularly ladle slag and furnace slag, with ash and slag waste generated by thermal power plants, enables the development of hybrid mineral additives possessing enhanced hydraulic

and pozzolanic activity. These hybrid additives make it possible to produce composite Portland cements whose mechanical strength is comparable to, or even exceeds, that of reference Portland cement grade PC400-Ad0, despite containing a significantly reduced proportion of clinker.

The active ash and slag (AASh) component—characterized by high reactivity—plays a pivotal role in the early stages of hydration. By intensively binding calcium hydroxide [$Ca(OH)_2$] from the pore solution, it accelerates the formation of calcium hydrosulfoaluminates, thereby contributing to the early strength gain of the cementitious matrix. Meanwhile, the more inert components of the hybrid additives, such as microsilica (MS), processed ladle slag (LS), and furnace slag (FS), continue to react over time, promoting the formation of secondary calcium silicate hydrates (C–S–H). These hydrates fill capillary pores, enhance microstructural densification, and contribute to the long-term strength and durability of the cement composite.

Comprehensive control testing of large-scale batches containing the optimal hybrid additive compositions was conducted at JSC Akhangarancement and JSC Bekabadcement. The results of these industrial-scale trials unequivocally confirmed the feasibility and effectiveness of replacing 25% to 45% of Portland cement clinker with the developed "green" hybrid additives. The resulting composite Portland cements reliably achieved strength classes of 400 to 500, in full compliance with regulatory standards and performance requirements.

These findings affirm the technological and environmental viability of the proposed hybrid systems and their potential for widespread application in sustainable cement manufacturing.

Conflicts of interest. On behalf of all authors, the corresponding author states that there is no conflict of interest.

CRediT author statement: **G. Begzhanova**: Conceptualization, Methodology, Software; **Z. Yakubzhanova**: Data curation, Writing draft preparation; **L Wang**: Visualization, Investigation; **A. Ruzmetova**: Supervision; **N. Makhsudova**: Software, Validation; **A. Ruzmetova**: Reviewing and Editing.

Acknowledgements. We express our deep gratitude to **Atabaev Farrukh Bakhtiyarovich**, Chief Scientific Researcher at the "STROM" Research Laboratory and Testing Center of the Institute of General and Inorganic Chemistry of the Academy of Sciences of Uzbekistan, for his practical assistance in conducting the experiments for this research. We also extend our sincere appreciation to **Khadzhiev Azamat Shamuratovich** for his translation support and language-related matters, as well as to the co-authors for their contributions to the writing and editing of the article.

Formatting of funding sources. This research did not receive any specific grant from funding agencies in the public, commercial, or not-for-profit sectors.

Cite this article as: Begzhanova GB, Yakubzhanova ZB, Wang L, Makhsudova ND, Ruzmetova ASh. Study of the suitability of industrial raw material resources as additives for Portland cement. Kompleksnoe Ispolzovanie Mineralnogo Syra = Complex Use of Mineral Resources. 2027; 341(2):71-82. https://doi.org/10.31643/2027/6445.19

Портландцементке қоспа ретінде өнеркәсіптік шикізаттың жарамдылығын зерттеу

[1*]Бегжанова Г.Б., [1] Якубжанова З.Б., [2]Wang L., [1]Махсудова Н.Ж., [3]Рузметова А.Ш.

[1] Өзбекстан Республикасының Ғылым академиясы, Жалпы және бейорганикалық химия институты, Ташкент
[2]Чжэцзян университеті, Энергетикалық инженерия колледжі, Ханчжоу, Қытай
[3] Әбу Райхан Беруни атындағы Ургенч мемлекеттік университеті, Өзбекстан

ТҮЙІНДЕМЕ

Бұл зерттеу композициялық портландцемент (КПЦ) өндірісінде өнеркәсіптік техногенді қалдықтарды гибридті минералдық қоспалар ретінде пайдалану мүмкіндігін зерттейді. Зерттеудің басты мақсаты – клинкер тұтынуын азайту және экологиялық таза құрылыс технологияларын ілгерілету. Қарастырылған материалдарға Ангрен жылу электр станциясынан алынған белсенді күл мен қож (БКҚ), микрокремнезем (МК), сондай-ақ «Өзметкомбинат» АҚ-ның болат өндірісі қалдықтары – ковш қожы (КҚ), пеш қожы (ПҚ) және қайта өңделген болат қожы (ҚБҚ) жатады. Аталған материалдардың химиялық, минералогиялық және механикалық қасиеттері ұлттық және халықаралық стандарттарға

Мақала келді: *5 маусым 2025*
Сараптамадан өтті: *1 қазан 2025*
Қабылданды: *25 қараша 2025*

сәйкес сипатталды. Олардың пуццоландық және гидравликалық белсенділігі қысымға төзімділік сынақтары және әктің сіңірілуін өлшеу арқылы бағаланды. Эксперименттік нәтижелер БКҚ-ның белсенділігі ең жоғары екенін көрсетті: ол клинкердің 45%-ға дейінгі мөлшерін механикалық беріктікке кері әсер етпей алмастыра алады. Белсенділігі төмен материалдармен (МК, ҚБҚ, ПҚ және КҚ) бірге қолданылғанда гибридті қоспалар синергетикалық әсер көрсетті. Атап айтқанда, БКҚ мен МК қоспасы ең жоғары пуццоландық белсенділік танытты: ол қоршаған сұйықтықтағы кальций оксиді (CaO) концентрациясының төмендеуімен және ерітінді сілтілігінің азаюымен расталды. Стьюденттің t-өлшемшарты арқылы жүргізілген статистикалық тексеру әрбір қоспаның тиімділігін дәлелдеді: алынған t-мағыналар олардың белсенді минералдық қоспалар ретінде жіктелуіне қажетті шектік мәндерден едәуір асып түсті. Зерттеу нәтижелері жергілікті өнеркәсіптік қалдықтар негізінде гибридті қоспалар арқылы «жасыл» КПЦ жасаудың мүмкіндігін қолдайды. Мұндай құрамдар көмірқышқыл газы шығарындыларын, энергия тұтынуды және табиғи ресурстардың сарқылуын айтарлықтай азайта отырып, цементтің пайдалану қабілетін сақтап қалады. Бұл тәсіл төмен клинкерлі және төмен көміртекті құрылыс материалдарына көшу жөніндегі жаһандық үрдістерге толық сәйкес келеді.

Түйін сөздер: өнеркәсіптік қалдықтар, болат балқытушы қож, микрокремнезем, қайта өңдеу, гибридті қоспалар, жасыл технология, энергия үнемдеу.

Авторлар туралы ақпарат:

Бегжанова Гулрух Бахтиярқызы — *Техника ғылымдарының докторы, Өзбекстан Ғылым академиясының Жалпы және бейорганикалық химия институтының STROM ғылыми-зерттеу зертханасы мен сынақ орталығының бас ғылыми қызметкері, Мырза Ұлықбек көшесі, 77, 100170, Ташкент, Өзбекстан. Email: gulrukh-begzhanova@rambler.ru; ORCID ID: https://orcid.org/0000-0002-0492-3246*

Якубжанова Зухра Бахтиярқызы — *PhD, Өзбекстан Ғылым академиясының Жалпы және бейорганикалық химия институтының STROM ғылыми-зерттеу зертханасы мен сынақ орталығының бас ғылыми қызметкері, Мырза Ұлықбек көшесі, 77, 100170, Ташкент, Өзбекстан. Email: farzona19@gmail.com; ORCID ID: https://orcid.org/0000-0002-9335-6238*

Lei Wang — *Профессор, Энергетикалық инженерия колледжі, Чжэцзян университеті, Ханчжоу, Чжэцзян, Қытай Халық Республикасы. Email: wanglei.leo@zju.edu.cn; ORCID ID: https://orcid.org/0000-0002-0336-7241*

Махсудова Нозима Жапарханқызы — *PhD, Өзбекстан Ғылым академиясының Жалпы және бейорганикалық химия институтының STROM ғылыми-зерттеу зертханасы мен сынақ орталығының кіші ғылыми қызметкері, Мырза Ұлықбек көшесі, 77, 100170, Ташкент, Өзбекстан. Email: nazima-25@mail.ru; ORCID ID: https://orcid.org/0000-0003-4579-6551*

Рузметова Айда Шоназарқызы — *PhD (техника ғылымдары бойынша), Ургенч мемлекеттік университетінің Әбу Райхон Беруни атындағы Химиялық технология факультетінің доценті, Ургенч, Өзбекстан. Email: aida0330@list.ru; ORCID ID: https://orcid.org/0009-0004-1008-4057*

Изучение пригодности промышленных сырьевых ресурсов в качестве добавок к портландцементу

[1*]Бегжанова Г.Б., [1]Якубжанова З.Б., [2]Wang L., [1]Махсудова Н.Ж., [3]Рузметова А.Ш.

[1] Институт общей и неорганической химии Академии наук Узбекистана, Ташкент
[2] Чжэцзянский университет, Колледж энергетического машиностроения, Ханчжоу, Китай
[3] Ургенчский государственный университет имени Абу Райхона Беруни, Узбекистан

Поступила: *5 июня 2025*
Рецензирование: *1 октября 2025*
Принята в печать: *25 ноября 2025*

АННОТАЦИЯ

В данном исследовании рассматривается возможность использования техногенных промышленных отходов в качестве гибридных минеральных добавок при производстве композиционного портландцемента (КПЦ) с целью снижения расхода клинкера и продвижения экологически безопасных строительных технологий. Изученные материалы включают активную золу и шлак (АЗШ) с Ангренской теплоэлектростанции, микросилику (микрокремнезем) (МС), а также переработанные отходы металлургического производства, такие как ковшевой шлак (КШ), печной шлак (ПШ) и переработанный сталеплавильный шлак (ПСШ) от АО "Узметкомбинат". Химические, минералогические и механические свойства этих материалов были охарактеризованы в соответствии с национальными и международными стандартами. Пуццолановая и гидравлическая активность оценивались методом испытания на прочность при сжатии и измерением поглощения извести. Экспериментальные результаты показали, что АЗШ обладает наивысшей активностью и способен заменять до 45% клинкера без ухудшения прочностных характеристик. В сочетании с менее активными компонентами (МС, ПСС, ПШ и КШ) гибридные добавки проявляют синергетический эффект. Среди них смесь АЗШ+МС показала наибольший пуццолановый эффект, что выражается в снижении концентрации оксида кальция (CaO) в окружающей жидкости и пониженной щелочности раствора. Статистическая проверка с использованием t-критерия Стьюдента подтвердила эффективность каждой добавки, поскольку значения t значительно превышали порог,

	необходимый для классификации их как активных минеральных добавок. Полученные результаты подтверждают возможность разработки «зеленого» КПЦ с использованием гибридных добавок на основе местных промышленных отходов, предлагая устойчивую альтернативу традиционным сырьевым материалам. Такие составы могут существенно снизить выбросы углекислого газа, потребление энергии и истощение природных ресурсов при сохранении эксплуатационных свойств цемента, что соответствует глобальным тенденциям к низкоклинкерным и низкоуглеродным строительным материалам.
	Ключевые слова: промышленные отходы, сталеплавильный шлак, микросилика, переработка, гибридные добавки, зелёные технологии, энергосбережение.
Бегжанова Гулрух Бахтияровна	***Информация об авторах:*** *Доктор технических наук, главный научный сотрудник Научно-исследовательской лаборатории и испытательного центра STROM Института общей и неорганической химии Академии наук Узбекистана, улица Мирзо Улугбека, 77, 100170, Ташкент, Узбекистан. Email: gulrukh-begzhanova@rambler.ru; ORCID ID: https://orcid.org/0000-0002-0492-3246*
Якубжанова Зухра Бахтияровна	*PhD, главный научный сотрудник Научно-исследовательской лаборатории и испытательного центра STROM Института общей и неорганической химии Академии наук Узбекистана, улица Мирзо Улугбека, 77, 100170, Ташкент, Узбекистан. Email: farzona19@gmail.com; ORCID ID: https://orcid.org/0000-0002-9335-6238*
Lei Wang	*Профессор, Колледж энергетического машиностроения, Чжэцзянский университет, Ханчжоу, Чжэцзян, Китайская Народная Республика. Email: wanglei.leo@zju.edu.cn; ORCID ID: https://orcid.org/0000-0002-0336-7241*
Махсудова Нозима Джапархановна	*PhD, младший научный сотрудник Научно-исследовательской лаборатории и испытательного центра STROM при Институте общей и неорганической химии Академии наук Узбекистана, улица Мирзо Улугбека, 77, 100170, Ташкент, Узбекистан. Email: nazima-25@mail.ru; ORCID ID: https://orcid.org/0000-0003-4579-6551*
Рузметова Айда Шоназаровна	*PhD, доцент факультета химической технологии Ургенчского государственного университета имени Абу Райхона Беруни, Ургенч, Узбекистан. Email: aida0330@list.ru; ORCID ID: https://orcid.org/0009-0004-1008-4057*

References

[1] Baruzdin A, Zakrevskaya L, Nikolaeva K, Bokarev D. Recycling construction waste for the purpose of synthesizing new composite materials. Ecology and Industry of Russia. 2023; 27(12):26-33. https://doi.org/10.18412/1816-0395-2023-12-26-33

[2] Khadzhiev A, Atabaev F. Influence of silica-containing additives on physical and mechanical properties of Portland Cement Co. Ltd Karakalpaksement. E3S Web of Conferences. 2023; 401:05051. https://doi.org/10.1051/e3sconf/202340105051

[3] Atabaev FB, Aripova MKh, Khadzhiev ASh, Tursunova GR, Tursunov ZR. Effect of multicomponent mineral additives on the microstructure and strength of composite cement. Kompleksnoe Ispolzovanie Mineralnogo Syra = Complex Use of Mineral Resources. 2027; 340(1):45-57. https://doi.org/10.31643/2027/6445.05

[4] Buriev AI, Iskandarova MI, Begzhanova GB. Influence of a high degree of filling on the properties of pozzolanic cement. RA Journal of Applied Research. 2023; 9(2):60-65. https://doi.org/10.47191/rajar/v9i2.02

[5] Amran M, Debbarma S, Ozbakkaloglu T. Fly ash-based eco-friendly geopolymer concrete: A critical review of the long-term durability properties. Construction and Building Materials. 2021; 270:121857. https://doi.org/10.1016/j.conbuildmat.2020.121857

[6] Liu X, et al. The physiochemical alterations of calcium silicate hydrate (C-S-H) under magnesium attack. Cement and Concrete Research. 2022. https://doi.org/10.1016/j.cemconres.2022.106901

[7] Iskandarova MI, et al. Improving properties of Portland cement using new types of composite additives. E3S Web of Conferences. 2023; 365:02013. https://doi.org/10.1051/e3sconf/202336502013

[8] Miller SA, Horvath A, Monteiro PJM. Readily implementable techniques can cut annual CO_2 emissions from the production of concrete by over 20%. Environmental Research Letters. 2016; 11(7):074029. https://doi.org/10.1088/1748-9326/11/7/074029

[9] Schneider M, Romer M, Tschudin M, Bolio H. Sustainable cement production—Present and future. Cement and Concrete Research. 2011; 41(7):642-650. https://doi.org/10.1016/j.cemconres.2011.03.019

[10] Damtoft JS, Lukasik J, Herfort D, Sorrentino D, Gartner EM. Sustainable development and climate change initiatives. Cement and Concrete Research. 2008; 38(2):115-127. https://doi.org/10.1016/j.cemconres.2007.09.008

[11] Scrivener KL, Martirena F, Bishnoi S, Maity S. Calcined clay limestone cements (LC3). Cement and Concrete Research. 2018; 114:49-56. https://doi.org/10.1016/j.cemconres.2017.08.017

[12] Dhandapani Y, Santhanam M. Assessment of pore structure and strength characteristics of blended cement with limestone and calcined clay. Cement and Concrete Composites. 2017; 78:124-133. https://doi.org/10.1016/j.cemconcomp.2017.01.003

[13] Zhang Y, Chen Q, Li J. Utilization of industrial waste in cement production: Chemical and mineralogical characteristics. Journal of Cleaner Production. 2020; 258:120789. https://doi.org/10.1016/j.jclepro.2020.120789

[14] Kumar R, Singh P, Verma M. Environmental and health risk assessment of cementitious materials with industrial by-products. Environmental Science and Pollution Research. 2021; 28(15):18825-18838. https://doi.org/10.1007/s11356-020-11902-7

[15] Lee SY, Kim JH. Mineralogical analysis and performance evaluation of technogenic raw materials for cement. Construction and Building Materials. 2019; 204:226-235. https://doi.org/10.1016/j.conbuildmat.2019.01.176

[16] Ahmed S, Al-Ghamdi SG. Carbon footprint reduction strategies in cement manufacturing using recycled industrial wastes. Journal of Environmental Management. 2018; 206:605-615. https://doi.org/10.1016/j.jenvman.2017.10.044

[17] Wang H, Zhao Z, Li X. Mitigating industrial dust pollution near cement plants: Techniques and impacts on public health. Atmospheric Environment. 2021; 244:117909. https://doi.org/10.1016/j.atmosenv.2020.117909

[18] Silva CM, Teixeira RF. Biodiversity preservation through sustainable mineral resource management in cement industries. Ecological Indicators. 2017; 76:227-235. https://doi.org/10.1016/j.ecolind.2016.12.042

[19] Torres A, Blanco A. Techno-economic analysis of energy and metallurgical waste valorization in cement composites. Resources, Conservation and Recycling. 2022; 176:105931. https://doi.org/10.1016/j.resconrec.2021.105931

[20] Gupta N, Rajput A. Durability and long-term performance of concrete with industrial waste additives: A review. Materials Today: Proceedings. 2020; 27:1300-1307. https://doi.org/10.1016/j.matpr.2020.02.587

[21] Chen L, Zhang Y. Development of industrial guidelines for sustainable cementitious materials. Sustainability. 2019; 11(3):741. https://doi.org/10.3390/su11030741

[22] Petrov V, Ivanov D. Economic and environmental benefits of synthetic mineral raw materials in cement industry modernization. Cement and Concrete Composites. 2023; 128:104387. https://doi.org/10.1016/j.cemconcomp.2022.104387

[23] Iskandarova M, Atabaev F, Tursunova G, Tursunov Z, Khadzhiev A. Composite Portland cements: Innovations and future directions in cement technology. Innovative Infrastructure Solutions. 2025. https://doi.org/10.1007/s41062-025-02067-x

[24] Iskandarova MI, Atabaev FB, Khadzhiev AS. Utilization of natural silicate rocks to reduce the carbon footprint in the cement industry. Kompleksnoe Ispolzovanie Mineralnogo Syra = Complex Use of Mineral Resources. 2026; 338(3):40-50. https://doi.org/10.31643/2026/6445.27

[25] Khadzhiev A, Abdullaev M, Yakubov Y, Jumaniyozov J. The effect of hybrid mineral additives on the genetic formation and physico-chemical processes of cement composites. E3S Web of Conferences. 2025; 633:08003. https://doi.org/10.1051/e3sconf/202563308003

[26] Atabaev FB, Aripova MKh, Khadzhiev ASh, Tursunova GR, Tursunov ZR. Effect of multicomponent mineral additives on the microstructure and strength of composite cement. Kompleksnoe Ispolzovanie Mineralnogo Syra = Complex Use of Mineral Resources. 2025; 1(322):45-57. https://doi.org/10.31643/2027/6445.05

Crossref
DOI: 10.31643/2027/6445.20
Mining & Mineral Processing

creative commons

Extraction of P_2O_5 from the mineralized mass of the Central Kyzylkum using acidic wastewater generated from cotton soapstock processing: scientific analysis based on equilibrium principles

[1]Baltayev U.S., [1*]Shamuratov S.X., [2]Alimov U.K, [3]Madaminov A.E., [4]Jabbarov M.E.

[1]Urgench State University named after Abu Rayhan Biruni, Uzbekistan
[2]Institute of General and Inorganic Chemistry, Academy of Sciences of the Republic of Uzbekistan, Tashkent
[3]Urgench State Pedagogical Institute, Uzbekistan
[4]Non-government Educational Institution Mamun University, Khiva, Uzbekistan

**Corresponding author email: shamuratovsx@gmail.com*

Received: *July 20, 2025*
Peer-reviewed: *October 16, 2025*
Accepted: *November 25, 2025*

ABSTRACT

This study explores the prospects of extracting phosphorus pentoxide (P_2O_5) from the mineralized mass of the Central Kyzylkum region using acidic wastewater (AWW) derived from cottonseed soapstock processing. The acidic components within the AWW were found to facilitate the decomposition of solid-phase phosphorite material. Experiments were conducted at 333 K under varying AWW-to-mineralized mass (AWW:MM) ratios ranging from 100:10 to 100:40. The concentration of P_2O_5 was determined using a photometric method at a wavelength of 440 nm. The research was based exclusively on the analysis of the solid phase, where the extent of the reaction was assessed through the quantity of precipitate formed. It was demonstrated that an increase in pH had a direct effect on P_2O_5 extraction. The reduction in CaO content followed an exponential trend, while the P_2O_5 release exhibited a logarithmic relationship with pH. The equilibrium reactions between ions were interpreted within the framework of chemical mechanisms. Experimental results were expressed through graphical analysis and regression modeling using OriginPro 2021. The obtained data were mathematically modeled with high reliability, as indicated by coefficients of determination (R^2) exceeding 0.95. This approach offers a cost-effective, waste-based alternative technological method for phosphorus extraction, utilizing industrial by-products while maintaining environmental and economic feasibility.

Keywords: Acidic wastewater, Central Kyzylkum mineralized mass, Ionic equilibrium, Mathematical modeling, Phosphorus pentoxide (P_2O_5), Photometric analysis, Solid-phase reaction.

Information about authors:

Baltaev Umidbek Sotimbayevich — *Candidate of Technical Sciences, doctoral student in the Faculty of Chemical Technologies, Urgench State University named after Abu Rayhan Biruni, 220100, H. Olimjon Street 14, Urgench, Uzbekistan. Email: umid.bo@urdu.uz; ORCID ID: https://orcid.org/0009-0004-5636-3318*

Shamuratov Sanjarbek Xusinbay ugli — *Doctor of Philosophy in Technical Sciences, Associate Professor at the Faculty of Chemical Technology, Urgench State University named after Abu Rayhan Biruni, 220100, H. Olimjon Street 14, Urgench, Uzbekistan. Email: shamuratovsx@gmail.com; ORCID ID: https://orcid.org/0000-0002-1040-1807*

Alimov Umarbek Kadirbergenovich — *Doctor of Technical Sciences, leading scientific researcher at the Institute of General and Inorganic Chemistry, Academy of Sciences of the Republic of Uzbekistan, 100170, Mirzo Ulugbek, 77, Tashkent, Uzbekistan. Email: umaralihonalimov@mail.ru; ORCID ID: https://orcid.org/0000-0001-5608-5304*

Madaminov Azimbek Egamberganovich — *Doctor of Philosophy in Pedagogical Sciences, Associate Professor in the Faculty of Natural and Applied Sciences, Urgench State Pedagogical Institute, 220100, Gurlan str, 1-A, Urgench city, Uzbekistan. ORCID ID: https://orcid.org/0000-0002-3482-8071*

Jabbarov Majidbek Erzodovich — *Non-government Educational Institution Mamun University, Khiva, Uzbekistan. Email: jabbarovmajidbek2@gmail.com; ORCID ID: https://orcid.org/0009-0001-5987-0057*

Introduction

In the fat and oil industry, soapstock—a by-product generated during the processing of cottonseed oil—occupies a significant position among production wastes. Soapstock is a complex mixture composed of soap-like compounds, phosphatides, residual oils, dissolved salts, and other impurities. Its direct disposal poses environmental and technological challenges, necessitating the development of appropriate recycling strategies [[1], [2], [3], [4], [5]].

The recycling process is typically carried out under strongly acidic conditions, resulting in the

formation of AWW enriched with reactive ions such as H^+, SO_4^{2-}, NO_3^-, and Cl^-. These wastewaters are characterized by high acidity, elevated salt concentrations, and the presence of organic matter. Due to their chemical composition, such effluents can be utilized as reactive media in various industrial processes. Notably, the solubility of metals and phosphorus compounds increases under acidic conditions, making acidic wastewater a promising secondary resource for mineral extraction [[6], [7], [8], [9]].

Phosphorite deposits located in the Central Kyzylkum region have been found to contain substantial amounts of phosphorus pentoxide (P_2O_5). The raw form of these deposits—referred to as mineralized mass—is not directly suitable for industrial use but can be upgraded through chemical processing. Alongside P_2O_5, the mineralized mass also contains significant levels of CaO, MgO, Al_2O_3, Fe_2O_3, CO_2, SO_3, F^-, and other oxides. Developing an efficient technology for the decomposition of this mass and the selective extraction of P_2O_5 is of considerable importance. Achieving this requires low-cost yet effective reagents [8].

AWW, derived from soapstock processing, is now being considered as one such reagent. This approach offers the potential for simultaneous recycling of two industrial wastes—soapstock and low-grade phosphorite—thus aligning with the concept of obtaining valuable products from waste materials and supporting principles of circular economy and sustainable resource use [[10], [11], [12], [13], [14]].

The conventional reagents commonly used for the extraction of phosphorus pentoxide (P_2O_5) are often expensive and pose environmental hazards [15]. In contrast, secondary AWW, particularly that derived from soapstock processing, offers both economic and technological advantages. It serves as a reactive medium that facilitates the dissolution of soluble components in phosphorite [16]. In acidic environments, minerals such as apatite and related phosphate compounds gradually undergo decomposition, releasing P_2O_5 in a soluble form into the solution. The efficiency of this process is highly dependent on factors such as pH, ionic composition, temperature, and the mass ratio between the reagent and the raw material [[17], [18], [19]].

AWW obtained from soapstock processing is rich in various ions, leading to the formation of complex reactions. In particular, H^+ and SO_4^{2-} ions engage in ion-exchange processes with cationic species, thereby enhancing the release of P_2O_5. A deeper theoretical and experimental investigation is required to fully understand these phenomena and to identify optimal operational parameters. Elucidating the reaction kinetics and equilibrium behavior is a fundamental scientific objective, as it could lead to the improvement of processing technologies for low-grade phosphate raw materials such as the Central Kyzylkum mineralized mass (MM) [[8], [17]]. Furthermore, this approach opens possibilities for the beneficial reuse of AWW within industrial applications [[20], [21], [22], [23], [24], [25], [26]].

The interaction of chemical components in such heterogeneous systems—especially from the standpoint of reaction equilibrium—demands rigorous physicochemical analysis. This complexity is evident in the mixed system comprising AWW generated from cottonseed soapstock processing and the mineralized mass (MM) from the Central Kyzylkum region. This mixture represents the contact zone between two distinct industrial-natural sources. Within the MM, P_2O_5 exists in multiple forms: readily soluble, partially bound, and insoluble phases. AWW, meanwhile, contains a high concentration of ionic species, including acidic anions (H^+, SO_4^{2-}, NO_3^-, Cl^-) and cations (Ca^{2+}, Mg^{2+}), making the system highly reactive [[15], [16], [17], [18], [19]].

Currently, there is insufficient empirical data on which specific ions directly influence the equilibrium state of the system or the selective solubilization of P_2O_5. The individual impact of each ion on the dissolution behavior of P_2O_5 has not been fully quantified. The reaction process involves simultaneous phenomena such as complex formation, ion exchange, and dissolution kinetics. However, the conditions under which each mechanism predominates or is suppressed remain unclear. The extent to which P_2O_5 is extracted at various AWW:MM ratios, its kinetic behavior, and equilibrium points have yet to be precisely established [[8], [15], [16], [17]].

Preliminary studies suggest that in certain mass ratios, the total yield of P_2O_5 decreases, while in others, it increases—indicating a highly nonlinear and complex equilibrium response. Furthermore, the formation and composition of precipitates resulting from the interaction of cations and anions during the process are not fully understood. There is no conclusive evidence on whether the P_2O_5 content within these precipitates remains chemically active or becomes inert. This uncertainty complicates the

assessment of the overall efficiency of P_2O_5 extraction in such systems.

Experimental data indicate that the solubility of phosphorus pentoxide (P_2O_5) varies significantly with changes in pH. However, a robust mathematical or statistical model describing this dependency has not yet been developed. Moreover, the functional relationship between P_2O_5 activity and its quantitative release during the reaction remains poorly understood. Critical parameters such as the time required to reach equilibrium in AWW, the duration of the reaction, and interionic competition are influenced by multiple factors, but a stable and unified analytical methodology to capture these effects does not currently exist.

There is a pressing need to determine the activity coefficients between the reacting components and to apply thermodynamic or quasi-kinetic approaches to describe this system. Practical experiments typically report only the percentage change in P_2O_5 content, yet fail to provide a theoretical basis for equilibrium constants or reaction pathways. Therefore, the development of a comprehensive theoretical model for the process is still lacking.

In addition, the state of P_2O_5 in the resulting precipitates—whether free, bound, or inert—has not been clearly established. The specific roles of other oxides present in the reaction, such as CaO, Fe_2O_3, and SO_3, have also not been thoroughly analyzed. In such a complex system, experimental data alone are insufficient; advanced mathematical modeling is also required. In particular, there is a lack of mathematical equations that describe equilibrium shifts as functions of AWW:MM ratios, pH levels, and temperature. As a result, scientific approaches to optimizing P_2O_5 extraction under ideal conditions remain incomplete [8].

This highlights the urgent need for an in-depth mathematical, chemical, and thermodynamic analysis of the system.

The primary objective of this study is to scientifically evaluate the feasibility of efficiently extracting P_2O_5 from the mineralized mass of the Central Kyzylkum region using acidic wastewater generated during the recycling of cottonseed soapstock. To achieve this aim, reaction efficiency will be studied under various AWW:MM mass ratios. For each ratio, the composition of the resulting precipitate, pH changes, and P_2O_5 extraction percentages will be experimentally determined [[8], [17]].

The results will be used to define practical expressions of reaction equilibrium and analyze the influence of controlling variables [[25], [26]]. Kinetic trends will be assessed based on the ratio between total and soluble forms of P_2O_5. The chemical and phase composition of the reaction products will be studied in detail to determine the thermodynamic direction of the extraction process. Interionic interactions, ion-exchange reactions, and equilibrium conditions in the solution will be modeled mathematically. The results of the model will be compared with experimental values to assess their consistency [16].

Ultimately, the optimal AWW:MM ratio and the most favorable pH range for maximum P_2O_5 extraction will be identified, leading to practical recommendations. Overall, this study is aimed at scientifically justifying the integrated utilization of two different industrial waste streams in a mutually beneficial and resource-efficient manner [[17], [18]].

The extraction of phosphorus pentoxide (P_2O_5) from the mineralized mass proceeds mainly through an acid–base ion exchange mechanism. The hydrogen ions (H^+) present in the acidic wastewater (AWW) react with tricalcium phosphate, the principal phosphate compound in the mineralized mass, according to the following reaction:

$$Ca_3(PO_4)_2 + 6H^+ \rightarrow 3Ca^{2+} + 2H_3PO_4$$

The resulting phosphoric acid (H_3PO_4) subsequently undergoes stepwise dissociation in the aqueous phase:

$$H_3PO_4 \rightleftharpoons H_2PO_4^- \rightleftharpoons HPO_4^{2-} \rightleftharpoons PO_4^{3-}$$

As the pH increases, this equilibrium shifts toward the right, leading to the release of more soluble phosphate ions (PO_4^{3-}). According to Le Chatelier's principle, the system tends to consume H^+ ions to restore equilibrium, which enhances the dissolution of phosphorus compounds.

Simultaneously, ion-exchange and complexation reactions occur between Ca^{2+} and the anionic species (SO_4^{2-}, Cl^-, NO_3^-) present in the AWW. These anions form stable calcium complexes, thereby accelerating the removal of P_2O_5 from the solid phase.

From a kinetic standpoint, the process follows an exponential decay law:

$$C = C_0 \cdot e^{-kt},$$

where C is the residual CaO concentration in the solid phase, and k is the rate constant. The exponential decrease in CaO content corresponds to the progressive release of P_2O_5 into solution, indicating that the dissolution rate slows down as the reaction approaches equilibrium.

Thus, the interdependence between CaO depletion and P_2O_5 solubilization defines the system's reaction kinetics [8].

Materials

In this study, two primary substances were selected as key objects of investigation: AWW generated during the processing of cottonseed soapstock, and the MM of the Central Kyzylkum region.

The AWW is a by-product formed during the neutralization and saponification stages in cottonseed oil refining. It is characterized by a high concentration of acidic components and represents an industrial effluent rich in reactive species. Analytical characterization of the AWW revealed the presence of various anions and cations, including oxygen- and hydrogen-containing species, as well as sulfate, nitrate, and chloride anions, and calcium and magnesium cations (see Table 1 for details).

Table 1 - Chemical Composition of AWW Generated in the Acid Processing Section of Cottonseed Soapstock

Component	Amount (mg/L)
H^+	100
SO_4^{2-}	48 145
Cl^-	38 116
NO_3^-	4 456
Mg^{2+}	1 824
Ca^{2+}	300
Na^+	9 710
K^+	1 745
NH_4^+	870
PO_4^{3-}	725
Total pH	**2.0**

Specifically, the concentrations of key ions in NOS were determined to be as follows: SO_4^{2-} – 48,145 mg/L, Cl^- – 38,116 mg/L, Mg^{2+} – 1,824 mg/L, and Ca^{2+} – 300 mg/L. These ionic constituents are capable of forming a highly reactive medium that can engage in chemical interactions with the phosphate components present in the MM [17].

Acidic Wastewater (AWW): obtained from the neutralization and saponification stages of cottonseed soapstock processing at the "Urganch yog'-moy" JSC. The wastewater contained H^+, SO_4^{2-}, Cl^-, and NO_3^- anions, as well as Ca^{2+} and Mg^{2+} cations. The pH of the solution was 1.7 ± 0.05, indicating a highly acidic medium.

The pH value of AWW was measured at 1.7, confirming its strongly acidic nature, which plays a critical role in driving ion exchange and dissolution reactions with MM constituents.

The second object of investigation in this study is the MM of the Central Kyzylkum, a natural ore material characterized by a high content of phosphorus compounds. The MM sample was pre-dried, ground, sieved, and subjected to chemical analysis. According to the results, the MM contains 12.57% P_2O_5, 43.17% CaO, 1.34% Fe_2O_3, 2.74% Al_2O_3, and 2.17% SO_3 (Table 2) [[8], [17]].

In this study, two primary substances were selected as the main experimental objects: AWW generated from the processing of cotton soapstock and the MM of the Central Kyzylkum, a natural material rich in phosphorus compounds.

AWW is a by-product of the neutralization and saponification stages during cottonseed oil refining, characterized by high concentrations of acidic components. Chemical analysis of AWW revealed the presence of oxygen, hydrogen, sulfate, nitrate, and chloride anions, as well as calcium and magnesium cations (see Table 1). In particular, the concentrations of SO_4^{2-}, Cl^-, Mg^{2+}, and Ca^{2+} were determined to be 48,145 mg/L, 38,116 mg/L, 1,824 mg/L, and 300 mg/L, respectively. These ions create a reactive environment capable of engaging in chemical interaction with phosphate compounds present in MM. The pH of AWW was measured to be 1.7, indicating a strongly acidic nature [[8], [17]].

Table 2 - Chemical Composition of the MM from the Central Kyzylkum

Component	Amount, %
P_2O_5	12.57
CaO	43.17
Fe_2O_3	1.34
Al_2O_3	2.74
MgO	1.41
SO_3	2.17
F	0.92
CO_2	9.26
SiO_2	3.47
H_2O	10.75
Other	12.60
Total	**100.00**

The second object of investigation, the mineralized mass of the Central Kyzylkum, is a naturally occurring deposit material with a high content of phosphorus compounds. The MM sample was pre-dried, ground, sieved, and subjected to chemical analysis. According to the results, MM contains 12.57% P_2O_5, 43.17% CaO, 1.34% Fe_2O_3, 2.74% Al_2O_3, and 2.17% SO_3 (Table 2). Additionally, minor quantities of MgO (1.41%) and fluorine (0.92%) were also detected. This composition makes MM a promising raw material for phosphorus extraction. The material was prepared in fractions with particle sizes ranging from 0.5 to 1 mm. Mineralized Mass (MM): collected from the Central Kyzylkum phosphorite deposits. The material was pre-dried, ground to 0.5–1 mm particles, and analyzed according to GOST 20851.2-75 for P_2O_5, CaO, Fe_2O_3, and SO_3 contents.

Both raw materials were stored in sealed glass containers at room temperature (298 K) before use.

Methods

All experiments were conducted under controlled laboratory conditions:

Reaction setup: A fixed 100 g of AWW was reacted with 10–40 g of MM (ratios 100:10 – 100:40) in 250 mL glass vessels at 333 K (60 °C), stirred at 600 rpm for 30 min.

Filtration and drying: The suspensions were vacuum-filtered, and the solid precipitates were dried at 333 K for 24 h.

Analysis of P_2O_5: Photometric method (formation of a yellow phosphomolybdate complex; λ = 440 nm) in accordance with *GOST 26727-2010*.

Analysis of CaO: Complexometric titration with EDTA using murexide indicator in alkaline medium (pH ≈ 12) per *GOST 4919.1-2008*.

Statistical processing: All measurements repeated n = 3; mean ± SD and 95% CI calculated in MS Excel; regression models and R^2 computed in OriginPro 2021.

All experimental stages strictly followed the laboratory methodology. Statistical processing of the data enabled assessment of experimental reliability, identification of functional relationships between variables, and development of predictive models. The experimental data on soluble P_2O_5, residual CaO in the precipitate, precipitate mass, and pH values were statistically analyzed [[27], [28], [29]]. Each experiment was repeated three times, and the average value was calculated using the following formula:

$$\bar{x} = \frac{1}{n}\sum_{i=1}^{n} x_i$$

To evaluate the dispersion between experimental trials, the standard deviation (S) was calculated using the following formula:

$$S = \sqrt{\frac{1}{n-1}\sum_{i=1}^{n}(x_i - \bar{x})^2}$$

The reliability of the data was analyzed using the dispersion and the coefficient of variation. The coefficient of variation V (%) was determined using the following formula:

$$V = \frac{S}{\bar{x}} \cdot 100$$

Statistical calculations were automated using built-in formulas in MS Excel.

Average values, standard deviations, and percentage dispersions were organized in a separate table. For each parameter, graphs were prepared using ORIGIN 21 PRO software. Before plotting, all data were arranged in XY pairs. The graphs were visualized in the "scatter with smooth line" or "scatter + line + error bar" modes. On each graph: The X-axis represents the mass ratio of NOS to MM, the Y-axis shows the corresponding values of P_2O_5 or CaO. Error bars (±S) were added to each data point to reflect the standard deviation. Using ORIGIN 21 PRO's interface, functional relationships were modeled through "fit linear" and "fit exponential" options. To evaluate the variation of P_2O_5 content as a function of the AWW:MM mass ratio, a linear regression equation was constructed as follows:

$$y = ax + b$$

here, a represents the slope (coefficient), and b is the intercept of the regression line. The accuracy of the model was assessed using the coefficient of determination (R^2). The closer the R^2 value is to 1, the better the model fits the experimental data. In ORIGIN 21 PRO, regression results were generated automatically. To describe the relationship between the reduction of soluble P_2O_5 and CaO, secondary (nonlinear) dependencies were also modeled. Since the variation in CaO–P_2O_5 concentrations often exhibits nonlinear behavior, an exponential model

was selected for this relationship. This model is expressed in the general form as follows [8]:

$$y = A(1 - e^{-kx})$$

Here, A represents the maximum asymptotic value, and k denotes the kinetic change coefficient. In the graphical analysis, model parameters were determined using iterative methods. For each model, values of R^2, Standard Error (SE), and Root Mean Square Error (RMSE) were automatically calculated. The regression equation and R^2 value were displayed directly on each graph. Graphical analyses were used solely to illustrate the statistical differences between experimental results. Error margins were represented in the form of error bars with transparent and fine lines. All graphs were exported in TIFF format at 300 dpi resolution. Each graph was fully annotated with a title, axis labels, units, and trend lines. The graphs were labeled with specific codes to ensure proper referencing in the "Results and Discussion" section. Graphs were visually differentiated by color, marker shape, and line thickness to align with the article's design format. When inserted into the article individually, all graphs retained their original legends and unit notations. In cases where model deviations were identified, additional polynomial regressions were tested but not adopted as primary models. Each experimental point was placed precisely on the graph, showing minimal deviations from the modeled curve. Data processing and visualization were seamlessly integrated between Excel and ORIGIN 21 PRO.

Results and Discussion

The experimental work was conducted using a laboratory-scale setup consisting of a 250 mL glass reactor equipped with a magnetic stirrer and temperature control. The acidic wastewater (AWW) and mineralized mass (MM) were reacted at various mass ratios (100:10, 100:15, 100:20, 100:25, 100:30, 100:35, 100:40) at a constant temperature of 333 K (60 °C) for 30 minutes. The obtained solid and liquid phases were separated by vacuum filtration.

The solid phase was analyzed for CaO and P_2O_5 contents before and after the reaction. The liquid phase was analyzed for pH and phosphate ion concentration. Experimental data were collected in triplicate (n = 3) and are presented in Table 3 and Figures 1–4.

It was found that as the mass ratio increased from 100:10 to 100:25, the extraction of P_2O_5 increased sharply, while CaO content in the solid phase decreased exponentially. Beyond a 100:30 ratio, the rate of change leveled off, indicating an approach to equilibrium. The observed trends confirm the effectiveness of using acidic wastewater as a reactive medium for phosphorus recovery.

All measurements were performed under reproducible conditions, ensuring high data reliability ($R^2 > 0.95$). The results obtained in this study represent original experimental findings of the research team and are not derived from external sources.

At the same time, significant shifts in CaO content were also recorded. At the 100:10 ratio, the CaO content was 23.92%, rising to 27.95% at 100:15, 28.66% at 100:20, and reaching 32.68% at 100:25. The steady increase in CaO indicates that the calcium oxide fractions in the MM composition are not fully involved in the reaction and remain in the solid precipitate. Especially at higher MM concentrations (100:30–100:40), CaO reached values from 35.48% to 36.96%. This suggests that as the activity of Ca^{2+} ions in the reaction medium approaches equilibrium, the reaction rate slows down (Table 3).

Table 3 - Changes in the amount of P_2O_5 and CaO in the solid phase depending on the AWW:MM ratio

AWW:MM Ratio	P_2O_5 Content (%)	CaO Content (%)
100:10	8.19	23.92
100:15	9.51	27.95
100:20	10.42	28.66
100:25	11.16	32.68
100:30	11.83	35.48
100:35	12.21	36.47
100:40	12.49	36.96

As seen from Table 3, the increase in P_2O_5 and CaO is almost linear within the range up to a AWW:MM ratio of 100:25. However, starting from 100:30, the increase slows down considerably. This indicates that the components in the precipitate phase are forming a large crystalline structure in the reactive medium. Although the excess mass after this point continues to accumulate P_2O_5 in the precipitate, its reactive activity decreases. The steady increase in CaO, particularly reaching a stabilization stage in the 100:35–100:40 range, indicates that this component has reached an

equilibrium state. This, in turn, suggests a decrease in the reaction potential between CaO and H^+ ions present in the NOS composition.

All results were obtained exclusively from the solid phase, and their experimental reliability was confirmed through triplicate analyses. It is clear that the increase in P_2O_5 and CaO in the precipitate phase correlates with an increase in reactive mass, but the effectiveness of their reactivity is clearly limited. This condition necessitates considering the AWW:MM ratio as a crucial determinant in optimizing the phosphate extraction process. Optimal efficiency was observed in the 100:20–100:25 range, which is evaluated as the most favorable in terms of equilibrium and kinetic activity conditions.

During the experiment, the chemical activity of the CaO component in MM was assessed in each AWW:MM ratio in relation to the H^+ ions in NOS. The primary role of CaO in the reaction medium is to participate in ion exchange and neutralization reactions with H^+ ions during the P_2O_5 extraction process. At a 100:10 ratio, the CaO content in the solid phase was 23.92%, indicating that a significant amount of Ca^{2+} ions had transferred into the AWW medium at the initial stage. At 100:15, this value increased to 27.95%, and at 100:20, to 28.66%, suggesting that ion exchange was still actively occurring at these stages. However, since these values represent the CaO remaining in the solid phase, the actual amount of Ca^{2+} that entered into ion exchange may have been higher.

The consistent increase of CaO at each stage implies that calcium compounds in MM either did not participate in the reaction or precipitated as a solid after the reaction. Notably, at a 100:25 ratio, the CaO content reached 32.68%, indicating a decrease in the participation of Ca^{2+} ions in the phosphate extraction reaction. To evaluate the depth of the reaction, the residual concentration of CaO in the solid phase—that is, the unreacted portion—was taken as a basis. The ion exchange reaction between Ca^{2+} ions and H^+ ions in the AWW medium is represented as follows:

$$Ca_3(PO_4)_2 + 6H^+ \rightarrow 3Ca^{2+} + 2H_3PO_4$$

This reaction proceeds completely only under conditions of sufficient acidity. At AWW:MM ratios of 100:30 and 100:35, the CaO content increased to 35.48% and 36.74%, respectively, indicating a decline in the reaction rate. At this stage, the calcium components in MM are participating less actively in ion exchange. The mismatch between the increasing CaO content in the solid phase and the comparatively slower growth of P_2O_5 also highlights changes in reaction kinetics. At the 100:40 ratio, the CaO content reached its maximum value — 36.96%, while the total P_2O_5 content was only 12.49%. This indicates a significant reduction in the chemical activity of CaO, which has transitioned from a reactive substance to an inert or semi-inert component. This phenomenon is likely due to the reaction of Ca^{2+} ions with carbonates, sulfates, or fluorides, forming insoluble compounds. At this point, the calcium component no longer neutralizes free H^+ ions in AWW but rather enters an equilibrium state resembling physical adsorption.

From a chemical standpoint, this process is related to the change in ionic strength of the NOS and the relative calcium content in MM components. As the amount of MM increases, more CaO remains in the solid phase, leading to reduced separation efficiency. Since the CaO values reported in Table 3.1 represent residual CaO, it is possible to determine the reaction depth at each stage. The 100:15–100:20 ratio range corresponds to the most active zone of reaction kinetics, as indicated by the relatively slower rate of CaO increase during this interval. This implies that ion exchange reactions were particularly active at these stages. Starting from the 100:25 ratio, the sharp rise in CaO content suggests the formation of precipitates saturated with inert solid-phase components. Moreover, changes in density and granulometric appearance observed at higher ratios further support that CaO accumulated in crystalline form.

Although the reaction temperature was consistently maintained at 333 K to support kinetic activity, the limited ion exchange surface area reduced the overall reaction efficiency. The increase of Ca^{2+} in the AWW supports the transformation of P_2O_5 into soluble forms, but this effect diminishes as MM increases. At each ratio, the measured CaO content was interpreted as the unreacted portion, allowing the differentiation between reactive and non-reactive fractions. General analysis shows that the CaO component is chemically active only during the initial stages. In later stages, it accumulates in the precipitate as a passive substance that slows down the reaction equilibrium, leading to a decrease in P_2O_5 separation efficiency. This makes identifying highly efficient reaction conditions especially important. Therefore, the 100:15 and 100:20 ratios represent the stages at which the CaO component in MM exhibits the highest chemical activity. Adding excess MM beyond this point does not enhance the reactivity; rather, it increases chemical inertness. These findings form a theoretical basis for more advanced mathematical modeling of the reaction mechanism.

To evaluate separation efficiency and component changes, experimental results from Table 3 were used to construct graphs in the "OriginPro 21" software. The graphs analyzed the dynamics of two main parameters — total P_2O_5 and CaO content. The results are presented in Figures 1 to 4.

Figure 1 illustrates the change in solid-phase P_2O_5 content as the NOS:MM ratio increases. Acidic ions in AWW wastewater gradually precipitated P_2O_5 from the MM composition into the solid phase. With each incremental ratio increase from 100:10 to 100:40, the P_2O_5 content rose from 8.19% to 12.49%. The graph shows a strong fit to the linear regression equation (R^2 = 0.9851), indicating high reliability of the experimental results. Phosphorus components reacted gradually, accumulating in the precipitate mainly in the form of orthophosphates. This graph reflects how the active components in MM interact with the acidic reagent. Since the R^2 value used in modeling exceeded 0.98, the presence of a linear relationship is confirmed. The direct growth trend of P_2O_5 demonstrates that the system operates in accordance with changes in the AWW:MM ratio.

The reaction proceeded at its maximum rate up to the 100:25 ratio, after which it appears to enter a saturation phase. The graph clearly distinguishes these stages and serves to identify the optimal ratio.

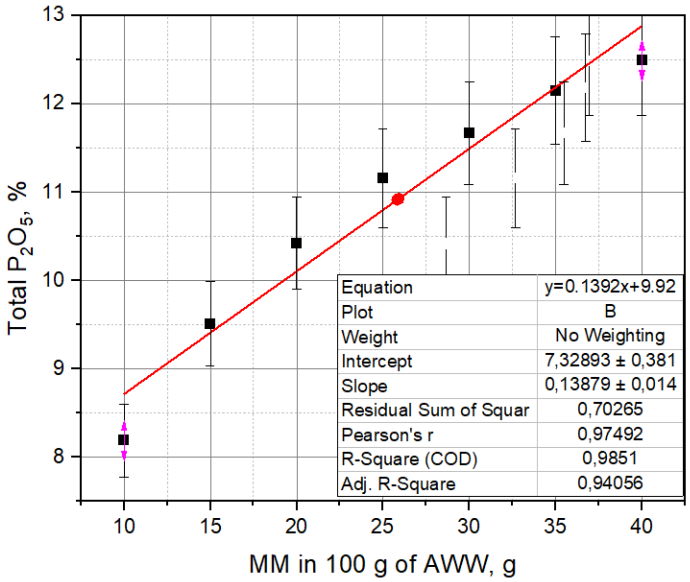

Figure 1 - Change in total P_2O_5 content relative to the AWW:MM ratio

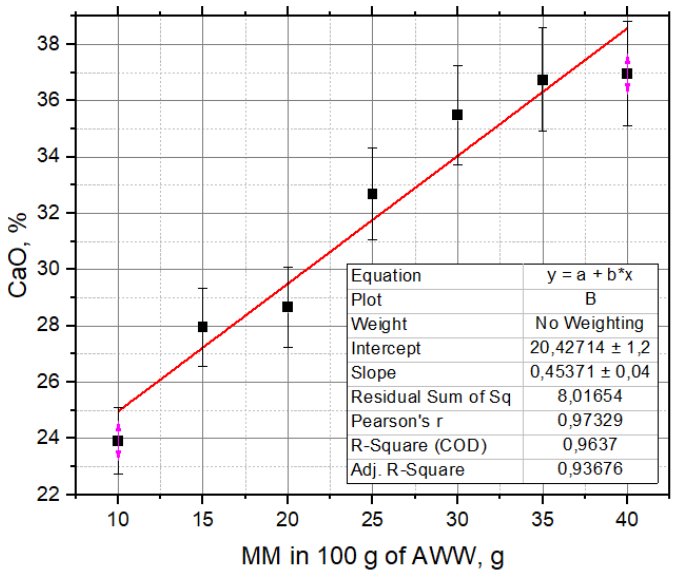

Figure 2 - Change in CaO content with respect to the NOS:MM ratio

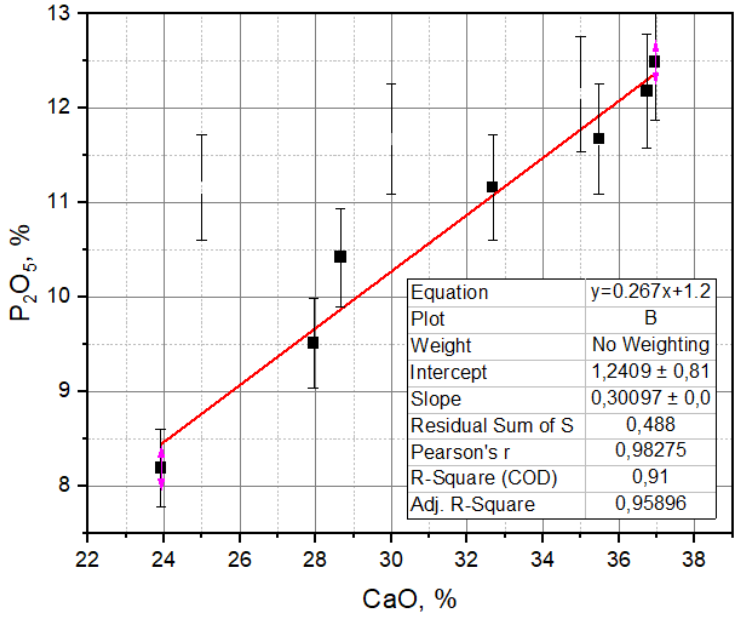

Figure 3 - Correlation between CaO reduction and P_2O_5 release

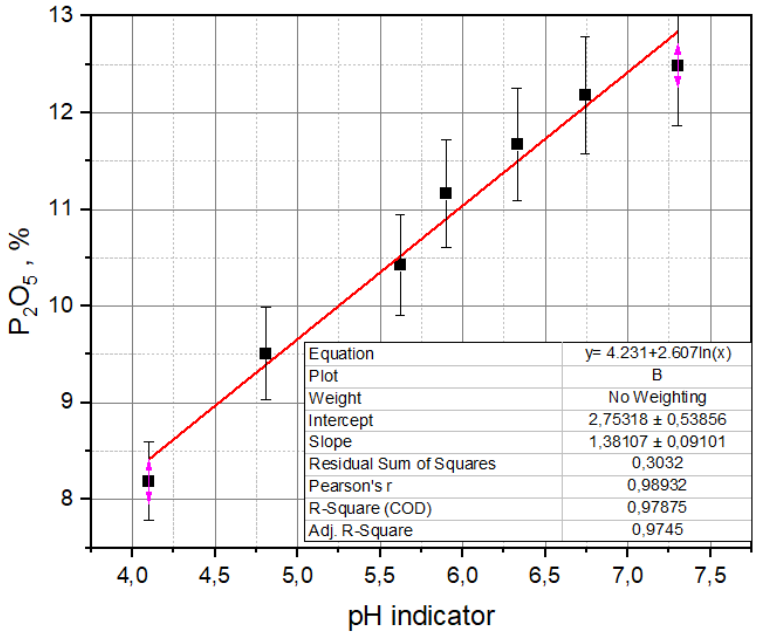

Figure 4 - Logarithmic relationship between pH and the solubility of P_2O_5

NOS:MM ratio of 100:10, the CaO content was 23.92%, increasing to 36.96% at a 100:40 ratio. This growth trend closely follows an exponential regression pattern, with a coefficient of determination $R^2 = 0.9637$. The acidic environment of the NOS component aimed to dissolve the CaO present in the MM. However, as the MM proportion increased, the degree of CaO participation in the reaction gradually slowed. This indicates a shift toward equilibrium in the reaction involving Ca^{2+} ions. Each incremental addition of MM did not result in a proportional transformation of CaO into a reactive, soluble form. Consequently, the graph displays a nonlinear curve bending toward saturation. The existence of an exponential regression implies that a significant portion of CaO remained in a residual, undissolved state within the precipitate. This graphical behavior clearly illustrates the reactivity threshold of CaO and marks the onset of the kinetic deceleration phase in the reaction process.

Figure 3 illustrates the linear relationship between the release of P_2O_5 and the reduction of CaO during the reaction. Each CaO ion that reacts

with H^+ contributes to the release of phosphorus into the solution in the form of orthophosphate. The linear regression displayed in the graph has an R^2 value of 0.91, indicating a strong correlation. Thus, one of the key factors influencing P_2O_5 release is the activity of Ca^{2+} ions in the equilibrium reaction. At each stage, the more CaO reacts, the more P_2O_5 transitions into a soluble form. This correlation is crucial for understanding the key stages of the release mechanism. Additionally, the graph clearly shows that the optimal AWW:MM ratio lies around 100:20 to 100:25. Adding MM beyond this range decreases the activity of CaO, which in turn hampers the release of P_2O_5. Therefore, the graph effectively demonstrates the boundaries of reaction activity and efficiency.

According to the analysis results, the amount of P_2O_5 released increased consistently with the rise in the pH value of the solution. This trend was confirmed to follow a logarithmic pattern. The obtained regression equation has the form $y = 4.23 + 2.607 \cdot \ln(x)$, which indicates a strong correlation (R^2 = 0.9934). The selection of a logarithmic model reflects the sensitivity of P_2O_5 solubility to equilibrium reactions in the chemical environment. An increase in pH, i.e., a rise in hydroxide ion concentration, helped maintain P_2O_5 in a complexed state, leading to its greater dissolution. These findings were validated through laboratory experiments. At pH = 7.3, the maximum P_2O_5 content reached 12.49%. This model may have practical significance in optimizing future industrial processes.

In extraction processes based on AWW, interionic equilibrium and kinetic limitations are the main factors determining the reaction efficiency. During the study, it was observed that the pH of a 10% AWW solution varied from 4.10 to 7.30, and within this range, significant changes occurred in the activity of hydroxide (OH^-), hydrogen (H^+), and other inorganic ions such as Ca^{2+}, PO_4^{3-}, $H_2PO_4^-$, and HPO_4^{2-}.

The AWW composition includes anions like SO_4^{2-}, Cl^-, and NO_3^-, and cations like Na^+ and K^+, which form ion pairs that contribute to ion-exchange reactions during extraction. In particular, when CaO is introduced into the medium, it rapidly hydrates to form $Ca(OH)_2$, which neutralizes free H^+ ions and increases the pH. This affects the equilibrium of phosphate ions forming P_2O_5 ($H_2PO_4^- \leftrightarrow HPO_4^{2-} \leftrightarrow PO_4^{3-}$) and influences their complex formation capacity.

The shift in ionic equilibrium responds sensitively to pH changes according to Le Chatelier's principle. As a result of these changes, Ca^{2+} and PO_4^{3-} ions in AWW may interact and form insoluble precipitates like $Ca_3(PO_4)_2$. However, with increasing pH, the solubility of PO_4^{3-} ions improves, enhancing their extractability.

Moreover, the presence of complex-forming agents such as EDTA (e.g., in a 0.2 M Trilon B solution) promotes the formation of strong complexes with divalent ions like Ca^{2+}. This displaces PO_4^{3-} ions from their bound state, facilitating the release and solubilization of phosphate. Such kinetics enable the system to quickly reach equilibrium.

According to the kinetic analysis of the process, in the initial stage, H^+ ions restrict phosphate dissolution, but these constraints are eliminated as pH increases. From a chemical perspective, the solubility of phosphate compounds forming P_2O_5 is governed by the following equilibrium reactions:

$$H_3PO_4 \rightleftharpoons H_2PO_4^- + H^+$$

$$H_2PO_4^- + H^+ \rightleftharpoons HPO_4^{2-} + H^+$$

$$HPO_4^{2-} + H^+ \rightleftharpoons HPO_4^{2-} + H^+$$

In addition, the following reaction chains are also observed:

$$Ca(OH)_2 \rightleftharpoons Ca^{2+} + 2\,OH^-$$

$$PO_4^{3-} + Ca^{2+} \rightleftharpoons Ca_3(PO_4)_2 \downarrow$$

As the pH increases and the solution becomes enriched with hydroxide ions, the kinetic barriers that previously prevented the formation of precipitates are reduced, thereby enhancing the degree of P_2O_5 extraction. This leads to a maximum phosphate solubility observed around pH 7.30. This phenomenon is fully consistent with the results presented in Figure 4.

From a kinetic perspective, the rate of reverse reactions decreases, causing the P_2O_5 release rate to approach equilibrium at a NOS:MM ratio of approximately 100:40. At this point, the release significantly slows down, indicating a state of kinetic saturation.

A comprehensive analysis of ionic equilibrium and chemical kinetics reveals that the mutual ratios of pH, Ca^{2+}, and PO_4^{3-} ions serve as key controlling factors. These relationships allow the development of highly accurate mathematical regression models for predictive simulation.

Conclusion

The AWW generated from the processing of cottonseed soapstock, containing active ions such as H^+, SO_4^{2-}, NO_3^-, and Cl^-, served as the reactive medium for extracting P_2O_5 from the mineralized mass of the Central Kyzylkum region. As the AWW:MM (mineral mass) mixing ratio increased from 100:10 to 100:40, the total extracted P_2O_5 percentage rose from 8.19% to 12.49%, indicating high selectivity of phosphorus dissolution into the solution phase. The efficiency of phosphorus extraction increased in correlation with rising pH values, which facilitated a decrease in H^+ ion concentration and promoted the release of free PO_4^{3-} ions into solution. The decline in CaO content followed an exponential trend described by the equation:$y = 12.28\ (1 - e^{(-0.085x)})$, with a high coefficient of determination ($R^2 = 0.9637$), reflecting the system's approach toward equilibrium kinetics. A logarithmic relationship between pH and P_2O_5 content was also established, expressed by the equation: $y = 4.23 + 2.607 \cdot \ln(x)$, with an excellent fit ($R^2 = 0.9934$), making this model a valuable predictive tool. Although the interaction between Ca^{2+} and PO_4^{3-} ions could potentially lead to the formation of $Ca_3(PO_4)_2$ precipitates, this process was effectively suppressed by controlling the pH level. The process analysis was based exclusively on the solid-phase composition; the chemical composition of the liquid phase reactants was not included. This approach enabled precise assessment of stepwise extraction kinetics. The research results—represented through graphical models (e.g., P_2O_5 and CaO content versus pH, logarithmic and exponential regressions)—were validated through modeling. The close interconnection among ionic equilibrium, kinetics, and chemical mechanisms ensured maximum P_2O_5 extraction efficiency. These findings provide a scientific basis for the development of an environmentally safer and economically efficient alternative technology for industrial-scale phosphorus recovery using acidic NOS solutions.

Conflicts of interest. On behalf of all authors, the corresponding author states that there is no conflict of interest.

CRediT author statement: **S. Shamuratov**: Conceptualization, Methodology, Software, Data curation, Writing draft preparation, Supervision, Software, Validation, Reviewing and Editing; **U. Baltaev, U. Alimov, A. Madaminov**: Visualization, Investigation.

Formatting of funding sources. This research did not receive any specific grant from funding agencies in the public, commercial, or not-for-profit sectors.

Cite this article as: Baltayev US, Shamuratov SX, Alimov UK, Madaminov AE, Jabbarov ME. Extraction of P_2O_5 from the mineralized mass of the Central Kyzylkum using acidic wastewater generated from cotton soapstock processing: scientific analysis based on equilibrium principles. Kompleksnoe Ispolzovanie Mineralnogo Syra = Complex Use of Mineral Resources. 2027; 341(2):83-96. https://doi.org/10.31643/2027/6445.20

Мақта майының сабын фракциясын өңдеу кезінде түзілетін қышқыл ағынды суларды (ҚҚС) пайдаланып, Орталық Қызылқұм шөлінің минералданған массасынан фосфор пентоксидін (P_2O_5) алу: тепе-теңдік принциптеріне негізделген ғылыми талдау

[1]Балтаев У.С., [1]Шамуратов С.Х., [2]Алимов У.К., [3]Мадаминов А.Э., [4]Жаббаров М.Э.

[1]Әбу Райхан Бируни атындағы Үргеніш мемлекеттік университеті, Өзбекстан
[2]Өзбекстан Республикасы Ғылым академиясының Жалпы және бейорганикалық химия институты, Ташкент
[3]Үргеніш мемлекеттік педагогикалық институты, Өзбекстан
[4]Мамун университеті мемлекеттік емес білім беру мекемесі, Хиуа, Өзбекстан

АННОТАЦИЯ

Бұл зерттеу мақта майының сабын фракциясын өңдеу кезінде түзілетін қышқыл ағынды суларды (ҚҚС) пайдаланып, Орталық Қызылқұм шөлінің минералданған массасынан фосфор пентоксидін (P_2O_5) алу перспективаларын қарастырады. ҚҚС құрамындағы қышқыл компоненттер қатты фазалы фосфоритті материалдың ыдырауына ықпал ететіні анықталды. Эксперименттер 333 К температурада, ҚҚС:минералданған масса (ҚҚС:ММ) арақатынасы 100:10-нан 100:40-қа дейін өзгертіліп жүргізілді. P_2O_5 концентрациясы 440 нм толқын ұзындығында фотометриялық әдіспен анықталды. Зерттеу тек қатты фаза талдауына

Мақала келді: *20 шілде 2025*
Сараптамадан өтті: *16 қазан 2025*
Қабылданды: *25 қараша 2025*

негізделіп, реакция дәрежесі түзілген тұнбаның мөлшері бойынша бағаланды. pH мәнінің жоғарылауы P_2O_5-тің бөлінуіне тікелей әсер ететіні көрсетілді. CaO мөлшерінің төмендеуі экспоненциалды заңдылыққа бағынды, ал P_2O_5 шығымы pH-пен логарифмдік байланыс көрсетті. Иондар арасындағы тепе-теңдік реакциялары химиялық механизмдер аясында түсіндірілді. Эксперименттік нәтижелер OriginPro 2021 бағдарламасы көмегімен графикалық және регрессиялық модельдеу арқылы талданды. Алынған деректердің сәйкестік коэффициенттері ($R^2 > 0.95$) бұл математикалық модельдердің сенімді екенін көрсетті. Бұл әдіс экологиялық және экономикалық тұрғыдан тиімді, өндірістік қалдықтарды пайдалану негізінде фосфорды бөлудің баламалы технологиясын ұсынады.

Түйін сөздер: қышқыл ағынды су, Орталық Қызылқұмның минералданған массасы, иондық тепе-теңдік, математикалық модельдеу, фосфор пентоксиді (P_2O_5), фотометриялық талдау, қатты фазалық реакция.

Авторлар туралы ақпарат:

Балтаев Үмітбек Сотымбайұлы
Техника ғылымдарының кандидаты, Әбу Райхан Беруни атындағы Үргеніш мемлекеттік университетінің химиялық технологиялар факультетінің докторанты, 220100, Х.Олимжон көшесі 14, Үргеніш, Өзбекстан. Email: umid.bo@urdu.uz; ORCID ID: https://orcid.org/0009-0004-5636-3318

Шамұратов Санжарбек Хусинбайұлы
Техника ғылымдары бойынша философия докторы (PhD), Әбу Райхан Беруни атындағы Үргеніш мемлекеттік университетінің химия-технология факультетінің доценті, 220100, Х.Олимжон көшесі 14, Үргеніш, Өзбекстан. Email: shamuratovsx@gmail.com; ORCID ID: https://orcid.org/0000-0002-1040-1807

Алимов Умарбек Кадирбергенович
Техника ғылымдарының докторы, Өзбекстан Республикасы Ғылым академиясының Жалпы және бейорганикалық химия институтының жетекші ғылыми қызметкері, Мирзо Улугбек, 77, 100170, Ташкент, Өзбекстан. Email: umaralihonalimov@mail.ru; ORCID ID: https://orcid.org/0000-0001-5608-5304

Мадаминов Азимбек Эгамберганович
Педагогика ғылымдары бойынша философия докторы (PhD), Үргеніш мемлекеттік педагогикалық институтының жаратылыстану және қолданбалы ғылымдар факультетінің доценті, 220100, Гүрлен көшесі, 1-А, Үргеніш, Өзбекстан. ORCID ID: https://orcid.org/0000-0002-3482-8071

Жаббаров Мажидбек Ерзодович
Мамун университеті мемлекеттік емес білім беру мекемесі, Хиуа, Өзбекстан. Email: jabbarovmajidbek2@gmail.com; ORCID ID: https://orcid.org/0009-0001-5987-0057

Извлечения пятиокиси фосфора (P_2O_5) из минерализованной массы Центрального Кызылкума с использованием кислотных сточных вод (КСВ), образующихся при переработке мыльной фракции хлопкового масла: научный анализ на основе принципов равновесия

[1]Балтаев У.С., [1]Шамуратов С.Х., [2]Алимов У.К., [3]Мадаминов А.Э., [4]Жаббаров М.Э.

[1]Ургенчский государственный университет имени Абу Райхона Беруни, Узбекистан
[2]Институт общей и неорганической химии Академии наук Республики Узбекистан, Ташкент
[3]Ургенчский государственный педагогический институт, Узбекистан
[4]Негосударственное образовательное учреждение Мамунский университет, Хива, Узбекистан

Поступила: *20 июля 2025*
Рецензирование: *16 октября 2025*
Принята в печать: *25 ноября 2025*

АННОТАЦИЯ

В данном исследовании рассматриваются перспективы извлечения пятиокиси фосфора (P_2O_5) из минерализованной массы Центрального Кызылкума с использованием кислотных сточных вод (КСВ), образующихся при переработке мыльной фракции хлопкового масла. Установлено, что кислотные компоненты КСВ способствуют разложению фосфоритного материала твердой фазы. Эксперименты проводились при температуре 333 К с варьированием соотношения КСВ: минерализованная масса (КСВ:ММ) от 100:10 до 100:40. Концентрация P_2O_5 определялась фотометрическим методом при длине волны 440 нм. Исследование было основано исключительно на анализе твердой фазы, где степень реакции оценивалась по количеству образовавшегося осадка. Показано, что повышение pH оказывает прямое влияние на извлечение P_2O_5. Снижение содержания CaO имело экспоненциальный характер, тогда как извлечение P_2O_5 логарифмически зависело от значения pH. Равновесные реакции между ионами были интерпретированы в рамках химических механизмов. Экспериментальные данные были представлены с помощью графического анализа и регрессионного моделирования в программе OriginPro 2021. Полученные математические модели обладали высокой достоверностью ($R^2 > 0.95$). Такой подход предлагает экономически эффективный и экологически безопасный альтернативный метод извлечения фосфора с использованием промышленных побочных продуктов.

	Ключевые слова: кислотные сточные воды, минерализованная масса Центрального Кызылкума, ионное равновесие, математическое моделирование, пентоксид фосфора (P_2O_5), фотометрический анализ, реакция в твёрдой фазе.
Балтаев Умидбек Сотимбаевич	***Информация об авторах:*** *Кандидат технических наук, докторант факультета химических технологий Ургенчского государственного университета имени Абу Райхана Беруни, 220100, улица Х. Олимджона, 14, Ургенч, Узбекистан. Email: umid.bo@urdu.uz; ORCID ID: https://orcid.org/0009-0004-5636-3318*
Шамуратов Санжарбек Хусинбай угли	*Доктор философии по техническим наукам (PhD), доцент химико-технологического факультета Ургенчского государственного университета имени Абу Райхана Беруни, 220100, улица Х. Олимджона, 14, Ургенч, Узбекистан. Email: shamuratovsx@gmail.com; ORCID ID: https://orcid.org/0000-0002-1040-1807*
Алимов Умарбек Кадирбергенович	*Доктор технических наук, ведущий научный сотрудник Института общей и неорганической химии Академии наук Республики Узбекистан, 100170, Мирзо Улугбек, 77, Ташкент, Узбекистан. Email: umaralihonalimov@mail.ru; ORCID ID: https://orcid.org/0000-0001-5608-5304*
Мадаминов Азимбек Эгамберганович	*Доктор философии по педагогическим наукам (PhD), доцент факультета естественных и прикладных наук Ургенчского государственного педагогического института, 220100, ул. Гурлана, 1-А, Ургенч, Узбекистан. ORCID ID: https://orcid.org/0000-0002-3482-8071*
Жаббаров Мажидбек Ерзодович	*Негосударственное образовательное учреждение Мамунский университет, Хива, Узбекистан. Email: jabbarovmajidbek2@gmail.com; ORCID ID: https://orcid.org/0009-0001-5987-0057*

References

[1] Dumont M-J, & Narine S S. Soapstock and deodorizer distillates from North American vegetable oils: Review on their characterization, extraction and utilization. Food Research International. Elsevier BV. 2007. https://doi.org/10.1016/j.foodres.2007.06.006

[2] Haas Michael J. Improving the Economics of Biodiesel Production through the Use of Low Value Lipids as Feedstocks: Vegetable Oil Soapstock. Fuel Processing Technology. Elsevier BV. 2005. https://doi.org/10.1016/j.fuproc.2004.11.004

[3] Dowd Michael K. Compositional Characterization of Cottonseed Soapstocks. Journal of the American Oil Chemists' Society. Wiley. 1996. https://doi.org/10.1007/bf02525458

[4] Barbusiński Krzysztof, Sławomir Fajkis, and Bartosz Szeląg. Optimization of Soapstock Splitting Process to Reduce the Concentration of Impurities in Wastewater. Journal of Cleaner Production. Elsevier BV. 2021. https://doi.org/10.1016/j.jclepro.2020.124459

[5] Ahmad Talha, Tarun Belwal, Li Li, Sudipta Ramola, Rana Muhammad Aadil, Abdullah, Yanxun Xu, and Luo Zisheng. Utilization of Wastewater from Edible Oil Industry, Turning Waste into Valuable Products: A Review. Trends in Food Science & Technology. Elsevier BV. 2020. https://doi.org/10.1016/j.tifs.2020.02.017

[6] Qasim Wael, and Mane A V. Characterization and Treatment of Selected Food Industrial Effluents by Coagulation and Adsorption Techniques. Water Resources and Industry. Elsevier BV. 2013. https://doi.org/10.1016/j.wri.2013.09.005

[7] Geetha Devi M, Shinoon Al-Hashmi Z S, and Chandra Sekhar G. Treatment of Vegetable Oil Mill Effluent Using Crab Shell Chitosan as Adsorbent. International Journal of Environmental Science and Technology. Springer Science and Business Media LLC. 2012. https://doi.org/10.1007/s13762-012-0100-4

[8] Chanda C, Ray Chaudhuri S, Mukherjee I. Sulphate-Reducing Bacteria in Wastewater Treatment Processes. In: Ray Chaudhuri, S. (eds) Application of Microbial Technology in Wastewater Treatment and Bioenergy Recovery. Clean Energy Production Technologies. Springer, Singapore. 2024. https://doi.org/10.1007/978-981-97-3458-0_4

[9] Rifi SK, et al. Study of the Performance of the Wastewater Treatment Plant in the Vegetable Oil Refining Industry. In: Souabi S, Anouzla A, Yadav S, Singh VP, Yadava RN. (eds) Wastewater Treatment Plants. Water Science and Technology Library. Springer, Cham. 2025; 130. https://doi.org/10.1007/978-3-031-87461-1_3

[10] Pintor Ariana MA, Andreia G Martins, Renata S Souza, Vítor JP Vilar, Cidália MS Botelho, and Rui AR Boaventura. "Treatment of Vegetable Oil Refinery Wastewater by Sorption of Oil and Grease onto Regranulated Cork – A Study in Batch and Continuous Mode." Chemical Engineering Journal. Elsevier BV. 2015. https://doi.org/10.1016/j.cej.2015.01.025

[11] Ahmad Ashfaq, Azizul Buang, and Bhat AH. Renewable and Sustainable Bioenergy Production from Microalgal Co-Cultivation with Palm Oil Mill Effluent (POME): A Review. Renewable and Sustainable Energy Reviews. Elsevier BV. 2016. https://doi.org/10.1016/j.rser.2016.06.084

[12] Hmidi K, Ksentini I, and Mansour . B. Treatment of Olive-Pomace Oil Refinery Wastewater Using Combined Coagulation-Electroflotation Process. Journal of Water Chemistry and Technology. Allerton Press. 2017. https://doi.org/10.3103/s1063455x17050046

[13] Mirshafiee Amir, Abbas Rezaee, and Rasol Sarraf Mamoory. A Clean Production Process for Edible Oil Removal from Wastewater Using an Electroflotation with Horizontal Arrangement of Mesh Electrodes. Journal of Cleaner Production. Elsevier BV. 2018. https://doi.org/10.1016/j.jclepro.2018.06.201

[14] Ahmad Talha, Rana Muhammad Aadil, Haassan Ahmed, Ubaid ur Rahman, Bruna CV Soares, Simone .Q Souza, Tatiana C Pimentel, et al. Treatment and Utilization of Dairy Industrial Waste: A Review. Trends in Food Science &amp. Technology. Elsevier BV. 2019. https://doi.org/10.1016/j.tifs.2019.04.003

[15] Kuznetsova AP, Lysenko ME, & Al-Shekhadat RI. Utilization of Waste-Derived Fatty Acid Feedstock for Polyhydroxyalkanoate Biosynthesis by Cupriavidus necator H16. Russ J Gen Chem. 2025. https://doi.org/10.1134/S1070363225130018

[16] Estrada R, Alon-alon K, Simbajon J, et al. Reduction of Acid Value of Waste Cooking Oil through Optimized Esterification via Central Composite Design. Circ.Econ.Sust. 2024; 4;1819–1834. https://doi.org/10.1007/s43615-024-00363-9

[17] Meti BS, Kulkarni SR, Jigajinni SK, Nainegali B. Food Industry By-Products and Waste Management. In: Yaradoddi, J.S., Meti, B.S., Mudgulkar, S.B., Agsar, D. (eds) Frontiers in Food Biotechnology. Springer, Singapore. 2024. https://doi.org/10.1007/978-981-97-3261-6_14

[18] Sotimboev Ilgizarbek, Umidbek Baltaev, Sanjarbek Shamuratov, Ruzimov Shamsiddin, Umarbek Alimov, and Mirzabek Saporboyev. Technical and Economic Efficiency of Processing Acidic Wastewater from the Oil and Fat Industry into Necessary Agricultural Products. E3S Web of Conferences. EDP Sciences. 2024. https://doi.org/10.1051/e3sconf/202456303072

[19] Turatbekova Aidai, Malokhat Abdukadirova, Sanjarbek Shamuratov, Bakhodir Latipov, Mirzabek Saporboyev, Jafar Shamshiyev, and Yusuf Makhmudov. Investigation of the Effect of Fertilizers on the Biochemical and Physical Characteristics of Carrots (Daucus Carota L.). E3S Web of Conferences. EDP Sciences. 2024. https://doi.org/10.1051/e3sconf/202456303074

[20] Sultonov B E, Kholmatov D S, Rasulov A A, and Temirov U Sh. Treatment of Phosphate Waste Generated during Thermal Processing of Phosphorites of the Central Kyzylkum. Obogashchenie Rud. Ore and Metals Publishing House. 2024. https://doi.org/10.17580/or.2024.04.06

[21] Shaymardanova Mokhichekhra, Kholtura Mirzakulov, Gavkhar Melikulova, Sakhomiddin Khodjamkulov, Abror Nomozov, and Oybek Toshmamatov. Studying of The Process of Obtaining Monocalcium Phosphate Based on Extraction Phosphoric Acid from Phosphorites of Central Kyzylkum. Baghdad Science Journal. College of Science for Women, University of Baghdad. 2024. https://doi.org/10.21123/bsj.2024.9836

[22] Sultonov B E, Nozimov E S, and Kholmatov D. S. Recycling of Local Phosphate Waste - Mineralized Mass into Activated Phosphorus Fertilizers. Chemical Science International Journal. Sciencedomain International. 2023. https://doi.org/10.9734/csji/2023/v32i6875

[23] Temirov Uktam, Nodir Doniyarov, Bakhrom Jurakulov, Najimuddin Usanbaev, Ilkhom Tagayev, and Abdurasul Mamataliyev. Obtaining Complex Fertilizers Based on Low-Grade Phosphorites. E3S Web of Conferences. EDP Sciences. 2021. https://doi.org/10.1051/e3sconf/202126404009

[24] Sedghkerdar Mohammad Hashem, Ehsan Mostafavi, and Nader Mahinpey. Investigation of the Kinetics of Carbonation Reaction with Cao-Based Sorbents Using Experiments and Aspen Plus Simulation. Chemical Engineering Communications. Informa UK Limited. 2015. https://doi.org/10.1080/00986445.2013.871709

[25] De Leonardis A, Macciola V, Iftikhar A. Present and Future Perspectives on the Use of Olive-Oil Mill Wastewater in Food Applications. In: Souabi, S., Anouzla, A. (eds) Wastewater from Olive Oil Production. Springer Water. Springer, Cham. 2023. https://doi.org/10.1007/978-3-031-23449-1_4

[26] Jeba RH, Hemada HM, Nadir AA, et al. Improving stability of frying oils and food quality with addition of dried olive mill wastewater. 2025; 9:75. https://doi.org/10.1038/s41538-025-00430-x

[27] Sun Ping, John R. Grace, C. Jim Lim, and Edward J. Anthony. Determination of Intrinsic Rate Constants of the $CaO–CO_2$ Reaction. Chemical Engineering Science. 2008; 63(1):47-56. https://doi.org/10.1016/j.ces.2007.08.055

[28] Fritz, Matthew S. An Exponential Decay Model for Mediation. Prevention Science. Springer Science and Business Media LLC. 2014; 15:611-622. https://doi.org/10.1007/s11121-013-0390-x

[29] Atashev E. Decomposition of Magnesite-Sparing Waste in Sulfuric Acid with a High Concentration: Empirical Modeling and Determination of Optimal Conditions. Kompleksnoe Ispolzovanie Mineralnogo Syra = Complex Use of Mineral Resources. 2025; 339(4):71–78. https://doi.org/10.31643/2026/6445.41

Crossref
DOI: 10.31643/2027/6445.21
Mining & Mineral Processing

creative commons

Polymer-bitumen compositions for improving the energy efficiency of road construction

[1*] Syzdyk A.G., [1] Seitenova G.Z., [2] Dyussova R.M., [1] Zhakmanova E.A., [1] Donbayeva E.

[1] L.N. Gumilyov Eurasian National University, Republic of Kazakhstan, Astana
[2] Toraighyrov University, Republic of Kazakhstan, Pavlodar

** Corresponding author email: ayazhanka.syzdyk@gmail.com*

Received: *May 6, 2025*
Peer-reviewed: *September 4, 2025*
Accepted: *November 26, 2025*

ABSTRACT

This article examines the effect of two types of polypropylene (H030 and H350) and petroleum residue on the bitumen modification process. Bitumen modification is one of the key methods for improving its physical and mechanical properties and enhancing the quality of road pavement. Currently, bitumen modification is widely used in road construction, playing a crucial role in improving its quality and energy efficiency. Studying the effect of polymers on the mechanical stability of bitumen is a relevant issue in increasing the durability of road surfaces. During the study, six different concentrations of polypropylene H030 and H350 were introduced into bitumen samples, and their main characteristics were compared. The obtained results demonstrated that polypropylene significantly alters the properties of bitumen, contributing to increased strength and durability of road pavements. Furthermore, the addition of petroleum residue enhances the rheological properties of the bitumen mixture, improving its adhesion. These studies provide essential data for improving bitumen used in road construction. The research results indicate that the use of polymer-modified bitumen increases the wear resistance of road surfaces, reduces crack formation, and enhances resistance to climatic factors. This, in turn, extends the service life of road pavements and reduces road maintenance costs. Long-lasting pavements help decrease energy consumption for bitumen production and road construction. The obtained data expand the possibilities for the effective use of polymer-modified bitumen mixtures in asphalt concrete production. Thus, the compatibility of bitumen and polypropylene has been studied, and their optimal compositions have been determined.

Keywords: bitumen, polypropylene, modified bitumen mixtures, petroleum residue, asphalt concrete, energy efficiency.

Information about authors:

Syzdyk Ayazhan Galymkyzy — *Master's student in the Faculty of Natural Sciences, L.N. Gumilyov Eurasian National University, Kazhymukan str., 13, 010000, Astana, Kazakhstan. E-mail: ayazhanka.syzdyk@gmail.com; ORCID ID: https://orcid.org/0009-0007-4435-0976*

Seitenova Gaini Zhumagalievna — *Candidate of chemical sciences, associate professor, Faculty of natural sciences, L.N. Gumilyov Eurasian National University, Satbayev str., 2, 010000, Astana, Kazakhstan. E-mail: gainiseitenova@gmail.com; ORCID ID: https://orcid.org/0000-0001-6202-3951*

Dyussova Rizagul Muslimovna — *Candidate of technical sciences, postdoctoral researcher, Toraighyrov University, Lomova str., 64, 140000, Pavlodar, Kazakhstan. E-mail: riza92@bk.ru; ORCID ID: https://orcid.org/0000-0003-3083-5255*

Zhakmanova Ekaterina Andreevna — *PhD student in the Faculty of Natural Sciences, L.N. Gumilyov Eurasian National University, Kazhymukan str., 13, 010000, Astana, Kazakhstan. E-mail: Ekaterina.zakmanova1998@gmail.com; ORCID ID: https://orcid.org/0000-0003-0545-5912*

Donbayeva Elvira — *Senior lecturer, Department of Chemistry, Faculty of Natural Sciences, L.N. Gumilyov Eurasian National University, 13 Kazhymukan str., 010000, Astana, Kazakhstan. E-mail: donbayeva_ek@enu.kz; ORCID ID: https://orcid.org/0009-0005-0762-1488*

Introduction

Research aimed at improving the quality of bitumen-based materials in road construction holds significant importance. Modification of bitumen is one of the key approaches to enhancing its physical and mechanical properties and ensuring the long-term durability of road pavements. Currently, polymer-modified bitumen mixtures are widely applied, as they improve thermal stability and increase mechanical strength [[1], [2]].

Bitumen is a complex organic binder composed of high-molecular-weight hydrocarbons and their derivatives. Its key properties include softening point, penetration depth, viscosity, plastic deformation capability, and wear resistance. These

parameters directly affect the quality of road surfaces [[3], [4]]. However, neat bitumen has several disadvantages; therefore, research is being actively carried out to improve its properties through various modifiers [5].

Among these, polymer modification occupies a special place. Polypropylene is one of the thermoplastic polymers frequently used in bitumen modification. It is characterized by high mechanical strength and chemical stability. Studies have shown that the addition of polypropylene increases the elastic modulus of bitumen, enhances its resistance to cracking, raises the softening point, and reduces penetration depth. These improvements make polymer-modified bitumen suitable for use under hot climatic conditions [[6], [7], [8], [9]].

Oil residues are also among the important compounds used to improve bitumen. Heavy fractions from oil refining reduce the viscosity of bitumen, enhance its low-temperature performance, and improve the homogeneity of the mixture [[10], [11]]. The combined use of polypropylene and oil residue enhances the elastic properties of bitumen and contributes to its long-term stability [12]. Such mixtures have been shown to exhibit greater crack resistance while also improving adhesion properties [13].

In recent years, research in this field has become increasingly relevant. First, studying the combined effect of polymers and oil residues aims to improve the quality of road pavements under various climatic conditions. Second, the use of recycled polymer waste is considered an environmentally friendly solution [[14], [15]]. In addition, current studies are also focused on investigating compatibility with nanocomposites and other functional additives [[16], [17]].

In this regard, the present study focuses on identifying the effect of polypropylene grades H030 and H350, together with oil residue, on the physical and mechanical properties of bitumen mixtures. Samples obtained at different concentrations were comparatively analyzed in terms of softening point and penetration depth. Moreover, the influence of the obtained results on the rheological characteristics of bitumen and asphalt concrete mixtures was also examined [[18], [19], [20]].

The scientific novelty of this study lies in the comparative analysis of the effects of polypropylene grades H030 and H350 on the properties of bitumen. Furthermore, for the first time, the combined use of polypropylene and oil residue has been comprehensively studied in relation to improving the structural stability and adhesion properties of the mixtures. The research was carried out on samples adapted to the climatic conditions of Kazakhstan, and the results obtained have practical significance for local road construction.

Experimental part

For the research, the following materials were used: bitumen of grade BND 100/130 provided by Pavlodar Oil Chemistry Refinery LLP (Kazakhstan). BND 100/130 bitumen possesses high viscosity and is widely applied in the production of road pavements with properties required for operation under various climatic conditions. Polypropylene grades PP H350 and PP H030 were supplied by “Neftekhim LTD” LLP and prepared in accordance with the National Standard of the Republic of Kazakhstan, ST RK 3191-2018. Polypropylene (PP) is a thermoplastic material based on propylene (propene). This polymer contributes to enhancing the strength, crack resistance, elasticity, and durability of polymer-modified bituminous (PMB) materials. Heavy oil residue of grade H603 was provided by Pavlodar Oil Chemistry Refinery LLP and used to regulate the viscosity and improve the technological properties of PMB mixtures. The addition of oil residue increased the fluidity of the material and ensured uniform distribution of the components within the mixture. This made it possible to achieve an optimal balance between viscosity and plasticity, thereby contributing to the durability and stability of road pavements.

The preparation of polymer-bitumen compositions is a multistage and complex process in which a modified structure is formed as a result of the physical and chemical interactions of the components. In this study, the compositions were prepared using a laboratory disperser unit.

Initially, the containers and equipment required for the experiment were thoroughly cleaned and dried to remove moisture residues. This step was essential to prevent the influence of external factors that could negatively affect the quality of the final product. Before use, all vessels were checked to ensure they were free of contamination and traces of moisture.

At the next stage, the bitumen was poured into a thermostable container and heated to the working temperature range of 120-150 °C. Such conditions reduce the viscosity of bitumen and allow better mixing with the polymer.

The required amount of polymer was then weighed in advance and calculated relative to the

mass of bitumen. The polymer concentration was selected depending on the modification level and the expected properties of the composition.

The preheated bitumen was combined with the measured polymer, and the mixture was stirred in the laboratory disperser. This process was carried out at 165-170 °C for up to 120 minutes. The mixing time and speed were determined based on the characteristics of the polymer used and the desired degree of dispersion. The high-speed stirrer ensured the uniform distribution of the components.

Once the mixture reached a homogeneous consistency, an additional maturation stage was carried out to strengthen the formation of molecular-level interactions between its constituents. During this period, the mixture was maintained at 160-170 °C for a specified duration.

The polymer-bitumen compositions prepared in this way were then subjected to standard testing. The softening point, penetration depth, and other characteristics were determined in accordance with the Standards of the Republic of Kazakhstan (ST RK). The compositions of the PMB mixtures are presented in the table below (Table 1):

Table 1 - Composition of PMB: proportion of bitumen, polypropylene, and oil residue

Sample No	1	2	3	4	5	6	7
Bitumen BND 100/130	100 %	95.7 %	95.1 %	94.5 %	93.5 %	93%	92%
PP H030 / PP H350	0	4%	4%	4%	4%	4%	4%
Oil residue	0	0.3%	0.9%	1.5%	2.5%	3%	4%

Table 1 presents the percentage composition of bitumen (BND 100/130), polypropylene (H030 or H350), and oil residue for each sample. These data characterize the exact formulations of the initial mixtures used in the study and form the basis for subsequent physical and mechanical testing.

Regarding the methods applied in the research, the penetration depth at 25 °C (with an accuracy of at least 0.1 mm) was evaluated in accordance with ST RK 1226-2003 using a digital automatic penetrometer, model 20-20670, produced by Infratest. According to the test procedure, PMB samples were first heated to 150 °C, then placed into a special container and cooled to 25 °C. A needle with a defined load (typically 100 g) was slowly applied to the surface of the sample. The penetration depth of the needle was measured in millimeters and recorded. This method makes it possible to objectively evaluate the viscosity of PMB materials and their suitability for various operating conditions.

The softening point (°C, minimum value) was determined using an automated device by Infratest, in accordance with ST RK 1227-2003. According to the test procedure, PMB samples were preheated to a temperature of 80-100 °C above the expected softening point but not lower than 120 °C and not exceeding 180 °C to remove moisture. The dehydrated PMB material was filtered, carefully stirred to eliminate air bubbles, and then poured in excess into two rings. After cooling to ambient temperature, the excess material was trimmed with a heated knife. The rings containing PMB material, along with steel balls cooled to (5 ± 1) °C, were placed into a water bath. The water temperature was then increased at a rate of (5.0 ± 0.5) °C per minute. The test continued until the steel ball penetrated the PMB material and touched the bottom plate, at which point the temperature was recorded as the softening point. Strict control of the heating rate ensured the accuracy of the test.

The ductility of bitumen was tested using a digital ductilometer, model 20-2356, in compliance with ST RK 1374-2005. Samples were prepared according to ST RK 1288-2004. Special “figure-eight” shaped molds were used, into which bitumen preheated to 150-180 °C was poured. The molds were then subjected to temperature conditioning. During testing, the samples were stretched in a water bath at 0 °C or 25 °C at a rate of 50 mm/min. The elongation length at break was recorded in centimeters. Each test was conducted on three parallel samples, and the arithmetic mean value was calculated. If the difference between results exceeded the allowable norm, the test was repeated. In cases where the sample did not break at an elongation of 1000 mm, the result was recorded as “>100 cm.”

Although standard testing methods were applied in this study, the influence of ecological factors, economic efficiency, and the probability of phase separation on the obtained results was not considered. These aspects represent the limitations of the study and require further in-depth investigation in the future.

Results and Discussion

In bitumen samples modified with polypropylene (PP H350) and oil residue, the penetration depth decreased with increasing concentration. This indicates an increase in bitumen hardness, meaning the transition of the material to a softened state at elevated temperatures slows down. In particular, for samples containing 1.5% and 2.5% oil residue, the penetration depth sharply decreased, reaching values of 31.4 mm and 47.5 mm, respectively.

The softening point generally showed an upward trend, indicating that the combined addition of polypropylene and oil residue improved the ability of bitumen to retain its shape at high temperatures.

In the sample with 4% oil residue, the softening point reached 66.2 °C, remaining at a relatively stable level compared to the initial value of 66 °C. This demonstrates enhanced thermal stability and strength of the bitumen.

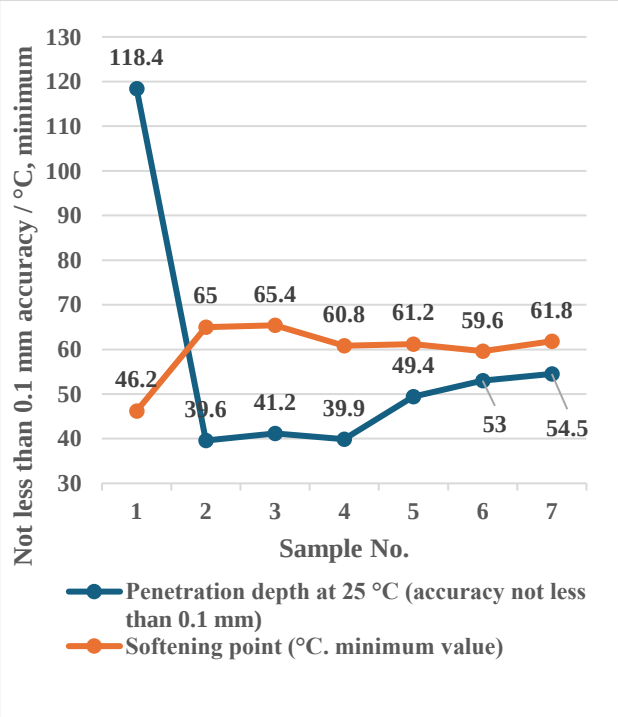

Figure 1 - Thermal Stability and Structural Changes of PMB Based on PP H030

In bitumen samples modified with polypropylene (PP H030) and 3-4% oil residue, the penetration depth increased from the initial 39.6 mm to 54.5 mm. At the same time, the softening point decreased from 65 °C to 61.8 °C.

Although the polypropylene content remained constant (4%), it was found that variations in the concentration of oil residue had a significant impact on the physical and mechanical properties of bitumen.

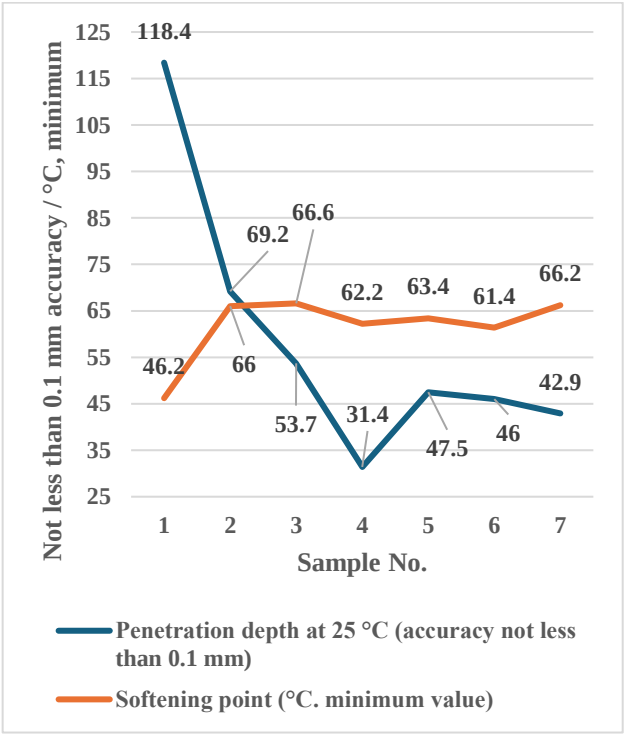

Figure 2 - Thermal Stability and Structural Changes of PMB Based on PP H350

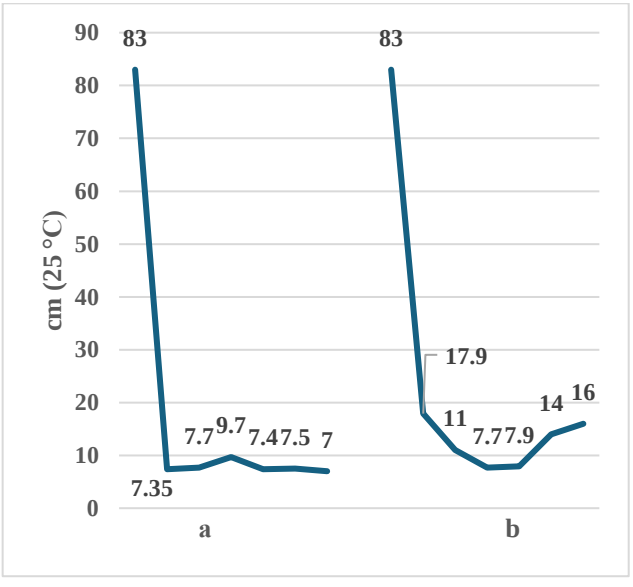

Figure 3 - Ductility of PMB mixtures (a - Bitumen + PP H030 + oil residue; b - Bitumen + PP H350 + oil residue)

As shown in Figures 1 and 2, all samples exhibited significant changes compared to the control sample (neat bitumen). This confirms the

combined effect of polypropylene and oil residue on the structure of bitumen.

While polypropylene increases the viscosity of bitumen and helps to maintain its softening point, oil residue partially balances this effect. Bitumen modified with H030 is sensitive to the concentration of oil residue: the softening point decreases slightly, but the penetration depth is initially higher. In contrast, H350-modified bitumen demonstrates greater stability and hardness at elevated temperatures, which makes it more suitable for roads subjected to heavy loads.

The ductility of bitumen samples modified with polypropylene (grades H030 and H350) and oil residue was evaluated at 25 °C. The results are presented in Figure 3.

Table 2 - Statistical data processing of the properties of polypropylene-modified bitumen

Parameters	PP H030	PP H350
Softening point (°C, minimum)	65.0-61.8	66.0-62.2
Standard deviation (°C)	1.8	2.0
Confidence interval (95%)	1.7	1.9
Penetration depth at 25 °C (accuracy 0.1 mm)	39.6-54.5	69.2-42.9
Standard deviation (mm)	5.5	10.1
Confidence interval (95%)	5.2	9.8
Ductility at 25 °C, cm	7-10	7-16
Mean value	8.2	11.3
Standard deviation	1.2	3.1
Confidence interval (95%)	7.5-8.9	9.8-12.8
Adhesion coefficient of oil residues	0.87	0.92
Standard deviation	0.03	0.04
Confidence interval (95%)	0.84-0.90	0.88-0.96

According to the results, the ductility of the original bitumen measured at 25 °C showed a high value (83 cm). In the modified mixtures, ductility values decreased significantly. This can be explained by the increase in hardness of the material and the limitation of its plastic deformation capacity as a result of polypropylene penetrating the bitumen structure. In the samples with grade H030, ductility was in the range of 7-10 cm, while in the mixtures based on H350 it was somewhat higher-ranging from 7 to 16 cm. This indicates that polypropylene of grade H350 possesses a better structure-forming ability and tends to distribute more uniformly within the bitumen matrix. As a result, mixtures based on H350 provide a more optimal balance between elasticity and strength. However, the decrease in ductility reflects a limitation of the plastic properties of bitumen, and therefore, future research should aim to identify compatible combinations of modifiers to improve this parameter.

The statistical data processing of the properties of polypropylene-modified bitumen is presented in the table (Table 2).

The data presented in Table 2 include the mean values, standard deviations, and 95% confidence intervals for the softening point, penetration depth at 25 °C, and adhesion coefficient of oil residues in bitumen samples modified with polypropylene. These results provide a quantitative basis for comparing the changes in the physical properties of the mixtures.

For each parameter, standard deviations and 95% confidence intervals were calculated to evaluate the reliability and stability of the obtained results. The data comparatively characterize the influence of PP H030 and PP H350 on the properties of bitumen. According to the results, mixtures based on polypropylene grade H350 demonstrated higher thermal stability, although they showed greater variability in penetration depth, indicating fluctuations in their properties. However, additional statistical methods (such as the t-test or ANOVA) were not applied to assess statistical significance. Therefore, future research should include a deeper statistical analysis of the results.

The reuse of polymer waste increases environmental efficiency, as it reduces the accumulation of plastic waste and transforms it into useful products for the construction sector. Oil residue, as an industrial by-product, can also be utilized, thereby reducing the environmental burden.

From an economic perspective, the application of polymer-bitumen mixtures reduces maintenance costs by extending the service life of road pavements. Moreover, with improved energy efficiency, expenditures on fuel and energy in bitumen production and road paving processes are also reduced.

Conclusions

The data, presented in this study, include the mean values, standard deviations, and 95% confidence intervals for the softening point, penetration depth at 25 °C, and adhesion coefficient of oil residues in bitumen samples modified with polypropylene. These results provide a quantitative basis for comparing the changes in the physical properties of the mixtures.

For each parameter, standard deviations and 95% confidence intervals were calculated to evaluate the reliability and stability of the obtained results. The data comparatively characterize the influence of PP H030 and PP H350 on the properties of bitumen. According to the results, mixtures based on polypropylene grade H350 demonstrated higher thermal stability, although they showed greater variability in penetration depth, indicating fluctuations in their properties. However, additional statistical methods (such as the t-test or ANOVA) were not applied to assess statistical significance. Therefore, future research should include a deeper statistical analysis of the results.

The reuse of polymer waste enhances environmental efficiency by reducing the accumulation of plastic waste and transforming it into useful products for the construction sector. Oil residue, as an industrial by-product, can also be utilized, thereby reducing the environmental burden.

From an economic perspective, the application of polymer-bitumen mixtures reduces maintenance costs by extending the service life of road pavements. Moreover, with improved energy efficiency, expenditures on fuel and energy in bitumen production and road paving processes are also reduced.

Conflicts of interest. The authors declare that they have no known financial or personal conflicts of interest that could have influenced the work reported in this paper.

CRediT author statement: **A. Syzdyk:** Concept development, research methodology, drafting of the initial manuscript; **G. Seytenova:** Scientific supervision, project leadership; **R. Dyussova:** Data analysis, document editing and revision; **E. Zhakmanova:** Research execution, preparation of materials, documentation; **E. Donbayeva:** Visualization, provision of available resources.

Acknowledgements. This research was conducted within the framework of program-targeted funding from the Science Committee of the Ministry of Science and Higher Education of the Republic of Kazakhstan. (Grant No. BR24992883 Creation of a scientific and technological park for petrochemicals and polymer materials to provide services and implement applied R&D results in the priority sectors of the country's economy).

Cite this article as: Syzdyk AG, Seitenova GZ, Dyussova RM, Zhakmanova EA, Donbayeva E. Polymer-bitumen compositions for improving the energy efficiency of road construction. Kompleksnoe Ispolzovanie Mineralnogo Syra = Complex Use of Mineral Resources. 2027; 341(2):97-104. https://doi.org/10.31643/2027/6445.21

Жол құрылысының энергия тиімділігін арттыруға арналған полимер-битум қоспалары

[1] Сыздық А.Ғ., [1] Сейтенова Г.Ж., [2] Дюсова Р.М., [1] Жакманова Е.А., [1] Донбаева Э.

[1] Л. Н. Гумилев атындағы Еуразия Ұлттық Университеті, Астана, Қазақстан
[2] Торайғыров университеті, Павлодар, Қазақстан

Мақала келді: *6 мамыр 2025*
Сараптамадан өтті: *4 қыркүйек 2025*
Қабылданды: *26 қараша 2025*

ТҮЙІНДЕМЕ

Бұл мақалада полипропиленнің екі түрі (H030 және H350) мен мұнай қалдықтарының битумды модификациялау процесіне әсері қарастырылады. Битумды модификациялау оның физикалық-механикалық қасиеттерін жақсарту арқылы жол жабындарының сапасын арттырудың маңызды тәсілдерінің бірі болып табылады. Қазіргі таңда битумды модификациялау жол құрылысында кеңінен қолданылып, оның сапасын және энергия тиімділігін арттыруда маңызды рөл атқарады. Полимерлердің битумның механикалық тұрақтылығына әсерін зерттеу жол жабындарының беріктігін арттыруда өзекті мәселе болып отыр. Зерттеу барысында битум үлгілеріне H030 және H350 полипропилендерінің 6 түрлі концентрациясы енгізіліп, олардың негізгі көрсеткіштері салыстырылды. Алынған нәтижелер полипропиленнің битум қасиеттерін айтарлықтай өзгертіп, жол жабынының

	беріктігі мен ұзақ мерзімділігін арттыруға ықпал ететінін көрсетті. Сонымен қатар, мұнай қалдығының қосылуы битум қоспасының реологиялық қасиеттерін жақсартуға мүмкіндік беріп, оның адгезиясын жоғарылатты. Бұл зерттеулер жол құрылысында қолданылатын битумды жақсарту үшін маңызды деректер береді. Зерттеу нәтижелері көрсеткендей, полимерлік модификацияланған битумның қолданылуы жол жабындарының тозуға төзімділігін арттырады, жарықшақтардың пайда болуын азайтады және климаттық факторларға төзімділігін күшейтеді. Бұл өз кезегінде жол төсемінің қызмет ету мерзімін ұлғайтуға және жол жөндеу шығындарын азайтуға мүмкіндік береді. Ұзақ мерзімді төсемдер битум өндірісіне және жол салуға жұмсалатын энергия шығындарын азайтуға көмектеседі. Алынған мәліметтер асфальтбетон өндірісінде полимер-модификацияланған битум қоспаларын тиімді пайдалану мүмкіндіктерін кеңейтеді. Осылайша, битум мен полипропиленнің үйлесімділігі зерттеліп, олардың оңтайлы құрамдары анықталды.
	Түйін сөздер: битум, полипропилен, модификацияланған битум қоспалары, мұнай қалдығы, асфальтбетон, энергия тиімділігі.
Сыздық Аяжан Ғалымқызы	***Авторлар туралы ақпарат:*** *Л.Н. Гумилев атындағы Еуразия ұлттық университеті, Жаратылыстану ғылымдары факультетінің магистранты, Қажымұқан көшесі, 13, 010000, Астана, Қазақстан. E-mail: ayazhanka.syzdyk@gmail.com; ORCID ID: https://orcid.org/0009-0007-4435-0976*
Сейтенова Гайни Жумагалиевна	*Химия ғылымдарының кандидаты, Л.Н. Гумилев атындағы Еуразия ұлттық университеті, Жаратылыстану ғылымдары факультетінің қауымдастырылған профессоры, Сәтпаев көшесі, 2, 010000, Астана, Қазақстан. E-mail: gainiseitenova@gmail.com; ORCID ID: https://orcid.org/0000-0001-6202-3951*
Дюсова Ризагуль Муслимовна	*Техника ғылымдарының кандидаты, Торайғыров университетінің пост докторанты, Ломов көшесі, 64, 140000, Павлодар, Қазақстан. E-mail: riza92@bk.ru; ORCID ID: https://orcid.org/0000-0003-3083-5255*
Жакманова Екатерина Андреевна	*Л.Н. Гумилев атындағы Еуразия ұлттық университеті, Жаратылыстану ғылымдары факультетінің PhD докторанты, Қажымұқан көшесі, 13, 010000, Астана, Қазақстан. E-mail: Ekaterina.zakmanova1998@gmail.com; ORCID ID: https://orcid.org/0000-0003-0545-5912*
Донбаева Эльвира	*Л.Н. Гумилев атындағы Еуразия ұлттық университеті, жаратылыстану ғылымдары факультеті, химия кафедрасының аға оқытушысы, Қажымұқан көшесі, 13, 010000, Астана, Қазақстан. E-mail: donbayeva_ek@enu.kz; ORCID ID: https://orcid.org/0009-0005-0762-1488*

Полимер-битумные композиции для повышения энергоэффективности дорожного строительства

[1] Сыздык А.Г., [1] Сейтенова Г.Ж., [2] Дюсова Р.М., [1] Жакманова Е.А., [1] Донбаева Э.

[1] Евразийский национальный университет имени Л. Н. Гумилёва, Астана, Казахстан
[2] Университет имени Торайгырова, Павлодар, Казахстан

Поступила: *6 мая 2025*
Рецензирование: *4 сентября 2025*
Принята в печать: *26 ноября 2025*

АННОТАЦИЯ

В данной статье исследовано влияние двух марок полипропилена (H030 и H350) и нефтяного остатка на процесс модификации битума. Модификация битума является одним из важных способов улучшения его физико-механических свойств и повышения качества дорожного покрытия. В настоящее время модификация битума широко применяется в дорожном строительстве, играя важную роль в повышении его качества и энергоэффективности. Изучение влияния полимеров на механическую стабильность битума является актуальной задачей в повышении прочности дорожного покрытия. В ходе исследования в образцы битума были введены шесть различных концентраций полипропилена H030 и H350, после чего проведено сравнение их основных характеристик. Полученные результаты показали, что полипропилен существенно изменяет свойства битума, способствуя повышению прочности и долговечности дорожного покрытия. Кроме того, добавление нефтяного остатка улучшает реологические свойства битумной смеси, повышая её адгезию. Эти исследования предоставляют важные данные для улучшения битума, применяемого в дорожном строительстве. Результаты исследования показали, что использование полимермодифицированного битума повышает износостойкость дорожного покрытия, снижает образование трещин и улучшает его устойчивость к климатическим факторам. Это, в свою очередь, увеличивает срок службы дорожного полотна и снижает затраты на его ремонт. Долговечные покрытия позволяют сократить энергозатраты на производство битума и укладку дороги. Полученные данные расширяют возможности эффективного применения полимермодифицированных битумных смесей в производстве асфальтобетона. Таким образом, изучена совместимость битума и полипропилена, определены их оптимальные составы.

	Ключевые слова: битум, полипропилен, модифицированные битумные смеси, нефтяной остаток, асфальтобетон, энергоэффективность.
Сыздык Аяжан Галымкызы	***Информация об авторах:*** *Магистрант факультета естественных наук Евразийского национального университета им. Л.Н. Гумилёва, ул. Кажымукана, 13, 010000, Астана, Казахстан. E-mail: ayazhanka.syzdyk@gmail.com; ORCID ID: https://orcid.org/0009-0007-4435-0976*
Сейтенова Гайни Жумагалиевна	*Кандидат химических наук, ассоциированный профессор факультета естественных наук Евразийского национального университета им. Л.Н. Гумилёва, ул. Сатпаева, 2, 010000, Астана, Казахстан. E-mail: gainiseitenova@gmail.com; ORCID ID: https://orcid.org/0000-0001-6202-3951*
Дюсова Ризагуль Муслимовна	*Кандидат технических наук, постдокторант Торайгыров Университета, ул. Ломова, 64, 140000, Павлодар, Казахстан. E-mail: riza92@bk.ru; ORCID ID: https://orcid.org/0000-0003-3083-5255*
Жакманова Екатерина Андреевна	*PhD докторант факультета естественных наук Евразийского национального университета им. Л.Н. Гумилёва, ул. Кажымукана, 13, 010000, Астана, Казахстан. E-mail: Ekaterina.zakmanova1998@gmail.com; ORCID ID: https://orcid.org/0000-0003-0545-5912*
Донбаева Эльвира	*Старший преподаватель, кафедра химии, факультет естественных наук, Евразийский национальный университет им. Л.Н. Гумилёва, ул. Кажымукана, 13, 010000, Астана, Казахстан. E-mail: donbayeva_ek@enu.kz; ORCID ID: https://orcid.org/0009-0005-0762-1488*

References

[1] Case P A, White M A. Polypropylene-modified bitumen: A review of the properties and current developments. Materials. 2020; 13(7):1495. https://doi.org/10.3390/ma13071495

[2] Zhang H, Yu J, Wu S. Effect of polypropylene fibers on the performance of asphalt mixtures. Applied Sciences. 2019; 9(4):742. https://doi.org/10.3390/app9040742

[3] Sengoz B, Topal A, Isikyakar G. The Effect of polypropylene fibres on the tensile performance of asphalt mixtures for road pavements. Materials Science and Engineering. 2020; 888(1):012082. https://doi.org/10.1088/1757-899X/888/1/012082

[4] Kondyurina I V, Kondyurin A V. Influence of polymer modification on bitumen properties. Periodica Polytechnica Civil Engineering. 2020; 64(1):170–179. https://doi.org/10.3311/PPci.11570

[5] Polacco G, Filippi S, Merusi F, Stastna J. Effects of Recycled Asphalt Pavement on the Stiffness and Fatigue Performance of Multigrade Bitumen Asphalt. Journal of Materials in Civil Engineering. 2015; 30(2):04014215. https://doi.org/10.1061/(ASCE)MT.1943-5533.0002150

[6] Lu X, Isacsson U. Modification of road bitumens with thermoplastic polymers. Polymer International. 2020; 69(3):215–224. https://doi.org/10.1002/pi.6405

[7] Onishchenko A, Stolyarova L, Bieliatynskyi A. Evaluation of the durability of asphalt concrete on polymer modified bitumen. Web of Conferences. 2020; 157:06005. https://doi.org/10.1051/e3sconf/202015706005

[8] Yildirim Y. Polymer modified asphalt binders. Construction and Building Materials. 2018; 25(2):781–789. https://doi.org/10.1016/j.conbuildmat.2018.10.007

[9] Sharma D K, Goyal P. Performance evaluation of polypropylene modified bitumen. International Journal of Scientific Research and Management. 2017; 5(12):7590–7595. https://doi.org/10.18535/ijsrm/v5i12.28

[10] Desidery L, Lanotte M. Variation of internal structure and performance of polyethylene- and polypropylene-modified bitumen during blending process. 2020; 133(15):50142. https://doi.org/10.1002/app.50142

[11] Zhou J, Wu S. Rheological properties of asphalt binders containing various anti-aging agents. Advances in Science and Engineering Research. 2020; 10(1):119–125. https://doi.org/10.35877/454RI.asci1119

[12] Schaur A, Unterberger S H, Lackner R. Impact of molecular structure of PP on thermo-rheological properties of polymer-modified bitumen. Construction and Building Materials. 2021; 278:122981. https://doi.org/10.1016/j.conbuildmat.2021.122981

[13] Zhang F, Yu J, Han J. Effect of polymer modification on the aging properties of bitumen. Road Materials and Pavement Design. 2021; 22(3):567–579. https://doi.org/10.1080/14680629.2021.1893209

[14] Kezhen Y, Lingyun Y, Daocheng W. High-Temperature Performance of Polymer-Modified Asphalt Mixes: Preliminary Evaluation of the Usefulness of Standard Technical Index in Polymer-Modified Asphalt. Polymers (Basel). 2019; 11(9):1404. https://doi.org/10.3390/polym11091404

[15] Sabzoi N, Yeong JB, Filippo G. Sustainable Polymers from Recycled Waste Plastics and Their Virgin Counterparts as Bitumen Modifiers: A Comprehensive Review. Polymers (Basel). 2021; 13(19):3242. https://doi.org/10.3390/polym13193242

[16] Qilin Y, Jiao L, Xiaowei W, Dawei W, Ning X, Xianming S. A review of polymer-modified asphalt binder: Modification mechanisms and mechanical properties. Cleaner Materials. 2024; 12:100255. https://doi.org/10.1016/j.clema.2024.100255

[17] Hasanain JK, Amir M, Shakir AB. Rheological and microstructural properties of nano-composite bitumen modified by nano-alumina and low-SBS content. Case Studies in Construction Materials. 2024; 20:e03244. https://doi.org/10.1016/j.cscm.2024.e03244

[18] Garcia-Morales M, Partal P, Navarro F J, Gallegos C. Effect of waste polymer addition on the rheology of modified bitumen. International Journal of Polymer Analysis and Characterization. 2017; 22(7):569–580. https://doi.org/10.1080/10916466.2017.1356853

[19] Polacco G, Stastna J, Biondi D. Asphalt modification with different polyethylene-based polymers. Fuel. 2016; 150:159–166. https://doi.org/10.1016/j.fuel.2015.12.038

[20] Yu J, Feng P, Zhang H, Wu S. Effect of organo-montmorillonite on aging properties of asphalt. Road Materials and Pavement Design. 2015; 16(1):193–207. https://doi.org/10.1080/14680629.2015.1030832

Crossref
DOI: 10.31643/2027/6445.22
Mining & Mineral Processing

creative commons

Innovative Adsorbent Materials for Efficient Silicon Extraction from Industrial Waters: A review

[1] Kylyshkanov M., [2]Gerassyova N., [1] Sharipov R., [1] Kuanysh A., [1] Maldybayev G., [1*]El-Sayed Negim, [3] Baigenzhenov O., [4] Bekbayeva L., [5]Khaldun M. Al Azzam, [1] Balgimbayeva U.

[1] Kazakh British Technical University, Almaty, Kazakhstan
[2]LLC Deep Core Analytics, Almaty, Kazakhstan
[3]Mining and Metallurgical Institute named after O.A. Baikonurov, Satbayev Unversity, Almaty, Kazakhstan
[4]Al-Farabi Kazakh National University, Almaty, Kazakhstan
[5] The University of Jordan, 11942, Amman, Jordan

** Corresponding author email: elashmawi5@yahoo.com*

Received: *October 27, 2025*
Peer-reviewed: *November 24, 2025*
Accepted: *November 26, 2025*

ABSTRACT
Silica fouling reduces the effectiveness and durability of membrane-based treatment systems, and silicon contamination in industrial water streams poses ongoing operational issues. With an emphasis on their processes, drawbacks, and applicability for various silica species, this article provides a comparative examination of the main silica removal technologies: ion exchange, reverse osmosis (RO), ultrafiltration (UF), electrocoagulation (EC), adsorption, and lime softening. Although they need a significant amount of chemical input and pH control, lime softening and ion exchange are efficient for dissolved silica. RO requires thorough preparation and offers broad-spectrum separation, although it is susceptible to silica scaling. While UF works well with colloidal and particulate silica, it is unsuccessful with monomeric forms. EC achieves excellent removal rates with less sludge by combining electrochemical destabilisation and crystallisation. Adsorption provides variable selectivity, low energy consumption, and compatibility with membrane systems, especially when employing tailored materials like activated alumina, iron oxide-coated media, and functionalised hybrids. In addition to outlining important techno-economic considerations for scaling up silica extraction methods in intricate industrial water matrices, the paper highlights new developments in adsorbent design, such as surface modification, hierarchical porosity, and regeneration techniques.

Keywords: silica, industrial, wastewater, treatment, adsorption.

Information about authors:

Manarbek Kylyshkanov — *Doctor of Physico-Mathematical Sciences, Laboratory of Advanced Materials and Technologies, Kazakh British Technical University, St. Tole bi, 59, 050000, Almaty, Republic of Kazakhstan. Email: kylyshkanov@mail.ru*

Gerassyova Natalya — *Doctoral student, LLC Deep Core Analytics, al-Farabi av., 17/1 b5B, 050059, Almaty, Kazakhstan. Email: tatoline2001@gmail.com*

Rustam Sharipov — *PhD, Assistant Professor, Laboratory of Advanced Materials and Technologies, Kazakh British Technical University, St. Tole bi, 59, 050000, Almaty, Kazakhstan. Email: r.sharipov@kbtu.kz*

Akzhunis Kuanysh — *Master student, Department of science and innovation, Kazakh British Technical University, St. Tole bi, 59, 050000, Almaty, Kazakhstan. Email: a.kuanysh@kbtu.kz*

Galymzhan Maldybayev — *PhD, Associate Professor, Laboratory of Advanced Materials and Technologies, Kazakh British Technical University, St. Tole bi, 59, 050000, Almaty, Kazakhstan. Email: g.maldybaev@kbtu.kz*

El-Sayed Negim — *PhD, Professor, School of Materials Science and Green Technologies, Kazakh British Technical University, St. Tole bi, 59, 050000, Almaty, Kazakhstan. Email: elashmawi5@yahoo.com*

Omirserik Baigenzhenov — *PhD, Professor, Mining and Metallurgical Institute named after O.A. Baikonurov, Satbayev Unversity 22 Satbaev str.,050013, Almaty, Kazakhstan. Email: o.baigenzhenov@satbayev.university*

Lyazzat Bekbayeva — *PhD, Associate Professor, National Nanotechnology Open Laboratory, Al-Faraby Kazakh National University, Al-Farabi av., 050040, Almaty, Kazakhstan. Email: lyazzat_bk2019@mail.ru*

Khaldun M. Al Azzam — *PhD, Professor, Department of Chemistry, Faculty of Science, The University of Jordan, 11942, Amman, Jordan. Email: azzamkha@yahoo.com*

Ulpan Balgimbayeva — *Doctoral student, School of Applied of Mathematics, Kazakh British Technical University, St. Tole bi, 59, 050000, Almaty, Kazakhstan. Email: u.balgimbaeva@kbtu.kz*

Introduction

In industrial water systems, silicon is predominantly found as silica (SiO_2), which exists in granular, colloidal, and ionic forms. In industrial applications, silicon is predominantly present as reactive silica (monomeric and soluble), colloidal silica (non-ionic and suspended), and particulate silica (such as sand or silt). Silica removal is the main goal of extraction procedures to reduce the

possibility of scaling and equipment deterioration. The specific form of silica is determined by variables such as pH, temperature, and the characteristics of the water source. The most effective removal techniques include lime softening, ion exchange, reverse osmosis, and advanced ceramic media filtration [1]. Silicon-containing wastewater is primarily produced during steam throughput or steam drive extraction used for thick oil development. Injected steam causes hydrolysis of underground silicon rocks, forming silicates and resulting in significant amounts of silicon-laden wastewater [[1], [2]]. Large-scale pipeline clogs can arise from silicate scale buildup in oilfield wastewater collection systems. Compared to other water sources, well water includes more silica, which can damage equipment, particularly in deep wells where temperatures are greater. High silica levels also hinder well-water treatment methods, so concentrations must be lowered to protect equipment and membranes. There are many methods used to reoval silicon from industrial wastes. Among these, the most widely employed techniques include adsorption, electroddialysis, reverse osmosis, chemical precipitation, ion exchange, solvent extraction/liquid membrane separation and electrolysis [[3], [4], [5]]. Adsorption has become a critical process across numerous industrial applications, including natural gas storage, pollution control, catalyst support, and particularly in gas separation and purification, owing to its low energy requirements, operational flexibility, and the wide variety of available adsorbents [[6], [7], [8], [9], [10]]. Additionally, adsorption processes are widely recognized as a standard technique for determining the surface area and pore size distribution of solid materials. This process is characterised by its non-toxicity, cost-effectiveness, environmental sustainability, and renewability. As a result, it is seen as a practical substitute for conventional treatment procedures and an efficient way to remove heavy metals from wastewater. The process of adsorption can be accomplished via chemisorption, which involves the creation of a chemical connection between the sorbate molecule and the adsorbent surface, or physical adsorption, which is controlled by weak intermolecular interactions. Due to the remaining valence forces from surface molecules, chemical adsorption results in the formation of a monomolecular layer of adsorbate on the surface. On the other hand, physical adsorption results from molecule condensation inside the solid's capillaries [[11], [12]]. Consequently, a thorough understanding of adsorption mechanisms is essential not only for the design and optimization of industrial adsorption processes but also for accurately characterizing the structure of porous solids. Several methods have been documented for the treatment of industrial effluents. Ion exchange involves swapping ions between electrolytes, or between an electrolyte solution and a complex. Its primary purpose is to employ solid materials such as minerals, clays, membranes, and resins to purify, separate, and disinfect ion-containing fluids. This mechanism may facilitate adsorption and takes place at the solid's surface. However, ion exchange is costly in terms of capital and operating expenses [13]. A common technique for recovering materials or purifying solutions is chemical precipitation, which turns dissolved compounds into solid particles. There are several methods for improving chemical precipitation. Sodium decanoate, carbamates, carbonates, sulphides, and polymers are examples of reagents that generate insoluble metal compounds as alternatives to hydroxide precipitation. Large volumes of sludge and silt containing heavy metals are produced by flocculation and coagulation, and this method is typically ineffective in eliminating trace pollutants [14]. Desalination, water purification, and chemical recovery are three applications where electrodialysis, a membrane-based separation technique that uses an electric potential to selectively remove ions from solutions, is very beneficial. Electric fields are used in electrodialysis, a non-thermal separation technique, to move ions across ion-exchange membranes. Positively charged ions (cations) can pass through cation-exchange membranes, while negatively charged ions (anions) can pass through anion-exchange membranes. These membranes are systematically arranged in alternating order between two electrodes within a configuration known as an electrodialysis stack [[15], [16], [17]]. Research indicates that the potential of an electrodialysis cell is largely independent of ion type, instead depending on operational conditions and cell configuration. Despite various drawbacks, electrodialysis has significant advantages for treating heavy metal-containing wastewater, including the ability to efficiently remove unwanted particles from water and produce highly concentrated streams for recovery [18]. But because this technique produces hazardous waste, cooperation with businesses that can recover and recycle metals from the resultant sludge is required. While, reverse osmosis is a

pressure-driven membrane process designed to remove dissolved salts, contaminants, and microorganisms from water by passing it through a semi-permeable membrane that permits the passage of water molecules while restricting larger solutes such as salts, organic compounds, and microbes [[19], [20], [21]]. This technology is extensively employed for desalination, water purification, and industrial fluid separation. In reverse osmosis, the natural osmotic flow is counteracted by applying pressure exceeding the osmotic pressure, thereby enabling the selective removal of impurities. But solvent extraction transfers a solute from one liquid phase (typically aqueous) to another immiscible phase (usually organic) based on solubility differences. Because of operational and financial concerns, it is rarely utilised in wastewater treatment, even though it enables the recovery of important species. Because a liquid membrane permits targeted solute movement between two aqueous phases, combining solvent extraction and membrane separation with a membrane can increase selectivity [[18], [19], [20]]. The electrolysis process is a significant electrochemical technique that utilises electrical energy to drive non-spontaneous chemical reactions, commonly for the decomposition of compounds or extraction of elements. It plays an essential role in fields such as metallurgy, water splitting, and electroplating. Electrolysis operates by passing a direct electric current through an electrolyte a medium containing free ions which induces chemical changes at the electrodes and facilitates the extraction of heavy metals [[22], [23], [24], [25]].

Common methods for removal silica from industrial waste. Lime Softening

By introducing lime (calcium hydroxide), which increases the pH and causes magnesium to precipitate as magnesium hydroxide, the lime softening method eliminates silica from water. During water softening, silica may be removed via precipitation with calcium carbonate or by adsorbing onto solids [26] . This precipitate adsorbs dissolved silica, and both are then removed via sedimentation and filtration. The effects of MgO slaking on silica removal and the mechanisms by which MgO removes silica were investigated [26]. At different pH levels (8.0–11.3), doses (100–1000 ppm), and contact periods (15–120 min), experiments were conducted to assess the silica removal efficiency of slaked and nonslaked MgO under warm lime sodtening operating temperatures (65–85 °C). There are two competing methods for removing silica: adsorption onto process-formed $Mg(OH)_2$ or precipitation as magnesium silicate complexes. Slaked MgO showed a lower percentage of silica removal under WLS conditions than nonslaked MgO, which was explained by higher silica adsorption on $Mg(OH)_2$ after slaking. According to research, the amount of magnesium in the water affects how well silica is removed by precipitation processes [27]. Furthermore, silica solubility can be impacted by temperature, pH level, salt concentration, silica concentration, and pressure [28]. The hot lime process has been shown to effectively remove both water hardness and silica. Additionally, studies indicate that lime softening can reduce silica content even when performed at ambient temperatures. Three chemical treatments lime-soda softening, sodium aluminate addition, and magnesium oxide for reducing silica in water purification systems were examined. Jar-tester experiments measured the effect of varying doses on silica concentrations. Magnesium oxide was the most cost-effective option for treating 30,000 cubic meters of water, possibly saving around US$1.8 - 2.1 million annually [29].

Ion exchange

By applying an anion exchange resin, which makes it easier for silica ions to be replaced with hydroxide ions and is regenerated using caustic agents like sodium hydroxide, ion exchange efficiently eliminates dissolved ionic silica from wastewater. Although this technique is quite effective at removing reactive silica, it needs to be treated first to transform the silica into its ionic form since ion exchange cannot deal with colloidal or particulate silicon. However, silica solubility is influenced by a range of factors, including temperature, pressure, pH, and ionic strength. For pH values below 9, solubility remains relatively constant; however, at higher pH levels, solubility increases as silicate ions form in addition to the monomer, which is in equilibrium with the solid phase. Salts lower silica solubility by increasing ionic strength [30]. Silica removal from hydrated lime was tested using ion exchange and UV spectrophotometry. By combining 10 mL of 2 M NaOH with 15 mL of 0.1 M HCl, the ideal technique reduced silica to 0.0054%. Sodium hydroxide reduces silica concentration and can limit silica accumulation on tube surfaces during water treatment [31]. The ideal conditions for silicon

removal from simulated wastewater were determined to be pH 6, a reaction time of 20 minutes, a current density of 27 mA/cm², and a temperature of 35 °C, based on single-factor and orthogonal experiments. Under the conditions of pH 8.0, reaction time of 20 minutes, current density of 27.2 mA/cm², and a temperature of 35 °C, the silicon concentration in Hongshan Oilfield wastewater decreased from 76.22 mg/L to 10.75 mg/L, achieving a silicon removal rate of 85.90% with an electrode mass loss of 0.0209 g. Calcium and magnesium ions greatly improve silica removal at pH 8. These findings inform industrial use of electrocoagulation to remove silicon from oilfield wastewater [1]. The removal of silica from water using the electro-Fenton (EF) advanced oxidation process was systematically evaluated. Experimental investigations varied several parameters, including pH, current density, reaction duration, monopolar versus bipolar system configurations, and inter-electrode distance. Results demonstrated that up to 95% silica removal was achieved after 40 minutes of operation at near-neutral pH utilizing a bipolar electrode arrangement. The extent of desilication increased proportionally with higher applied current densities. Optimal silica removal consistently occurred at near-neutral pH values [32]. The separate pretreatment of removing silica was explored using several methods. Testing was done on precipitation using $Fe(OH)_3$, $Al(OH)_3$, silica gel, and a strongly basic anion (SBA) exchange resin. While some aluminium remained and aluminosilicate colloids were not eliminated, $Al(OH)_3$ was the most successful, removing nearly all the dissolved silica. With a silica removal rate of up to 94%, the SBA resin also demonstrated good performance [33].

Reverse osmosis for silica removal

A semipermeable membrane is used in the popular water purification process known as reverse osmosis (RO) to eliminate impurities. Nevertheless, silica cannot be successfully removed by RO alone; pretreatment and scale control are required to avoid silica fouling. The many types of silica dissolved, colloidal, and particulate present difficulties for RO membranes. Although some particle silica is eliminated by RO, dissolved reactive silica frequently gets through and may subsequently result in chronic scaling. Pretreatment strategies for silica removal from reverse osmosis (RO) feed water encompass softening and coagulation, seed precipitation and aggregation, tight ultrafiltration, ion exchange, adsorptive media, and electrocoagulation. To mitigate RO membrane fouling under silica-rich conditions, common approaches include antiscalant dosing, pH optimization, and intermediate concentrate softening [[33], [30]]. Examined were the behaviour of silica scaling and its elimination in RO membrane processes, paying special emphasis to the gallic acid (GA)-based cleaning mechanism. Even at the lowest starting concentrations of silicic acid, silica scale accumulation caused a steady drop in membrane flow over time. Nonetheless, GA was quite successful in cleaning silica-fouled RO membranes; in the first half hour, it removed 81.87% of the silica scale, recovering 89.7% of the initial flow. GA's ability to clean is ascribed to its ability to adsorb onto silica scale particles, creating a surface complex that changes into a 1:3 complex that dissolves in water. Silica deposits on the membrane surface are gradually broken down by this contact.

These results enhance knowledge of the relationships between GA and silica scaling and provide important information for creating effective silica scale cleaning methods [34]. As feed water concentration rises, increasing osmotic pressure limits water recovery in reverse osmosis. However, this restriction has no effect on membrane distillation (MD), a thermally driven membrane desalination method. This study examined pH adjustment to reduce silica scaling in the MD process. When feed water pH was below 5 or above 10, negligible scaling occurred at silica concentrations up to 600 mg/L, whereas scaling peaked at neutral pH (6–8). The study also evaluated cleaning techniques; performance was momentarily restored by dissolving some silica scale with NaOH solutions that had a pH higher than 11. Re-exposed to supersaturated silica, however, caused quicker scaling than with fresh membranes because residual silica remained on membrane surfaces [35]. The electromagnetic field (EMF) influenced the performance of the RO system by reducing membrane scaling, altering the characteristics of the formed scales, and lowering the rate at which normalized water permeability declined. EMF treatment demonstrated efficacy in removing pre-existing scales and precipitates from water pipelines and storage tanks. It was only partially successful in getting rid of existing scaling on RO membranes, though. According to membrane autopsy, the scales that developed on the membrane surface when exposed to an electromagnetic field (EMF) had a

soft, powdery texture that made it easy to remove them with a simple water rinse. After examining the many ways that EMF impacted the RO membrane, the magnetohydrodynamic effect was shown to be the main one. This study presents EMF as a chemical-free method for controlling membrane scaling and maintaining RO performance during brackish groundwater desalination, providing detailed discussion on mechanisms and future perspectives [36].

Ultrafiltration (UF)

Ultrafiltration (UF) is a membrane-based separation technology extensively utilised in industrial water treatment processes, particularly for silica removal. This technique uses semi-permeable membranes that function at low to moderate pressures (1–10 bar) and have pore diameters that are normally between 0.01 and 0.1 microns. UF may be used to remove particulate and colloidal silica, but it cannot extract dissolved (reactive) silica because it efficiently separates suspended solids, colloidal particles, and high-molecular-weight solutes from water. Several factors influence the efficacy of ultrafiltration, including pH which affects silica speciation and membrane charge; temperature which impacts viscosity and flux; transmembrane pressure where higher levels increase flux but may also promote fouling; and crossflow velocity which plays a crucial role in reducing concentration polarization and fouling [[37], [38]]. Feed solution pH significantly affects electrodialysis with ultrafiltration (EDUF) using polyethersulfone (PES) membranes by altering membrane selectivity through electrostatic interactions with peptides. These effects can cause high molecular weight peptides to accumulate softly. EDUF at pH 9 efficiently isolates cationic peptides (<400 Da) in KCl and restricts anionic peptide variety in KCl 1. A two-step UF–EDUF method using UF permeate as feed is being tested to better understand the influence of high molecular weight peptides [39]. The role of solution chemistry in PES ultrafiltration membrane fouling by silica nanoparticles and natural organic matter was assessed under controlled pH, ionic strength, and calcium conditions. The Lifshitz–van der Waals, electrostatic, and acid–base interactions were measured using the Extended Derjaguin–Landau–Verwey–Overbeek (xDLVO) theory. The main force behind adhesion and cohesion was found to be acid–base attraction, and fouling rose with decreasing pH, increasing ionic strength, and increasing calcium. In complicated colloidal systems, the inverse relationship between estimated interaction energy and fouling potential highlights the usefulness of xDLVO theory in forecasting membrane behaviour [[40], [41]]. To investigate how adding and then removing silica (SiO_2) nanoparticles affected the membrane's shape, hydrophilicity, and separation performance, an ultrafiltration membrane based on polysulfone (PSf) was designed. Three types of membranes were prepared pristine PSf, PSf/SiO_2 composite, and acid-washed PSf/$WSiO_2$ and characterized systematically. Pure water flux tests showed that the PSf/$WSiO_2$ membrane had higher permeability compared to the other samples, while the PSf/SiO_2 membrane had lower fouling during bovine serum albumin filtration. These findings indicate that introducing and subsequently removing sacrificial fillers can influence transport properties and performance in PSf-based ultrafiltration membranes [42]. Silica was eliminated using a semi-batch adsorption method that included hollow fibre ultrafiltration membranes and iron oxy/hydroxide agglomerates (IOAs). Adsorbent dose, residence period, and silica content were the main factors investigated. Maximum adsorption occurred within 15 minutes, matching batch results. Higher silica concentrations increased, while greater adsorbent dosages decreased, adsorption capacity. The ultrafiltration membrane separated loaded adsorbent without significant fouling before breakthrough. A simple model accurately predicted breakthrough curves [43].

Electrocoagulation for Silica Removal

Electrocoagulation (EC) uses a direct electric current to dissolve metal electrodes usually aluminum or iron which release ions that bind with and remove silica from water. This chemical-free procedure minimises sludge and eliminates the need for additional chemicals by forming solid floc that is easy to remove, making it an effective substitute for conventional industrial and geothermal water treatment techniques [[44], [45]]. An electrochemical reaction serves as the foundation for the electrocoagulation (EC) process. The anode, such as aluminium, oxidises and dissolves when a direct current is supplied, releasing metal ions into the water. Water reduction results in the production of hydroxide ions at the cathode, which causes hydroxide creation. The metal ions released from the anode subsequently react with these hydroxide ions to form metal hydroxides, such as aluminum hydroxide. These metal hydroxides function as coagulants, aggregating with dissolved silica to produce stable hydroxy-aluminosilicate polymers

and other flocs. Because of their size, these flocs can be eliminated by filtering or sedimentation procedures [[44], [45], [46]]. The following elements affect the EC process: iron is good for both silica and sulphide, whilst aluminium is good for silica; Results are influenced by electrical factors, including voltage, time, and current density; Flow rate reducing power consumption and increasing efficiency by optimising flow rate and electrode spacing; and Conductivity and pH in water chemistry affect treatment efficacy and cost. [47], [44], [48], and [49]. Electrocoagulation is an effective and energy-efficient approach for removing silica and hardness from oil-sands produced water. Key operating parameters including charge loading, current density, flow rate, and polarity reversal period significantly influence removal efficiency and system performance. Over 80% silica removal was made possible under ideal circumstances (8 mA cm^{-2} current density and 1000–1500 C L^{-1} charge loading), with aluminium electrodes surpassing iron in terms of pollutant reduction and operating costs. Extended polarity reversal intervals further enhanced removal efficiency while reducing energy consumption and cell voltage. These findings highlight the potential of EC, particularly Al-based systems, as a scalable and cost-effective solution for silica-rich industrial wastewater treatment [48]. Meanwhile, the aluminium electrode is frequently used in electrocoagulation (EC) to remediate wastewater that contains SiO_2. The effectiveness of SiO2 removal using iron was increased by methodically optimising the current density, plate spacing, plate-to-water ratio, and electrode passivation control. A multiphysical field linked simulation model was also used to examine the temperature field, velocity, concentration, and electricity distributions inside the silica removal system. An optimal silica removal rate of 97.4% was achieved with a theoretical iron consumption of 0.251 g Fe/L, an adsorption capacity of 660 mg SiO2/(g Fe L), and electricity usage of 0.312 Wh/L. Simulation results demonstrated that EC promotes mass and heat transfer within the cell, and anodes featuring square holes are more effective in enhancing the iron corrosion rate [49]. Fouling and scaling from silica are major challenges in membrane desalination. Studies of pretreatment and SDI tests found silicate salts stay insoluble in brackish and seawater, and fouling does not relate to silica levels between 15–200 mg/L. Electrocoagulation using Al^{3+} is more effective than Fe^{3+}, reaching 90.2% silica removal efficiency for brackish water containing roughly 28 mg/L silica [50]. The use of hybrid coagulants composed of polyaluminum nitrate sulfate (PANS) and three polyamines (PAs) with different molecular weights for silica removal was investigated. For each polymer, four hybrids with varying PANS-to-polyamine ratios (5–20%) were examined at five doses (500–2,500 mg/L) and two beginning pHs (8.4 and 10.5). In terms of silica removal, all hybrids performed better than PANS at pH 8.4; they needed lower doses (500 vs. 2,500 mg/L) and were best at 5% polyamine (over 50% vs. PANS's 30%). At pH 10.5, all products removed up to 90% of the material with no variation in efficiency. Generally speaking, hybrids eliminated more COD than PANS, particularly at higher pH values. While PA molecular weight did not affect silica removal, higher weights improved COD removal. Mechanism analysis indicated that PANS promoted sweep flocculation, whereas hybrids combined sweep flocculation with patch formation [51]. The influence water quality affects dissolved silica removal using electrocoagulation with aluminum electrodes was studied. Experiments were performed on replacement water (RW) and cooling tower blowdown water (CTBW), both assessed at a small pilot scale with a continuous flow system including electrocoagulation, flocculation, sedimentation, and sand filtration. Key variables evaluated included silica removal efficiency, aluminum usage, head loss, and voltage. Treatment costs for all water types were considered. The Al^{3+}/silica removal ratio ranged from 1.09 to 1.33 for RW and was 0.85 for CTBW [52].

Adsorption for removal silica

An effective method for removing silica from water is adsorption, which makes use of substances like silica-based adsorbents, activated alumina, and iron-based compounds. Activated alumina's remarkable selectivity and regeneration capabilities make it particularly beneficial. Additionally, composite materials, including magnetic iron–aluminum hydroxide nanoparticles, provide the benefit of magnetic separation, facilitating straightforward recovery processes [[53], [54], [55], [56]]. Absorbent materials include activated alumina, which is a commonly used and well-researched adsorbent, particularly for complex industrial wastewaters, due to its selectivity for silica and capacity for regeneration. Although they are also used, iron-based absorbents such iron (III) hydroxide and similar substances have the potential to create deposits that make regeneration procedures more difficult. To improve stability and

adsorption performance, a variety of silica-based materials are used, such as mesoporous silica and silica aerogels, occasionally with additional metal oxides. To make separation and reuse easier, composite materials like magnetic iron-aluminum hydroxide nanoparticles combine silica adsorption capabilities with magnetic qualities [[57], [58], [59], [60], [61]]. Surface contacts, pH, and the chemical affinity of silica species for the adsorbent are all factors that affect adsorption. Strong pH dependence characterises the adsorption process; for example, adsorption onto activated alumina is pH-dependent, whereas iron-based adsorbents work best at pH 9. As shown with gallic acid-modified resins, chemisorption—the formation of chemical bonds between silica and the adsorbent occurs sometimes [[53], [57], [62], [63]]. Adsorption and chemical precipitation were used to study the removal of reactive silica from synthetic solutions and industrial anodising waste streams. Seven precipitants and twelve commercial adsorbents were evaluated. Ferrolox (based on iron (III) hydroxide) was the most effective adsorbent, particularly at pH 9, producing 16.22 mg/g for synthetic solutions and 11.25 mg/g for wastewater. According to molecular modelling, Ferrolox and silica species formed a hydroxo-complex during the silica removal process. Magnesium chloride was removed up to 87% in precipitation, and the most important factor was found to be pH (variance value 81.42) [57]. The effectiveness of boehmite (γ-AlOOH) as an adsorbent for silica removal was assessed. Both chemical and physical adsorption processes were shown by kinetic analysis, and the pseudo-second-order model suggested the existence of chemisorption. At concentrations more than 50 mg/L, the silica adsorption isotherm complied with the Freundlich model, and mesoporous structures facilitated silica adsorption in tap water. According to this study, γ-AlOOH can be used as an adsorbent to alleviate silica-related issues in a variety of sectors [56]. At a SiO_2 concentration of 200 mg/L, with a dosage of 0.10 g/L, pH 10.5, and temperature of 303 K, integrated chemical precipitation using Fennofix type FF40 and evaporation achieved 96% silicon removal. This result is marginally higher than reported silicon removal rates for precipitation using CaO (93%) and electro-coagulation (95%) at initial SiO_2 concentrations of 954 mg/L and 250 mg/L, respectively. Both chemical precipitation and evaporation were able to treat thermo-mechanical pulping (TMP) whitewater of varying strengths, as the treated effluents complied with the regulatory silicon limit of less than 50 mg/L [63]. Magnesium oxide effectively removes soluble silica from water via adsorption, especially when combined with hot-process lime-soda softening, without increasing lime or soda ash usage. The process aligns with Langmuir and Freundlich isotherms and reduces the solids content of treated water, unlike chemical reagents such as ferric sulphate. While final traces of silica are hardest to eliminate, practical applications have shown reductions from 6.3 ppm to 0.6 ppm and from 56 ppm to 1 ppm in full-scale and natural water treatments, respectively [64]. Core-shell composite magnetic $Al(OH)_3@Fe_3O_4$ nanoparticles were created as adsorbents to extract silica from brackish water. Silica adsorption is made possible by the $Al(OH)_3$ shell, while magnetic separation is made simple by the Fe_3O_4 core.

At 2 g L^{-1}, these nanomaterials removed approximately 95% and 80% of silica from solutions with initial concentrations of 0.5 and 2 mM, respectively. After four cycles, regeneration with 0.05 M NaOH retained reusability and removal effectiveness of around 40%. The presence of silica polymerisation on the $Al(OH)_3$ shell during adsorption was verified by spectroscopic investigations. Utilising these nanoparticles in reverse osmosis showed decreased silica scaling and enhanced water recovery, suggesting that they might be used for effective brackish water treatment and inland desalination [[65], [66]]. Ferric hydroxide ($Fe(OH)_3$) and ferric chloride ($FeCl_3$) were investigated for the removal of silica from integrated circuit (IC) effluent. $Fe(OH)_3$ absorbed 94.6% of reactive silica in less than 60 minutes, whereas optimised $FeCl_3$ decreased turbidity by 97.2%. Adsorption was modelled using PHREEQC and suited the Langmuir isotherm, showing silica polymerisation on iron surfaces. Silica may be effectively removed from industrial effluent by using both $FeCl_3$ and $Fe(OH)_3$ [67].

Conclusions

Removing silica from industrial water is vital for preventing membrane fouling and maintaining efficiency. In addition to their advantages, traditional techniques including electrocoagulation, ion exchange, reverse osmosis, ultrafiltration, and

lime softening have disadvantaged such high chemical usage, high energy costs, and restricted compatibility. The selective removal of reactive and colloidal silica using adsorption, particularly with improved materials, requires less energy and produces less sludge. Research on enhanced adsorbents via regeneration, porous architectures, and surface modification is essential to creating scalable and cost-effective solutions. The development of efficient and sustainable water treatment systems for silicon management can be facilitated by incorporating these developments.

Conflicts of interest. Authors declare no conflict of interest.

CRediT author statement: **M. Kylyshkanov:** Conceptualization, Methodology, Software; **R. Sharipov**: Data curation, Writing draft preparation; **G. Maldybayev**: Visualization, Investigation; **A. Kuanysh**: Supervision; **E. Negim**: Software, Validation; **N. Gerassyova, L.. Bekbayeva, O. Baigenzhenov, U. Balgimbaeva**: Reviewing and Editing.

Acknowledgements. This research was funded by the Committee of Science of the Ministry of Science and Higher Education of the Republic of Kazakhstan (Grant No. BR28713471 Development of methods for increasing the extraction of uranium from uranium-containing solutions by effectively reducing the content of silicon compounds).

Cite this article as: Kylyshkanov M, Gerassyova N, Sharipov R, Kuanysh A, Maldybayev G, El-Sayed Negim, Baigenzhenov O, Bekbayeva L, Khaldun M Al Azzam, Balgimbayeva U. Innovative Adsorbent Materials for Efficient Silicon Extraction from Industrial Waters: A review. Kompleksnoe Ispolzovanie Mineralnogo Syra = Complex Use of Mineral Resources. 2027; 341(2):105-116. https://doi.org/10.31643/2027/6445.22

Өнеркәсіптік ағынды сулардан кремнийді тиімді бөліп алу үшін инновациялық адсорбент материалдары: Шолу

[1] Қылышканов М., [2]Герасёва Н., [1] Шарипов Р., [1] Қуаныш А., [1] Малдыбаев Г., [1]El-Sayed Negim, [3] Байгенженов Ө., [4]Бекбаева Л., [5] Khaldun M. Al Azzam, [1] Балгимбаева У.

[1]Қазақстан-Британ Техникалық Университеті, Алматы, Қазақстан
[2]ЖШС Deep Core Analytics, Алматы, Қазақстан
[3]О. А. Байқоңыров атындағы Тау-Кен Металлургия Институты, Сәтбаев Университеті, Алматы, Қазақстан
[4]Әл-Фараби атындағы Қазақ Ұлттық Университеті, Алматы, Қазақстан
[5]Иордания университеті, 11942, Амман, Иордания

Мақала келді: *27 қазан 2025*
Сараптамадан өтті: *24 қараша 2025*
Қабылданды: *26 қараша 2025*

ТҮЙІНДЕМЕ

Кремнеземмен ластану мембраналық тазарту жүйелерінің тиімділігі мен ұзақ мерзімді беріктігін төмендетеді, ал өнеркәсіптік су ағындарында кремнийдің болуы тұрақты пайдалану кезінде елеулі қиындықтар тудырады. Бұл мақалада кремнийді кетірудің - ион алмасу, кері осмос (КО), ультрафильтрация (УФ), электрокоагуляция (ЭК), адсорбция және әкпен жұмсарту сияқты негізгі технологияларына олардың жұмыс істеу процестері, кемшіліктері мен әртүрлі кремнезем түрлеріне қолданылу ерекшеліктері тұрғысынан салыстырмалы талдау жүргізіледі. Олар айтарлықтай мөлшерде химиялық заттарды және pH бақылауын қажет етсе де, әкпен жұмсарту және ион алмасу әдістері еріген кремнеземді кетіруде тиімді. Кері осмос кең ауқымды бөлу қабілетіне ие болғанымен, алдын ала дайындықты қажет етеді және кремнезем тұнбасының түзілуіне бейім. Ультрафильтрация коллоидты және дисперсті кремнеземді тиімді жояды, дегенмен, ол мономерлі түрлерге қатысты тиімсіз. Электрокоагуляция электрохимиялық тұрақсыздандыру мен кристалдану процестерінің үйлесуі нәтижесінде аз көлемді шлам түзе отырып, жоғары жою тиімділігін қамтамасыз етеді. Адсорбция әдісі әсіресе белсендірілген глиноземді, темір оксиді негізіндегі қаптамаларды және функционалдандырылған гибридтер сияқты арнайы материалдарды пайдаланған жағдайда айнымалы селективтілікке, төмен энергия тұтынуға және мембраналық жүйелермен жақсы үйлесімділікке ие. Сонымен қатар, күрделі өнеркәсіптік су матрицаларынан кремнеземді кетіру әдістерін кеңейтудің негізгі техникалық және экономикалық аспектілерін талдаумен қатар, мақалада адсорбентті жобалаудағы соңғы жетістіктер, мысалы, беттік модификация, иерархиялық кеуектілік және регенерация әдістері талқыланады.

Түйін сөздер: кремний диоксиді, өнеркәсіптік, ағынды сулар, тазарту, адсорбция.

Манарбек Қылышқанов	***Авторлар туралы ақпарат:*** *Физ.-мат. ғ. докторы, Перспективті материалдар мен технологиялар, Қазақстан-Британ Техникалық Университеті, Төле би көшесі, 59, 050000, Алматы, Қазақстан. Email: kylyshkanov@mail.ru*
Наталья Герасёва	*Докторант, ЖШС Deep Core Analytics, Аль-Фараби даңғылы, 17/1 к5Б, 050059, Алматы, Қазақстан. Email: tatoline2001@gmail.com*
Рустам Шарипов	*PhD, ассистент-профессор, Перспективті материалдар мен технологиялар, Қазақстан-Британ Техникалық Университеті, Төле би көшесі, 59, 050000, Алматы, Қазақстан. Email: r.sharipov@kbtu.kz*
Ақжүніс Қуаныш	*Магистрант, Ғылым және инновация департаменті, Қазақстан-Британ Техникалық Университеті, Төле би көшесі, 59, 050000, Алматы, Қазақстан. Email: a.kuanysh@kbtu.kz*
Ғалымжан Малдыбаев	*PhD, қауымдастырылған-профессор, Перспективті материалдар мен технологиялар, Қазақстан-Британ Техникалық Университеті, Төле би көшесі, 59, 050000, Алматы, Қазақстан. Email: g.maldybaev@kbtu.kz*
El-Sayed Negim	*PhD, Материалтану және жасыл технологиялар мектебінің профессоры, Қазақстан-Британ Техникалық Университеті, Төле би көшесі, 59, 050000, Алматы, Қазақстан. Email: elashmawi5@yahoo.com*
Өмірсерік Байгенженов	*PhD, Профессор, О.А. Байқоңыров атындағы Тау-Кен Металлургия Институты, Сәтбаев Университеті, Сәтбаев көшесі, 22., 050013, Алматы, Қазақстан. Email:o.baigenzhenov@satbayev*
Ләззат Бекбаева	*PhD, Қауымдастырылған-профессор, Ашық Түрдегі Нанотехнологиялық Зертхана,Әл-Фараби атындағы Қаз¥У 71, әл-Фараби даңғылы, 050040, Алматы, Қазақстан. Email: lyazzat_bk2019@mail.ru*
Khaldun M. Al Azzam	*PhD, Профессор, Иордания университетінің химия кафедрасы, ғылым факультеті, 11942, Амман, Иордания. Email: azzamkha@yahoo.com*
Улпан Балгимбаева	*Докторант, Қолданбалы Математика мектебі, Қазақстан-Британ Техникалық Университеті, Төле би көшесі, 59, 050000, Алматы, Қазақстан. Email: u.balgimbaeva@kbtu.kz*

Инновационные адсорбирующие материалы для эффективного извлечения кремния из промышленных вод: Обзор

[1] Кылышканов М., [2]Герасёва Н., [1] Шарипов Р., [1] Куаныш А., [1] Малдыбаев Г., [1]El-Sayed Negim, [3] Байгенженов О., [4]Бекбаева Л., [5] Khaldun M. Al Azzam, [1] Балгимбаева У.

[1] Казахстанско-Британский технический университет, Алматы, Казахстан
[2]ТОО Deep Core Analytics, Алматы, Казахстан
[3]Горно-металлургический институт им. О. А. Байконурова, Сатпаев университет, Алматы, Казахстан
[4]Казахский национальный университет им. Аль-Фараби, Алматы, Казахстан
[5] Иорданский университет, 11942, Амман, Иордания

Поступила: *27 октября 2025*
Рецензирование: *24 ноября 2025*
Принята в печать: *26 ноября 2025*

АННОТАЦИЯ

Загрязнение кремнеземом снижает эффективность и долговечность мембранных систем очистки, а присутствие кремния в промышленных водных потоках создаёт постоянные эксплуатационные проблемы. В данной статье проводится сравнительный анализ основных технологий удаления кремнезема - ионного обмена, обратного осмоса (ОО), ультрафильтрации (УФ), электрокоагуляции (ЭК), адсорбции и умягчения известью - с акцентом на их механизмы, недостатки и применимость к различным формам кремнезема. Несмотря на необходимость использования значительного количества химических реагентов и контроля pH, известковое умягчение и ионный обмен эффективны для удаления растворённого кремнезема. ОО требует тщательной предварительной подготовки, но обеспечивает широкий диапазон разделения, хотя и подвержен образованию осадков кремнезема. УФ эффективно удаляет коллоидный и частично дисперсный кремнезем, однако не справляется с мономерными формами. ЭК демонстрирует высокие показатели удаления при меньшем объёме осадка благодаря сочетанию электрохимической дестабилизации и кристаллизации. Адсорбция характеризуется переменной селективностью, низким энергопотреблением и совместимостью с мембранными системами, особенно при использовании специально разработанных материалов - активированного оксида алюминия, покрытий на основе оксида железа и функционализированных гибридов. Помимо анализа ключевых технико-экономических аспектов масштабирования методов удаления кремнезема из сложных промышленных водных матриц, в статье также рассматриваются последние достижения в области проектирования адсорбентов, такие как модификация поверхности, иерархическая пористость и методы регенерации.

Ключевые слова: диоксид кремния, промышленные, сточные воды, очистка, адсорбция.

Манарбек Кылышканов	***Информация об авторах:*** *Д.физ.-мат.наук, Перспективные материалы и технологии, Казахстанско-Британский технический университет, ул. Толе би, 59, 050000, Алматы, Казахстан. Email: kylyshkanov@mail.ru*
Наталья Герасёва	*Докторант, ТОО Deep Core Analytics, проспект Аль-Фараби, 17/1 к5Б, 050059, Алматы, Казахстан. Email: tatoline2001@gmail.com*
Рустам Шарипов	*PhD, Ассистент-профессор, руководитель Лаборатории перспективных материалов и технологий, Казахстанско-Британский технический университет, ул. Толе би, 59, 050000, Алматы, Казахстан. Email: r.sharipov@kbtu.kz*
Акжунус Куаныш	*Магистрант, Департамент науки и инноваций, Казахстанско-Британский технический университет, ул. Толе би, 59, 050000, Алматы, Казахстан. Email: a.kuanysh@kbtu.kz*
Галымжан Малдыбаев	*PhD, Ассоциированный-профессор, Перспективные материалы и технологии, Казахстанско-Британский технический университет, ул. Толе би, 59, 050000, Алматы, Казахстан. Email: g.maldybaev@kbtu.kz*
El-Sayed Negim	*PhD, Профессор Школы материаловедения и зеленых технологий, Казахстанско-Британский технический университет, ул. Толе би, 59, 050000, Алматы, Казахстан. Email: elashmawi5@yahoo.com*
Омирсерик Байгенженов	*PhD, Профессор, Горно-металлургический институт им.О.А.Байконурова, Сатбаев Университет, ул. Сатпаева, 22, 050013, Алматы, Казахстан. Email: o.baigenzhenov@satbayev*
Ляззат Бекбаева	*PhD, Ассоциированный-профессор, Лаборатория нанотехнологии открытого типа, КазНУ им. Аль-Фараби 71, проспект Аль-Фараби, 050040, Алматы, Казахстан. Email: lyazzat_bk2019@mail.ru*
Khaldun M. Al Azzam	*PhD, Профессор, Кафедра химии, Факультет естественных наук, Иорданский университет, 11942, Амман, Иордания. Email: azzamkha@yahoo.com*
Улпан Балгимбаева	*Докторант, Школа прикладной математики, Казахстанско-Британский технический университет, ул. Толе би, 59, 050000, Алматы, Казахстан. Email: u.balgimbaeva@kbtu.kz*

References

[1] Teng W, Liu S, Zhang X, Zhang F, Yang X, Xu M, Hou J. Reliability Treatment of Silicon in Oilfield Wastewater by Electrocoagulation. Water. 2023; 15:206. https://doi.org/10.3390/w15010206

[2] Wang XJ, Goual L, Colberg PJS. Characterization and treatment of dissolved organic matter from oilfield produced waters. J. Hazard. Mater. 2012; 217:164–170.

[3] Fu F, Wang Q. Removal of heavy metal ions from wastewaters: A review. J. Environ. Manage. 2011; 92:407-418. https://doi.org/10.1016/j.jenvman.2010.11.011

[4] Hubicki Z, Kolodynska D. Selective Removal of Heavy Metal Ions from Waters and Waste Waters Using Ion Exchange Methods. Ion Exch. Technol. 2012, 193-240. https://doi.org/10.5772/51040

[5] Ghosh P, Samanta AN, Ray S. Reduction of COD and removal of Zn2+ from rayon industry wastewater by combined electro-Fenton treatment and chemical precipitation. Desalination. 2011; 2661(3):213-217. https://doi.org/10.1016/j.desal.2010.08.029

[6] Liu Q, Li Y, Chen H, et al. Superior adsorption capacity of functionalised straw adsorbent for dyes and heavy-metal ions. J. Hazard. Mater. 2020, 382. https://doi.org/10.1016/j.jhazmat.2019.121040

[7] Asere TG, Stevens CV, Du Laing G. Use of (modified) natural adsorbents for arsenic remediation: a review. Sci. Total Environ. 2019; 676:706-720. https://doi.org/10.1016/j.scitotenv.2019.04.237

[8] Xu H, Zhu S, Xia M, et al. Rapid and efficient removal of diclofenac sodium from aqueous solution via ternary core-shell CS@ PANI@ LDH composite: experimental and adsorption mechanism study. J. Hazard. Mater. 2021, 402. https://doi.org/10.1016/j.jhazmat.2020.123815

[9] Xu H, Zhu S, Xia M, et al. Three-dimension hierarchical composite via in-situ growth of Zn/Al layered double hydroxide plates onto polyaniline-wrapped carbon sphere for efficient naproxen removal. J. Hazard. Mater. 2022, 423. https://doi.org/10.1016/j.jhazmat.2021.127192

[10] Xu Y, Zhang Q, Jiang G, et al. Activated Carbon Loaded with Ti^{3+} Self-Doped TiO_2 Composite Material Prepared by Microwave Method. J. of Materi Eng and Perform. 2022; 31:2810–2822. https://doi.org/10.1007/s11665-021-06421-9

[11] Khan ZH, Gao M, Qiu W, et al. Mechanisms for cadmium adsorption by magnetic biochar composites in an aqueous solution. Chemosphere. 2020; 246. https://doi.org/10.1016/j.chemosphere.2019.125701

[12] Khan A, Naeem A, Mahmood T, et al. Mechanistic study on methyl orange and congo red adsorption onto polyvinyl pyrrolidone modified magnesium oxide. Int. J. Environ. Sci. Technol. 2022; 19(4):2515-2528. https://doi.org/10.1007/s13762-021-03308-z

[13] Barakat M A. New trends in removing heavy metals from industrial wastewater. Arabian Journal of Chemistry. 2011; 4(4):361-377

[14] Guillaume Hopsort, Quentin Cacciuttolo, David Pasquier. Electrodialysis as a key operating unit in chemical processes: From lab to pilot scale of latest breakthroughs. Chemical Engineering Journal. 2024; 494:153111.

[15] Gmar S, Chagnes A, Lutin F, Muhr L. Application of Electrodialysis for the Selective Lithium Extraction Towards Cobalt, Nickel and Manganese from Leach Solutions Containing High Divalent Cations/li Ratio, Recycling. 2022; 7:14. https://doi.org/10.3390/recycling7020014

[16] Zimmermann P, Tekinalp O, Deng L, Wilhelmsen Ø, Burheim OS. Electrodialysis for Removal of Impurities in Silver Electrowinning, Meet. Abstr. MA2023-01. 2023, 1608. https://doi.org/10.1149/ma2023-01241608mtgabs

[17] Kumar Y, Khalangre A, Suhag R, Cassano A. Applications of Reverse Osmosis and Nanofiltration Membrane Process in Wine and Beer Industry. Membranes. 2025; 15:140. https://doi.org/10.3390/membranes15050140

[18] Charcosset C. Ultrafiltration, Microfiltration, Nanofiltration and Reverse Osmosis in Integrated Membrane Processes. In Integrated Membrane Systems and Processes. Basile A, Charcosset C, Eds, Wiley: Hoboken, NJ, USA. 2016, 1-22. ISBN 978-1-118-73908-2.

[19] Pati S, La Notte D, Clodoveo ML, Cicco G, Esti M. Reverse Osmosis and Nanofiltration Membranes for the Improvement of Must Quality. Eur. Food Res. Technol. 2014; 239:595–602.

[20] Poonguzhali E, Fathima Aadilah Mohamed Ali, Ashish Kapoor, Prabhakar S. Performance of membrane assisted solvent extraction with homologous solvents for the removal and recovery of phenol, Desalination and Water Treatment. 2022; 251:64-78. https://doi.org/10.5004/dwt.2022.28117

[21] Poonguzhali E, Ashish Kapoor, Prabhakar S. Membrane assisted process intensification and optimization for removal and recovery of phenol from industrial effluents, Separation and Purification Technology. 2023; 319:124026. https://doi.org/10.1016/j.seppur.2023.124026

[22] Sanika Bhokarikar, Poojitha P, Vijay Vaishampayan, Adithya Sridhar, Gurumoorthi P, Ashish Kapoor. Chapter Thirteen - Parameters affecting the efficiency of extraction systems in the food industries, Editor(s): Seid Mahdi Jafari, Sahar Akhavan-Mahdavi, In Unit Operation and Processing Equipment in the Food Industry. Extraction Processes in the Food Industry, Woodhead Publishing. 2024, 397-434. https://doi.org/10.1016/B978-0-12-819516-1.00010-7

[23] Ming Li, Chuanying Liu, Anting Ding, Chengliang Xiao. A review on the extraction and recovery of critical metals using molten salt electrolysis. Journal of Environmental Chemical Engineering. 2023; 11(3):109746.

[24] https://doi.org/10.1016/j.jece.2023.109746

[25] Yin T, Chen L, Xue Y, Zheng Y, Wang X, Yan Y, Zhang M, Wang G, Gao F, Qiu M. Electrochemical behavior and underpotential deposition of Sm on reactive electrodes (Al, Ni, Cu and Zn) in a LiCl-KCl melt. Int J. Min. Met. Mater. 2020; 27(12):1657–1665.

[26] Yin T, Xue Y, Yan Y, Ma Z, Ma F, Zhang M, Wang G, Qiu M. Recovery and separation of rare earth elements by molten salt electrolysis, Int J. Min. Met. Mater. 2021; 28(6):899–914.

[27] Roalson S R, Kweon J, Lawler D F, & Speitel G E, Jr. Enhanced Softening: Effects of Lime Dose and Chemical Additions. Journal AWWA. 2003; 95(11):97-109. https://doi.org/10.1002/j.1551-8833.2003.tb10496.x

[28] Kailun Z, David P, Maryam J, Qingye L. Effect of MgO Slaking on Silica Removal during Warm Lime Softening of SAGD Produced Water. Industrial & Engineering Chemistry Research. 2021; 60(4):1839-1849. https://doi.org/10.1021/acs.iecr.0c05484

[29] Hermosilla D, Ordóñez R, Blanco L, de la Fuente E, and Blanco A. pH and Particle Structure Effects on Silica Removal by Coagulation. Chemical Engineering Tecnology. 2012; 35(9):1632–1640.

[30] Alsayer IA. A Comparative Study of the Effect of Sodium Aluminate, Magnesium Oxide, and Calcium Hydroxide on the Concentration of Silicon Dioxide in RO Water Plants. Journal of Chemical Engineering of Japan. 2025; 58(1). https://doi.org/10.1080/00219592.2025.2544885

[31] Lunevich L. Aqueous Silica and Silica Polymerisation. IntechOpen. 2020. https://doi.org/10.5772/intechopen.84824

[32] Bifa Shimelis, Abel Saka, Leta Tesfaye Jule, Bulcha Bekele, Mesfin Redi, Nagaprasad N, Esakkiraj ES, Stalin B, Krishnaraj Ramaswamy. Preparation of hydrated lime quality for water treatment: to reduce silica concentration from hydrated lime up to standard specification, Desalination and Water Treatment. 2022; 251:35-42. https://doi.org/10.5004/dwt.2022.28089

[33] Fathi Djouider, Essam Banoqitah, Abdulsalam Alhawsawi, Laboratory study of the silica removal in water by electro-Fenton method: Effect of operational parameters, Desalination and Water Treatment. 2024; 317:100118. https://doi.org/10.1016/j.dwt.2024.100118

[34] Salvador Cob S, Hofs B, Maffezzoni C, Adamus J, Siegers WG, Cornelissen ER, Genceli Güner FE, Witkamp GJ. Silica removal to prevent silica scaling in reverse osmosis membranes, Desalination. 2014; 344:137-143. https://doi.org/10.1016/j.desal.2014.03.020

[35] Park Y-M, Yeon K-N, Park C-H. Silica treatment technologies in reverse osmosis for industrial desalination: A review. Environmental Engineering Research. 2020; 25(6):819-829. https://doi.org/10.4491/eer.2019.353

[36] Shuqin B, Jue H, Niqi A, Ru Y, Wei D. Scaling and cleaning of silica scales on reverse osmosis membrane: Effective removal and degradation mechanisms utilizing gallic acid, Chemosphere. 2024% 352:141427. https://doi.org/10.1016/j.chemosphere.2024.141427

[37] Wenbin J, Xuesong X, David J, Lu L, Huiyao W, Pei X. Effectiveness and mechanisms of electromagnetic field on reverse osmosis membrane scaling control during brackish groundwater desalination, Separation and Purification Technology. 2022; 280:119823. https://doi.org/10.1016/j.seppur.2021.119823

[38] Firdaous L, Dhulster P, Amiot J, Doyen A, Lutin F, Ve´zina L-P, Bazinet L. Investigation of the large-scale bioseparation of an antihypertensive peptide rom alfalfa white protein hydrolysate by an electromembrane process, J. Membr. Sci. 2010; 355:175–181.

[39] Springer F, Laborie S, Guigui C. Removal of SiO2 nanoparticles from industry wastewaters and subsurface waters by ultrafiltration: Investigation of process efficiency, deposit properties and fouling mechanism, Separation and Purification Technology. 2013; 108:6-14. https://doi.org/10.1016/j.seppur.2013.01.043

[40] Cyril Roblet, Alain Doyen, Jean Amiot, Laurent Bazinet. Impact of pH on ultrafiltration membrane selectivity during electrodialysis with ultrafiltration membrane (EDUF) purification of soy peptides from a complex matrix. Journal of Membrane Science. 2013; 435:207-217. https://doi.org/10.1016/j.memsci.2013.01.045

[41] Sun Y, Zhang R, Sun C, Liu Z, Zhang J, Liang S, Wang X. Quantitative Assessment of Interfacial Interactions Governing Ultrafiltration Membrane Fouling by the Mixture of Silica Nanoparticles (SiO_2 NPs) and Natural Organic Matter (NOM): Effects of Solution Chemistry. Membranes. 2023; 13:449. https://doi.org/10.3390/membranes13040449

[42] Yangbo Q, Stef D, Long-Fei R, Changmei Z, Chao W, Jiahui S, Lei X, Yan Z, Bart VdB. Progress of Ultrafiltration-Based Technology in Ion Removal and Recovery: Enhanced Membranes and Integrated Processes. ACS EST Water. 2023; 3(7):1702–1719. https://pubs.acs.org/doi/10.1021/acsestwater.2c00625

[43] Samin H, Ali N. Enhanced water flux through ultrafiltration polysulfone membrane via addition-removal of silica nano-particles: Synthesis and characterization J. Appl. Polym. Sci. 2016; 133:43556. https://doi.org/10.1002/app.43556

[44] Shemer H, Melki-Dabush N, & Semiat R. Removal of silica from brackish water by integrated adsorption/ultrafiltration process. Environ Sci Pollut Res. 2019; 26:31623–31631. https://doi.org/10.1007/s11356-019-06363-9

[45] Mroczek EK, Graham D, Bacon L. Removal of arsenic and silica from geothermal fluid by electrocoagulation, Journal of Environmental Chemical Engineering. 2019; 7(4):103232. https://doi.org/10.1016/j.jece.2019.103232

[46] Teng W, Liu S, Zhang X, Zhang F, Yang X, Xu M, & Hou J. Reliability Treatment of Silicon in Oilfield Wastewater by Electrocoagulation. Water. 2023; 15(1):206. https://doi.org/10.3390/w15010206

[47] Pranjal P Das, Mukesh Sharma, Mihir K Purkait. Recent progress on electrocoagulation process for wastewater treatment: A review, Separation and Purification Technology. 2022; 292:121058. https://doi.org/10.1016/j.seppur.2022.121058

[48] Héline C, Anh L-TP. Effective removal of silica and sulfide from oil sands thermal in-situ produced water by electrocoagulation. Journal of Hazardous Materials. 2019; 380:120880. https://doi.org/10.1016/j.jhazmat.2019.120880

[49] Mudasar M, Nael Y, Behzad F-H, Edward PLR. Influence of operating conditions on the removal of silica and hardness by continuous electrocoagulation. Journal of Environmental Chemical Engineering. 2022; 10(6):108899. https://doi.org/10.1016/j.jece.2022.108899

[50] Minghui L, Shuang M, Xi W, Mingmei W, Yutong Z, Zhanpeng Y, Erqiang W, Hui Z Tianyan X. Effective removal of dissolved silica from white carbon black wastewater by iron electrode electrocoagulation: Process optimization and simulation. Journal of Water Process Engineering. 2022; 47:102812. https://doi.org/10.1016/j.jwpe.2022.102812

[51] Xin Z, Mengjia L, Mohd AMI, Cameron Crombie, Veeriah Jegatheesan. Performance of precipitation and electrocoagulation as pretreatment of silica removal in brackish water and seawater,Process Safety and Environmental Protection. 2019; 126:18-24. https://doi.org/10.1016/j.psep.2019.03.024

[52] Isabel L, Ruben M, Rosa C, Angeles B. Efficiency of polyaluminum nitrate sulfate–polyamine hybrid coagulants for silica removal. Desalination and Water Treatment. 2016; 57(38):17973-17984. https://doi.org/10.1080/19443994.2015.1091992

[53] Iván EV-M, Alejandra M-D, Sara P-C, Silvia LG-S. Electrocoagulation to Remove Silica from Cooling Towers Water. Tecnologia Y Ciencias Del Agua. 2014; 5(3):41-51.

[54] Miranda R, Latour I, & Blanco A. Silica Removal from a Paper Mill Effluent by Adsorption on Pseudoboehmite and γ-Al_2O_3. Water. 2021; 13(15):2031. https://doi.org/10.3390/w13152031

[55] Salvador Cob S, Yeme C, Hofs B, Cornelissen ER, Vries D, Gencelli Güner FE, Witkamp GJ. Towards zero liquid discharge in the presence of silica: Stable 98% recovery in nanofiltration and reverse osmosis. Sep. Purif. Technol. 2015; 140:23–31.

[56] Sasan K, Brady PV, Krumhansl JL, Nenoff TM. Exceptional selectivity for dissolved silicas in industrial waters using mixed oxides. J. Water Process. Eng. 2017; 20:187–192.

[57] Minehiko S, Ngan PTT, Takaomi K. Mesoporous γ-AlOOH as an adsorbent for silica removal from aqueous solutions. Desalination and Water Treatment. 2024; 317:100084. https://doi.org/10.1016/j.dwt.2024.100084

[58] Andrea AA-H, Virginia H-M, Rigoberto T-G, María AP-C, Miguel A M-M, Norma A Rangel-Vázquez, Francisco J. Cervantes, Water reclamation from anodizing wastewaters by removing reactive silica with adsorption and precipitation methods. Journal of Environmental Management. 2023; 326(A):116683. https://doi.org/10.1016/j.jenvman.2022.116683

[59] Gulcihan GK, Elena A, Huseyin D, Ramón M-M. Low-cost silica xerogels as potential adsorbents for ciprofloxacin removal. Sustainable Chemistry and Pharmacy. 2021; 22:100483. https://doi.org/10.1016/j.scp.2021.100483

[60] Shakeel Z, Nisar A, Zarshad A, Muhammad B, Bushra A, Sajjad H, Saima G, Farman A, Rashid A, Sabir K, Hafiz MNI. Silica-based nanomaterials as designer adsorbents to mitigate emerging organic contaminants from water matrices. Journal of Water Process Engineering. 2020; 38:101675. https://doi.org/10.1016/j.jwpe.2020.101675

[61] Ismail A, Ali SA, Saheed G, Nadeem B, Billel S, Sohaib A. Facile engineering of mesoporous silica for the effective removal of anionic dyes from wastewater: Insights from DFT and experimental studies. Heliyon. 2023; 9(11):e21356. https://doi.org/10.1016/j.heliyon.2023.e21356

[62] Maldybayev G, Shayakhmetova R, Nurzhanova S, Sharipov R, Negim E-S, Alimzhanova A, Osipov P, Mukhametzhanova A, Usman A. Synthesis of Chemical Adsorbents for Purification of Heavy Oil Residues. International Journal of Technology. 2024; 15(3):792-802.

[63] Shuxuan C, Shuqin B, Ru Y, Cong D, Wei D. Continuous silicic acid removal in a fixed-bed column using a modified resin: Experiment investigation and artificial neural network modeling. Journal of Water Process Engineering. 2022; 49:102937. https://doi.org/10.1016/j.jwpe.2022.102937

[64] Toni SH, Tonni AK, Mika ETS. Removal of silicon from pulping whitewater using integrated treatment of chemical precipitation and evaporation. Chemical Engineering Journal. 2010; 158(3):584-592. https://doi.org/10.1016/j.cej.2010.01.058

[65] Betz LD, Noll CA, Maguire JJ. Adsorption Process for Removal of Soluble Silica From Water. Journal of Fluids Engineering. 63(8):713-720. https://doi.org/10.1115/1.4019615

[66] Guan YF, Marcos-Hernández M, Lu X, Cheng W, Yu HQ, Elimelech M, Villagrán D. Silica Removal Using Magnetic Iron-Aluminum Hybrid Nanomaterials: Measurements, Adsorption Mechanisms, and Implications for Silica Scaling in Reverse Osmosis. Environ Sci Technol. 2019; 53(22):13302-13311. https://doi.org/10.1021/acs.est.9b02883

[67] Baca Ehren D. Comprehensive Silica Removal with Ferric Compounds for Industrial Wastewater Reuse. Master thesis. 2017. https://digitalrepository.unm.edu/ce_etds/176

Crossref

DOI: 10.31643/2027/6445.23
Mining & Mineral Processing

Investigation of the effect of a modified additive on the strength characteristics of foam concrete

[1*]Askerbekova A.M., [1]Dyussembinov D.S., [1]Shashpan Zh.A., [2]Abduova A.A., [2]Kambarov M.A.

[1] L.N. Gumilyov Eurasian National University, Astana, Kazakhstan
[2] M. Auezov South Kazakhstan Research University, Shymkent, Kazakhstan

** Corresponding author email: arai_09.91@mail.ru*

Received: *August 1, 2025*
Peer-reviewed: *October 11, 2025*
Accepted: *December 1, 2025*

ABSTRACT

The article presents the second stage of the investigate the effect of the modified additive on the strength characteristics of foam concrete. This work describes a method for manufacturing foam concrete samples, selects a modifying additive composition with different percentages of components, and analyzes their strength characteristics. The purpose of introducing plasticizing additives (post-alcohol bard) in foam concrete D600 to reduce water consumption and the expected increase in strength. To evaluate the changes in strength, samples were made and tested in compression at the age of 3, 7, 14, and 28 days of normal moisture curing. According to research results, the use of such additives can significantly reduce formwork removal times, increase the load-bearing capacity of structures, and expand the scope of application of foam concrete—even to structural and thermal insulation products. Additives improve not only strength but also structural uniformity, reducing the number of macropores and increasing the density of the material.

Keywords: cement paste, post-alcohol bard, modified additive, compressive strength, plasticizer, foaming agent.

Information about authors:

Askerbekova Arailym Myrzakhankyzy — *PhD. student, Department of Technology of Industrial and Civil Construction, L.N. Gumilyov Eurasian National University, Astana, Kazakhstan. Email: aria_09.91@mail.ru; ORCID ID: https://orcid.org/0000-0002-4356-053X*

Dyussembinov Duman Serikovich — *C.t.s., Assistant Professor of the Department of Technology of Industrial and Civil Construction, L.N. Gumilyov Eurasian National University, Astana, Kazakhstan. Email: dusembinov@mail.ru; ORCID ID: https://orcid.org/0000-0001-6118-5238*

Shashpan Zholaman Amangeldievich — *D.t.s., Assistant Professor of the Department of Technology of Industrial and Civil Construction, L.N. Gumilyov Eurasian National University, Astana, Kazakhstan. Email: zholamanalmatykz@gmail.com; ORCID ID: https://orcid.org/0000-0002-6236-0525*

Abduova Aisulu Alshynbekovna — *C.t.s., Assistant Professor of the* Department of Ecology, *M. Auezov South Kazakhstan Research University, Shymkent, Kazakhstan. Email: aisulu.abduova@mail.ru; ORCID ID: https://orcid.org/0000-0001-5389-6953*

Kambarov Medet Abdildaevich — *C.t.s., Assistant Professor of the Department of Building materials and expertise in construction, M. Auezov South Kazakhstan Research University, Shymkent, Kazakhstan. Email:* medet_2030*@mail.ru; ORCID ID: https://orcid.org/0000-0001-6397-1451*

Introduction

In Kazakhstan, the concentration of the workforce in large cities has led to the widespread construction of apartment buildings and high-rise buildings, as well as the dynamic development of the construction industry. In addition, based on the “Nurly Zher” housing and utilities development program for 2020-2025 and the “7-20-25” program, extended until 2029, it is necessary to use building materials with low raw material consumption to provide the population with quality housing in the shortest possible time [[1] [,2]].

Among such building materials is foam concrete — a lightweight, porous material with excellent thermal and sound insulation properties, distinguished by its economic efficiency and environmental safety, which makes it highly demanded in modern construction [3].

Currently, various methods of improving the efficiency of foam concrete are of particular interest. Research into the strength characteristics of foam concrete, research into the resistance of foam concrete to chemical and physical aggressive factors, and research into the use of various binders in the production of foam concrete are of great

importance. In addition, the use of foam concrete significantly reduces the cost and duration of construction, which is important in modern conditions for solving housing problems [[4], [5], [6], [7]].

Also, due to the thermal insulation properties of foam concrete, it saves energy and is an effective material that can be used in construction in regions with a harsh continental climate. This material can be obtained from a mixture of cement, sand, and foam [[8], [9], [10], [11]].

Since it is an inexpensive building material that saves energy spent on heating buildings and consumes less raw materials, its improvement with the addition of modern additives allows for the production of foam concrete with a specified structure.

In modern concrete technology, various organic and inorganic additives are widely used, which significantly affect the physical and chemical processes of cement hardening and modify the structure of concrete, ensuring its strength and durability. An analysis of technical literature shows that among the additives used, plasticizing additives—thinners that significantly reduce the water demand of concrete mixtures without reducing their mobility—are of great importance. Surface-active substances, either specially synthesized or by-products of various industries, many of which are environmentally unsafe, are widely used as plasticizers for cement mixtures [[12], [13], [14]].

The main objective of our research work is to develop a technology for producing non-autoclaved thermal insulation foam concrete from industrial waste. In this article, we must investigate the effect of the modified additive on the strength characteristics of foam concrete.

In this research work to accomplish the objective, the following tasks were carried out:

1. The optimal formulation of the additive was selected based on varying percentages of its components.

2. Samples with different additive compositions were prepared under laboratory conditions.

3. The physical and mechanical properties of the experimental samples were investigated in the laboratory.

Materials and methods of research

In order to successfully achieve the set goals and objectives of this study, as well as to ensure the reliability and accuracy of the experimental results, construction materials that fully comply with current technical standards and regulatory requirements were selected and applied.

Cement – As the primary binding material, Portland cement of grade M400 was used. This type of cement is widely recognized for its high strength characteristics and consistent performance in construction applications. Its use ensured the structural integrity and uniformity of the test samples throughout the experiment.

Modified additive – The key component of the modified mixture was post-alcohol bard, a liquid by-product derived from ethyl alcohol production. This organic waste product was introduced into the cement mixture in varying dosages of 2.5%, 5.0%, 7.5%, and 10%, with 2.5% intervals, in order to assess its effect on the properties of the resulting material. The bard was supplied in liquid form by the Idabul Distillery (JSC "Idabul Distillery"), ensuring consistent quality and composition for laboratory use.

Post-alcohol bard is used as a plasticizing additive and is supplied in liquid form from JSC Aydabul Distillery. In Kazakhstan, the largest producers of ethyl alcohol are several companies, including Talgar-alcohol (Talgar), Adil JSC (Ust-Kamenogorsk), Altyn Omir (Kostanay region), etc. Ethyl alcohol is sold on the Kazakh market mainly through domestic trade. Currently, most bardu distilleries are processed in one way or another, mainly for feed. At the same time, 10-15 liters of bard per 1 liter of alcohol, depending on the technology [[15], [16]].

3. As a hardening accelerator, gypsum was introduced into the cement mixture to intensify the setting and early strength development processes. This additive was applied in varying dosages — specifically 1.0%, 1.5%, 2.0%, and 2.5% of the total mass of cement — with increments of 0.5%. The use of gypsum in these proportions made it possible to evaluate its influence on the rate of hardening and overall physical-mechanical characteristics of the resulting material.

The incorporation of gypsum as a hardening accelerator in foam concrete enhances the cement hydration process, resulting in improved structural uniformity, increased early strength, and reduced setting time [[17], [18]].

The synthetic foaming agent ‘Neoplast, art. 55’ meets the requirements of TU 2381-008-90275031-2011. It is used to produce thermal insulation (ρ_{avg}=400-500 kg/m^3) and thermal insulation-structural (ρ_{avg}=600-900 kg/m^3) foam concretes based on cement binder using the ‘dry mineralisation’ method of foam production. The foaming agent is a pore former that provides a cellular structure for concrete, as well as helping to reduce its density, improve its thermal and sound insulation properties, and facilitate the laying and moulding of mixtures [19].

a) b) c)

Polyfractional sand | Post-alcohol bard | The synthetic foaming agent

Figure 1 – Raw materials for foam concrete

a) b) c)

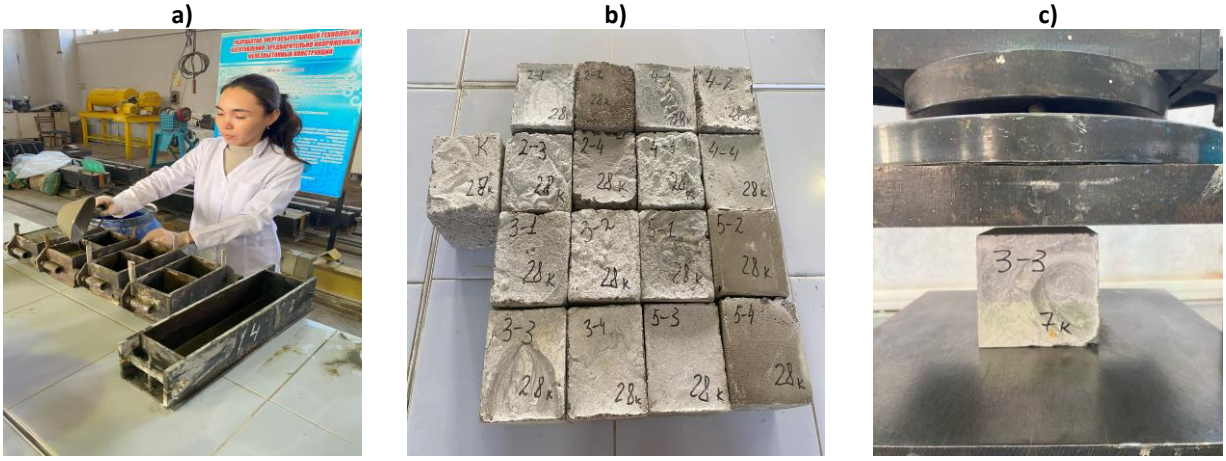

Figure 2 – Samples of the foam concrete D600: The process of foam concrete sample preparation (a), Prepared foam concrete samples (b), Compression test of samples (c)

Figure 1 illustrates several construction materials used in the experiment, while Figure 2 shows the process of sample preparation and testing.

The foam formed by adding a foaming agent is a key factor in foam concrete production technology. Its multiplicity determines the structure of the material, having a significant impact on its porosity, density, and strength characteristics.

The optimal ratio of the modifier additive to cement was evaluated in stages as part of the study. At the initial stage of the research, attention was focused on examining how the composition of the modifying additive influences the setting time of the cement paste. This allowed for the identification of optimal component ratios that contribute to more efficient hardening processes [18]. In the subsequent stage, a series of experiments was conducted to determine the compressive strength of foam concrete samples. These tests were performed in relation to varying concentrations of the modified additive introduced into the mixture, enabling an assessment of its impact on the mechanical performance of the final product.

For each type of sample, cubes measuring 10x10x10 cm were made. The compressive limits were determined in accordance with GOST 10180-2012 "Concrete. Methods for determining strength using control samples" at 3, 7, 14, and 28 days using press equipment. The subject of this study was a foam concrete, prepared using M400-grade cement and the synthetic foaming agent Neoplast. The mixtures were produced both without any additives and with the inclusion of post-alcohol bard, utilizing

Table 1 – Composition of compared samples of the foam concrete D600

Number	Type of sample	Cement, g	Sand, g	Gypsum, g	Post-alcohol bard, g	Foaming agent, g	Water, g
1	Type 1 Reference sample	400	200	-	-	1.25	230
2	Type 2-1	397	200	3	7.5	1.25	222.5
3	Type 2-2	397	200	3	15	1.25	215
4	Type 2-3	397	200	3	22.5	1.25	207.5
5	Type 2-4	397	200	3	30	1.25	200
6	Type 3-1	395.5	200	4.5	7.5	1.25	222.5
7	Type 3-2	395.5	200	4.5	15	1.25	215
8	Type 3-3	395.5	200	4.5	22.5	1.25	207.5
9	Type 3-4	395.5	200	4.5	30	1.25	200
10	Type 4-1	394	200	6	7.5	1.25	222.5
11	Type 4-2	394	200	6	15	1.25	215
12	Type 4-3	394	200	6	22.5	1.25	207.5
13	Type 4-4	394	200	6	30	1.25	200
14	Type 5-1	392.5	200	7.5	7.5	1.25	222.5
15	Type 5-2	392.5	200	7.5	15	1.25	215
16	Type 5-3	392.5	200	7.5	22.5	1.25	207.5
17	Type 5-4	392.5	200	7.5	30	1.25	200

polyfractional sand. The sand was pre-measured and packaged in 200-gram portions to ensure consistency across all test samples.

The study focused on evaluating the impact of a modified additive, introduced in varying percentages, on the strength properties of foam concrete. To achieve this, the preparation of the foam concrete mixture was carried out in two distinct stages. In the first stage, all mineral components—such as cement and sand—were thoroughly mixed to form a homogeneous dry mixture. In the second stage, foam was saturated with air and turned into a persistent fine bubbly foamin in the foam generator and then carefully integrated into the mineral mixture. This stepwise approach ensured uniform distribution of the foam throughout the mass, contributing to the consistency and reliability of the resulting material's properties.

The compressive strength of foam concrete was assessed using six different mixture compositions, comprising a total of 17 test samples. Each composition included a combination of mineral components, modified additives, foam, and water. Among these, the reference mixture—designated as Type-1—contained only cement, gypsum, foam, and water, without any additive. This control mixture served as the baseline for comparing the performance of all other modified formulations.

For each composition, the optimal water-to-binder ratio was individually determined to ensure consistency and reliability in test results. To evaluate the efficiency and compatibility of the modified additive with Portland cement, a series of mixture compositions was developed. The detailed characteristics and component ratios of these formulations are presented in Table 1.

Results and Discussion

In our research, the selection of additives was guided by their primary mechanisms of action and their potential to enhance the performance of the cementitious material. The modified additive used in this study is a combination of gypsum and post-alcohol bard — a by-product of ethyl alcohol production that also serves as a plasticizer. The experimental results demonstrated that the simultaneous application of gypsum and post-alcohol bard has a synergistic effect, significantly improving the physical and mechanical properties of the cement mixture. This combined use enhances the setting behavior, workability, and overall strength development of the material, making it a promising solution for foam concrete production.

Experimental results revealed that foam concrete samples containing the modified additive (post-alcohol bard) maintained their integrity and did not degrade when exposed to water. This

observation confirms the effectiveness of the additive as a water-resistant modifier. A key component of post-alcohol bard is casein—a natural protein — which undergoes polymerization upon interaction with the fine aggregates in the concrete mix. This reaction leads to the formation of additional contact films within the structure, which enhance the cohesion between particles and significantly improve the material's overall water resistance.

Studies have shown that the strength of foam concrete with additives at 3 days of age and beyond is higher than that of foam cement mixture without additives (Type 1). In samples with additives, the intensive hardening period lasts up to 28 days, thereby achieving greater strength.

The degradation or failure of foam concrete is closely related to the degree of structural integrity and the quality of the bonds between its cellular elements. The more uniform and well-formed these internal connections are, the greater the material's resistance to external stresses and long-term durability [20].

It is well established that the strength of foam concrete is a complex, integrated property influenced by a variety of interrelated factors. These include the quality and characteristics of the raw components, the precise formulation of the mixture, the consistency and workability (fluidity) of the foam concrete, the molding techniques employed during sample preparation, and the specific conditions under which the hardening and curing processes take place. Each of these factors plays a critical role in determining the final mechanical performance of the material.

Figure 3 shows the compressive strength of D600 foam concrete. It compares the control sample (without additives) with samples containing a modified additive. Tests were done on days 3, 7, 14, and 28 to see how strength developed and how the additive affected the results.

Figure 3 presents a graph illustrating the variation in compressive strength of the samples over the curing period.

The Type 1 reference samples (without additives) exhibited the lowest compressive strength values at all curing stages (3, 7, 14, and 28 days), with average strength ranging from 0.61 to 2.20 MPa.

Type 2-1 samples demonstrated slightly higher strength than the Type 1 reference samples by 1.6% in 3 days, 3.2% in 7 days, 7.5% at 14 days, and 2.3% at 28 days. However, their strength remained lower than that of the Type 2-2 samples by 11.4%, 3%, 1.71%, and 6.25% in the corresponding curing periods. The average compressive strength of Type 2-1 samples ranged from 0.62 to 2.25 MPa.

Samples of Type 2-2 demonstrated compressive strength values exceeding those of the Type 1 reference samples by 14.7% on day 3, 6.4% on day 7, 9.3% on day 14, and 9.1% on day 28. However, their strength was lower than that of Type 2-3 samples by 7.1% (day 3), 2.9% (day 7), 1.13% (day 14), and 2.8% (day 28). The average compressive strength of Type 2-2 samples ranged from 0.7 MPa to 2.4 MPa over the 28-day curing period.

Samples of Type 2-3 showed even greater strength improvements compared to the reference (Type 1) samples, with increases of 22.9% (day 3), 9.6% (day 7), 10.6% (day 14), and 12.2% (day 28). However, their strength remained lower than that of Type 2-4 samples by 5.1% (day 3), 6.8% (day 7), 4.3% (day 14), and 3.9% (day 28). The average strength values for Type 2-3 samples ranged between 0.75 MPa and 2.47 MPa throughout the hardening period.

Samples of Type 2-4 exhibited compressive strength values significantly higher than those of the Type 1 reference samples, with increases of 26.5% at 3 days, 17.6% at 7 days, 15.6% at 14 days, and 16.8% at 28 days. However, compared to Type 3-1 samples, their strength values were 2.5% (3 days), 7.5% (7 days), 7.03% (14 days), and 3.4% (28 days) lower. The average compressive strength of Type 2-4 samples ranged from 0.79 MPa to 2.57 MPa during the 28-day curing period.

Samples of Type 3-1 showed even more pronounced strength gains over the Type 1 reference mix, exceeding it by 32.7% on day 3, 27.2% on day 7, 24.3% on day 14, and 20.9% on day 28. However, when compared to the Type 3-2 samples, their strength values were slightly lower by 4.7% (3 days), 0.6% (7 days), 5.2% (14 days), and 7.6% (28 days). The average strength for Type 3-1 samples ranged from 0.81 MPa to 2.66 MPa throughout the testing period.

Samples of Type 3-2 demonstrated noticeably higher compressive strength values compared to the Type 1 reference samples, with increases of 39.3% at 3 days, 28.0% at 7 days, 31.25% at 14 days, and 30.9% at 28 days. However, when compared to Type 3-3 samples, their strength values were lower by 6.6% (3 days), 5.3% (7 days), 5.8% (14 days), and 2.7% (28 days). The average compressive strength of Type 3-2 samples ranged from 0.85 MPa to 2.88 MPa over the curing period.

a)

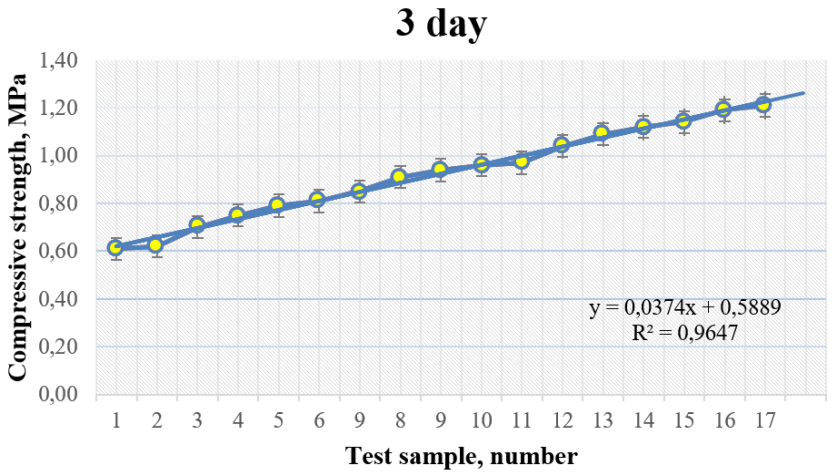

b)

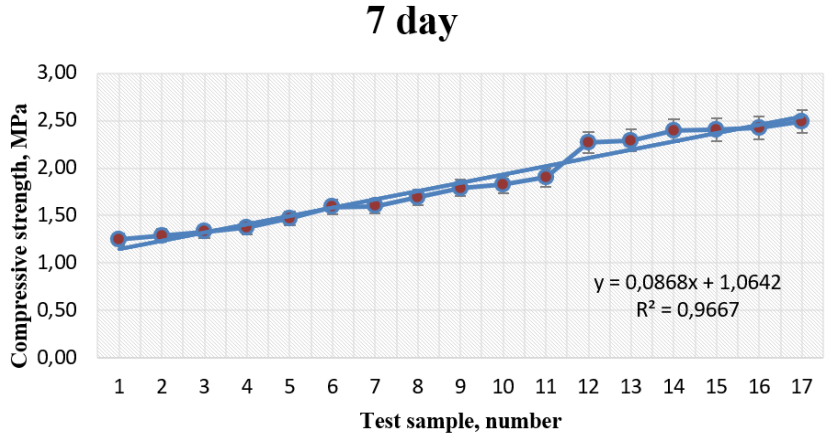

c)

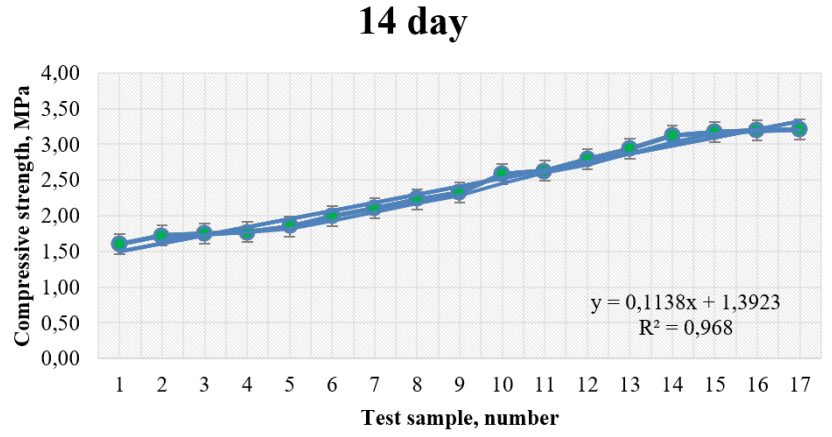

d)

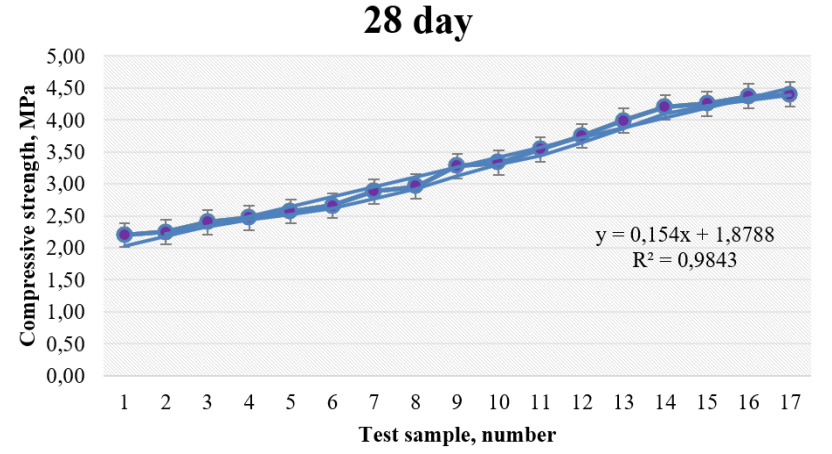

Figure 3 - Plots of growth of compressive strength of the tested samples: 3 day (a) 7 day (b), 14 day (c), 28 day (d)

Samples of Type 3-3 showed even greater improvements in strength relative to the reference Type 1 mix, with increases of 49.2% (3 days), 35.2% (7 days), 39.3% (14 days), and 34.5% (28 days). Nevertheless, they showed slightly lower values compared to Type 3-4 samples—by 3.2% (3 days), 5.6% (7 days), 3.9% (14 days), and 9.7% (28 days). The average compressive strength for Type 3-3 samples ranged from 0.91 MPa to 2.96 MPa.

Samples of Type 3-4 exhibited a significant increase in compressive strength over the Type 1 reference samples: 54.1% at 3 days, 43.2% at 7 days, 45.0% at 14 days, and 49.1% at 28 days. However, these results were still slightly below those of the Type 4-1 samples—by 2.1% (3 days), 2.2% (7 days), 10.0% (14 days), and 2.4% (28 days). The average compressive strength of Type 3-4 samples ranged from 0.94 MPa to 3.28 MPa.

Samples of Type 4-1 demonstrated significant increases in compressive strength compared to the Type 1 reference samples—57.4% at 3 days, 46.4% at 7 days, 61.25% at 14 days, and 51.3% at 28 days. Despite this, their strength values were slightly lower than those of Type 4-2 samples, with differences of 1.03% (3 days), 3.7% (7 days), 1.9% (14 days), and 5.9% (28 days). The average strength values for Type 4-1 ranged from 0.96 MPa to 3.33 MPa.

Samples of Type 4-2 exhibited even greater improvements over the Type 1 reference mix, with compressive strength increases of 59.0% (3 days), 52.0% (7 days), 64.3% (14 days), and 61.0% (28 days). However, when compared to Type 4-3 samples, their strength values were lower by 6.7% (3 days), 16.3% (7 days), 5.7% (14 days), and 32.3% (28 days). The average strength for Type 4-2 samples ranged from 0.97 MPa to 3.54 MPa.

Samples of Type 4-3 showed particularly high compressive strength, outperforming the Type 1 reference samples by 70.5% at 3 days, 81.6% at 7 days, 74.3% at 14 days, and 70.4% at 28 days. Nonetheless, their strength remained slightly below that of Type 4-4 samples—by 4.6% (3 days), 0.87% (7 days), 5.1% (14 days), and 6.0% (28 days). The average strength values for Type 4-3 ranged from 1.04 MPa to 3.75 MPa.

Samples of Type 4-4 demonstrated considerable improvements in compressive strength compared to the Type 1 reference samples, with increases of 78.6% at 3 days, 83.2% at 7 days, 83.7% at 14 days, and 81.1% at 28 days. However, their strength values were slightly lower than those of Type 5-1 samples—by 2.7% (3 days), 4.2% (7 days), 5.8% (14 days), and 5.0% (28 days). The average compressive strength for Type 4-4 samples ranged from 1.09 MPa to 3.99 MPa.

Samples of Type 5-1 outperformed the Type 1 reference mix with compressive strength increases of 83.6% (3 days), 91.2% (7 days), 95.0% (14 days), and 90.0% (28 days). When compared to Type 5-2, however, they showed slightly lower strength values—by 1.7% (3 days), 0.4% (7 days), 1.6% (14 days), and 1.2% (28 days). The average strength ranged from 1.12 MPa to 4.20 MPa.

Samples of Type 5-2 showed further increases in compressive strength relative to Type 1, with gains of 86.8% (3 days), 92.0% (7 days), 98.1% (14 days), and 93.2% (28 days). Nevertheless, they were slightly outperformed by Type 5-3 samples—by 4.2% (3 days), 0.8% (7 days), 0.6% (14 days), and 2.7% (28 days). The average strength values for Type 5-2 ranged from 1.14 MPa to 4.25 MPa.

Samples of Type 5-3 displayed a nearly twofold increase in compressive strength compared to the reference Type 1 samples, with increases of 95.1% (3 days), 93.6% (7 days), 99.3% (14 days), and 98.6% (28 days). However, their values were slightly lower than those of Type 5-4—by 1.6% (3 days), 2.8% (7 days), 0.6% (14 days), and 0.7% (28 days). The average compressive strength of Type 5-3 samples ranged from 1.19 MPa to 4.37 MPa.

Samples of Type 5-4 exhibited the highest compressive strength values among all tested compositions. Compared to the Type 1 reference samples, the strength of Type 5-4 samples increased by 98.4% at 3 days, 99.2% at 7 days, and reached a full 100% improvement at both 14 and 28 days. These results indicate a doubling of strength relative to the control mixture. The average compressive strength of Type 5-4 samples ranged from 1.21 MPa to 4.40 MPa, confirming the superior effectiveness of this composition in enhancing the mechanical performance of foam concrete.

The analysis of the experimental results indicates that for sample types 2-1 through 5-4, the compressive strength at 28 days ranges from 2.25 MPa to 4.40 MPa, whereas the reference sample (Type 1) demonstrated a strength of 2.20 MPa. This means that in the most effective cases, the compressive strength nearly doubles compared to the control sample.

The data also show that the hardening process occurs not only during the early stages but continues progressively over time, with a steady increase in strength. This consistent development of mechanical properties suggests that the use of a plasticizing additive contributes significantly to the long-term structural performance of foam concrete.

Overall, the incorporation of the modified additive positively influences both early and late strength gain, enhancing the material's durability and reliability.

It has been established that all the additives studied have a positive effect on compressive strength, starting from the early stages of hardening (3 days) and especially by 28 days.

The most intense increase in strength is observed between 14 and 28 days, which indicates the prolonged action of the additives and improvement of cement hydration processes in the cellular structure of foam concrete.

Samples of types 2-1 to 3-2 showed a moderate increase in strength, ranging from 2.3% to 30.9% on day 28 compared to the reference sample. This indicates an initial positive effect of the additives, but without a radical change in the structure of the material.

Starting with samples of type 3-3 and above, the increase in strength became more pronounced, which is associated with the use of more effective or combined modifying compositions.

Type 5-4 samples demonstrated the highest strength — up to 4.40 MPa on day 28, which is 100% higher than the reference samples (2.20 MPa). This result indicates the high effectiveness of complex additives in improving the structure and density of foam concrete.

By the third day, strength had increased from 1.6% to 98.4%, confirming the accelerated hardening of foam concrete in the presence of active additives.

On the 7th day, an increase from 3.2% to 99.2% was observed, and on the 14th day, from 7.5% to 100%, reflecting the gradual strengthening of the structure and the completion of the main hydration processes.

Maximum strength values are reached on day 28, with an increase from 2.3% to 100%, depending on the type of sample. The kinetics of foam concrete hardening were studied, and it was found that the modifying additive accelerates the hardening of foam concrete.

Conclusion

The results obtained from the study support the recommendation of incorporating effective complex additives—particularly those used in sample types 4-3 through 5-4—into the production of non-autoclaved foam concrete with a density of D=600. The use of these additives has been shown to significantly enhance the strength and long-term durability of the material.

One of the key factors contributing to this improvement is the reduction in the water-cement ratio, made possible by the hydrophilic properties of the modifying additive. This leads to a denser and stronger concrete matrix. At the same time, the hydrophobic action of the additive reduces the material’s water absorption capacity, thereby improving its resistance to moisture and increasing its durability under service conditions.

The integration of such additives into foam concrete mixtures not only improves mechanical performance but also offers important practical advantages: it enables faster formwork removal, increases the load-bearing capacity of structural elements, and broadens the range of possible applications for foam concrete—including its use in both structural and thermal insulation products.

Additives improve not only strength but also structural uniformity, reducing the number of macropores and increasing the density of the material.

The analysis showed that correctly selected and dosed modifying additives can significantly improve the strength characteristics of non-autoclaved foam concrete grade D=600, in some cases almost doubling them. This makes the material more competitive and expands its application in modern construction, including energy-efficient building envelopes.

CRediT author statement: **A. Askerbekova**: conceptualization; **D. Dyusembinov**: writing—original draft preparation; **Zh.Shashpan**: formal analysis; **A. Abduova**: resources; **M. Kambarov**: critical review of content.

Acknowledgements. The authors would like to express their gratitude to the research and production center "ENU-lab" for conducting laboratory tests of foam concrete.

This research has been/was/is funded by the Committee of Science of the Ministry of Science and Higher Education of the Republic of Kazakhstan (Grant No. BR21882278 «Establishment of a construction and technical engineering centre to provide a full cycle of accredited services to the construction, road-building sector of the Republic of Kazakhstan»).

All authors have read and agreed to the published version of the manuscript.

Cite this article as: Askerbekova AM, Dyussembinov DS, Shashpan ZhA, Abduova AA, Kambarov MA. Investigation of the effect of a modified additive on the strength characteristics of foam concrete. Kompleksnoe Ispolzovanie Mineralnogo Syra = Complex Use of Mineral Resources. 2027; 341(2):117-127. https://doi.org/10.31643/2027/6445.23

Модификацияланған қоспаның көбікті бетонның беріктік сипаттамаларына әсерін зерттеу

[1]Аскербекова А.М., [1]Дюсембинов Д.С., [1]Шашпан Ж.А., [2]Абдуова А.А., [2]Камбаров М.А.

[1]Л.Н. Гумилев атындағы Еуразия ұлттық университеті, Астана, Қазақстан
[2] М.Әуезов атындағы Оңтүстік Қазақстан зерттеу университеті, Шымкент, Қазақстан

Мақала келді: *1 тамыз 2025*
Сараптамадан өтті: *11 қазан 2025*
Қабылданды: *1 желтоқсан 2025*

ТҮЙІНДЕМЕ

Мақалада модификацияланған қоспаның көбікті бетонның беріктік сипаттамаларына әсерін зерттеудің екінші кезеңі ұсынылған. Бұл жұмыста көбікті бетон үлгілерін дайындау әдісі сипатталып, әртүрлі пайыздық құрамдағы компоненттермен модификациялаушы қоспаның құрамы таңдалып, олардың беріктік сипаттамаларына талдау жүргізілді. D600 маркалы көбікті бетонға пластификаторлық қоспа (спирттен кейінгі барда) енгізудің мақсаты – су шығынын азайту және беріктікті арттыру. Беріктік өзгерістерін бағалау үшін 3, 7, 14 және 28 тәулікте қалыпты ылғалдандыру жағдайында қысу сынақтарына арналған үлгілер дайындалды. Зерттеу нәтижелері бойынша мұндай қоспаларды қолдану қалыптан босату уақытын айтарлықтай қысқартуға, конструкциялардың көтергіш қабілетін арттыруға және көбікті бетонды қолдану аясын кеңейтуге – тіпті конструкциялық және жылу оқшаулағыш бұйымдар үшін де – мүмкіндік беретіні анықталды. Қоспалар тек беріктікті ғана емес, сонымен қатар құрылымның біртектілігін де жақсартады, макрокеуектер санын азайтады және материалдың тығыздығын арттырады.

Түйін сөздер: цемент қоспасы, спирттен кейінгі барда, модификацияланған қоспа, қысу кезіндегі беріктік, пластификатор, көбіктендіргіш.

Авторлар туралы ақпарат:

Аскербекова Арайлым Мырзаханкызы — *PhD докторанты, Өнеркәсіптік және азаматтық құрылыс технологиясы кафедрасы, Л.Н. Гумилев атындағы Еуразия ұлттық университеті, Астана, Қазақстан. Email: aria_09.91@mail.ru; ORCID ID: https://orcid.org/0000-0002-4356-053X*

Дюсембинов Думан Серикович — *Т.ғ.к., Өнеркәсіптік және азаматтық құрылыс технологиясы кафедрасының доценті, Л.Н. Гумилев атындағы Еуразия ұлттық университеті, Астана, Қазақстан. Email: dusembinov@mail.ru; ORCID ID: https://orcid.org/0000-0001-6118-5238*

Шашпан Жоламан Амангелдіұлы — *Т.ғ.д., Өнеркәсіптік және азаматтық құрылыс технологиясы кафедрасының доценті, Л.Н. Гумилев атындағы Еуразия ұлттық университеті, Астана, Қазақстан. Email: zholamanalmatykz@gmail.com; ORCID ID: https://orcid.org/0000-0002-6236-0525*

Абдуова Айсулу Алшынбековна — *Т.ғ.к., Экология кафедрасының доценті, М.Әуезов атындағы Оңтүстік Қазақстан зерттеу университеті, Шымкент, Қазақстан. Email: aisulu.abduova@mail.ru; ORCID ID: https://orcid.org/0000-0001-5389-6953*

Камбаров Медет Абдильдаевич — *Т.ғ.к., Құрылыс материалдары және құрылыстағы сараптама кафедрасының доценті, М.Әуезов атындағы Оңтүстік Қазақстан зерттеу университеті, Шымкент, Қазақстан. Email: medet_2030@mail.ru; ORCID ID: https://orcid.org/0000-0001-6397-1451*

Исследование влияния модифицированной добавки на прочностные характеристики пенобетона

[1]Аскербекова А.М., [1]Дюсембинов Д.С., [1]Шашпан Ж.А., [2]Абдуова А.А., [2]Камбаров М.А.

[1]Евразийский национальный университет имени Л.Н. Гумилева, Астана, Казахстан
[2]Южно-Казахстанский исследовательский университет имени М.Ауэзова, Шымкент, Казахстан

Поступила: *1 августа 2025*
Рецензирование: *11 октября 2025*
Принята в печать: *1 декабря 2025*

АННОТАЦИЯ

В статье представлен второй этап исследования влияния модифицированной добавки на прочностные характеристики пенобетона. В данной работе описан способ изготовления образцов пенобетона, подобран состав модифицирующей добавки с различным процентным содержанием компонентов и проведен анализ их прочностных характеристик. Цель введения пластифицирующих добавок (послеспиртовой барды) в пенобетон D600 - снижение расхода воды и ожидаемое повышение прочности. Чтобы оценить изменения в прочности, были изготовлены образцы и испытаны на сжатие в возрасте 3, 7, 14 и 28 дней

	при нормальном увлажнении. Согласно результатам исследований, использование таких добавок позволяет значительно сократить сроки распалубки, повысить несущую способность конструкций и расширить сферу применения пенобетона - даже для конструкционных и теплоизоляционных изделий. Добавки улучшают не только прочность, но и однородность структуры, уменьшая количество макропор и повышая плотность материала.
	Ключевые слова: цементная смесь, послеспиртовая барда, модифицирующая добавка, прочность на сжатие, пластификатор, пенообразователь.
Аскербекова Арайлым Мырзаханкызы	***Информация об авторах:*** *Докторант PhD, Кафедра Технология промышленного и гражданского строительства, Евразийский национальный университет имени Л.Н. Гумилева, Астана, Казахстан. Email: aria_09.91@mail.ru; ORCID ID: https://orcid.org/0000-0002-4356-053X*
Дюсембинов Думан Серикович	*К.т.н., доцент кафедры Технология промышленного и гражданского строительства, Евразийский национальный университет имени Л.Н. Гумилева, Астана, Казахстан. Email: dusembinov@mail.ru; ORCID ID: https://orcid.org/0000-0001-6118-5238*
Шашпан Жоламан Амангельдиевич	*Д.т.н., доцент кафедры Технология промышленного и гражданского строительства, Евразийский национальный университет имени Л.Н. Гумилева, Астана, Казахстан. Email: zholamanalmatykz@gmail.com; ORCID ID: https://orcid.org/0000-0002-6236-0525*
Абдуова Айсулу Алшынбековна	*К.т.н., доцент кафедры Экология, Южно-Казахстанский исследовательский университет имени М.Ауэзова, Шымкент, Казахстан. Email: aisulu.abduova@mail.ru; ORCID ID: https://orcid.org/0000-0001-5389-6953*
Камбаров Медет Абдильдаевич	*К.т.н., доцент кафедры Строительные материалы и экспертиза в строительстве, Южно-Казахстансикй исследовательский университет имени М.Ауэзова, Шымкент, Казахстан. Email: medet_2030@mail.ru; ORCID ID: https://orcid.org/0000-0001-6397-1451*

References

[1] Postanovlenie Pravitel'stva Respubliki Kazahstan. Gosudarstvennaya programma zhilishchno-kommunal'nogo razvitiya Nұrly-ZHer na 2020-2025 gody [State Program of Housing and Communal Development Nurly-Zher for 2020-2025]. utv. 31 dekabrya 2019 goda, №1054 (in Russ.). https://adilet.zan.kz/rus/docs/P1900001054

[2] Postanovlenie Pravleniya Natsionalnogo Banka Respubliki Kazakhstan [Resolution of the Board of the National Bank of the Republic of Kazakhstan]. utv. 19 dekabrya 2022 goda № 123. O vnesenii izmeneniy v postanovleniye Pravleniya Natsionalnogo Banka Respubliki Kazakhstan [On Amendments to the Resolution of the Board of the National Bank of the Republic of Kazakhstan]. utv. 31 maya 2018 goda № 107 Ob utverzhdenii Programmy ipotechnogo zhilishchnogo kreditovaniya 7-20-25. Novyye vozmozhnosti priobreteniya zhilia dlya kazhdoy semi [On the Approval of the Mortgage Housing Loan Program 7-20-25: New Opportunities for Every Family to Purchase Housing]. (in Russ.). https://online.zakon.kz/Document/?doc_id=36871886&pos=6;-108#pos=6;-108

[3] Jalalov ShG, Otsokov KA. Sposoby povysheniya effektivnosti penobetona [The ways of increase of efficiency of foam concrete]. Vestnik Dagestanskogo gosudarstvennogo tekhnicheskogo universiteta. Tekhnicheskiye nauki [Herald of Dagestan State Technical University. Technical Sciences]. 2016;42(3):167-174. (In Russ.). https://doi.org/10.21822/2073-6185-2016-42-3-167-175

[4] Liu J, Ge T, Wu Y, Chen R. Effect of Sand-to-Cement Ratio on Mechanical Properties of Foam Concrete. Buildings. 2022; 12(11):1969. https://doi.org/10.3390/buildings12111969

[5] Liu J, Ren Y, Chen R, Wu Y, Lei W. The Effect of Pore Structure on Impact Behavior of Concrete Hollow Brick, Autoclaved Aerated Concrete and Foamed Concrete. Materials. 2022; 15(12):4075. https://doi.org/10.3390/ma15124075

[6] Lukpanov RE, Dyusembinov DS, Altynbekova AD, Yenkebayev SB, Zhantlesova ZhB. Issledovaniye fiziko-mekhanicheskikh svoystv peska i tsementa dlya proizvodstva penobetona [Research physical and mechanical properties of sand and cement for foam concrete production]. Vestnik Kazakhskoy golovnoy arkhitekturno-stroitel'noy akademii. Stroitel'nyye konstruktsii i materialy [Bulletin of Kazakh Leading Academy of Architecture and Construction. Building structures and materials]. 2023; 1(87):217- 228. (In Russ.). https://doi.org/10.51488/1680-080X/2023.1-21

[7] Zhongwei Liu, Kang Zhao, Chi Hu, and Yufei Tang. Effect of water-cement ratio on pore structure and strength of foam concrete. Hindawi Publishing Corporation. Advances in Materials Science and Engineering. 2016. http://dx.doi.org/10.1155/2016/9520294

[8] Abdyushkurov F, Sabitov E, Kirghizbayev A, Duzelbayev S. Building materials and products, Nur-Sultan, L.N. Gumilyov Eurasian National University. 2021, 458.

[9] Al-Khazraji AA. Use of plasticizers in cement concrete. Journal of Advanced Research in Dynamical and Control Systems. 2020; 12(3):599-607. https://doi.org/10.5373/JARDCS/V12I3/20201229

[10] Arvind Vishavkarma, Kizhakkumodom Venkatanarayanan Harish. Development of eco-friendly and cost-effective foam concrete using high-volume supplementary cementitious materials: Analysis of microstructural, mechanical, and durability properties. Construction and Building Materials. 2025; 458. https://doi.org/10.1016/j.conbuildmat.2024.139584

[11] Dhasindrakrishna K, et al. Collapse of fresh foam concrete: Mechanisms and influencing parameters. Cement and Concrete Composites. 2021; 122:104151.

[12] Cherkasov VD, Buzulukov VI, Emelianov AI. Perspektivnaya plastifitsiruyushchaya dobavka dlya tsementnykh sistem iz poslespirtovoy bardy [A promising plasticizing additive for cement systems made from distillery stillage]. Vestnik Volzhskogo regionalnogo otdeleniya Rossiyskoy akademii arkhitektury i stroitelnykh nauk [Bulletin of the Volga Regional Branch of the Russian Academy of Architecture and Construction Sciences]. 2014; 17:264-266. (in Russ.).

[13] Shi M, et al. Mix proportion optimization and early strength development in modified foam concrete: an experimental study. Mater. Res. Express. IOP Publishing. 2023; 10(6):065507.

[14] Baronins J, et al. The Effect of Raw Materials and Mechanical Activation Stages on Properties of Foamed Concrete: SSRN Scholarly Paper. Rochester, NY. 2024, 4728421.

[15] Serova RF, Tkach EV, Seydinova GA, Stasilovich EA. Issledovaniye sposobov utilizatsii promyshlennykh otkhodov dlya proizvodstva gazobetona [Research into methods of industrial waste utilization for aerated concrete production]. Vestnik Trudy universiteta. Seriya: Stroitelstvo. Transport [Bulletin of the University's Proceedings. Series: Construction. Transport]. Karagandy. 2020; 2(79):74-78. (in Russ.).

[16] Altynbekova AD, Lukpanov RE, Dyussembinov DS, Askerbekova AM, Talal Awwad. Effect of a complex modified additive based on post-alcohol bard on the strength behavior of concrete. Kompleksnoe Ispolzovanie Mineralnogo Syra = Complex Use of Mineral Resources. 2023; 327(4):5-14. https://doi.org/10.31643/2023/6445.34

[17] Miryuk OA. Resursosberezheniye v tekhnologii stroitelnykh materialov [Resource conservation in building materials technology]. Almaty. Evero. 2013, 280. (in Russ.).

[18] Askerbekova AM, Dyusembinov DS, Skripnikova NK, Altynbekova AD, Iztleuov GM. The effect of a complex modified additive on the quality of the production of foam concrete products. Bulletin of D. Serikbaev EKTU, Technical sciences. 2024; 2:5-15. https://doi.org/10.51885/1561-4212_2024_2_5

[19] Cherkasov VD, Emelyanov AI, Kiselev EV. Obtaining efficient foam from secondary products of ethyl alcohol production. Expert: theory and practice. 2023; 1(20):160-162. (In Russ.). https://doi.org/10.51608/26867818_2023_1_160

[20] Vinokurova OV, Baranova AA. On the question of choosing the optimal water-cement ratio in the production of thermal insulating foam concrete. Bulletin of BSTU named after V.G. Shukhov. 2022; 11:19–29. https://doi.org/10.34031/2071-7318-2022-7-11-19-290

Crossref
DOI: 10.31643/2027/6445.24
Mining & Mineral Processing

creative commons

Physicochemical Analysis of Water-Soluble Sodium Silicate Obtained from Modified Raw Materials

[1*]Madaminov D.Q., [2] Atashev E.A., [3]Matmurotov B.Y., [4]Radjapov O.B., [5]Masharipov R.M.

[1]Khorezm Mamun Academy, Khiva, Uzbekistan
[2] Urgench State University named after Abu Rayhon Beruni, Uzbekistan
[3]Tashkent State Medical University, Uzbekistan
[4] Urgench Innovation University, Uzbekistan
[5]Mamun University, Khiva, Uzbekistan

** Corresponding author email: dilshodbek-md@mail.ru*

Received: *September 9, 2025*
Peer-reviewed: *October 17, 2025*
Accepted: *December 1, 2025*

ABSTRACT

This article investigates the physicochemical properties of water-soluble sodium silicate synthesized from modified raw materials. During the research process, several compositions of soluble glass samples were prepared, and their structural characteristics were analyzed using infrared (IR) spectroscopy. In addition, X-ray fluorescence (XRF) analysis was employed to determine the chemical composition of the products and the distribution of their components. The results demonstrated that two of the studied compositions are considered promising in terms of technological and physicochemical parameters. In particular, the third composition provided the most optimal outcome, exhibiting superior stability, structural homogeneity, and practical applicability of the soluble glass. The findings of this study highlight the potential for developing energy-efficient technologies for the production of water-soluble sodium silicate based on local and modified raw materials. The results of infrared spectroscopic analysis showed that the BMK-3 sample exhibited significantly more stable and intense Si–O–Na bonds compared to other analyzed samples and compositions. This phenomenon is explained by the structural uniformity of the composition, the balance of cation–anion interactions, and the strength of the glass network structure. Therefore, the third composition is recommended as the most promising sample.

Keywords: water-soluble sodium silicate, modification of raw materials, IR analysis, X-ray fluorescence, optimal composition, physicochemical properties.

Information about authors:

Madaminov Dilshodbek Quranboyevich — *Doctoral student, Khorezm Mamun Academy, Markaz Street 1, Khiva, Uzbekistan. Email: dilshodbek-md@mail.ru; ORCID ID: https://orcid.org/0009-0004-9696-8899*

Atashev Elyor Atashevich — *Doctor of Philosophy in Technical Sciences, Associate Professor at the Faculty of Chemical Technology, Urgench State University named after Abu Rayhon Beruni, 220100, H. Olimjon Street 14, Urgench, Uzbekistan. Email: elyor.a@urdu.uz; ORCID ID: https://orcid.org/0000-0003-4070-5665*

Matmurotov Bakhtishod Yangibayevich — *Doctor of Philosophy in Chemistry (PhD), Senior Lecturer at the International Faculty, Tashkent State Medical University, 100109, Forobiy Street 2, Almazar District, Tashkent, Uzbekistan. E-mail: b.matmurotov@mail.ru; ORCID ID: https://orcid.org/0009-0002-1175-3588*

Radjapov Odilbek Babanazarovich — *Associate Professor, Department of Social and Humanities of the Faculty of Social and Humanities of Urgench Innovation University, 220100, Gurlan Street 2, Urgench, Uzbekistan. Email: radjapovodilbek@urgiu.uz; ORCID ID: https://orcid.org/0009-0006-2851-1429*

Masharipov Ravqat Madraximovich — *Doctor of Philosophy in Pedagogical Sciences (PhD), Associate Professor at the Faculty of Psychology and General Professional Sciences, Mamun University, 2 Bo'l-Xovuz Street, Qibla Tozabog' Makhalla, Khiva, Khorezm Region, Uzbekistan. E-mail: ravqatmasharipov@gmail.com*

Introduction

Water-soluble sodium silicates belong to the group of alkali metal silicates and are primarily obtained from a mixture of silicon dioxide and sodium oxide. Many researchers believe that the terms *"soluble glass"* and *"liquid glass"* are interchangeable. However, the concept of *"liquid glass"* is much broader, as it refers to all aqueous solutions of alkali silicates, regardless of their method of production, type of cation, concentration, or polymeric structure of silica [[1], [2]].

While soluble glass serves as a raw material for the production of liquid glass, the latter can also be synthesized through the dissolution of silica in alkalis, as well as by dissolving amorphous or crystalline, hydrated or anhydrous powdered alkali silicates. Liquid glass may be potassium-based, sodium-based, lithium-based, or ammonium-based.

Both substances are considered large-tonnage products of inorganic synthesis [[3], [4], [5], [6]].

A key feature of liquid glass production lies in its environmental friendliness, the availability of raw materials, and its low cost. The composition of soluble glass is expressed as $R_2O{\cdot}SiO_2$. In terms of physical properties, it exists as silicate lumps (solid pieces) and as an aqueous solution, which represents the actual liquid glass. The molar ratio between alkali metal oxides and silica, known as the silicate modulus (*n*), ranges from 2.0 to 4.0. Depending on the type of raw material used, soluble glasses are categorized as soda, soda-sulfate, or sulfate-based, while by composition they are classified as sodium, potassium, mixed, or double. In construction, sodium-based liquid glasses are most widely applied, followed to a lesser extent by potassium-based glasses [7].

Liquid glass is classified according to the following parameters:

1. type of cation: sodium, potassium, lithium, or organic bases;
2. silicate modulus;
3. absolute content of R_2O and SiO_2;
4. content of impurities such as oxides of iron, aluminum, calcium, magnesium, and sulfur;
5. density of the solution.

The density of sodium liquid glass ranges from ρ = 1.30–1.60 g/cm³ with a silicate modulus *n* = 2.0–3.5, while potassium liquid glass typically has a density of ρ = 1.25–1.40 g/cm³ and *n* = 2.8–4.0 [8]. Due to their wide compositional range, liquid glasses may contain various cations, silicate anions ranging from monomeric to highly polymerized forms, and silica in different structural and aggregate states. Consequently, their properties also vary within a wide range [9].

A specific feature of soluble glass lies in the gradual change of its chemical composition during operation. With decreasing alkalinity, transformation toward silica sols occurs, accompanied by changes in the physicochemical nature of the solution. Conventional sodium and potassium glasses occupy only a narrow segment within this diversity of systems [10].

The process of silicate formation from glass melt is multistage in nature, proceeding sequentially and often simultaneously through high-temperature reactions between components in both solid and liquid phases. The main transformations occurring during heating include: removal of hygroscopic moisture at 110–120 °C; elimination of crystallohydrate moisture, which may form upon moistening of the raw mixture, at 200 °C; polymorphic transitions of sodium carbonate at 235 °C; polymorphic transformations of quartz at 575 °C; and dissociation of potassium carbonate. At 800–900 °C, solid-phase silicate formation reactions begin, while at 855 °C, melting of mixture components is initiated. In the range of 900–1400 °C, eutectic phases are formed within the $R_2O–SiO_2$ system, followed by the melting of alkali–quartz compounds and the dissolution of silica. At 1400 °C, glass mass formation occurs, after which the melt undergoes cooling. In the case of sodium soluble glass, the reactions typically begin at approximately 380 °C [[11], [12], [13], [14]].

$$Na_2CO_3 + SiO_2 \xrightarrow{®} Na_2O \cdot nSiO_2 + CO_2. \quad (1)$$

The complete binding of sodium carbonate is observed at temperatures of 920–950 °C. During this process, the product consists of sodium metasilicate, silica, and alkali silicate, forming a glass-like solid structure. With increasing temperature, this mass undergoes a series of physicochemical transformations associated with the dissolution of silica, which leads to an increase in the melt volume and the formation of an excess amount of material of up to approximately 30% [[15], [16], [17]].

The minimum temperature for the formation of an alkali silicate melt is 780 °C; however, to obtain a homogeneous melt of industrial composition, a temperature of 1250 °C is required. During the glass-forming process, quartz residues gradually dissolve in the viscous sodium silicate melt, resulting in the formation of a zone enriched with SiO_2. As saturation of this zone increases, the solubility of sand decreases, while the excess amount of silica is removed through diffusion driven by the concentration gradient [18].

The diffusion rate determines the rate of glass formation and depends on temperature, viscosity, surface tension of the melt, as well as the intensity of mixing. To clarify the glass mass—removing visible gas inclusions and achieving homogenization to obtain a uniform mass—a temperature of 1400 °C is required [[19], [20]].

Experimental part

In this study, the chemical structure of sodium silicate samples was investigated using infrared (IR)

spectral analysis. The analyses were performed on a *Shimadzu Fourier-transform IR spectrometer* within the range of 4000–400 cm^{-1}, with a resolution of 4 cm^{-1}. Sample preparation was carried out using the potassium bromide (KBr) pellet technique: pre-dried and finely ground samples were uniformly mixed with KBr and compressed into transparent pellets using a specialized press. The characteristic absorption bands observed in the spectra were used to identify functional groups present in the sodium silicate structure. The elemental composition of the synthesized glass samples was analyzed using X-ray fluorescence spectroscopy (XRF). This method enables the accurate detection of both major and minor components in glass without destruction of the sample. The analyses were conducted with a modern XRF analyzer equipped with an Rh-anode X-ray tube, operating at 50 kV and 40 mA. The samples were prepared either in pressed pellet form or fused with a flux. The identified elements included the main oxides - SiO_2, Na_2O, Al_2O_3, Fe_2O_3, MgO, and CaO - as well as minor components such as K_2O, TiO_2, and P_2O_5. The analytical results were presented in the form of spectra, images, and tables. Data processing and phase interpretation were carried out using specialized software packages such as *Spectra Plus* and *Shimadzu XRF Manager*. Calibration of the instruments was performed using international standard reference materials (SRM, NIST). The applied analytical methods demonstrated several advantages, including rapid analysis, high accuracy, non-destructive sample preparation, and broad elemental coverage. These features are of critical importance for the comprehensive evaluation of glass composition and the analysis of technological processes.

Results and Discussion

The infrared spectroscopic (IR) analysis of the sample was carried out, and the obtained IR spectra are presented in Figures 1, 2, 3, and 4. In the spectrum of the sample shown in Figure 1, several distinct absorption bands were observed. The high-frequency sharp peaks at 3732, 3691, 3667, and 3610 cm^{-1} correspond to the Si–OH hydroxyl groups. The broad absorption band in the range of 3519–3193 cm^{-1} is attributed to hydrogen-bonded –OH groups and molecular water.

The characteristic deformations related to silicate structures were identified at 1245 and 1139 cm^{-1}, which correspond to Si–O–Si linkages in sodium silicate. Additionally, the absorption band at 1022 cm^{-1} indicates the presence of Si–O^-–Na vibrational groups coordinated with sodium, which is a distinctive feature of sodium silicate.

In the spectrum of the sample shown in Figure 2, a broad absorption band at 3436 cm^{-1} was identified, corresponding to –OH groups and molecular water, although present in very small amounts. The absorption bands at 2361 and 2342 cm^{-1} are typically associated with the vibrational modes of residual CO_2 carbonates, which may indicate that the sample absorbed CO_2 from the atmosphere. A strong absorption peak observed at 1033 cm^{-1} is attributed to the Si–O–Si stretching vibrations and, to some extent, to Si–O^-–Na vibrations, which are characteristic for sodium silicate. The band at 912 cm^{-1} corresponds to Si–O^- groups coordinated with sodium, confirming features typical of soluble glass. Furthermore, the absorption peaks at 777 and 687 cm^{-1} represent the bending vibrations of Si–O–Si bonds, while the bands at 581 and 454 cm^{-1} correspond to the skeletal vibrations of the silicate framework, indicating the structural stability of the silicate network.

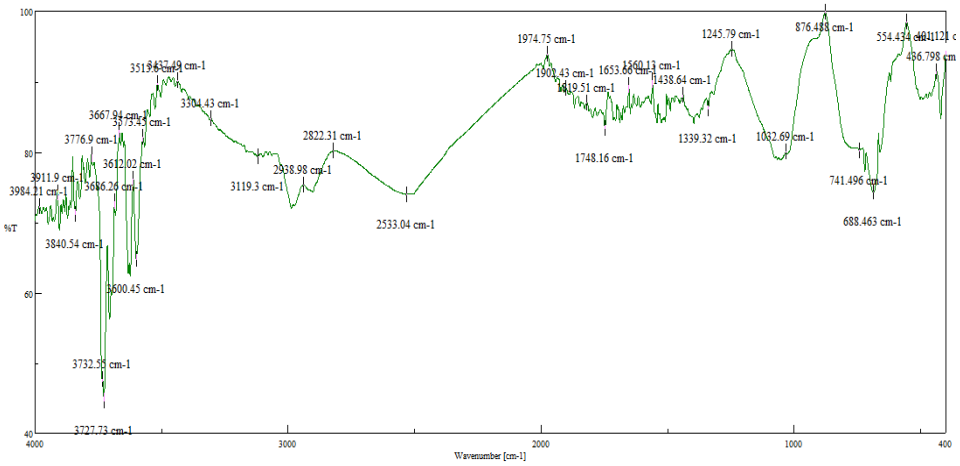

Figure 1 - IR spectroscopic analysis of Sample 1 of soluble sodium silicate

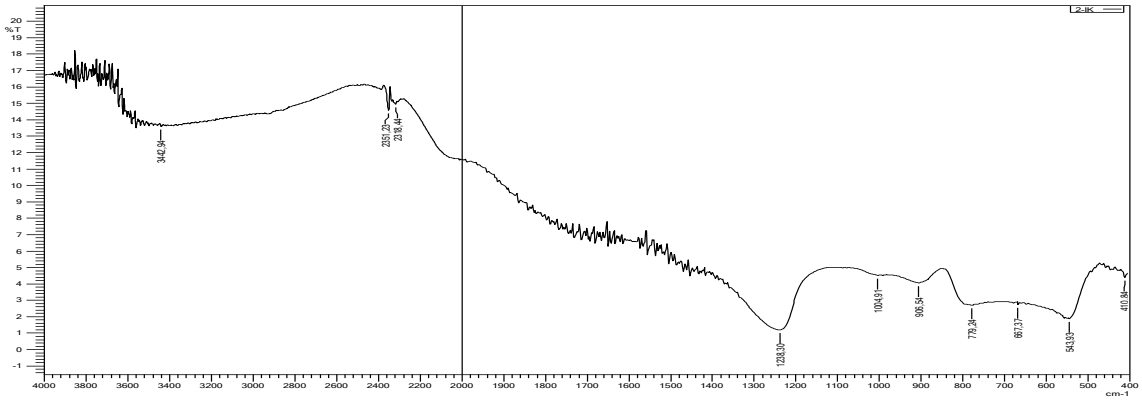

Figure 2 - IR spectroscopic analysis of Sample 2 of soluble sodium silicate

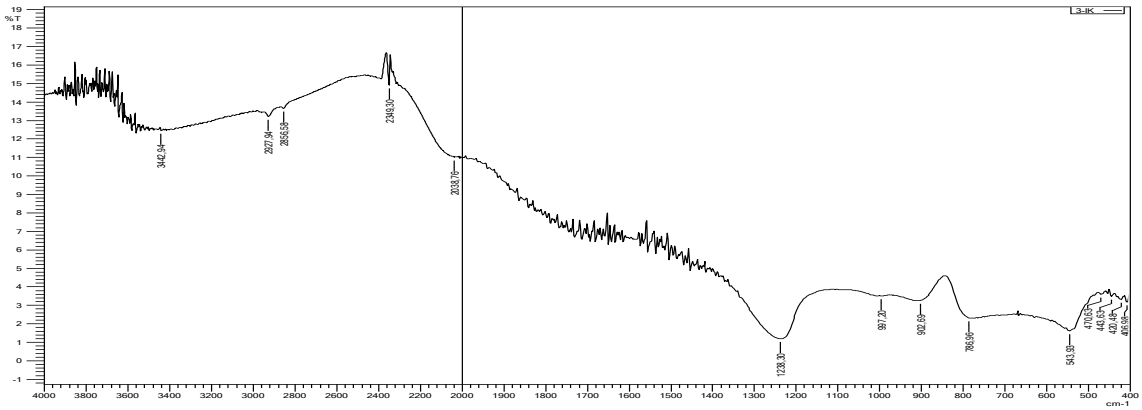

Figure 3 - IR spectroscopic analysis of Sample 3 of soluble sodium silicate

In the spectrum of the sample shown in Figure 3, a broad absorption band at 3434 cm^{-1} was observed, corresponding to the –OH groups and molecular water. The absorption peaks at 2361 and 2336 cm^{-1} are typically attributed to the vibrational modes of CO_2 carbonate groups. A strong and sharp band at 1030 cm^{-1} is assigned to the Si–O–Si stretching vibrations, while the absorption band at 912 cm^{-1} indicates the presence of $Si–O^-$ groups coordinated with sodium, a characteristic feature of soluble glass.

Additionally, the absorption bands at 787 and 719 cm^{-1} correspond to the bending vibrations of Si–O–Si bonds, whereas the peaks at 654, 614, and 454 cm^{-1} are associated with the skeletal vibrations of the silicate framework, reflecting the stability and integrity of the silicate network structure.

According to the results of the spectrum shown in Figure 4, the broad absorption bands in the range 3957–3610 cm^{-1} correspond to the O–H stretching vibrations of hydroxyl groups. The peaks at 2929 cm^{-1} and 2854 cm^{-1} are attributed to the C–H stretching vibrations of methyl or methylene groups. The absorption at 2358 cm^{-1} is assigned to CO_2 molecules, which may have been absorbed from the surrounding atmosphere. The band at 1994 cm^{-1} can be related to complex Si–O–Si vibrations or mixed vibrational modes.

The absorption range 1732–1566 cm^{-1} indicates the presence of C=O groups, which may belong to carboxyl or carbonate compounds, as well as possible H–O–H bending vibrations of molecular water. A very strong absorption band between 1054–995 cm^{-1} is attributed to the Si–O–Si stretching vibrations of the silicate framework. The bands at 823–761 cm^{-1} correspond to Si–O deformation vibrations within the silicate structure, while the absorptions at 665–472 cm^{-1} are associated with the Si–O bending vibrations characteristic of sodium silicates.

The spectrum clearly demonstrates that sodium silicate is the main component. The presence of organic residues (C–H, C=O bands) suggests that the sample was derived from a waste-based or mixed raw material system. In the lower-frequency region (400–800 cm^{-1}), the presence of distinct absorption bands further confirms the inorganic silicate network structure. Overall, this spectrum is typical of soluble sodium silicate synthesized from waste-containing or mixed-component systems.

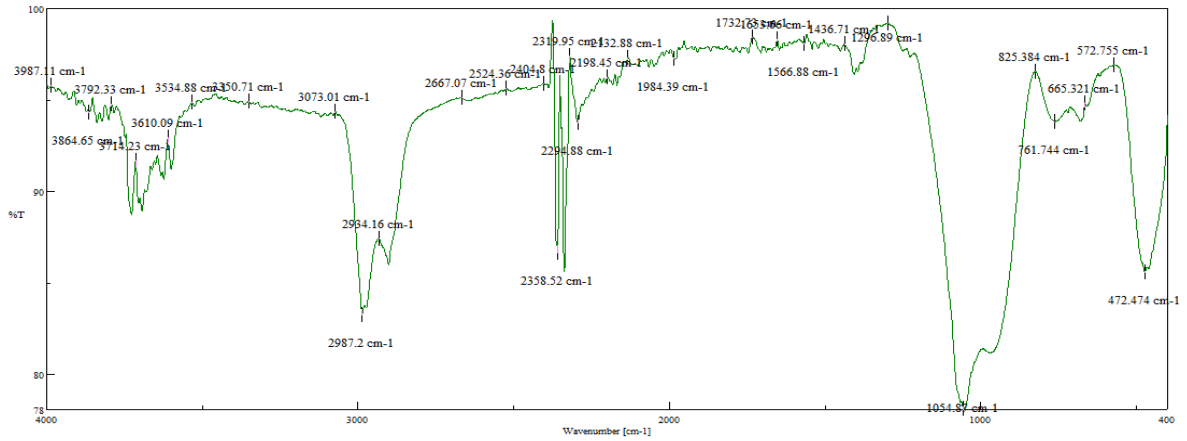

Figure 4 - IR spectroscopic analysis of Sample 4 of soluble sodium silicate

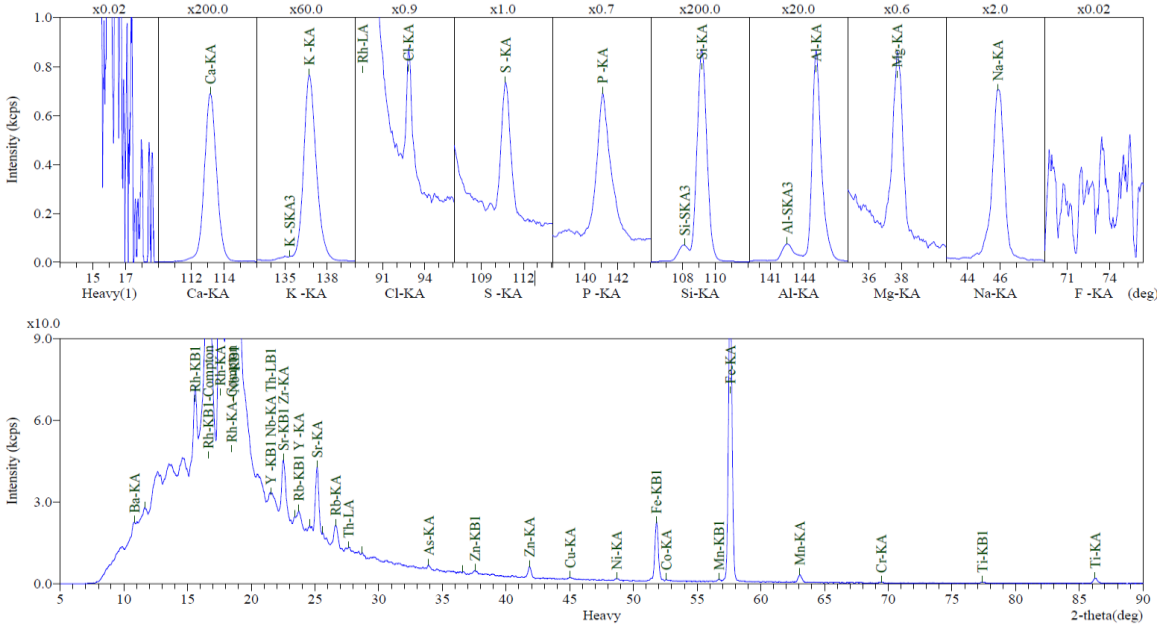

Figure 5 - X-ray fluorescence (XRF) analysis of soluble sodium silicate, Sample 3

Table 1 - Chemical composition of soluble sodium silicate

Sample	Oxide content, wt.%									LOI, wt.%
	SiO_2	Al_2O_3	Fe_2O_3	CaO	MgO	K_2O	Na_2O	TiO_2	P_2O_5	
Sample - 3	67.9	1.74	1.86	1.77	0.844	1.79	23.0	0.2	0.02	0.876

Based on the results of the IR spectroscopic analysis, the characteristics of Sample 3 revealed properties and features typical of soluble glass.

To further verify these findings, an X-ray fluorescence (XRF) analysis was carried out in order to determine the oxide composition of Sample 3 and to evaluate its compliance with the requirements of GOST 13079–2021, as well as to calculate the silicate modulus (fig. 5 and Tab. 1).

The chemical composition of the obtained samples was analyzed based on Table 1, and it was determined that their main components are SiO_2, Na_2O, CaO, Al_2O_3, and Fe_2O_3 oxides. The SiO_2 content of 67.9% plays an important role in ensuring the structural stability of the glass. Na_2O (23.0%) is the main compound required for the synthesis of soluble glass. Its sufficient amount accelerates the bonding process with SiO_2 and increases solubility. CaO (1.77%) and MgO (0.844%) serve as additional modifier oxides that improve the mechanical strength and thermal resistance of the glass mass. However, their excessive content may reduce the solubility of the glass. Fe_2O_3 was found in a concentration of 1.86%, and a higher amount of this oxide can negatively affect the quality of the glass. In addition, other impurities such as Cl^- and SO_4^{2-}, if

present in significant amounts, can also have a detrimental effect. Therefore, technological regulation of their concentration is of great importance.

Conclusions

In all spectra, broad peaks were observed in the range of 3200–3600 cm^{-1}, indicating the presence of hydroxyl groups. Higher peak intensity suggests that the sample has better potential for dissolution during liquid glass production. Strong Si–O–Si stretching vibrations were observed in the range of 1000–1200 cm^{-1} across all four spectra. To determine the most suitable composition, the peaks should be sharp and well-defined, without additional side signals, as this indicates a well-developed silicate network. Si–O bending vibrations were present in the range of 450–800 cm^{-1} in all samples. In the spectra of Figures 3 and 4, a distinct peak around 470 cm^{-1} was observed, confirming the presence of a fully polymerized silicate structure. In Figures 2 and 3, weak peaks in the range of 1450–1500 cm^{-1} were detected, suggesting the presence of small amounts of carbonates and organic impurities, which can lower the quality of the solution. In this study, a peak at 2358 cm^{-1} was detected, corresponding to absorbed CO_2, likely introduced from the surrounding atmosphere. Although this can be removed during processing, excessive amounts may negatively influence product quality. Based on these observations, the first sample revealed OH groups but also noticeable carbonate impurities. The second sample showed strong Si–O peaks, but additional signals in the range of 1400–1500 cm^{-1} were present. The third sample exhibited distinct silicate peaks, with a strong peak at 470 cm^{-1}, indicating a well-polymerized structure. The fourth sample contained Si–O peaks but also CO_2 traces at 2358 cm^{-1}. Overall, the third sample spectrum was determined to be the most suitable for liquid glass production. This is attributed to its sharp and strong Si–O–Si peaks, high degree of polymerization, lower carbonate (CO_2) impurities, and balanced OH content related to moisture. Comparative analysis of the chemical composition confirmed that the third sample was optimal for liquid glass synthesis. This is due to the balanced ratio of SiO_2 and Na_2O, along with relatively lower levels of harmful impurities such as Fe_2O_3 and SO_4^{2-}. These findings demonstrate the potential of producing liquid glass through energy-efficient technologies based on waste-derived raw materials.

Conflicts of interest. On behalf of all authors, the corresponding author states that there is no conflict of interest.

CRediT author statement: **E. Atashev**: Conceptualization, Methodology, Software; **D. Madaminov**: Data curation, Writing draft preparation, Visualization, Investigation, Supervision, Software, Validation; **О. Раджабов**: Reviewing and Editing.

Acknowledgements. We would like to express our deep gratitude to **Atashev Elyor Atashevich**, *Doctor of Philosophy in Technical Sciences, Associate Professor* of the Faculty of Chemical Technologies at Urgench State University named after Abu Rayhon Beruni, for his practical assistance in conducting the experiments for this research. We also extend our sincere appreciation to **Radjapov Odilbek Babanazarovich** for his support in translation and language-related matters, and to my colleague Azamat Shomuratovich Khadjiev for his valuable contributions to the writing and editing of this article.

Formatting of funding sources. This research did not receive any specific grant from funding agencies in the public, commercial, or not-for-profit sectors.

Cite this article as: Madaminov DQ, Atashev EA, Matmurotov BY, Radjapov OB, Masharipov RM. Physicochemical Analysis of Water-Soluble Sodium Silicate Obtained from Modified Raw Materials. Kompleksnoe Ispolzovanie Mineralnogo Syra = Complex Use of Mineral Resources. 2027; 341(2):128-135. https://doi.org/10.31643/2027/6445.24

Модификацияланған шикізаттан алынған суда еритін натрий силикатының физика-химиялық талдауы

[1*]Мадаминов Д.Қ., [2]Аташев Э.А., [3]Матмуротов Б.Я., [4]Раджабов О.Б., [5]Машарипов Р.М.

[1] Хорезм Мамун академиясы, Хива, Өзбекстан
[2] Әбу Райхан Бируни атындағы Үргеніш мемлекеттік университеті, Өзбекстан
[3]Ташкент мемлекеттік медицина университеті, Өзбекстан
[4]Үргеніш инновациялық университеті, Өзбекстан
[5]Мамун университеті, Хива, Өзбекстан

Мақала келді: *9 қыркүйек 2025*
Сараптамадан өтті: *17 қазан 2025*
Қабылданды: *1 желтоқсан 2025*

ТҮЙІНДЕМЕ
Мақалада модификациялық шикізаттар негізінде синтезделген еритін натрий силикатының үлгілерінің физика-химиялық қасиеттері зерттелді. Зерттеу барысында әртүрлі құрамдағы еритін шыны үлгілері дайындалып, олардың құрылымы инфрақызыл (ИҚ) спектроскопия әдісі арқылы талданды. Сонымен қатар, өнімдердің химиялық құрамын және компоненттердің таралуын анықтау мақсатында рентгенофлуоресценттік (РФ) талдау әдісі қолданылды. Алынған нәтижелер зерттелген құрамдардың екеуінің технологиялық және физика-химиялық көрсеткіштері бойынша болашағы бар екенін көрсетті. Ал үшінші құрам еритін шынының жоғары тұрақтылығын, құрылымдық консистенциясын және практикалық қолданудағы тиімділігін қамтамасыз ететін оңтайлы нәтижелер көрсетті. Зерттеу нәтижелері жергілікті және модификацияланған шикізат негізінде еритін натрий силикатын өндіру үшін энергия үнемдейтін технологияларды әзірлеу мүмкіндігін анықтайды. ИК-спектроскопиялық талдау нәтижелері бойынша үшінші үлгінің спектрограммасында Si–O–Na байланыстары басқа зерттелген үлгілер мен құрамдармен салыстырғанда анағұрлым тұрақты және жоғары интенсивтілік байқалды. Бұл құбылыс құрамның құрылымдық біртектілігімен, катион-анион байланыстарының тепе-теңдігімен және шыны торының беріктігімен түсіндіріледі. Осыған байланысты ВМК-3 құрамы ең болашағы зор үлгі ретінде ұсынылады.

Түйін сөздер: еритін натрий силикаты, модификациялық шикізат, ИҚ талдау, рентген флуоресценция, оңтайлы құрам, физика-химиялық қасиеттер.

Авторлар туралы ақпарат:

Мадаминов Дилшодбек Куранбоевич
Докторант, Хорезм Мамун академиясы, Марказ көшесі, 1, Хива, Өзбекстан. Email: dilshodbek-md@mail.ru; ORCID ID: https://orcid.org/0009-0004-9696-8899

Аташев Элёр Аташевич
Техника ғылымдары бойынша философия докторы, Әбу Райхон Беруни атындағы Үргеніш мемлекеттік университетінің химия-технология факультетінің доценті, 220100, Үргеніш, Х.Олимжон, 14, Өзбекстан. Email: elyor.a@urdu.uz; ORCID ID: https://orcid.org/0000-0003-4070-5665

Матмуротов Бахтишод Янгибоевич
Химия ғылымдары бойынша философия докторы (PhD), Ташкент мемлекеттік медицина университетінің Халықаралық факультетінің аға оқытушысы, 100109, Алмазар ауданы, Фараби көшесі, 2-үй, Ташкент, Өзбекстан. E-mail: b.matmurotov@mail.ru; ORCID ID: https://orcid.org/0009-0002-1175-3588

Раджапов Одилбек Бабаназарович
Доцент, Әлеуметтік және гуманитарлық ғылымдар кафедрасы, Әлеуметтік және гуманитарлық ғылымдар факультеті, Ургенч инновациялық университеті, 220100, Гурлан к-сі, 2, Ургенч Өзбекстан. Email: radjapovodilbek@urgiu.uz; ORCID ID: https://orcid.org/0009-0006-2851-1429

Машарипов Равкат Мадрахимович
Педагогика ғылымдары бойынша философия докторы (PhD), Мамун университетінің Психология және жалпы кәсіби пәндер факультетінің доценті, Хорезм облысы, Қыбла Тозабоғ МАӘ, Бөл-хауз көшесі, 2-үй, Хива, Өзбекстан. E-mail: ravqatmasharipov@gmail.com

Физико-химический анализ водорастворимого силиката натрия, полученного из модификационного сырья

[1*]Мадаминов Д.Қ., [2]Аташев Э.А., [3]Матмуротов Б.Я.[4]Раджабов О.Б. [5]Машарипов Р.М.

[1]Хорезмская академия Мамуна, Хива, Узбекистан
[2] Ургенчский государственный университет имени Абу Райхона Беруни, Ургенч, Узбекистан
[3]Ташкентский государственный медицинский университет, Ташкент, Узбекистан
[4]Ургенчский инновационный университет, Ургенч, Узбекистан
[5]Университет Мамуна, Хива, Узбекистан

Поступила: *9 сентября 2025*
Рецензирование: *17 октября 2025*
Принята в печать: *1 декабря 2025*

АННОТАЦИЯ
В данной статье изучены физико-химические свойства образцов растворимого силиката натрия, синтезированных на основе модификационного сырья. В процессе исследования были подготовлены образцы растворимого стекла различного состава, структура которых проанализирована методом инфракрасной (ИК) спектроскопии. Кроме того, для определения химического состава продуктов и распределения компонентов был применён метод рентгенофлуоресцентного (РФ) анализа. Полученные результаты показали, что два из исследованных составов являются перспективными по своим технологическим и физико-химическим показателям. В частности, третий состав продемонстрировал оптимальные результаты, обеспечив высокую стабильность растворимого стекла, структурную согласованность и эффективность в практическом применении. Результаты исследования свидетельствуют о возможности разработки энергосберегающих технологий производства растворимого силиката натрия на основе местного и модификационного сырья. Результаты ИК-спектроскопического анализа показали, что в спектрограмме образца ВМК-3 связи Si–O–Na проявляются значительно более устойчивыми и интенсивными по сравнению с другими исследованными образцами и составами. Данное явление объясняется структурной однородностью состава, сбалансированностью катион-анионных взаимодействий и прочностью стеклосеточной структуры. В связи с этим третий состав рекомендуется как наиболее перспективный образец.

Ключевые слова: растворимый силикат натрия, модификационное сырьё, ИК-анализ, рентгенофлуоресценция, оптимальный состав, физико-химические свойства.

Мадаминов Дилшодбек Куранбоевич	***Информация об авторах:*** *Докторант Хорезмской академии Мамуна, ул. Марказ, 1, Хива, Узбекистан. Email: dilshodbek-md@mail.ru; ORCID ID: https://orcid.org/0009-0004-9696-8899*
Аташев Элёр Аташевич	*Доктор философии в области технических наук (PhD), доцент факультета химической технологии Ургенчского государственного университета имени Абу Райхона Беруни, 220100, Ургенч, улица Х. Олимжона, 14, Узбекистан. Email: elyor.a@urdu.uz; ORCID ID: https://orcid.org/0000-0003-4070-5665*
Матмуротов Бахтишод Янгибоевич	*Доктор философии в области химических наук (PhD), старший преподаватель Международного факультета Ташкентского государственного медицинского университета, Узбекистан, 100109, Алмазарский район, ул. Фараби, д. 2, Ташкент, Узбекистан. E-mail: b.matmurotov@mail.ru; ORCID ID: https://orcid.org/0009-0002-1175-3588*
Раджапов Одилбек Бабаназарович	*Доцент кафедры Социальные и гуманитарные науки факультета Социальные и гуманитарные науки Ургенчского инновационного университета, 220100, ул. Гурлан, 2, Ургенч, Узбекистан. Email: radjapovodilbek@urgiu.uz; ORCID ID: https://orcid.org/0009-0006-2851-1429*
Машарипов Равкат Мадрахимович	*Доктор философии в области педагогических наук (PhD), доцент факультета психологии и общепрофессиональных дисциплин Университета Мамуна, Хорезмская область, МФЙ Кибла Тозабог, ул. Буль-хауз, д. 2, Хива, Ургенч. E-mail: ravqatmasharipov@gmail.com*

References

[1] Matinfar M, & Nychka J A. A review of sodium silicate solutions, Structure, gelation, and syneresis. Advances in Colloid and Interface Science; 2023; 322:103036. https://doi.org/10.1016/j.cis.2023.103036

[2] Minju N, Nair B N, & Savithri S. Sodium silicate-derived aerogels: effect of processing parameters on their applications. RSC Advances. 2021; 11:15301–15322. https://doi.org/10.1039/D0RA09793D

[3] Adinaev Kh A, Kadirova Z R. Physico-chemical analysis of quartz sand and technological waste used as a main raw material for glass production // Journal of Chemical Technology and Metallurgy. 2024; 59(3):599-604.

[4] Boyjanov Islom, Djabberganov Djakhangir, Matyaqubova Karomat, Khudayberganov Erkaboy and Sitmuratov Tulkinbek. Phase transformations and physico-mechanical properties of ceramic tiles from Lower Amu Darya raw materials for sustainable construction in earth and environmental engineering. E3S Web of Conferences. 2025; 633:08001. https://doi.org/10.1051/e3sconf/202563308001

[5] Buranova D, Matchanov S, & Atashev E. Physicochemical and mineralogical characterization of Sultan Uwais feldspar for sustainable glass manufacturing in earth and environmental sciences. E3S Web of Conferences. 2025; 633:06001. https://doi.org/10.1051/e3sconf/202563306001

[6] Adinaev KhA, Kadyrova ZR, Shilova OA. Synthesis of Lead-Containing Glass Crystalline Materials with Various Crystallization Nucleators. Glass Physics and Chemistry. 2024; 50(2):160-67.

[7] Adinaev KhA, Ismatov AA. IR spectroscopic and electron microscopic investigations of colored lead silicate glasses. Russian journal of applied chemistry. 2010; 83(12):2205-2209.

[8] Richet P, Bottinga Y, Tequi C. Heat-capacity of sodiumsilicate liquids. J. Am. Ceram. Soc. 1984; 67(1):6-8.

[9] Toplis MJ. Quantitative links between microscopic properties and viscosity of liquids in the system SiO_2–Na_2O. Chem. Geol. 2001; 174(1–3):321-331.

[10] Lavrov R V, Mironovich L M. A novel method for preparing a batch of silicate glasses using sodium and potassium hydroxides. Glass Phys. Chem. 2018; 44(2):145–151.

[11] Lavrov R. A method of activation of a quartz-containing raw material component of a glass batch with sodium hydroxide. The American Ceramic Society. 25 th International Congress on Glass (ICG 2019). Boston, Massachusetts, USA. 2019, 94.

[12] Anas SM, Alam M, Saifi F, Jumaniyozov K, Saidova D. CEL-FE numerical analysis of blast wave pressure on buried pipeline subjected to subsurface and surface detonations, and dynamic response, E3S Web of Conferences. 2024; 563:02016. https://doi.org/10.1051/e3sconf/202456302016

[13] Jumaniyozov K, & Adambaeva F. Study on the Production of Glass-Ceramics from Diabase Rocks: A case study of Uzbekistan. In E3S Web of Conferences. EDP Sciences. 2024; 563:02028.

[14] Kulkarni S, Singh D, Hussain L, Balaji V, Sharma A, Jumaniyozov K, & Kenjaeva K. Finite element analysis of bonded, riveted and hybrid joints in glass fibre epoxy composite laminates for aircraft structure. In E3S Web of Conferences. EDP Sciences. 2024; 563:02006.

[15] Kulkarni Santosh, et al. Finite element analysis of bonded, riveted and hybrid joints in glass fibre epoxy composite laminates for aircraft structure. E3S Web of Conferences. EDP Sciences. 2024; 563.

[16] Kulkarni S, et al. Finite element analysis of bonded, riveted and hybrid joints in glass fibre epoxy composite laminates for aircraft structure. E3S Web of Conferences. EDP Sciences. 2024; 563:02006.

[17] Lesovik VS, Zagorodnyuk LK, Babaev Z K, & Dzhumaniyazov Z B. Analysis of the Causes of Brickwork Efflorescence in the Aral Sea Region. Glass Ceram. 2020; 77:277–279. https://doi.org/10.1007/s10717-020-00287-4

[18] Aripova MK, and Ruzibaev BR. Synthesis of glass in the system quartz – kaolin – dolomite. Glass Ceram. 2009; 66:378-380. https://doi.org/10.1007/s10717-010-9205-8

[19] Aripova MK, Mkrtchyan RV, & Érkinov FB. On the Possibility of Enriching Quartz Raw Materials of Uzbekistan for the Glass Industry. Glass Ceram. 2021; 78:120-124. https://doi.org/10.1007/s10717-021-00359-z

[20] Trang An Duong, Farrukh Erkinov, Mastura Aripova, Chang Won Ahn, Byeong Woo Kim, Hyoung–Su Han, Jae–Shin Lee, Ferroelectric–to–relaxor crossover in KNN–based lead–free piezoceramics. Ceramics International. 2021; 47(4):4925-4932. https://doi.org/10.1016/j.ceramint.2020.10.066

МАЗМҰНЫ
СОДЕРЖАНИЕ
CONTENTS

Техникалық редакторлар:
Г.К. Қасымова, Н.М.Айтжанова, Т.И. Қожахметов

Компьютердегі макет:
Г.К. Қасымова

Дизайнер:
Г.К. Қасымова, Н.М.Айтжанова

“Металлургия және кен байыту институты” АҚ
050010, Қазақстан Республикасы, Алматы қаласы, Шевченко к-сі, 29/133

Жариялауға 02.12.2025 жылы қол қойылды

Технические редакторы:
Г.К. Касымова, Н.М. Айтжанова, Т.И. Кожахметов

Верстка на компьютере:
Г.К. Касымова

Дизайнер:
Г.К. Касымова, Н.М.Айтжанова

АО “Институт металлургии и обогащения”
050010, г. Алматы, Республика Казахстан. ул. Шевченко, 29/133

Подписано в печать 02.12.2025 г.

Technical editors:
G.K. Kassymova, N.M. Aitzhanova, T.I. Kozhakhmetov

The layout on a computer:
G.K. Kassymova

Designer:
G.K. Kassymova, N.M. Aitzhanova

“Institute of Metallurgy and Ore Beneficiation” JSC
050010, Almaty city, the Republic of Kazakhstan. Shevchenko str., 29/133

Signed for publication on 02.12.2025